Biologically-Inspired Systems

Christian Hamm *Editor*

Evolution of Lightweight Structures

Analyses and Technical Applications

Springer

Biologically-Inspired Systems

Volume 6

Series Editor
Stanislav N. Gorb
Christian Albrecht University of Kiel, Kiel, Germany

Motto: Structure and function of biological systems as inspiration for technical developments

Throughout evolution, nature has constantly been called upon to act as an engineer in solving technical problems. Organisms have evolved an immense variety of shapes and structures from macro down to the nanoscale. Zoologists and botanists have collected a huge amount of information about the structure and functions of biological materials and systems. This information can be also utilized to mimic biological solutions in further technical developments. The most important feature of the evolution of biological systems is multiple origins of similar solutions in different lineages of living organisms. These examples should be the best candidates for biomimetics. This book series will deal with topics related to structure and function in biological systems and show how knowledge from biology can be used for technical developments in engineering and materials science. It is intended to accelerate interdisciplinary research on biological functional systems and to promote technical developments. Documenting of the advances in the field will be important for fellow scientists, students, public officials, and for the public in general. Each of the books in this series is expected to provide a comprehensive, authoritative synthesis of the topic.

More information about this series at http://www.springer.com/series/8430

Christian Hamm
Editor

Evolution of Lightweight Structures

Analyses and Technical Applications

Springer

Editor
Christian Hamm
Bionic Lightweight Constructions and
Functional Morphology
Alfred-Wegener-Institut Helmholtz-
Zentrum für Polar- und Meeresforschung
Bremerhaven
Germany

ISSN 2211-0593 ISSN 2211-0607 (electronic)
Biologically-Inspired Systems
ISBN 978-94-017-9397-1 ISBN 978-94-017-9398-8 (eBook)
DOI 10.1007/978-94-017-9398-8

Library of Congress Control Number: 2015930397

Springer Dordrecht Heidelberg New York London

Printed on acid-free paper

Springer is part of Springer Science+Business Media (www.springer.com)

Preface

This book is based on the hypothesis that evolution created a large variety of fantastic, very efficient lightweight structures as a result of the adaptation to diverse environmental factors, i.e. significant mechanical challenges and the need to build lightly and/or economically.

The focus of this book is on planktonic organisms, where there is good evidence that an arms race between predators such as copepods and their floating prey—diatoms and radiolarians—leads to a large, continuously changing pool of species with individual (defensive) lightweight structures (see Knoll and Kotrc, Chap. 1). Due to a very patchy fossil record, it is impossible to follow the development of feeding tools of copepods to a similar extent—but we do see the results of the arms race: the gnathobases of copepods are not only highly developed in their complex geometries, they also have a sophisticated multi material composition (see Michels and Gorb, Chap. 3).

Diatoms and radiolarians are unicellular organisms and thus restricted to sizes between a few µm and 1 mm. They use amorphous silica as the main building material, which is very convenient as it makes, unlike crystalline minerals, any form possible—even in the size range between a few nm and a mm. The process of biomineralization is initiated by small amounts of organic components and recent research has shown that there is not only one, but a large variety of chemical components involved in this process (Ehrlich and Witkowski, Chap. 4). This makes diatom silica a composite, and an additional structuring of interfaces between organic and inorganic components most likely results in anisotropic, strong material properties. This would be consistent with theoretical mechanics: the best lightweight solutions are a combination of sophisticated structures and composite materials.

The resolution of microscopes with regard to resolving the diatom composite structure qualitatively and quantitatively in 3D is, however, so far unsatisfactory. Layers of silica seem to have a size of 30–40 nm, and the organic layers are even thinner, so that a reasonable material model could not be realized within the project. Although virtually all other structural biogenic materials are also composites, there is one group of organisms, where composites are very common, and which also combine silica with organic materials: higher plants. Especially in equisetales and graminaceae silica structures (phytoliths) are very abundant. Since many

publications have already dealt with fibre orientation of wood and plant stems, Keutmann and Speck (Chap. 9) focus on the detection and potential mechanical function of phytoliths in higher plants.

Light weight structures are also an issue in much larger marine organisms, such as echinodermata, especially sea urchins. They use $CaCO_3$ to build their skeletons and have also optimized their mechanical strength to reduce mortality by predation; the selection pressure to build light structures is probably based on their need for mobility and to save energy necessary to build a $CaCO_3$-skeleton. The fossil record is excellent and the geometries of the solitary organisms are less restricted by growth processes than they are in trees or snails. A variety of fascinating typical lightweight principles of sea urchin skeletons are described by Nebelsick et al. in Chap. 8.

Since evolutionary processes have led to fantastic lightweight solutions, especially in diatoms, but are not easily accessible for engineers, Chap. 5 (Kooistra and Pohl) summarizes a variety of interesting principles and gives examples of how they could be applied in the technical world.

Hierarchically organized—fractal—structures are very common in nature. Especially diatom shells are known for honeycomb structures which are interlaced within each other. In other cases they have different stiffening devices such as ribs, honeycombs, and undulations which are combined in different dimensions. This design is advantageous if a massive outer skin, resulting in the best second moment of area, is for whatever reason not applicable. In the case of diatoms, high permeability is required to ensure efficient uptake of nutrients. Other (including technical) reasons could be the need for transparency or a production process.

The combination of complex fractally structured geometries with modern fibre reinforced plastic materials is a highly challenging task, as multiple branchings are the rule and have to be solved. In Chap. 7 by Milwich, an innovative method is described to produce geometrically complex Carbon Fibre Composite (CFC) structures. Mechanical tests revealed very promising properties, e.g. for robot structures. Thus, with the rapid development of production technologies, the near future will see considerable progress in this field.

A highly aesthetic solution for an exhibition pavilion made of thin glass fibre reinforced plastic is described by Pohl (Chap. 6). This ambitious project shows how a combination of lightweight principles from nature, human intuition, and innovative manufacturing approaches can lead to a highly attractive product with the potential for upscaling. In this case, the design aspect is very important and has been successfully realized—visitors of the pavilion were enthusiastic.

An innovative, powerful method which combines several principles of the evolutionary optimization process is the ELiSE method (Chap. 10). It uses the full potential of a synthesis of (a) natural lightweight principles, (b) the innovation strength of ecosystems due to a high biodiversity, and (c) the power of the optimization process. It has thus a higher similarity to the natural process of structure evolution than most other methods used in bionics, but at the same time complies with industrial approaches of product development. An example for this method is given in Chap. 11, where an offshore foundation has been developed on the basis of the ELiSE process.

Most of the chapters contain results of the Helmholtz Virtual Institute Plankton-Tech, which integrated basic research on the biology of lightweight structures with approaches to transfer them to technical structures. We are very grateful for this substantial support by the Helmholtz Society. It is evident that the combination of basic research, applied research and technical realization presented here shows but a snapshot of the increasing tendency to use principles from nature to design clever, environmentally friendly and sustainable technical solutions. I hope it became visible that only substantial effort, dedication, and interdisciplinary cooperation leads to progress in this field and I expect that similar constellations and projects will further improve both our knowledge on fascinating principles in nature and our ability to use them for our own benefit.

2015

Christian Hamm
Bremerhaven
Germany

Structure and Function of Biological Systems as Inspiration for Technical Developments

Throughout evolution, organisms have evolved an immense variety of materials, structures, and systems. This book series deals with topics related to structure-function relationships in diverse biological systems and shows how knowledge from biology can be used for technical developments (bio-inspiration, biomimetics).

Contents

Contributors

Janina F. Dynowski Stuttgart State Museum of Natural History, Stuttgart, Germany

Department of Geosciences, University of Tübingen, Tübingen, Germany

H. Ehrlich TU Bergakademie Freiberg, Freiberg, Germany

Stanislav N Gorb Department of Functional Morphology and Biomechanics, Institute of Zoology, Christian-Albrechts-Universität zu Kiel, Kiel, Germany

Jan Nils Grossmann Institute of Zoology, Graduate Program: Bionics-Interactions across Boundaries to the Environment, University of Bonn, Bonn, Germany

Zentrum für Wissenschafts- und Technologietransfer, Hochschule Bonn-Rhein-Sieg, University of Applied Sciences, Grantham Allee, Augustin, Germany

Christian Hamm Bionic Lightweight Constructions and Functional Morphology, Alfred-Wegener-Institut Helmholtz-Zentrum für Polar- und Meeresforschung, Bremerhaven, Germany

Rene von der Hellen WeserwindGmbHOffshoreConstructionGeorgsmarienhütte GmbH, Bremerhaven, Germany

WeserWind GmbH Offshore Construction Georgsmarienhütte, Bremerhaven, Germany

Piotr Jurkojc Bionic Lightweight Constructions and Functional Morphology, Alfred-Wegener-Institut Helmholtz-Zentrum für Polar- und Meeresforschung, Bremerhaven, Germany

Inga C. Keutmann Plant Biomechanics Group, Botanic Garden of the Albert-Ludwig University, Faculty of Biology, Freiburg im Breisgau, Germany

Andrew H. Knoll Department of Earth and Planetary Sciences, Harvard University, Cambridge, MA, USA

Wiebe H. C. F. Kooistra Stazione Zoologica Anton Dohrn, Villa Comunale, Naples, NA, Italy

Benjamin Kotrc Department of Earth and Planetary Sciences, Harvard University, Cambridge, MA, USA

Sebastian Möller Bionic Lightweight Constructions and Functional Morphology, Alfred-Wegener-Institut Helmholtz-Zentrum für Polar- und Meeresforschung, Bremerhaven, Germany

Björn Melzer Plant Biomechanics Group, Botanic Garden of the Albert-Ludwig University, Faculty of Biology, Freiburg im Breisgau, Germany

Jan Michels Department of Functional Morphology and Biomechanics, Institute of Zoology, Christian-Albrechts-Universität zu Kiel, Kiel, Germany

Biological Oceanography, Geomar, Düsternbrooker Weg 20, Kiel, Germany

Markus Milwich Institut für Textil-und Verfahrenstechnik Denkendorf, Denkendorf, Germany

Hochschule Reutlingen, Reutlingen, Germany

James H. Nebelsick Department of Geosciences, University of Tübingen, Tübingen, Germany

Nils Niebuhr Bionic Lightweight Constructions and Functional Morphology, Alfred-Wegener-Institut Helmholtz-Zentrum für Polar- und Meeresforschung, Bremerhaven, Germany

Göran Pohl Faculteit Bouwkunde, Facade Research Group/office, TU Delft/Pohl Architekten, Erfurt, Germany

Faculty of Architecture and The Built Environment, Architectural Engineering + Technology, TU Delft, Delft, The Netherlands

Robin Seidel Plant Biomechanics Group, Botanic Garden of the Albert-Ludwig University, Faculty of Biology, Freiburg im Breisgau, Germany

Daniel Siegel Bionic Lightweight Constructions and Functional Morphology, Alfred-Wegener-Institut Helmholtz-Zentrum für Polar- und Meeresforschung, Bremerhaven, Germany

Thomas Speck Plant Biomechanics Group, Botanic Garden of the Albert-Ludwig University, Faculty of Biology, Freiburg im Breisgau, Germany

Freiburg Materials Research Center (FMF), Freiburg im Breisgau, Germany

Christian Tötzke Helmholtz-Zentrum Berlin for Materials and Energy, Berlin, Germany

Ralf Thomann Freiburg Materials Research Center (FMF) and Institute of Macromolecular Chemistry of the Albert-Ludwig University, Freiburg im Breisgau, Germany

A. Witkowski TU Bergakademie Freiberg, Freiberg, Germany

University of Szczecin, Szczecin, Poland

Chapter 1
Protistan Skeletons: A Geologic History of Evolution and Constraint

Andrew H. Knoll and Benjamin Kotrc

1.1 Introduction

The ninth century Persian polymath, Abu-Bakr Muhammed ibn Zakariya al-Razi first divided the material world into the categories of animal, vegetable and mineral (Strathern 2005). Although this classification would guide alchemists well into the Age of Enlightenment, even cursory inspection shows that the world is not so simple. Many animals and plants precipitate minerals, as do a broad array of microorganisms whose existence could not have been known to al-Razi. Bacterial metabolism induces the precipitation of carbonates, sulfides and oxides from pore waters in sediments (Konhauser and Riding 2012), and at least a few bacteria precipitate magnetite within their cytoplasm to guide movement (Frankel et al. 1998). Eukaryotic organisms precipitate a variety of minerals intracellularly, serving a range of functions that includes the regulation of buoyancy, gravity sensing, magnetotaxis, and storage (Raven and Knoll 2010). Of particular interest are those eukaryotes, large and small, that precipitate mineralized skeletons: tests, scales, spicules, sclerites, shells and bones.

More than 50 biominerals have been recorded in eukaryotic organisms, half of them containing calcium and a quarter crystallographically amorphous (Weiner and Dove 2003). Overwhelmingly, however, the minerals found in skeletons are Ca-phosphates (especially dahllite), calcium carbonate (calcite and aragonite), or amorphous silica. How are skeletal biominerals distributed among organisms, and what features of function and environment account for this distribution? How, as well, have biomineralizing eukaryotes evolved through time?

A. H. Knoll (✉) · B. Kotrc
Department of Earth and Planetary Sciences, Harvard University, Cambridge, MA 02138, USA
e-mail: aknoll@oeb.harvard.edu

B. Kotrc
e-mail: kotrc@mit.edu

C. Hamm (ed.), *Evolution of Lightweight Structures,* Biologically-Inspired Systems 6,
DOI 10.1007/978-94-017-9398-8_1

1.2 The Phylogenetic Distribution of Biomineralized Skeletons

Molecular research has begun to resolve evolutionary relationships among eukaryotic organisms. Most treatments recognize half a dozen "superkingdoms" within the Eukarya, although branching relationships among these major clades remain a topic of debate (e.g., Burki et al. 2008; Parfrey et al. 2010; Walker et al. 2011; Fig. 1.1). Our understanding of skeletal biomineralization derives principally from animals, giving the impression that calcium carbonate is the most widespread

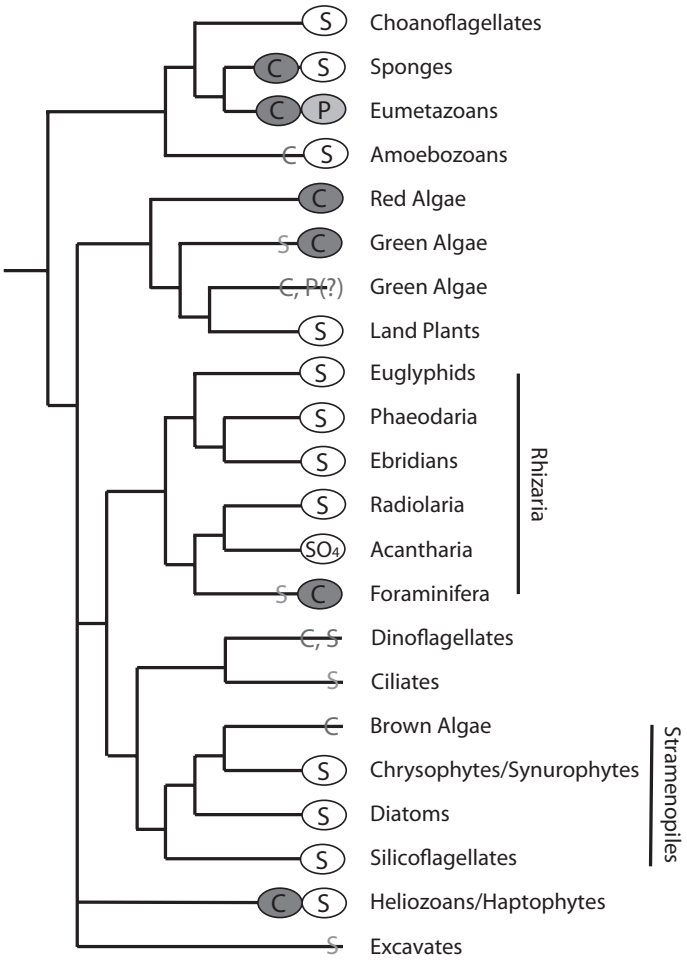

Fig. 1.1 A phylogeny of biomineralizing eukaryotes, drawn from papers cited in the text. Letters in ovals indicate major occurrence of biomineralized skeletons of calcium carbonate (C), Ca-phosphate (P), amorphous silica (S), or, uniquely in the case of acantharians (strontium sulfate). *Grey* letters indicate minor occurrences within a clade

means of mineralizing skeletal elements. Calcite and/or aragonite strengthen external skeletons in a number of phyla including the sponges, cnidarians, brachiopods, bryozoans, molluscs, annelid worms, and arthropods (e.g., Knoll 2003; Cuif et al. 2011; Wallace et al. 2012). Echinoderms also precipitate skeletal plates of calcite, but do so internally, beneath a thin layer of epidermis, and tunicates, as well, precipitate aragonitic spicules within their bodies. Among living animals, phosphatic skeletons are formed externally by some brachiopods, internally by vertebrates and, rarely, as minor components of arthropod exoskeletons (Bentov et al. 2012); fossils indicate that phosphatic skeletons were more widespread during the Cambrian Period, characterizing early chaetognath teeth and skeletons in a limited number of now extinct lineages (Zhuravlev and Wood 2008; Maloof et al. 2010). Silica biomineralization is even more restricted among animals, characterizing only early branching sponges (Müller et al. 2007), with minor occurrences in calcareous brachiopods and a few arthropods (references in Knoll 2003). Among seaweeds, calcite and aragonite also dominate skeletal biomineralization, occurring among the green, red, and brown algae (Raven and Giordano 2009). Land plants are different, precipitating amorphous silica within epidermal cells (Raven 1983).

The greater phylogenetic distribution of mineralized skeletons reflects a second short-coming of al-Razi's classification. Many eukaryotes are neither animal nor vegetable, instead belonging to diverse clades grouped informally (and paraphyletically) as protists, and these microscopic eukaryotes paint a different picture of skeletal biomineralization. Testate and scale-forming organisms are widely, if discontinuously distributed among protists. They may serve a number of functions, but ballast and defense against predation probably explain many such structures (e.g., Cohen and Knoll 2012). Calcite mineralizes the tests of some foraminiferans (Lipps 1973) and the scales of coccolithophorid algae (Young and Henriksen 2003), and rare occurrences of carbonate biomineralization have been reported among dinoflagellates and in at least one amoebozoan. Phosphatic biomineralization, however, is exceedingly rare in protists, being reported only in the scales of a single freshwater green phytoflagellate (Domozych et al. 1991; but see Raven and Knoll 2010) and in the test lining of a freshwater amoebozoan (Hedley et al. 1977). In contrast, amorphous silica occurs in diverse protistan clades (Preisig 1994, Fig. 1.1), including the choanoflagellates, rhizarians (four or more independent origins), haptophytes, heliozoans, amoebozoans (at least three independent origins), and stramenopiles (at least three origins). New occurrences continue to be discovered, for example, the report of a ciliate that coats its resting spores with granules of amorphous silica (Foissner et al. 2009).

Among biomineralizing protists, acantharians desrve mention for a unique feature: they fashion spiculate tests and cysts of celestite ($SrSO_4$) (Decelle et al. 2013). Non-skeletal Sr and Ba sulfates are precipitated by phylogenetically diverse protists and appear to function in the perception of gravity or buoyancy control (Raven and Knoll 2010). Molecular sequence comparisons place acantharians within the traditionally defined polycystine Radiolaria (Kunimoto et al. 2006, Krabberod et al. 2011), and so it is noteworthy that some radiolarians precipitate celestite crystals within their cytoplasm. It may be that members of this group repurposed this

biomineralizing capacity to precipitate skeletal celestite tests on a molecular template inherited from radiolarian ancestors (Raven and Knoll 2010; Decelle et al. 2012). Today, acantharians place a key role in the distribution of strontium in the oceans (De Decker 2004; Decelle et al. 2013)

A comparison between microscopic and macrosocpic eukaryotes prompts a simple question: why should silica precipitation be so prominent among microscopic eukaryotes, when Ca-minerals dominate in the macroscopic biota?

1.3 Silica Use by Protists

Silica might seem an unusual choice for skeletal mineralization, given its low concentrations in seawater and most terrestrial environments. The physiological cost of biomineralization, however, scales with saturation state, not with absolute abundance. Seawater becomes saturated with respect to amorphous silica at concentrations of about 60 ppm, and in pre-diatom oceans, it is likely that marine waters were commonly at or near this saturation state (Siever 1992), or even higher (Grenne and Slack 2003). Silica concentrations can also be high in rivers, lakes and groundwaters—waters that are commonly undersaturated with respect to calcium carbonate minerals.

Of course, the upper ocean is also oversaturated with respect to calcium carbonate minerals, and so saturation sate alone cannot account for the widespread use of silica in protestant skeletons. Perhaps the key lies in material properties. Amorphous silica can be fashioned into complex structures on a scale of microns or less, enabling silica-precipitating microorganisms to make strong, lightweight structures with pores and struts that are little approximated by carbonate-precipitating protists. Moreover, both observation and experiment show that amorphous silica precipitates readily on long chain polyamines and structural proteins such as chitin and collagen which, themselves, can be fashioned into structures of outstanding complexity on micron- or even submicron spatial scales (Ehrlich 2010). That is, many protists, whether mineralized or not, fashion organic scales of exquisite complexity. The advantage, then, of amorphous silica in protistan biomeralization may be that it can reinforce those fine-sccale constructions free of the crystallographic constraints that influence carbonate biomineralization (e.g., Young and Henriksen 2003). Together, the constructional properties of these organic molecules and the silica that binds to them may account for the repeated evolution of silica biomineralization in scale- and test-forming protists.

Our understanding of silica biomineralization in protists stems almost entirely from laboratory studies of diatoms (reviewed by Kröger and Poulsen 2008; Wallace et al. 2012). The concentration of orthosilicic acid in the internal vesicles where frustule formation occurs is commonly high relative to the ambient environment, indicating that diatoms can pump silica across membranes (Hildebrand 2000). Nucleation appears to occur on a polysaccharide-rich organic template, catalyzed by long chain polyamines and silaffin proteins (Kröger and Poulsen 2008). Silicification in sponges involves a different set of organic constituents (references in Wallace et al.

2012), demonstrating that distinct proteins and polysaccharides have been recruited for silica skeletogenesis in different silicifying clades. In this regard, it is curious that preliminary molecular research on silica precipitation in choanoflagellate loricae (e.g., Gong et al. 2010) indicates that silicon transporters in this group are related to those in diatoms, implying lateral genetic transfer (Marron et al. 2013). Not much is known about the molecular biology of silicification in radiolaria or other groups.

Various functions have been inferred for silicified tests and scales in protists. Defense against grazers is commonly invoked, and Hamm et al. (2003; Hamm 2005) have demonstrated experimentally that diatom frustules have a mechanical strength that would deter mandibulate microzooplankton predators such as copepods, euphausiids, and, in fresh water, cladocerans. Indeed, a portion of the diatoms ingested by both copepods and euphausiids has been observed to survive passage through the gut unscathed (Fowler and Fisher 1983). Other functions have been proposed for diatom frustules, involving buoyancy, light modulation, catalysis of carbon assimilation, maintenance of shape and orientation, and defense against viruses (references in Finkel and Kotrc 2010)—these are not mutually exclusive hypotheses. Whether the siliceous scales of chrysophytes, heliozoans and prymensiophytes would protect against microarthropod grazing is open to question, but they might well deter protistan predators such as ciliates. A correlation between the test morphology and feeding mode of radiolarians suggests that siliceous tests in these protists may also play a role in providing shape and structure to the cytoplasm (Matsuoka 2007), supporting prey-capturing pseudopodia analogous to the vertebrate skeletomuscular system (Anderson 1983), and perhaps in orienting cells within the water column (Haeckel 1887). Sorting out functional hypotheses might be aided by surveying the geologic history of silica-precipitating protists.

1.4 A Short History of Protistan Biomineralization

The oldest eukaryotic microfossils that might be interpreted in terms of defense against predators are vase-shaped tests and scales, both found in 800–740 million year old (Ma) rocks. 10–30 μm scales preserved in platform carbonates from northwestern Canada were originally interpreted as siliceous, based largely on comparisons to scales formed today by chrysophyte algae (Allison and Hilgert 1986). In a restudy, Cohen et al. (2011) used Raman and fluorescence spectroscopy to show that the scales actually consist of apatite in an organic matrix. Systematic investigation of scales freed by acid digestion from host rocks documents some three dozen morphospecies, the highest diversity of eukaryotic fossils found to date in any pre-Ediacaran rocks (Cohen and Knoll 2012). Many protists form scales, but none of the ca. 800 Ma scales can be allied unambiguously to an extant clade. Indeed, it remains an open question whether the apatite within the fossils reflects biomineralization or early diagenetic phosphatization, as observed in small shelly fossils from Cambrian strata. If the observed phosphate was emplaced diagenetically, it is probable that the scales were originally organic, as we know of no fossils in which phosphate has replaced pre-existing silica.

The other microfossils of interest are assemblages of ca. 100 μm long, vase-shaped tests found in 740–780 Ma rocks from around the world but preserved especially well in the Grand Canyon. At least some of these tests can be assigned to clades of testate amoebae in the Amoebozoa (Porter et al. 2003). A subpopulation displays abundant ovoid holes 5–10 μm in maximum dimension and arranged in a hexagonally close-packed pattern. Porter et al. (2003) hypothesized that these holes reflect the positions of scales that covered the test in life, much like the extant testate rhizarian *Euglypha*. More recent molecular clock estimates suggest that euglyphids originated long after 750 Ma, requiring that any comparison with the Grand Canyon fossils reflect analogy rather than homology (Berney and Pawlowski 2006). Also, whether the inferred scales were siliceous or not remains unknown. Thus, while pre-Edicaran rocks preserve evidence for protistan defensive structures and include possible candidates for early skeletal biomineralization, it is only in the Ediacaran Period that we begin to see unambiguous evidence of mineralized skeletons.

Microbial reefs from late Ediacaran (550–542 Ma) platform carbonates contain locally abundant populations of at least three biomineralizing animals. As in the case of older protists, both the systematic relationships and original mineralogy of these fossils remain questions for debate. Much opinion, however, places tubular *Cloudina* and goblet-shaped *Namacalathus* among the Cnidaria, and the *Namapoeikea* with calcareous sponges (Grotzinger et al. 2000; Wood et al. 2002). All had thin calcified surfaces, possibly aragonitic in *Namapoeikea*, but less readily interpreted in the other taxa (Porter 2010).

A new age of biomineralization began with the Cambrian Period. Molecular clock estimates suggest that silica-precipitating sponges evolved as much as 750–800 Ma (Sperling et al. 2010), but unambiguous spicules occur only basal Cambrian rocks (Antcliffe et al. 2014), when a radiation of both hexactinellids and siliceous demosponges first brought sponges to biogeochemical prominence in the marine silica cycle (Maliva et al. 1989; Carrera and Botting 2008). Calcareous sponges also radiated in Cambrian oceans, most prominently the ecologically important but stratigraphically short-lived archaeocyathids (Debrenne 2007). Cnidarians show evidence of Cambrian diversification, but massively calcifying corals spread only during the succeeding Ordovician Period (Park et al. 2011). And among bilaterian animals, calcareous and, to a lesser extent, phosphatic skeletons evolved independently in diverse phyla, filling most of the skeletal morphospace that would be occupied during the Phanerozoic Eon (Thomas et al. 2000). There is broad agreement that the polyphyletic (Knoll 2003) evolution of mineralized skeletons reflects an increase in metazoan predation, at least in part (Bengtson and Conway Morris 1992). Despite the evolution of mineralized skeletons in many clades, however, skeletons played a relatively minor role in the carbonate cycle of Cambrian oceans (Pruss et al. 2010, 2012; Creveling et al. 2013). The evolution of biomineralized structures reflects cost:benefit ratios, and in this context, the limited biogeochemical importance of carbonate skeletons in Cambrian oceans may relate to limited predation pressure (and hence, low benefit, given the cost of skeleton precipitation), warm oceans with anoxia in subsurface water masses (a circumstance that, like ocean acidification, increases the cost of carbonate precipitation by lowering saturation level; Knoll and

Fischer 2011), or both. Only with renewed Ordovician diversification did highly calcified, sessile benthic invertebrates become established as dominant constituents of marine carbonates (Pruss et al. 2010).

What about Cambrian protists? Did they participate in the "Great Leap Forward" of biomineralization? Protists certainly radiated in Cambrian oceans along with animals; this is seen clearly in the records of cysts made predominantly by algae (Knoll 1994; Vidal and Moczydlowska 1997) and in the diversification of benthic foraminiferans with agglutinated skeletons (McIlroy et al. 2001). The main actors in protist biomineralization, however, appear to have been the silica-precipitating Radiolaria. Radiolarian fossils have been described from lower Cambrian strata (Pouille et al. 2011) and show gradual diversification throughout the period. Like animals, however, radiolarians really emerged as important components of the marine silica cycle with renewed expansion during the Ordovician Period (Maliva et al. 1989; Won and Iams 2011).

Among animals, novel instances of skeletal biomineralization tailed off after the Ordovician Period, but this does not seem to be true of protists. The vagaries of preservation may bias the protistan record toward younger occurrences, as may the ecological restriction of some biomineralizing clades to fresh water and wet soil, environments less likely to be preserved in older successions. Nonetheless, innovations in protistan biomineralization appear to have continued and, likely, accelerated over the past 500 million years (Fig. 1.2). Foraminifera, for example, can have organic, agglutinated, or calcareous tests (Lipps 1973). While molecular clocks suggest

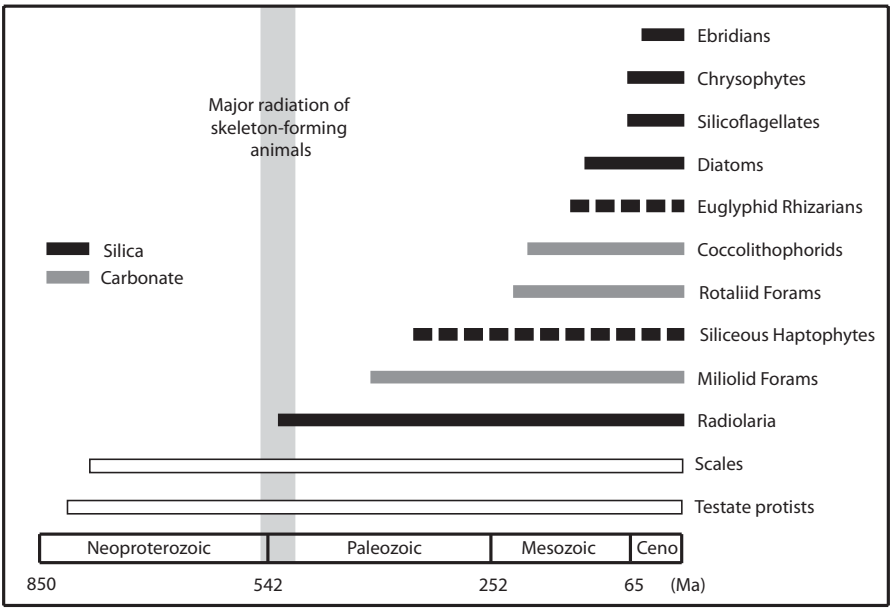

Fig. 1.2 Geologic history of biomineralizing protistan clades, drawn from the fossil record (*solid lines*) or molecular clock estimates (*dashed lines*). Data sources cited in text

a Neoproterozoic origin for the clade (Groussin et al. 2011), the oldest widely accepted foram fossils are agglutinated tests in Cambrian rocks (McIlroy et al. 2001). Calcareous tests emerged with the mid-Paleozoic radiation of miliolids and, again, with the independent acquisition of calcitic tests by rotaliids during the Triassic Period (Groussin et al. 2011). Haptophyte algae also evolved calcitic scales (coccoliths) toward the end of the Triassic Period, about 210 Ma (Young and Henriksen 2003).

Experiments have shed light on calcification in both forams and coccolithophorid haptophytes, and in both cases, ions derived from seawater are pumped into a membrane-defined space where carbonate (in at least some cases, initially as amorphous calcium carbonate) forms on a macromolecular template, perhaps facilitated by physiological modulation of pH (e.g., Paasche 2002; Marsh 2003; Erez 2003; Bentov et al. 2009). Together, the radiation of coccolithophorids and the polyphyletic (Ujiié et al. 2008) expansion of calcified forams into the marine plankton changed the nature of carbonate deposition in the oceans (Zeebe and Westbroek 2003).

Despite the early evolution of scales in eukaryotes (Cohen and Knoll 2012), silica biomineralization of protistan scales also appears to be, in large part, a much younger phenomenon. Molecular clocks suggest that prymensiophytes with siliceous scales appeared no earlier than about 300 Ma (Berney and Pawlowski 2006). Euglyphid rhizarians, known to produce siliceous scales that tile their tests, are thought on the basis of molecular clock estimates to have Mesozoic origins (Berney and Pawlowski 2006; Brown and Sorhannus 2010), and the siliceous microfossils of ebridians, placed within the Rhizaria on the basis of molecular sequence comparions (Hoppenrath and Leander 2006), date back only to the Paleocene (Ernissee and McCartney 1992). Similarly, the array of silica-precipitating clades within the stramenopiles—chrysophytes, synurophytes, dictyochophytes (silicoflagellates), and diatoms (Andersen 2004)—appear on the basis of both fossils and molecular clocks to characterize only Mesozoic and younger ecosystems (chapters in Falkowski and Knoll 2007; Brown and Sorhannus 2010).

Diatoms, of course, are the crown jewels among silica-precipitating protists, fashioning frustules of SiO_2 that inspire technological innovations in lightweight design (Gordon et al. 2009). Diatoms first appear as fossils in uppermost Jurassic rocks and diversify through the Cretaceous Period and into the Cenozoic Era, both in the oceans and in non-marine environments (Kooistra et al. 2007). These algae may be responsible for as much as 20% of Earth's total primary production, and they dominate the marine silica cycle, quantitatively removing dissolved silica from surface water masses (Maliva et al. 1989; Maldonado et al. 2011). Moreover, the ballast provided by mineralized frustules contributes to the dominant influence of diatoms in marine export production (Smetacek 1999).

This brief outline of the evolutionary history of biomineralizing protists prompts two questions: why silica and why so late in the evolutionary day? As noted above, the first question finds answer in the material properties of amorphous silica and the biomolecules onto which it is precipitated. Amorphous silica can be formed into strong porous and strutted structures on lengths scales of less than a micron, making it ideal for protistan biomineralization. In some ways, the question of mineral utilization should really be: why don't animals and macroscopic algae make greater structural use of silica, and here the answer probably lies in its low solubility in

fresh and marine waters—there simply isn't enough silica in seawater to make large skeletons from a physiologically realistic volume of water (Wallace et al. 2012). Silica—found in freshwater water algae, soil protists and vascular plants—also fits the environmental constraints of terrestrial environments: most rivers, lakes and groundwaters are undersaturated with respect to calcite and aragonite.

Why so many armored protists (both siliceous and calcareous) gained importance only during the past 200 million years is a more intriguing question. As noted earlier, scales have been produced by protists since the Neoproterozoic Era (Cohen and Knoll 2012), and while it is impossible to know whether or not groups such as testate amoebozoans, testate rhizarians, and heliozoans precipitated silica in these oceans, there is little evidence for such biosynthesis, and any protistan biomineralization must have played an insignificant role in the marine silica cycle (Maliva et al. 1989). The late geological appearance of siliceous scales certainly has a phylogenetic component to it: silica-precipitating haptophytes and stramenopiles did not exist before the latest Paleozoic or early Mesozoic Era. This, however, does not by itself resolve the issue, as silica precipitation requires a functional as well as phylogenetic explanation.

The Mesozoic to earliest Cenozoic appearance of siliceous skeletons in diatoms, silicoflagellates, chrysophytes, and ebridians, along with the evolution of calcitic tests in coccolithophroids and the expansion of calcified forams into the water column, might find ecological explanation in an increase in predation by microzooplankton. A general increase in predation pressure in the oceans occurred on this time scale (Vermeij 1977), as did a shift in shelf primary producers from green flagellates and cyanobacteria to dinoflagellates, coccolithophorids and diatoms (Falkowski et al. 2004). Perhaps radiating primary producers precipitated evolutionary changes in microzooplankton and throughout marine food webs (e.g., Knoll 2013), with predation pressure feeding back onto both photosynthetic and heterotrophic protists. A nearly monotonic increase in $^{87}Sr/^{86}Sr$ of seawater over the past 150 million years also suggests that erosional fluxes—including silica—from continents to the oceans increased over this interval (Richter et al. 1992). Over time, then, silica flux may have increased even as surface reservoir size declined.

1.5 The Evolutionary Consequences of Diatom Radiation for Silica Biomineralizers

Despite the widespread removal of carbonates from the oceans by marine animals and protists, surface oceans remain oversaturated with respect to calcite and aragonite, and there is little evidence that carbonate precipitation by any one clade has influenced the evolutionary trajectories of other calcareous species. This is, however, not the case for biological participants in the marine silica cycle. Skeleton-forming organisms deplete silica levels in surface oceans to values an order of magnitude lower than those that characterized seawater before the advent of siliceous skeletons (Siever 1992), and one might reasonably expect that the secular decline in silica availability has impacted the evolutionary trajectories of silica-precipitating animals and protists.

Consistent with paleontological evidence that they first evolved in silica-rich Neoproterozoic and Cambrian oceans, sponges (at least the few species that have been examined experimentally) show maximum uptake efficiency at dissolved silica levels much higher than those found in modern surface oceans (Maldonado et al. 2011). Siliceous sponges can be locally important in coastal ecosystems (Maldonado et al. 2010), but the fossil record indicates that they have progressively declined in ecological importance among shelf communites through the late Mesozoic and Cenozoic eras (Maliva et al. 1989). Indeed, when grown at silica concentrations similar to those inferred for a pre-diatom world, some modern sponges produce spicule morphologies not seen in the geologic record since the Jurassic Period (Maldonado et al. 1999). It has been hypothesized that the inefficient uptake of silica by sponges relative to diatoms accounts for their ecological retreat to deeper waters (Maldonado et al. 2012)—diatom success, then, has impacted sponge evolution by restricting many silica-precipitating species to deeper seafloors where silica concentrations are relatively high and diatoms that compete for silica are absent.

Much like sponges, the Radiolaria also evolved in silica-rich oceans. Their fossil record has revealed a remarkable trajectory of morphological change, especially over the course of the Cenozoic Era. During the same time interval that the diatoms rose to their present-day diversity and dominance over the marine silica cycle, the shell weight of radiolarians in low latitude oceans declined severalfold (Harper and Knoll 1975). Morphological measurement has since shown that this decline is due to a decrease in silicification, rather than a reduction in size, with shell walls becoming thinner and more porous through time (Lazarus et al. 2009). Although most modern surface ocean waters have extremely low silica concentrations, this is not true of the high-latitude Southern Ocean, where upwelling has supplied silica-rich water to the surface since the late Eocene Epoch. Interestingly, radiolarian assemblages from those southern high latitude regions do not show a reduction in silicification over the Cenozoic (Lazarus et al. 2009), further supporting the conclusion that the evolutionary trends in radiolarian biomineralization happened in response to changing silica availability. Radiolarians also appear to be less common in shelf environments than they were in earlier oceans (Racki and Cordey 2000), arguably another habitat shift in response to the radiation of diatoms across continental shelves.

Though the known fossil record of the silicoflagellates extends only to the Mesozoic Era (Bukry 1981), the decline of silica availability in surface waters of Cenozoic oceans should still have affected their evolution. Although there appears to have been no change in the average silicification of silicoflagellates over the past 60 million years (van Tol and Finkel 2012) of the sort seen in Radiolaria, shifting costs and benefits of biomineralization may nonetheless have impacted silicoflagellate evolution. Silicoflagellates with spines show quite a different trajectory of morphological change from those without spines, which are also larger. While the larger, spineless forms decreased in size and eventually became extinct, the smaller, spined forms increased the number of spines while their size remained constant. Van Tol and Finkel (2012) suggested that these two groups may have employed two different strategies to avoid predation—large cell size versus anti-grazing spines. Because of their larger surface to area ratio and consequently higher nutrient uptake rate, the benefit of spines in the smaller, spined forms could have outweighed the

rising metabolic costs of uptake with declining silica availability, even as those costs began to exceed the benefit of large size for the spineless forms.

Diatoms may have been the major agents of geochemical change in the Phanerozoic silica cycle, but one might nonetheless expect these changes to have affected their own evolution. Indeed, anecdotal evidence suggests that robust and heavily silicified diatoms are common in Cretaceous and early Cenozoic assemblages, but are gradually replaced by more delicate forms (Armstrong and Brasier 2005; Barron and Baldauf 1995). For example, the Cretaceous species of the genus *Hemiaulus* are heavily silicified, while those occurring in Cenozoic deposits are more lightly silicified (Round et al. 1990). This pattern was borne out in a semi-quantitative survey of three well-preserved diatom assemblages spanning from the Early Cretaceous to the Neogene, which showed a decline in percent silicification of frustule walls (Finkel and Kotrc 2010). While thinner walls are more common in the younger assemblages, the pattern is complicated by the observation that silicification is actually inversely proportional to wall thickness. Thus, while there are more thinner-walled forms with time, these lack the larger pores and chambered, multiple-layer structure of many thicker-walled forms, meaning the decline in percent silicification cannot be predicted by wall thickness alone.

Studies of extant diatoms grown in culture under varying silica concentrations have also shed light on how declining silica availability has affected diatom evolution. When measured across a range of concentrations, the kinetics of silica uptake in diatoms seem to be multiphasic, which may suggest that multiple silica uptake systems evolved over the course of declining silica concentrations (Finkel et al. 2010). While the degree of silicification and the frustule micromorphology of several species changed with silica concentration in culture experiments, the oldest species examined was also the most heavily silicified—consistent with having evolved in a higher-silica oceans than the younger, less-silicified species.

This is not to suggest that silica alone has driven morphological trends in the evolution of diatoms or any other clade; surely silicifying organisms have responded through time to secular variations in nutrient abduance, temperature, ocean circulation and grazing pressure. Nonetheless, research on the fossil records of several silica-precipitating clades indicates that the remarkable evolutionary success of diatoms in the world's oceans, with its attendant consequences for silica availability in surface water masses, has impacted the evolution of all major participants in the marine silica cycle—including diatoms, themselves.

1.6 Summary

Both living and fossil protists show evidence of skeletal biomineralization, documenting a structurally and mineralogically diverse range of lightweight bioconstructions. Protistan fossils and phylogeny do not follow predictions made on the basis of animal biology: Biomineralization predominantly uses amorphous silica, and new silica-precipitating clades have continued to arise through time. The material properties of amorphous silica and the biomolecules on which it precipitates open

up new opportunites for complex microstructures that play a number of roles in protistan biology, including—but not restricted to—defense against microarthropod grazers. At the same time, the remarkable rise of diatoms to ecological prominence in the oceans has depleted silica concentrations in the mixed layer of most oceans, imposing a significant constraint on the evolution of protists that participate in the marine silica cycle. The bioconstructions observed in living marine protists reflect both the opportunities and constraints associated with silica biomineralization, and the increasingly more economical use of silica through time documented for some clades, has the potential to guide future thinking about improving biomimetic designs while conserving materials. In this respect, the long evolutionary history of biomineralizing protists may inspire novel approaches to technology.

References

Allison CW, Hilgert JW (1986) Scale microfossils from the early Cambrian of northwest Canada. J Paleontol 60:973–1015

Andersen RA (2004) Biology and systematics of heterokont and haptophyte algae. Amer J Bot 91:1508–1522

Anderson OR (1983) Radiolaria. Springer, New York

Antcliffe JB, Callow RHT, Brasier MD (2014) Giving the early fossil record of sponges a squeeze. Biol Rev. doi:10.1111/brv.12090

Armstrong H, Brasier M (2005) Microfossils. Blackwell Publishing, Malden

Barron J, Baldauf J (1995) Cenozoic marine diatom biostratigraphy and applications to paleoclimatology and paleoceanography. (In: Blome CD, Whalen PM, Reed KM (eds) Siliceous Microfossils.) Paleontol Soc Short Courses Paleontol 8:107–118

Bengtson S, Conway Morris S (1992) Early radiation of biomineralizing phyla. In: Lipps JH, Signor PW (eds) Origin and early evolution of the Metazoa. Plenum, New York, pp 447–481

Bentov S, Brownlee C, Erez J (2009) The role of seawater endocytosis in the biomineralization process in calcareous foraminifera. Proc Nat Acad Sci USA 51:21500–21504

Bentov S, Zaslansky P, Al-Sawalmih A et al (2012) Enamel-like apatite crown covering amorphous mineral in a crayfish mandible. Nature Comm 3:839. doi:10.1038/ncomms1839

Berney C, Pawlowski J (2006) A molecular time-scale for eukaryote evolution recalibrated with the continuous microfossil record. Proc R Soc Lond Ser B 273:1867–1872

Brown JW, Sorhannus U (2010) A molecular genetic timescale for the diversification of autotrophic stramenopiles (Ochrophyta): Substantive underestimation of putative fossil ages. PLOS ONE 5(9). doi:10.1371/journal.pone.0012759

Bukry D (1981) Synthesis of silicoflagellate stratigraphy for Maestrichtian to Quaternary marine sediment. Soc of Econ Paleont Min Spec Pub 32:433–444

Burki F, Shalchian-Tabrizi K, Pawlowski J (2008) Phylogenomics reveals a new 'megagroup' including most photosynthetic eukaryotes. Biology Lett 4:366–369

Carrera MG, Botting JR (2008) Evolutionary history of cambrian spiculate sponges: implications for the Cambrian evolutionary fauna. Palaios 23:124–138

Creveling JC, Knoll AH, Fernández Remolar D et al (2013) Geobiology of a Lower Cambrian carbonate platform, Pedroche Formation, Spain. Palaeogeogr Palaeoclimatol Palaeoecol 386:459–478

Cohen PA, Knoll AH (2012) Neoproterozoic scale microfossils from the Fifteen Mile Group, Yukon Territory. J Paleontol 86:775–800

Cohen PA, Schopf JW, Butterfield NJ et al (2011) Phosphate biomineralization in mid-Neoproterozoic protists. Geology 39:539–542

Cuif J-P, Dauphin Y, Sorauf JE (2011) Biominerals and fossils through time. Cambridge University Press, Cambridge
Debrenne F (2007) Lower Cambrian archaeocyathan bioconstructions. Comptes Rendus Palevol 6:5–19
Decelle J, Suzuki N, Mahe F et al (2012) Molecular phylogeny and morphological evolution of the Acantharia (Radiolaria). Protist 163:435–450
Decelle J, Martin P, Paborstava K et al (2013) Diversity, ecology and biogeochemistry of cyst-forming Acantharia (Radiolaria) in the oceans. PLoS ONE 8:(Article Number)e53598
De Decker P (2004) On the celestite-secreting Acantharia and their effects on seawater strontium to calcium ratios. Hydrobiologia 517:1–13
Domozych D, Wells B, Shaw P (1991) Basket scales of the green-alga, *Mesostigma viride*—chemistry and ultrastructure. J Cell Sci 100:397–407
Ehrlich H (2010) Chitin and collagen as universal and alternative templates in biomineralization. Int Geol Rev 52:661–699
Erez J (2003) The source of ions for biomineralization in foraminifera and their implications for paleoceanographic proxies. Rev Mineral Geochem 54:115–149
Ernissee JJ, McCartney K (1992) Ebridians. In: Lipps JH (ed) Fossil prokaryotes and protists. Blackwell Scientific, Oxford, pp 131–140
Falkowski P, Knoll H (eds) (2007) The evolution of primary producers in the sea. Elsevier, Burlington
Falkowski PG, Katz ME, Knoll AH et al (2004) The evolution of modern eukaryotic phytoplankton. Science 305:354–360
Finkel ZV, Kotrc B (2010) Silica use through time: macroevolutionary change in the morphology of the diatom fustule. Geomicrobiol J 27:596–608
Finkel ZV, Matheson KA, Regan KS et al (2010) Genotypic and phenotypic variation in diatom silicification under paleo-oceanographic conditions. Geobiology 8:433–445
Foissner W, Weissenbacher B, Krautgartner W-D et al (2009) A cover of glass: first report of biomineralized silicon in a ciliate, Maryna umbrellata (Ciliophora: Colpodea). J Euk Microbiol 56:519–530
Fowler S, Fisher N (1983) Viability of marine phytoplankton in zooplankton fecal pellets. Deep-Sea Res 30:963–969
Frankel RB, Bazylinski DA, Schüler D (1998) Biomineralization of magnetic iron minerals in magnetotactic bacteria. J. Supramol Sci 5:383–390
Gong N, Wiens M, Schröder HC et al (2010) Biosilicification of loricate choanoflagellate: organic composition of the nanotubular siliceous costal strips of *Stephanoeca diplocostata*. J Exp Biol 213:3575–3585
Gordon R, Losic D, Tiffany MA et al (2009) The glass menagerie: diatoms for novel applications in nanotechnology. Trends Biotechnol 27:116–127
Grenne, T, Slack, JF (2003) Paleozoic and Mesozoic silica-rich seawater: evidence from hematitic chert (jasper) deposits. Geology 31:319–322
Grotzinger JP, Watters, Knoll AH (2000) Calcareous metazoans in thrombolitic bioherms of the terminal Proterozoic Nama Group, Namibia. Paleobiology 26:334–359
Groussin M, Pawlowski J, Yang Z (2011) Bayesian relaxed clock estimation of divergence times in foraminifera. Mol Phyl Evol 61:157–166
Haeckel E (1887) Report on the Radiolaria collected by H.M.S. Challenger during the years 1873–1876. Rep Sci Results, Challenger, Zool. 18:clxxxviii + 1803 p
Hamm CE (2005) The evolution of advanced mechanical defenses and potential technological applications of diatom shells. J Nanosci Nanotechnol 5:108–199
Hamm CE, Merkel R, Springer O et al (2003) Architecture and material properties of diatom shells provide effective mechanical protection. Nature 421:841–843
Harper HE Jr, Knoll AH (1975) Silica, diatoms, and Cenozoic radiolarian evolution. Geology 3:175–177
Hedley R, Ogden C, Mordan N (1977) Biology and fine structure of Cryptodifflugia oviformis (Rhizopdea: Protozoa). Bull Br Mus Nat Hist (Zool.) 30:313–328

Hildebrand M (2000) Silicic acid transport and its control during cell wall silicification in diatoms. In: Bäuerlein E (ed) Biomineralization. Springer, Weinheim, pp 171–188
Hoppenrath M, Leander BS (2006) Ebriid phylogeny and the expansion of the Cercozoa. Protist 157:279–290
Knoll AH (1994) Proterozoic and Early Cambrian protists: evidence for accelerating evolutionary tempo. Proc Nat Acad Sci USA 91:6743–6750
Knoll AH (2003) Biomineralization and evolutionary history. Rev Mineral Geochem 54:329–356
Knoll AH (2013) Systems paleobiology. Geol Soc Am Bull 125:3–13
Knoll AH, Fischer WW (2011) Skeletons and ocean chemistry: the long view. In: Gattuso JP, Hansson L (eds) Ocean acidification. Oxford University Press, Oxofrd, pp 67–82
Konhauser KO, Riding R (2012) Bacterial biomineralization. In: Knoll AH, Canfield DE, Konhauser KO (eds) Fundamentals of geobiology. Wiley-Blackwell, Chichester, pp 105–130
Kooistra WHCF, Gersonde R, Medlin LK et al (2007) The origin and evolution of the diatoms: their adaptation to a planktonic existence. In: Falkowski P, Knoll AH (eds) The evolution of primary producers in the sea. Elsevier, Burlington, pp 207–249
Krabberød AK, Brate J, Dolven JK et al (2011) Radiolaria divided into Polycystina and Spasmaria in combined 18S and 28S rDNA phylogeny. PLoS ONE 6:e23526
Kröger N, Poulsen N (2008) Diatoms-from cell wall biogenesis to nanotechnology. Ann Rev Genet 42:83–107
Kröger N, Sumper M (2004) Silica formation in diatoms: the function of long-chain polyamines and silaffins. J Mater Chem 14:2059–2065
Kunitomo Y, Sarashina I, Iijima M et al (2006) Molecular phylogeny of acantharian and polycystine radiolarians based on ribosomal DNA sequences, and some comparisons with data from the fossil record. European J Protistol 42:143–153
Lazarus DB, Kotrc B, Wulf G et al (2009) Radiolarians decreased silicification as an evolutionary response to reduced Cenozoic ocean silica availability. Proc Nat Acad Sci USA 106:9333–9338
Lipps JH (1973) Test structure in Foraminifera. Ann Rev Microbiol 27:471–488
Maldonado M, Carmona MC, Uriz MJ et al (1999) Decline in Mesozoic reef-building sponges explained by silicon limitation. Nature 401:785–788
Maldonado M, Riesgo A, Bucci A et al (2010) Revisiting silicon budgets at a tropical continental shelf: Silica standing stocks in sponges surpass those in diatoms. Limnol Oceanogr 55: 2001–2010
Maldonado M, Navarro L, Grasa A et al (2011) Silicon uptake by sponges: a twist to understanding nutrient cycling on continental margins. Nature Sci Rep 1:1–8
Maldonado M, Cao H, Cao X et al (2012) Experimental silicon demand by the sponge Hymeniacidon perlevis reveals chronic limitation in field populations. Hydrobiologia 687:251–257
Maliva R, Knoll AH, Siever R (1989) Secular change in chert distribution: a reflection of evolving biological participation in the silica cycle. Palaios 4:519–532
Maloof AC, Porter SM, Moore JL et al (2010) The earliest Cambrian record of animals and ocean geochemical change. Geol Soc Am Bull 122:1731–1774
Marron AO, Alston MJ, Heavens D, Akam M, Caccamo M, Holland PWH, Walker G (2013) A family of diatom-like silicon transporters in the siliceous loricate choanoflagellates. Proc Roy Soc Biol Sci 280:20122543
Marsh ME (2003) Regulation of $CaCO_3$ formation in coccolithophores. Comp Biochem Physiol B Biochem Mol Biol 136:743–754
Matsuoka A (2007) Living radiolarian feeding mechanisms: new light on past marine ecosystems. Swiss J Geosci 100:273–279
McIlroy D, Green OR, Brasier MD (2001) Palaeobiology and evolution of the earliest agglutinated Foraminifera: *Platysolenites, Spirosolenites* and related forms. Lethaia 34:13–29
Müller WEG, Li J, Schröder HC et al (2007) The unique skeleton of siliceous sponges (Porifera; Hexactinellida and Demospongiae) that evolved first from the Urmetazoa during the Proterozoic: a review. Biogeosciences 4:219–232
Parfrey LW, Grant J, Tekle YI et al (2010) Broadly sampled multigene analyses yield a well- resolved eukaryotic tree of life. Syst Biol 59:518–533

Park T-Y, Woo J, Lee D-J et al (2011) A stem-group cnidarian described from the mid-Cambrian of China and its significance for cnidarian evolution. Nature Comm. doi:10.1038/ncomms1457

Paasche E (2002) A review of the coccolithophorid *Emiliania huxleyi* (Prymnesiophyceae), with particular reference to growth, coccolith formation and calcification—photosynthesis interactions. Phycologia 40:503–529

Porter SM (2010) Calcite and aragonite seas and the de novo acquisition of carbonate skeletons. Geobiology 8:256–277

Porter SM, Meisterfeld R, Knoll AH (2003) Vase-shaped microfossils from the Neoproterozoic Chuar Group, Grand Canyon: A classification guided by modern testate amoebae. J Paleontol 77:409–429

Pouille L, Obut O, Danelian T et al (2011) Lower Cambrian (Botomian) polycystine radiolaria from the Altai Mountains (southern Siberia, Russia). Comptes rendus Palevol 10:627–633

Preisig HR (1994) Siliceous structures and silicification in flagellated protists. Protoplasma 181:29–42

Pruss SA, Finnegan S, Fischer WW et al (2010) Carbonates in skeleton-poor seas: new insights from Cambrian and Ordovician strata of Laurentia. Palaios 25:73–84

Pruss SA, Clemente H, LaFlamme M (2012) Early (Series 2) Cambrian archaeocyathan reefs of southern Labrador as a locus for skeletal carbonate production. Lethaia 45:401–410

Racki G, Cordey F (2000) Radiolarian palaeoecology and radiolarites: is the present the key to the past? Earth-Sci Rev 52:83–120

Raven JA (1983) The transport and function of silicon in plants. Biol Rev 58:179–207

Raven JA, Giordano M (2009) Biomineralization by photosynthetic organisms: evidence of coevolution of the organisms and their environment? Geobiology 7:140–154

Raven JA, Knoll AH (2010) Non-skeletal biomineralization in protists: matters of moment and gravity. Geomicrobiol J 27:1–13

Raven JA, Waite AM (2004) The evolution of silicification in diatoms: inescapable sinking and sinking as escape? New Phytol 162:45–61

Richter FM, Rowley DB, Depaolo DJ (1992) Sr isotope evolution of seawater—the role of tectonics. Earth Planet Sci Lett 109:11–23

Round FE, Crawford RM, Mann DG (1990) The diatoms: biology & morphology of the genera. Cambridge Univ Press, Cambridge

Siever R (1992) The silica cycle in the Precambrian. Geochim Cosmochim Acta 56:3265–3272

Sperling EA, Robinson JM, Pisani D et al (2010) Where's the glass? Biomarkers, molecular clocks, and microRNAs suggest a 200-Myr missing Precambrian fossil record of siliceous sponge spicules. Geobiology 8:24–36

Strathern P (2005) A brief history of medicine: from Hippocrates' four humours to Crick and Watson's double helix. Robinson, London

Thomas RDK, Shearman RM, Stewart CW (2000) Evolutionary exploitation of design options by the first animals with hard skeletons. Science 288:239–1242

Ujiié Y, Kimoto K, Pawlowski J (2008) Molecular evidence for an independent origin of modern triserial planktonic foraminifera from benthic ancestors. Mar Microapelontol 69:334–340

van Tol HM, Irwin AJ, Finkel ZV (2012) Macroevolutionary trends in silicoflagellate skeletal morphology: the costs and benefits of silicification. Paleobiology 38:391–402

Vermeij GJ (1977) The Mesozoic marine revolution: evidence from snails, predators and grazers. Paleobiology 3:245–258

Vidal G, MoczydlowskaVidal M (1997) Biodiversity, speciation, and extinction trends of Proterozoic and Cambrian phytoplankton. Paleobiology 23:230–246

Walker G, Dorrell RG, Schlacht A, Dacks JB (2011) Eukaryotic systematics: a user's guide for cell biologists and parasitologists. Parasitology 138:1638–1663

Wallace AF, Wang D, Hamm LM et al (2012) Skeletal formation in eukaryotes. In: Knoll AH, Canfield DE, Konhauser K (eds) Fundamentals of geobiology. Wiley-Blackwell, Chichester, pp 150–187

Weiner S, Dove PM (2003) An overview of biomineralization processes and the problem of the vital effect. Rev Mineral Geochem 54:1–29

Won M-Z, Iams WJ (2011) Earliest Arenig radiolarians from the Cow Head Group, western Newfoundland. J Paleontol 85:156–177

Wood RA, Grotzinger JP, Dickson JAD (2002) Proterozoic modular biomineralized metazoan from the Nama Group, Namibia. Science 296:2383–2386

Yoshida M, Noel M, Nakayama T et al (2006) A haptophyte bearing siliceous scales: ultrastructure and phylogenetic position of Hyalolithus neolepis gen. et sp. nov. (Prymnesiophyceae, Haptophyta). Protist 157:213–234

Young J, Henriksen K (2003) Mineralization within vesicles: the calcite of coccoliths. Rev Mineral Geochem 54:189–215

Zeebe RE, Westbroek P (2003) A simple model for the $CaCO_3$ saturation state of the ocean: the "Strangelove", the "Neritan", and the "Cretan" ocean. Geochem Geophy Geosystems. doi:10.1029/2003GC000538

Zhuravlev AYu, Wood RA (2008) Eve of biomineralization: controls on skeletal mineralogy. Geology 36:923–926

Zlatogursky VV (2012) *Raphidiophrys heterophryoidea* sp nov (Centrohelida: Raphidiophryidae), the first heliozoan species with a combination of siliceous and organic skeletal elements. Eur J Protistol 48:9–16

Chapter 2
Morphospaces and Databases: Diatom Diversification through Time

Benjamin Kotrc and Andrew H. Knoll

2.1 Introduction

The diversity of diatom form has been a source of fascination and inspiration since diatom frustules were first described by the 19th Century pioneers of micropaleontology (Ehrenberg 1838; Haeckel 1904) and their shapes applied to Art Nouveau architecture and design, like René Binet's design for the Printemps department store (Proctor 2006) or Hendrik Petrus Berlage's jewelry imitating chain-forming diatoms (Netherlands Architecture Institute 2012). Many thousands of extant diatom species have been described (Mann and Droop 1996), their shapes representing a wide range of variations on a basic pill-box Bauplan—from circles to triangles, needles, and curves—with staggering variety in the geometrically arranged, hierarchical pore structure (Round et al. 1990), lending an aesthetic that evidently appealed to turn-of-the-century designers. With biomimetic design advancing from superficial aesthetic inspiration to an application of underlying structural and evolutionary principles, renewed interest in diatoms warrants efforts toward a deeper understanding of their diversification, a cardinal feature of any clade's evolutionary history.

The fossil record provides two windows on clade diversification history: taxonomic diversity and morphological disparity. The former, often referred to as taxonomic richness or simply as diversity, is the familiar measure that tallies numbers of taxa (commonly species). The latter, disparity for short, describes the variety of shapes or the "within-group variance of form" (Erwin 2007) by directly quantifying organismal morphology. In a sense, diversity and disparity both measure variety of form, because fossil taxonomy is, of course, itself based on morphology. It is

B. Kotrc (✉)
Department of Earth and Planetary Sciences, Harvard University, Cambridge, MA 02138, USA
e-mail: kotrc@mit.edu

A. H. Knoll
Department of Earth, Atmospheric and Planetary Sciences, Massachusetts Institute of Technology, Cambridge, MA 02138, USA
e-mail: aknoll@oeb.harvard.edu

C. Hamm (ed.), *Evolution of Lightweight Structures,* Biologically-Inspired Systems 6,
DOI 10.1007/978-94-017-9398-8_2

also intuitive, however, that the two approaches measure this variety in very different ways. As an extreme example, a collection containing one species of fish, one species of elephant, and one species of insect has the same taxonomic diversity as a collection of three fish species, though the former clearly represents much greater morphological disparity.

We have two tie points on both the taxonomic and the morphological diversification of diatoms—their origin and their present diversity and disparity—from which we can trivially infer a net increase through time. But the more interesting questions about what happened in between are less trivial. What were the trajectories of diatom diversity and disparity through time? Has there been a monotonic increase, or was an early rise followed by stasis or even decline? Did diversity and disparity vary in lockstep or independently?

While the fossil record of diatoms extends back to at least the early Cretaceous Period (Gersonde and Harwood 1990) and includes many occurrences from nonmarine environments, the most robust and abundant data come from deep-sea sediments of the Cenozoic Era. Although it does not represent the entire clade's evolutionary history, we focus on this record here because it allows us to consider the biases that uneven sampling through time may impart to our view of evolutionary history and process.

2.2 Reconstructing Taxonomic Diversity

Conventionally, the Cenozoic history of marine planktonic diatom diversity describes a steep, almost monotonic rise of about an order of magnitude (Spencer-Cervato 1999). This view plays a central role in a number of evolutionary narratives involving the diatoms, including their coevolution with grasses (Falkowski et al. 2004) and whales (Marx and Uhen 2010), their role in reshaping the silica cycle, and its effect on radiolarians (Lazarus et al. 2009). Although widely accepted, this view has recently been challenged (Rabosky and Sorhannus 2009). The conventional diversity curve is generated from Neptune, a large database of marine microfossil occurrences reported from the Deep Sea Drilling Program and Ocean Drilling Program, representing several decades of micropaleontological research (Lazarus 1994; Spencer-Cervato 1999). The diversity history derived from these occurrences is not, however, a unique result, since different methodological choices can be made in taxon counting, dealing with data imperfections, and accommodating secular variations in sampling intensity. Each of these can change substantially the diversity curve generated.

Taxon counting. In order to get from database to diversity curve, occurrence data need to be divided into time bins (in our examples below, of 2 million year duration) and the number of taxa in each bin counted. Traditionally, this has been done by counting taxa as present in all time bins between their earliest and latest occurrences, then tallying taxa known to have existed in each time bin regardless

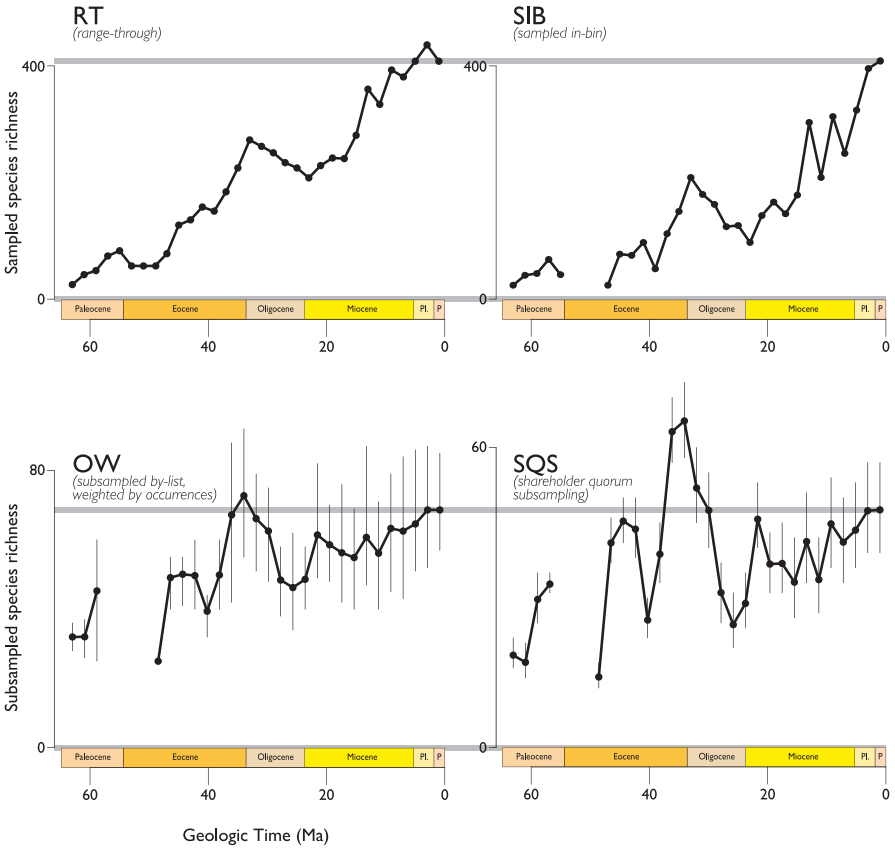

Fig. 2.1 Diatom diversity through time over the Cenozoic era, based on analysis of the Neptune database by range-through taxon counting (RT), sampled-in-bin taxon counting (SIB), subsampling by-lists, weighted by occurrences (OW), and shareholder quorum subsampling (SQS)

of whether observed or inferred. This "range-through" method (RT, see Fig. 2.1) has an advantage over simply counting taxa observed, or sampled in-bin (SIB, see Fig. 2.1), because it takes into account variations in preservation and sampling from one bin to another. For example, in Fig. 2.1, the plot of diatom diversity from Neptune using RT taxon counting makes up for missing data between 54–48 Ma; diversity during that interval was clearly not zero, as a literal reading of the SIB curve might imply.

Despite its advantage in accounting for 'Lazarus taxa' (taxa that appear to go extinct, only to reappear later in the record; Flessa and Jablonski 1983), however, the RT method has fallen out of favor among some paleobiologists because it imparts a number of undesirable and potentially severe biases: the Signor-Lipps effect, the Pull of the Recent, and other edge effects reviewed by Alroy (2010a). The SIB sampling method is preferred over RT and other methods such as tallying only those

taxa known to cross the boundary between adjacent time bins because it is immune to these biases, and the bin-to-bin sampling differences that remain can be counteracted with corrections like the part-timer sampling probability, which effectively performs a temporally localized range-through among adjacent time bins (Alroy 2008). While the diversity curve for the Neptune diatom data obtained by SIB taxon counting does differ from the conventional curve obtained using RT in the details, the curves are rather similar in shape to first order.

Data quality. Generally, paleontologists worry that the fossil record underestimates the true ranges of taxa (e.g. Marshall 1990), but the record of marine microfossils is so unusually rich that the opposite has been suggested for the Neptune database. Marine microfossils can appear outside of their true range due to "RATs", that is, because of the physical **r**eworking of sediments (erosion and redeposition in a stratigraphically younger position), errors in the **a**ge model assigning a fossil occurrence to the wrong time bin, or **t**axonomic error (Lazarus 2011). For the curve that has become the canonical depiction of diatom diversity, these problems were addressed by manually excluding occurrences in Neptune considered unreliable, including occurrences near depositional hiatuses (Spencer-Cervato 1999). The effect of all but the most severe instances of reworking can be obviated by setting sufficiently wide time bins, and misplaced occurrences far from the true range of a taxon are much less of an issue for SIB than RT taxon counting. Nonetheless, outliers could also be identified for removal by applying hat-shaped models of the rise and fall in occurrences through a taxon's range (Liow and Stenseth 2007; Liow et al. 2010), but a much simpler method recently proposed just trims a certain calibrated percentage of occurrences from the beginning and end of a taxon's range—aptly named Pacman profiling (Lazarus et al. 2012a).

Sampling biases. An arguably graver concern for the accurate reconstruction of diatom paleodiversity is that the amount of data in the Neptune database greatly increases with time, as shown in Fig. 2.2. This is worrisome because it is easy to imagine a situation where true diatom diversity in fact remained constant, but a steadily increasing number of samples through time captures more species from younger intervals, giving a false impression of rising diversity. Although this concern was noted in the first explorations of the Neptune dataset (Spencer-Cervato 1999), it was only recently addressed in detail (Rabosky and Sorhannus 2009).

Such temporal sampling biases are common in paleontological datasets, for a number of reasons. In general, older sediments are less abundant than younger ones. For microfossils from deep-sea drilling cores more specifically, sediments are progressively destroyed as ocean crust becomes subducted by plate tectonic processes, making older sediments less common. Perhaps more importantly, the deep drilling commonly required to reach older sediments is expensive, and requires drilling through younger sediments for which samples are usually also collected. Finally, diatoms undergo a series of diagenetic mineral transitions as burial temperatures and pressures increase, making the preservation of recognizable morphological features less likely with age (DeMaster 2003). In recent decades, paleobiologists have directed much research effort towards developing numerical methods to correct for these sampling biases.

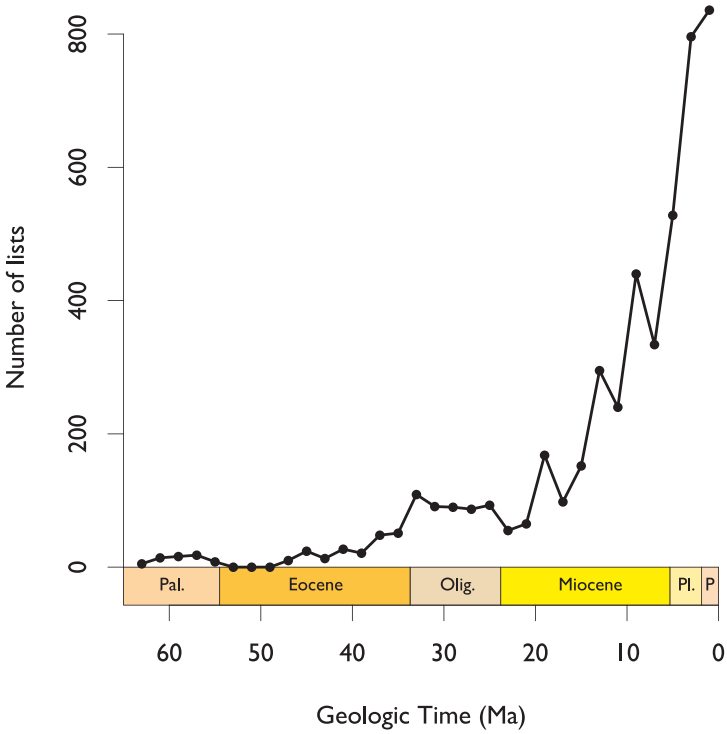

Fig. 2.2 Number of lists (of taxa found at a particular depth in a particular borehole) in the Neptune database through the Cenozoic era

Subsampling methods. The idea at the heart of these methods is that we can obtain a more accurate reconstruction of diversity history if we measure diversity using a standardized, comparable sample size in each time bin. It is important to note that the goal of such subsampling methods is not to get closer to the true absolute values of diversity (as range-through taxon counting does, for example), but rather to reconstruct the relative shape of the diversity curve as accurately as possible. The basic procedure underlying these methods involves randomly drawing items from the full data set of the time bin in question until some quota is reached. The number of taxa in that subsample are then tallied and the process is repeated a large number of times to obtain an average diversity and an associated confidence interval for that time bin. This whole process, in turn, is repeated for all time bins, using the same quota for each.

The well-established subsampling methods all use a uniform quota of items, but differ in how items are drawn and how the quota is set. For example, in classical rarefaction (CR, Miller and Foote 1996), occurrences are drawn from the full dataset until a quota of some fixed number of occurrences is reached. The items drawn can also be taxonomic lists, which in the case of the Neptune data means the list of taxa found in a particular borehole at a particular depth. In this case, the quota can be simply set as a number of lists, in which case the method is

referred to as by-lists, unweighted subsampling (UW, Alroy 2000), or as a number of occurrences, (weighted by occurrence subsampling, or OW for short, Alroy 1996). In practice (at least for the Neptune diatom data set), these methods give broadly similar results.

Subsampling methods were only recently applied to diatoms (Rabosky and Sorhannus 2009), painting a picture of diatom diversification very different from curves generated from RT and SIB tabulations of Neptune data (Fig. 2.1). A representative diversity curve generated by OW subsampling (Fig. 2.1 OW), similar to those produced by CR and UW subsampling, still shows a net increase over the Cenozoic Era, but the total increase is only about twofold. Perhaps more importantly, maximum diversity is sited in the late Eocene Epoch, with tabulated diversity falling substantially through the Oligocene, before recovering through the Neogene Period.

Another method of subsampling, which uses a quota measured by the sum of squared occurrences (O2W), has also been applied to diatoms and results in an even flatter diversity curve with a still more pronounced Eocene-Oligocene diversity peak (Rabosky and Sorhannus 2009). The reasoning that underpins this method (Alroy 2000) is a little complicated, but can be understood by considering how taxon occurrences are recorded. A paleontologist describing the species in a sample will examine specimens, i.e. individual fossils, recording new species as they are encountered. Because not all taxa are equally abundant, the common taxa will be found quickly, while rare taxa are only likely to be counted after many specimens have been examined. This results in an asymptotic collector curve (or accumulation curve), in which taxa discovered are plotted against specimens examined (or sampling effort expended). The O2W method attempts to account for this non-linear relationship between specimens and species. Unfortunately, diversity estimates under this method have been found to be strongly biased when the geographic structure of diversity changes through time (Bush et al. 2004), so we do not show O2W results here.

A major shortcoming of all of the fixed-quota subsampling methods is that they can systematically undersample intervals with high diversity, because uniform sampling is not necessarily fair sampling (Alroy 2010a). Consider an ideal case where there has been no change in the true diversity through time, but an increase in sampling results in an apparent increase in diversity: in this situation, fixed-quota methods will theoretically perform well. But if there has been a true increase in diversity in addition to an increase in sampling, these methods may artificially flatten the resulting diversity curve, because more diverse intervals will require more sampling to capture the same proportion of the total (true) diversity. As an extreme example, consider that a population of five species can be sampled completely with 100 occurrences, while the same size sample will underestimate radically the diversity of a population with 500 species. When we allow for the possibility that true diversity can vary widely, it makes intuitive sense to allow the quota of items drawn in subsampling to vary also—and from this perspective, we can also see that the level to which we ought to standardize samples is not a fixed amount of sampling, but some amount of sampling that aims to return a fixed proportion of the total diversity, or coverage.

A recently published subsampling method, shareholder quorum subsampling (SQS), is based on this principle of taxonomic coverage (Alroy 2010a). The method is named by analogy to a corporate shareholder's meeting, where a quorum of shareholders needs to be present such that the sum of their shares meets a threshold proportion of the total shares in the company. In SQS, we can think of taxa as shareholders and their share of the frequency distribution (proportion of total occurrences) as shares. Occurrences are drawn much as before, but rather than stopping at a certain number of occurrences or lists, samples are drawn until a 'shareholder quorum' is reached—that is, until the sum of the frequencies of sampled taxa exceeds some threshold. The number of lists or occurrences it takes to reach this quota is free to vary, making this method philosophically quite distinct from the uniform sampling methods like CR, UW or OW.

In order to ensure that the proportion of frequencies drawn represents a certain proportion of taxonomic coverage, however, we need to know how taxonomically complete each sample is—that is, we need an estimate of coverage. Another way to think of this problem is to consider the observed frequency distribution to overestimate the frequency of those taxa observed in favor of those taxa not observed, whose frequencies are rounded down to zero. We need an estimate of how much of the underlying, true frequency distribution has been muted by such rounding down. One such estimate, used commonly in ecology, uses the proportion of observations that are singletons, i.e. taxa only seen once in that sample, calculated as Good's u (Good 1953). In ecology these observations are individuals, but the approach can be extended to compiled paleontological data where these observations are occurrences (i.e. the presence of a taxon at a particular location and stratigraphic position, irrespective of its abundance; Alroy 2010a). While for the purposes of ecological studies, singletons are those taxa that occur only once in a sample area such as a quadrat, Alroy (2010a) argued that for paleontological data the best analogical equivalent was to count singletons as taxa occurring only in a single publication.

We applied a modified version of this basic SQS algorithm to the diatom occurrence data from Neptune. Because of the way micropaleontological data are collected (the occurrence of a set of taxa reported over a stratigraphic range), taxa will almost always have more than one occurrence in any given publication. Instead, we used taxa occurring only in a single borehole in place of singletons.

Our results for SQ subsampling of the Neptune diatom data (Fig. 2.1, SQS) are broadly similar to those of the fixed-quota subsampling methods (Fig. 2.1, OW), suggesting that true diversity increased only slightly over the Cenozoic Era. Much as under the fixed-quota methods, peak diversity is reached in the latest Eocene/earliest Oligocene, but under SQS this peak is exaggerated, suggesting that diversity then was significantly higher than today—similar to the results of the O2W method (Rabosky and Sorhannus 2009).

In spite of the obvious sampling bias in the Neptune data, the largely stationary view of Cenozoic diatom diversity suggested by subsampling methods has not been universally accepted by micropaleontologists. A potential vulnerability of subsampling methods, including SQS, is that they may not give accurate results if there are large changes in relative abundance structure (or evenness) through time (Lazarus et al. 2012b). We can understand this problem by considering the relative

frequency distribution of a time interval—a rank-ordered plot of the proportion of occurrences of each taxon (such that the extent along the x-axis represents total diversity). Fixed-quota subsampling methods can be thought of as sampling all taxa falling above a threshold 'veil line' of some relative frequency (Alroy 2010a). The failing of these methods, addressed by SQS, can be visualized by considering what happens if the diversity increases, but the shape of this distribution stays the same: because each taxon now has a smaller relative frequency, a greater proportion of the taxa falls under the veil line, underestimating diversity under subsampling. Under SQS, a constant area under this curve is sampled, so even if the total diversity increases, the same proportion of the frequency distribution will be recovered—and, if the shape of the distributions stays the same, the same proportion of total diversity. If the shape of the frequency distribution were to change drastically, however, SQS might not work as well.

Empirically, the diatom occurrence data in Neptune do show a change in frequency distribution from more even to more uneven, and it has been argued that these changes may cause subsampling methods (including SQS) to mask a true rise in diversity (Lazarus et al. 2012b). If we imagine SQS subsampling to recover a fixed area under a rank-ordered relative frequency distribution (see supplement to Alroy 2010b), the area under a flat curve (an equitable frequency distribution) will sample a greater proportion of the total diversity than the same area under a hollow curve (an uneven frequency distribution). Lazarus et al. (2012b) apply an empirical correction factor to account for the changes in frequency distribution and recover a rise in diatom diversity more similar to the canonical view. A similar correction factor with even greater leverage is used to account for an increase in provinciality through time, particularly regarding the development on an endemic polar fauna (Lazarus et al. 2012b).

Lazarus et al. (2012b) marshal further support for the conventional view of diatom diversification from a catalogue of about 500 diatom species' ranges compiled from both marine and land-based sections under expert curation against taxonomic and stratigraphic error. The curve generated is similar in form to the canonical diatom diversity curve (Spencer-Cervato 1999), albeit showing a net increase that is slightly less steep. This data set has certainly been better flushed of "RATs" (the sorts of errors described in the section on data quality above) than Neptune, but the question of sampling bias arguably remains: while there is no strong correlation in this compilation between diversity in a time bin and the number of publications from which this diversity is derived (Lazarus et al. 2012a), the relationship between a taxonomic or biostratigraphic publication and the amount of sampling it represents is not clear and not necessarily fixed.

To summarize, the taxonomic window on diatom diversification provides an uncertain picture of Cenozoic diatom evolution. Interpreted at face value, the fossil record suggests a steep Cenozoic rise in species richness, whether from deep-sea occurrences in the Neptune database (Spencer-Cervato 1999) or from a biostratigraphic catalogue of first and last appearances (Lazarus et al. 2012a). When the stark secular rise in the amount of available data is taken into account using item quota (Rabosky and Sorhannus 2009) or SQS subsampling methods, however, a

more stationary pattern emerges, showing at most a modest overall increase in species richness and peak diversity around the Eocene/Oligocene boundary. With changes in relative abundance potentially biasing the results of these subsampling methods, we are left with a level of uncertainty about the true diversification history of the diatoms. Recalling that there is another window on diversification, however, we turn to the history of diatom morphological disparity to gain another perspective on this question.

2.3 Reconstructing Evolution in Shape Space

In common paleobiological usage, disparity describes a quantification of morphological differences among organisms (Wills 2001, p. 56). Unlike species richness for diversity, there is no singular metric for disparity; commonly used measures can be more easily understood in the conceptual framework of morphospace—a mathematical construct used to quantify and describe organismal morphology.

Morphospaces. Morphospaces are n-dimensional mathematical spaces describing the form of a group of organisms. As such, morphospaces are an example of what, in the context of ecology, Lewontin (1969, p. 13) called "the concept of the vector field in n-dimensional space," which he described as "the most fundamental [concept] we have for dealing with the transformations of complicated dynamical systems in time." Familiar, conceptually related notions include adaptive landscapes (Wright 1932) and niche space (Hutchinson 1978, p. 158), but rather than gene alleles or ecological variables, the axes of morphospaces represent morphological characters or parameters. Each point in morphospace represents a particular, unique morphology, and it can either be occupied (i.e. represent a morphology actually realized by an organism) or not.

With this framework in mind, we can consider the morphological disparity of a group as a description of how the group is distributed in morphospace—are the taxa spread out widely (signifying large morphological differences) or clustered together (signifying morphological similarity)? As discussed in more detail below, this spatial distribution of taxa can be quantified in a number of ways, leading to multiple metrics of disparity. Before considering how to measure morphospace occupation, however, it is worth briefly examining the different ways in which morphospaces can be constructed.

Morphospaces are often divided into two kinds, those whose axes are parameters of a shape-generating function, called generative or theoretical morphospaces, and those whose axes are measurements of organisms, called empirical morphospaces (McGhee 1999). Theoretical morphospaces generally have only a few axes and thus a small number of dimensions that is easy to visualize; the first and best-known example is Raup's (1966) classic morphospace of coiled shells. Empirical morphospaces, in contrast, often have a very large number of axes (representing a large number of measured morphological characters) and generally require an

ordination procedure such as principal components analysis (PCA) or principal coordinates analysis (PCO) for visualization and analysis, an approach pioneered by Foote (1989). Because of this, empirical morphospaces have been described as having axes that are data-dependent or unstable, since different measurements of the same morphology will result in different ordinated axes (McGhee 1999). Seen from a more general perspective, however, the distinction between theoretical and empirical morphospaces can become conceptually and mathematically blurred if the latter are considered in their full, unordinated dimensionality (sometimes called "raw morphospaces," Eble 2000): the number of axes could then be seen as the most significant difference between the two. From this perspective, both sorts of morphospace can be used to investigate the realms of unrealized as well as realized morphologies—although theoretical morphospaces can undoubtedly generate a wider range of unrealized form than empirical morphospaces can.

Limitations of theoretical morphospaces. While there is broad consensus that theoretical morphospaces are preferable because their use of explicit, measurement-independent growth models that allow one to explore a wider range of unexplored as well as impermissible forms (e.g. Erwin 2007), their application is unfortunately not always possible (McGhee 1999, p. 26). Growth models for theoretical morphospaces are more readily devised for organisms with accretionary or branching growth (e.g. Raup 1966; Niklas 1999), but mathematical shape models with a reasonable number of parameters can only reproduce so many aspects of form. The applicability of generative morphospaces with a small number of parameters is thus limited in a two ways that are well illustrated by the case of the diatoms: the range of overall forms that can be generated, and the difficulty of including complex and higher-order morphological features.

Previous diatom morphospaces. The diversity of fundamental forms that can be generated by a mathematical model with a few parameters is limited. In diatoms, for example, capturing the great variety of different symmetries of the valve in plan view alone (circular-elliptical, triangular, rectangular, curved, isopolar or heteropolar, and so on) in a generative model would require many parameters, and even then the plan-view outline shape says nothing about the obviously important three-dimensional shape of the valve. Generative shape models that have been developed for the diatoms are thus by necessity limited both in terms of covering only a subset of the full taxonomic and morphological diversity, and in terms of describing a subset of the overall frustule morphology. Examples include models for a particular species (Stoermer and Ladewski 1982) or genus (Mou and Stoermer 1992), a more widely applicable model describing only valve outlines (Arita and Ohtsuka 2004), and a model based on 3D parametric equations limited to a group of asymmetrical pennate diatoms (Pappas 2005). While generative morphospaces of this nature have been profitably applied to questions of taxonomic distinction or morphological evolution within particular groups, they capture neither the total diversity of overall diatom form, nor the higher-order features of diatom morphology such as pore arrangement, spines, processes, or the raphe—even though these may well be of biological and evolutionary significance.

We are thus led to an empirical morphospace approach in trying to understand the Cenozoic evolution in morphospace of the marine diatoms in as a whole. This approach has been successfully applied to many other groups with complex morphologies, highlighting important features that are hard to model with simple geometric models (e.g. Foote 1991; Lupia 1999; Boyce and Knoll 2002). Under the auspices of the PlanktonTech initiative, we conducted an empirical morphospace study of Cenozoic marine planktonic diatoms, the detailed methodology and results of which are published elsewhere (Kotrc and Knoll 2015a, b). Summarized briefly, this approach involved quantifying the morphology of Cenozoic diatom taxa using a large number of morphological characters to construct a morphospace, applying an ordination procedure to visualize this morphospace, and then populating the morphospace through time based on the fossil record. Since the Neptune database is a readily available compilation of fossil diatom occurrences, we used it to populate the morphospace. Because an analysis at the species level would be intractable (there are over 1,000 diatom species in Neptune), we chose to work at the genus level; our final analysis included 140 genera (for complete methods and data see Kotrc 2013, Kotrc and Knoll 2014; Kotrc and Knoll 2015a, b).

Choice and coding of characters. We used descriptions of frustule morphology and taxonomic descriptions of the genera in Neptune to compile a list of morphological characters. In formulating these characters, we were careful to strictly describe morphology independent of taxonomy or phylogeny—meaning that structures were quantified by their similarity in form regardless of whether they are equivalent in development or evolutionary origin. In some cases, this meant bridging substantial gaps in the nomenclature used to describe structures in different groups within the diatoms, for example the terms applied to the arrangement of pores in centric diatoms ("areolation") versus in pennate diatoms ("striation"). This strictly morphological approach distinguishes morphospace analysis from morphometric approaches in which the importance of choosing homologous characters is often strongly emphasized (e.g. Rohlf and Bookstein 1990). It has the advantage of allowing the evolutionary exploration of form on its own merit, independent of how this form is achieved phylogenetically or developmentally. Our final analysis included 100 morphological characters, coded as unordered, discrete character states (including many binary characters), allowing us to account for both intrageneric variation and the categorical nature of many characters (such as the presence or absence of a raphe, a slit along the valve face of some diatoms that enables locomotion).

Ordination. The resulting morphological character codings for each genus define a 100-dimensional, categorical morphospace, a "raw morphospace" in the sense alluded to above. Visualizing this morphospace requires that we find a lower-dimensional projection of the relative locations of our genera, something that can be accomplished with PCO, a method analogous to the more familiar PCA that works with unordered discrete characters. This transformation results in a representation of the morphospace along continuous axes, the first two of which (the two capturing the greatest amount of the information in the full-dimensional morphospace) are shown on the left in Fig. 2.3.

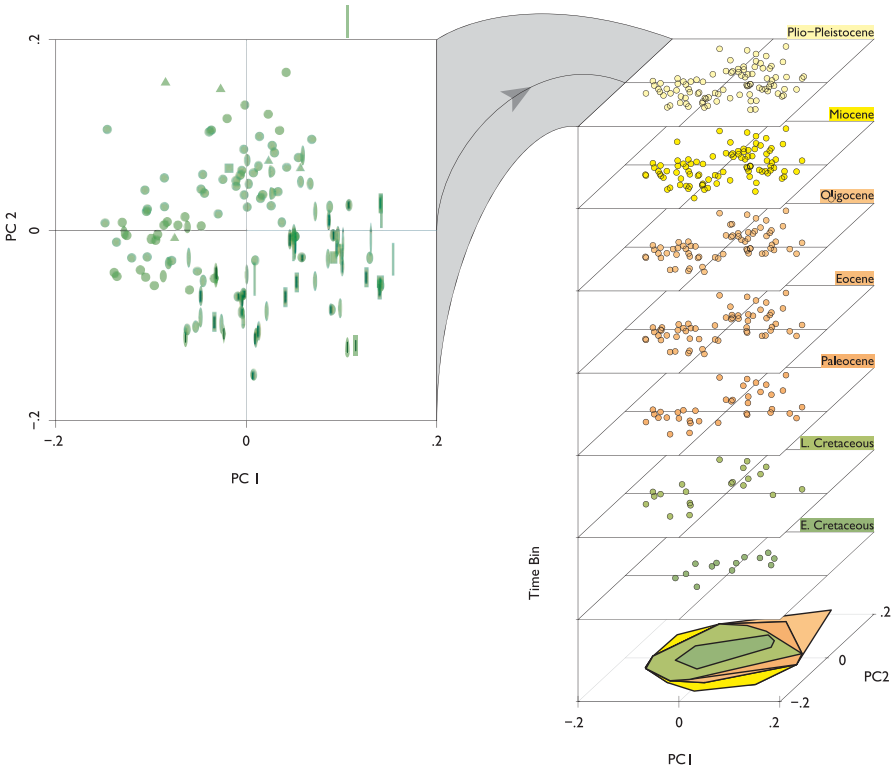

Fig. 2.3 Left: first two principal coordinate (PCO) axes of marine planktonic diatom morphospace; plot symbols reflect states morphological characters describing valve shape in plan view and presence/absence of raphe. Right: the same plot populated through time using occurrence data from the Neptune database; colored polygons below show convex hull areas enclosing points in time bins above of the corresponding color

Visualization. Empirical morphospace plots resulting from ordination procedures like this one can be hard to interpret if the only information presented is the location of genera on ordinated axes of mysterious meaning. Providing representative images of morphologies at selected locations is helpful, but because we have morphological data for each of the points, it can make sense to modify the shape of plot points themselves to reflect morphological character states. In the left panel of Fig. 2.3, we have represented the states of three characters relating to the plan (valve) view shape of each genus: the overall shape (elliptical, triangular, square, or ovate.), the aspect ratio, and the presence or absence of a raphe. The plot shows equant forms toward the top left, and elongate forms with and without raphes toward the bottom right. For examples of these morphologies, we refer the reader to the excellent SEM images in Round et al. (1990). This division reflects the largest-scale taxonomic division within the diatoms—centrics versus pennates—and raises the question to what extent phylogenetic structure is evident in morphospace.

Morphospace and phylogeny. Comparing the proximity of genera in morphospace to their proximity on a molecular phylogenetic tree shows only a very weak correlation; phylogenetic proximity at finer levels of resolution beyond the centric-pennate divide is not a good predictor of proximity in morphospace (Kotrc and Knoll 2015a). For example, the two major subdivisions within the pennate diatoms (raphids and araphids) do not appear to occupy distinct regions of morphospace. This may seem surprising, considering diatom phylogenies from before the molecular era broadly agree with molecular ones. It helps to remember, however, that morphological phylogenies identify key features with defined polarities, called synapomorphies, signifying inclusion in groups; this morphospace, in contrast, consists of equally weighted characters.

These results seem to suggest that the major groups of diatoms iteratively recolonized already-occupied regions of morphospace. In the case of the raphe, for example, this might make sense if we consider that—in providing for locomotion—it represents a key innovation in the radiation of diatoms in benthic and terrestrial environments. The taxa in our analysis come from the marine plankton, however, where—in the absence of substrates upon which to locomote—this innovation may have been of relatively little consequence. As a result, raphid diatoms in the plankton may have radiated to fill ecological niches indistinct from those occupied by their araphid cousins, resulting in overlapping occupation of morphospace.

While on the topic of diatom phylogenies, we divert briefly to consider that a clade's diversification history can also been addressed from a phylogenetic perspective directly, something commonly achieved using molecular phylogenies of their extant members and "lineage through time" plots. While such an approach could be taken for the diatoms (perhaps even using a phylogeny derived from morphological data, such as the data matrix underlying the morphospace analysis here), we point out the limited inferences that can be drawn from such analyses. Diversification rates result from a balance between origination and extinction, and as Quental and Marshall (2010) showed, molecular phylogenies are sensitive to the former, but blind to the latter. As an example, they compare a diversification history for whales derived from a molecular phylogeny, suggesting a history of unchecked diversification since the Oligocene (Steeman et al. 2009), to one based on the group's rather complete fossil record, which reveals a sharp decline in diversity from the Late Miocene to the present, a worrying discrepancy due to extinctions not revealed by the molecular phylogeny.

Returning to morphospace, molecular clocks suggest that the four major groups of diatoms (the raphid and araphid pennates and two groups of centric diatoms, the radial centrics and bi- and multipolar centrics) had diverged by the late Cretaceous Period (e.g. Kooistra et al. 2007). Given the apparent overlap of these groups in morphospace, we might expect to see broad morphological stasis across the Cenozoic Era. Fortunately, we can further explore this question by extending our morphospace back through time using the fossil data from Neptune.

Morphospace through time. The right hand side of Fig. 2.3 shows the occupation of the two-dimensional morphospace plot on the left through geologic time, tilted to an oblique view, for several Cenozoic time bins (with the youngest at the

top). The polygons at the bottom of the plot are convex hulls enclosing the points in each of the time bins above in the corresponding colors; convex hulls being the shape that would be made by stretching a rubber band around the points in a time bin and thus describe the extent of occupied morphospace. While the Cenozoic assemblages cover a larger area of the plot than the Cretaceous ones, the area does not increase very much through the Cenozoic Era. One interesting observation is that the quadrant at the center of pennate diatom morphology (the bottom right) is sparsely occupied up until the Miocene. This general impression of how morphospace has been occupied through time can be quantified much more rigorously by calculating metrics of disparity for each time bin in the Neptune data set.

Metrics of disparity. Many different ways of measuring disparity have been devised. A thorough review of these different metrics is beyond the scope of this chapter (for more detailed treatments see Wills et al. 1994; Ciampaglio et al. 2001; Erwin 2007), but a key point is that these metrics do not all describe the same aspects of morphospace occupation. To illustrate this notion, we present two disparity metrics here: convex hull volume and mean pairwise distance. The former is a higher-dimensional extension of the rubber band method introduced in Fig. 2.3; instead of measuring the area enclosed by the polygon, the volume or hypervolume enclosed in three or more dimensions is calculated. While convex hull volume is a measure of the total extent of morphospace occupied, the latter metric—as implied by its name—measures the average distance between pairs of taxa, measured as the proportion of character state mismatches out of possible matches.

It is not hard to see that because these metrics describe different aspects of morphospace occupation—the total extent of occupied morphospace and the degree of dispersion of taxa in morphospace, respectively—they can give different answers regarding disparity trends through time. In the case of diatom morphospace, for example, mean pairwise distance (Fig. 2.4, top left panel) stays roughly constant through time, while convex hull volume (Fig. 2.4, top right) shows a substantial increase (regardless of how may dimensions are considered in the volume calculation). While these results would appear to be at odds if we were to consider disparity as a monolithic concept, inspection of the stacked morphospace plot in Fig. 2.3 makes clear which aspects of morphospace occupation they describe: on the one hand, the total extent of occupied morphospace is increasing as new genera expand into previously unoccupied morphologies, while on the other hand, the number of genera is increasing, leading to a roughly constant (or slightly increasing) "packing" of genera into the occupied region. We can thus think of mean pairwise distance as representing something of a density measure and convex hull volume as the total extent of occupied morphospace. As is the case in Fig. 2.4, the density (mean pairwise distance) can remain roughly constant as occupied morphospace (convex hull volume) expands, but only if there is a commensurate rise in diversity.

Sampling. This increase in the number of genera in morphospace raises an interesting question about sampling. Since we spent much of the first half of this chapter voicing concern about the possibility that the evident rise in taxonomic diversity may simply be an artifact of sampling, it seems natural to ask: could sampling also

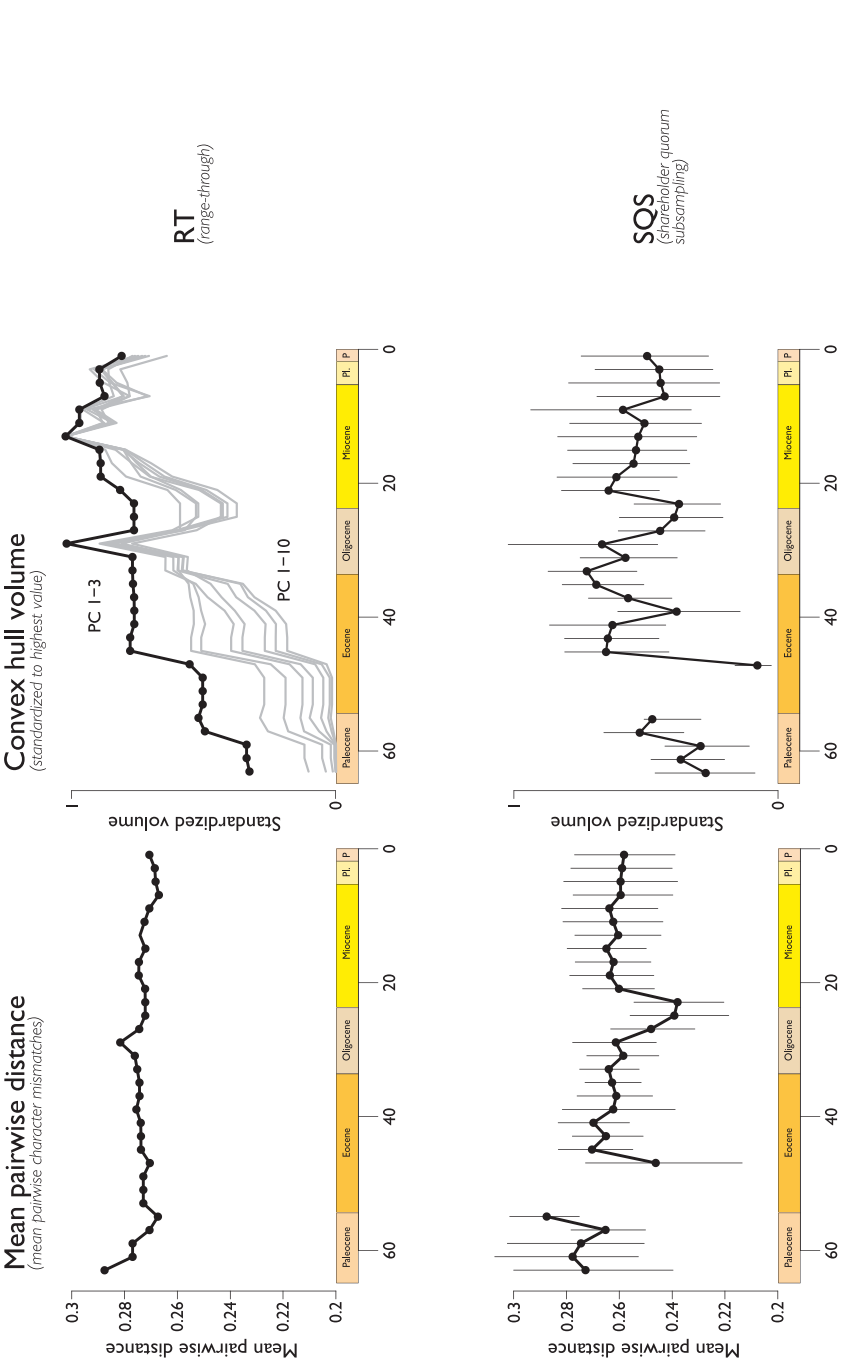

Fig. 2.4 Metrics of diatom disparity through time under in-bin sampling of the Neptune occurrence data taken at face value (*top row*) and shareholder quorum subsampling of the same dataset (*bottom row*). Plots on the left show the average dissimilarity (or morphological distance) between taxa measured as the proportion of character state mismatches to possible matches, plots on the right show the volume of convex hulls enclosing genera present in each time bin (in the top plot, 3–10 dimensions, in the bottom plot, 3 dimensions only)

affect metrics of morphological disparity? Although we introduced disparity as a different window onto the diversification history of a clade, it is based on the same fossil record and is thus subject to the same geological sources of bias. Studies on the effect of sampling on disparity metrics have suggested the use of mean pairwise distance, which has been observed to be more robust to variations in sampling than other disparity measures (Foote 1992; Ciampaglio et al. 2001; Butler et al. 2012). As we have just seen, however, considering one disparity metric alone limits analysis to just one aspect of morphospace occupation. While it is always possible to consider the effect of increasing numbers of taxa in a morphospace indirectly, for example, by rarefaction to a standardized number of taxa (Foote 1992), we can do better in the unique situation where a morphospace has been populated using a database of fossil occurrences. In this case, we can apply those subsampling metrics (discussed above) developed for addressing sampling bias in studies of taxonomic diversity to our morphospace, and calculate metrics of disparity under subsampling.

The results of applying SQS to the diatom morphospace and calculating our two chosen disparity metrics are shown in the bottom half of Fig. 2.4. Mean pairwise distance does not appear to be significantly impacted by the subsampling exercise, lending further support to the notion that this metric is robust to sampling variations. For convex hull volume, in contrast, the increasing trend over the Cenozoic seems to all but disappear, revealing a much more stationary pattern through time. When sampling is taken into account, then, disparity metrics paint a picture of relative Cenozoic stasis in diatom morphological evolution that stands in agreement with both the comparison between morphospace and phylogeny and the results of subsampled taxonomic diversity.

2.4 Synthesis

The fossil record provides us with two windows onto the Cenozoic diversification history of diatoms, through taxonomic diversity and morphological disparity. When read at face value, the record suggests steep Cenozoic diversification from both a view through diversity and through convex hull volume, a disparity measure describing the total extent of occupied morphospace; mean pairwise distance, in contrast, suggests a stationary pattern through Cenozoic time. When secular trends in sampling intensity are taken into account using both well-established and new subsampling methods, however, the records through both windows broadly suggest stasis, a pattern also predicted from a comparison of morphospace and molecular phylogeny. While disparity as measured by mean pairwise distance seems to be robust to sampling, the other results—disparity as well as diversity—hinge upon whether we believe that subsampling algorithms do a better job at uncovering true diversity history than a literal reading of the fossil record, or whether they simply trade sampling bias for another bias resulting from changing relative abundance distributions.

A similar pattern has been discovered in another group of open ocean microfossils, the planktonic foraminifera: a literal reading of their deep-sea record also suggests a steep and roughly monotonic rise in species richness through Cretaceous and Cenozoic time, but, when sampling is accounted for by either subsampling or modeling, a much more gradual rise is recovered, with peak diversity in the Cretaceous (Lloyd et al. 2012a). And the fossil record of cocclithophorids also contrasts a literal reading of the Cretaceous-Cenozoic record with results obtained when sampling is taken into account (Lloyd et al. 2012b).

Without the compelling empirical suggestion of a Cenozoic rise in diatom diversity, it is worth considering whether an unfettered diversification would be expected *a priori.* The answer is not immediately obvious, but surely requires consideration of the relationship between phytoplankton diversity and both physical and chemical oceanography—as highlighted, for example, by global marine ecosystem models that implicate the role of resource availability and dispersal in controlling phytoplankton diversity (Follows et al. 2007). While these oceanographic factors are undoubtedly linked to climate, how exactly changes in climate would be expected to affect diatom diversity is a question deserving of further attention. We do note the correspondence between the high rates of diversity change around the Eocene-Oligocene boundary and the major shift in the Earth's climate system observed around that time. The decline in diatom diversity, particularly pronounced in the subsampled results, coincides broadly with a sharp drop in ocean temperature (about 5°C cooling in the high latitudes, Liu et al. 2009), thought to be driven by the establishment of circum-Antarctic circulation (Kennett 1982) and/or decreases in atmospheric CO2 (Pagani et al. 2005).

If the pattern of relative Cenozoic stasis in diversity and disparity to which the results presented here point is accurate, most of the marine planktonic diatoms' diversification was a Mesozoic to earliest Cenozoic event, perhaps prompting a reexamination of evolutionary narratives in which a Cenozoic rise in diatom diversity features prominently. In many of these narratives, however, diatom diversity merely stands as a proxy for diatom participation in the silica cycle, yet the number of taxa is only one factor in their importance to silica cycling. It is also conceivable that there were changes through time in diatom abundance or the rate of diatomaceous sediment deposition. Such changes could, at least theoretically, be independent of diversity; consider, for example, that in the Southern Ocean diatom ooze belt, perhaps the most important area of diatomaceous silica deposition today, sediments are dominated by just one species, *Fragilariopsis kerguelensis,* constituting up to 60 to 90% of total diatom abundance (Zielinski and Gersonde 1997). In addition to its abundance, *F. kerguelensis* is rather heavily silicified, illustrating also the potential role of changes in silicification to the diatoms' biogeochemical impact. The origination of even a small number of such numerically dominant or robustly silicified taxa could potentially expand the diatoms' role in the silica cycle to an extent much greater than the concomitant taxonomic diversification. Indeed, as described in the discussion of subsampling methods above, frequency distributions in the Neptune database indicate an increase in dominance through time compatible with such a scenario.

From the perspective of diatoms serving as starting points for biologically inspired design, one implication of an early exploration of morphospace might be that fossil morphologies ought to be considered alongside those of extant diatoms. Particularly if the maximum range of diatom form was achieved early in the Cenozoic, fossils from that time period may provide a range of biological constructions of engineering value not available in recent forms.

There are also important limitations of this study that must be considered. We have only considered the taxonomic and morphological diversity of marine planktonic diatoms here, although these only account for as estimated one-tenth the total diversity of diatoms (Kooistra et al. 2007). While we are not aware of systematic compilations of global diversity history of either benthic or freshwater diatoms, we expect the trajectories may be different than in the marine plankton—freshwater diatoms, for instance, being dominated by the pennate clade, whereas centric diatoms predominate in the marine planktonic realm (Round et al. 1990). Constructing a morphospace capable of representing the full taxonomic and temporal sweep of a clade as large and diverse as the marine planktonic diatoms also requires trade-offs in the level of morphological detail that can be recorded. For example, changes in the degree of silicification of diatom frustules are not well captured by the morphological characters in this study, since these are not necessarily visible in those characters that can be coded cohesively at the genus level. If predictions from the fossil record of radiolarians (Lazarus et al. 2009) and semi-quantitative observations of the diatom fossil record (Finkel and Kotrc 2010) hold true, diatoms ought to show a reduction in silicification over the Cenozoic Era, a pattern of interest to engineers seeking structures that maximize strength with minimal use of constructional material. Such trends may be best investigated by looking at morphological changes within long-ranging genera (such as *Stephanopyxis*), where insight might be gained to how nature does more with less. For figured examples of such morphologies, we refer the reader to Gombos (1980), Olshtynskaya (1990 and 2002), Sims (1986, 1988 and 1990), and Round et al. (1990, particularly pp. 144, 166, 172, 182–189, 202, 216, 226–229, 268–279, 316, 330, 416 and 564).

References

Alroy J (1996) Constant extinction, constrained diversification, and uncoordinated stasis in North American mammals. Palaeogeogr Palaeoclimatol Palaeoecol 127:285–311

Alroy J (2000) New methods for quantifying macroevolutionary patterns and processes. Paleobiology 26:707–733

Alroy J, Aberhan M, Bottjer DJ et al (2008) Phanerozoic Trends in the Global Diversity of Marine Invertebrates. Science 321:97–100

Alroy J (2010a) Fair sampling of taxonomic richness and unbiased estimation of origination and extinction rates. Paleontol Soc Pap 16:558–80

Alroy J (2010b) The shifting balance of diversity among major marine animal groups. Science 329:1191–1193

Arita S, Ohtsuka T (2004) Describing the valve outlines of Navicula species using a newly described arc-constitutive model. Diatom 20:191–198

Boyce CK, Knoll AH (2002) Evolution of developmental potential and the multiple independent origins of leaves in Paleozoic vascular plants. Paleobiology 28(1):70–100
Bush AM, Markey MJ, Marshall CR (2004) Removing bias from diversity curves: the effects of spatially organized biodiversity on sampling-standardization. Paleobiology 30(4):666–686
Butler R, Brusatte S, Andres B, Benson R (2012) How do geological sampling biases affect studies of morphological evolution in deep time? A case study of pterosaur (Reptilia: Archosauria) disparity. Evolution 66:147–162
Ciampaglio CN, Kemp M, McShea DW (2001) Detecting changes in morphospace occupation patterns in the fossil record: characterization and analysis of measures of disparity. Paleobiology 27(4):695–715
DeMaster DJ (2003) The Diagenesis of Biogenic Silica: Chemical Transformations Occurring in the Water Column, Seabed, and Crust. In: Holland HD, Turekian KK (eds) Treatise on Geochemistry, vol 7. Pergamon, Oxford, pp 87–98
Eble GJ (2000) Theoretical morphology: state of the art. Paleobiology 26(3):520–528
Ehrenberg CG (1838) Die Infusionsthierchen als vollkommene Organismen. Ein Blick in das tiefere organische Leben der Natur. Leopold Voss, Leipzig
Erwin DH (2007) Disparity: morphological pattern and developmental context. Palaeontology 50(1):57–73
Falkowski PG, Katz ME, Knoll AH, Quigg A, Raven JA, Schofield O, Taylor FJR (2004) The evolution of modern eukaryotic phytoplankton. Science 305:354–360
Finkel ZV, Kotrc B (2010) Silica use through time: macroevolutionary change in the morphology of the diatom fustule. Geomicrobiol J 27:596–608
Flessa KW, Jablonski D (1983) Extinction is here to stay. Paleobiology 9(4):315–321
Follows MJ, Dutkiewicz S, Grant S, Chisholm SW (2007) Emergent biogeography of microbial communities in a model ocean. Science 315:1843–1846
Foote M (1989) Perimeter-based Fourier analysis: a new morphometric method applied to the trilobite cranidium. J Paleont 63(6):880–885
Foote M (1991) Morphological and taxonomic diversity in a clade's history: the Blastoid record and stochastic simulations. Contrib Mus Paleo Univ Mich 28(6):101–140
Foote M (1992) Rarefaction analysis of morphologic and taxonomic diversity. Paleobiology 18:1–16
Gersonde R, Harwood DM (1990) Lower Cretaceous diatoms from ODP Leg 113 Site 693 (Weddell Sea). Part 1. Vegetative cells. Proc ODP Sci Results 113:365–402
Gombos AM (1980) The early history of the Diatom family Asterolampraceae. Bacillaria 3:227–272
Good IJ (1953) The population frequencies of species and the estimation of population. Biometrika 40:237–264
Haeckel E (1904) Kunstformen der Natur. Bibliographisches Institut, Leipzig
Hutchinson, GE (1978) An introduction to population ecology. Yale University Press, New Haven
Kennett JP (1982) Marine geology. Prentice-Hall, Englewood Cliffs
Kooistra WHCF, Gersonde R, Medlin LK, Mann DG (2007) The origin and evolution of the diatoms: their adaptation to a planktonic existence. In: Falkowski PG, Knoll AH (eds) Evolution of primary producers in the sea. Elsevier Academic Press, Burlington
Kotrc B (2013) Evolution of silica biomineralizing plankton. PhD thesis, Harvard University
Kotrc B, Knoll AH (2014) Data from: A morphospace of planktonic marine diatoms, parts I and II. Dryad Digital Repository. http://dx.doi.org/10.5061/dryad.js64t
Kotrc B, Knoll AH (2015a) A morphospace of planktonic marine diatoms. I. Two views of disparity through time. Paleobiology (in press)
Kotrc B, Knoll AH (2015b) A morphospace of planktonic marine diatoms. II. Sampling standardization and spatial disparity partitioning. Paleobiology (in press)
Lazarus DB (1994) Neptune: a marine micropaleontology database. Math Geol 26(7):817–832
Lazarus DB (2011) The deep-sea microfossil record of macroevolutionary change in plankton and its study. Geol Soc Lond Spec Publ 358(1):141–166
Lazarus DB, Kotrc B, Wulf G, Schmidt DN (2009) Radiolarians decreased silicification as an evolutionary response to reduced Cenozoic ocean silica. PNAS 106(23):9333–9338

Lazarus DB, Weinkauf M, Diver P (2012a) Pacman profiling: a simple procedure to identify stratigraphic outliers in high-density deep-sea microfossil data. Paleobiology 38(1):144–161
Lazarus DB, Barron J, Türke A, Diver P, Renaudie J (2012b) Diversity history of Cenozoic planktic marine diatoms. The Micropalaeontological Society AGM and warm world symposium, British Geological Survey, Nottingham, UK, Nov. 11th–13th
Lewontin RC (1969) The meaning of stability. Brookhaven Symp Biol 22:13–24
Liow LH, Stenseth NC (2007) The rise and fall of species: implications for macroevolutionary and macroecological studies. Proc R Soc B 274:2745–2752
Liow LH, Skaug HJ, Ergon T, Schweder T (2010) Global occurrence trajectories of microfossils: environmental volatility and the rise and fall of individual species. Paleobiology 36(2):224–252
Liu Z, Pagani M, Zinniker D et al (2009) Global cooling during the Eocene-Oligocene climate transition. Science 323(5981):1187–1190
Lloyd GT, Pearson PN, Young JR, Smith AB (2012a) Sampling bias and the fossil record of planktonic foraminifera on land and in the deep sea. Paleobiology 38(4):569–584
Lloyd GT, Young JR, Smith AB (2012b) Comparative quality and fidelity of deep-sea and land-based nannofossil records. Geology 40(2):155–158
Lupia R (1999) Discordant morphological disparity and taxonomic diversity during the Cretaceous angiosperm radiation: North American pollen record. Paleobiology 25(1):1–28
Mann DG, Droop SJM (1996) Biodiversity, biogeography and conservation of diatoms. Hydrobiologia 336(1):19–32
Marshall, CR (1990) Confidence intervals on stratigraphic ranges. Paleobiology 16:1–10
Marx FG, Uhen MD (2010) Climate, critters, and cetaceans: Cenozoic drivers of the evolution of modern whales. Science 327(5968):993–996
McGhee GR (1999) Theoretical morphology: the concept and its applications. Columbia University Press, New York.
Miller AI, Foote M (1996) Calibrating the Ordovician radiation of marine life: implications for Phanerozoic diversity trends. Paleobiology 22:304–309
Mou D, Stoermer EF (1992) Separating *Tabellaria* (Bacillariophyceae) shape groups: a large sample approach based on Fourier descriptor analysis. J Phycol 2:386–395
Netherlands Architecture Institute. Accessed 8/1/2012. http://schatkamer.nai.nl/system/pictures/546/original/BERL_251-5_900px.jpg?1348145419
Niklas KJ (1999) Evolutionary walks through a land plant morphospace. J Exp Bot 50(330):39–52
Olshtynskaya AP (1990) Morphology of the diatom genus *Pseudopodosira*. In Proceedings of the 10th International Diatom Symposium, Joensuu, Finland, August 28-September 2, 1988, 93–101. Simola H (ed). Koeltz Scientific Books
Olshtynskaya AP (2002) Morphological and taxonomic characteristics of some Paleogene diatoms of Ukraine. Int J Algae 4:118–126
Pagani M, Zacho JC, Freeman KH, Tipple B, Bohaty S (2005) Marked decline in atmospheric carbon dioxide concentrations during the Paleogene. Science 309(5734):600–603
Pappas JL (2005) Theoretical morphospace and its relation to freshwater Gomphonemoid–Cymbelloid diatom (Bacillariophyta) lineages. J Biol Systems 13(4):385–398
Proctor R (2006) Architecture from the cell-soul: René Binet and Ernst Haeckel. J Arch 11(4): 407–424
Quental TB, Marshall CR (2010) Diversity dynamics: molecular phylogenies need the fossil record. Trends Ecol Evol 25(8):434–441
Rabosky DL, Sorhannus U (2009) Diversity dynamics of marine planktonic diatoms across the Cenozoic. Nature 457:183–186
Raup DM (1966) Geometric analysis of shell coiling: general problems. J Paleontol 40(5): 1178–1190
Rohlf FJ, Bookstein FL (eds) (1990) Proceedings of the Michigan morphometrics workshop. The Univ. of Mich. Mus. of Zoology Spec. Pub. 2
Round FE, Crawford RM, Mann DG (1990) The diatoms: biology & morphology of the genera. Cambridge University Press

Sims PA (1986) *Sphynctolethus* Hanna, *Ailuretta* gen. nov., and evolutionary trends within the Hemiauloideae. Diatom Res 1:241–269

Sims PA (1988) The fossil genus *Trochosira*, its morphology, taxonomy and systematics. Diatom Res 3(2):245–257

Sims PA (1990) The fossil diatom genus *Fenestrella*, its morphology, systematics and palaeogeography. Beiheft zur Nova Hedwigia 100:277–288.

Spencer-Cervato C (1999) The Cenozoic deep sea microfossil record: explorations of the DSDP/ODP sample set using the Neptune database. Palaeontologia Electronica 2

Steeman, ME, Hebsgaard MB, Fordyce RE et al (2009) Radiation of extant Cetaceans driven by restructuring of the oceans. Syst Biol 58:573–585

Stoermer EF, Ladewski TB (1982) Quantitative analysis of shape variation in type and modern populations of Gomphoneis herculeana. Nova Hedwigia Beih 73:347–386

Wills MA (2001) Morphological disparity: a primer. In: Adrain JM, Edgecombe GD, Lieberman BS (eds) Fossils, phylogeny, and form: an analytical approach. Kluwer, New York

Wills MA, Briggs DEG, Fortey RA (1994) Disparity as an evolutionary index: a comparison of Cambrian and recent arthropods. Paleobiology 20(2):93–130

Wright S (1932) The roles of mutation, inbreeding, crossbreeding and selection in evolution. Proc Sixth Int Congr Genet 1:356–366

Zielinski U, Gersonde R (1997) Diatom distribution in Southern Ocean surface sediments (Atlantic sector): implications for paleoenvironmental reconstructions. Palaeogeogr Palaeoclimatol Palaeoecol 129:213–250

Chapter 3
Biomineralization in Diatoms: The Organic Templates

H. Ehrlich and A. Witkowski

3.1 Introduction

Naturally occurring silica-containing skeletons are nanoorganized composites where organic components mostly of proteinaceous origin are functional parts of broad variety of skeletal architectures (Wong Po Foo et al. 2006). Diverse proteinaceous materials have been proposed to regulate biosilicification in vivo in organisms including plants (Perry et al. 1984), diatoms (Kröger et al. 1999, 2002; Kröger and Sumper 2004), other protists (Schultz et al. 2001), and sponges (Cha et al. 1999; Weaver and Morse 2003; Müller et al. 2005; Ehrlich et al. 2010). Siliceous planktonic organisms, including diatoms, provide an abundant assemblage of unusual skeletal structures. Diatoms are fascinating because of their biosilica cell walls that are hierarchically organized structures from nano to micro scale. These bioconstructs determine design and development of novel artificial approaches with respect to lightweight structures (Hamm et al. 2003; Hamm and Smetacek 2005) and advanced materials (Gordon and Parkinson 2005; Kröger and Sandhage 2010).

The diatom cell's rigidity is provided by the skeleton—the silica frustule (Hecky et al. 1973). Their shapes vary from circular/triangular to bipolar, and their sizes from two up to a few hundred micrometers. Some even grow to an exceptional 5500 µ5. They are broadly categorized into radial forms with nanostructured pore patterns (centrics) or bilateral symmetries (pennates) (Round et al. 1990; Yang et al. 2011). The highly specialized nanostructure of a cell wall determines photonic properties on nanoscale being involved in photosynthesis, staving off predators due to their sturdy structure, and acting as a counterbalance to turgor pressure (see for review Yang et al. 2011). Therefore, a better understanding of the principles of

H. Ehrlich (✉) · A. Witkowski
TU Bergakademie Freiberg, Freiberg, Germany
e-mail: hermann.ehrlich@physik.tu-freiberg.de

A. Witkowski
University of Szczecin, Szczecin, Poland

C. Hamm (ed.), *Evolution of Lightweight Structures,* Biologically-Inspired Systems 6,
DOI 10.1007/978-94-017-9398-8_3

biomineralization in diatoms is a worthwhile challenge for the scientific community (Ehrlich 2010; Patwardhan 2011; Sheppard et al. 2012).

According to the established point of view (see Tesson and Hildebrand 2010), both organic compounds and organelles in the diatom's cell are involved in the formation of mineralized nanostructures of their frustules. For example, the Silica Deposition Vesicles (SDV) are examples of specialized compartments where silica structures are synthetized. After this process is completed, the entire formation undergoes exocytosis and forms the new frustule. Soluble silicic acid is the form for silicon transport into the cell, however, it is thought that solid silica structures are as condensed inside the SDV.

There are numerous candidates among organic molecules as main players in diatom biosilicification. But while the common biomineralization pathway is unclear, it has been well established that biomineralization of tissue in living organisms is determined and regulated by corresponding organic molecules that are able to nucleate and to control the formation and growth of the mineral phase. This process is usually termed as "templating", and has become somewhat generic though, denoting numerous proposed organic-inorganic interactions, including molecular as well as structural affinities (Subburaman et al. 2006). The term of "template for mineralization" seems appropriate with respect to the aminoacids, peptides, polypeptides, proteins (structural or/and acidic), glyco- and proteoglycans, lipids and polysaccharides (cellulose, chitin) as well as other biomolecules which possess the "templating activity" on such stages of biomineralization process as transport, nucleation, as well as growth and stabilization of corresponding biocomposite.

There are no doubts that especially molecular recognition between inorganic and organic species is crucial for generating of such complex structures. It is suggested that both individual interactions or combinations of interfacial or non-bonding interactions including hydrogen bonding, electrostatic, stereo-chemical and hydrophobic effects are essential for mineralization process (Patwardhan et al. 2007). Principally, templates provide both the preferential locations for nucleation sites and control the orientation of corresponding mineral phase (De Yoreo and Vekilov 2003). Stephen Mann in his fundamental work (Mann 2001) proposed that a key mediator of controlled biomineralization is represented by some kind of insoluble macromolecular framework: *"The matrix subdivides the mineralization spaces, acts as a structural framework for mechanical support, and is interfacially active in nucleation*." It is involved in subdivision of mineralization spaces, is interfacially active during nucleation and functions as a mechanical support. Characterization of organic substances which are associated with diatom silica has identified four classes of biomolecules likely to be the key players in biosilicification on nanoscale, however there are doubts whether these molecule classes can resemble some kind of "structural framework for mechanical support" in diatoms. Specifically modified (poly)peptides known as silaffins, acidic polypeptides called silacidins, as well as unique long chain polyamines (LCPAs), (see for review Tesson and Hildebrand 2010) and recently discovered cingulins from diatom's microrings (Scheffel et al. 2011) are definitively involved in biosilicification process on molecular level. Combinations of these biomolecules can be formed via electrostatic interactions. Due to this process, broad variety of nanoscale structures can be observed after in vi-

tro precipitation of silicic acid, however obtained products only partially resemble structural morphologies of diatom silica (see for review Wieneke et al. 2011).

Mostly, they lack the degree of architectural complexity of mesoscale silica structure observed in diatoms, which suggests that some alternative components of cellular origin are involved. We think that the best candidate in this case is nanofibrillar β-chitin recently discovered within cell walls of well investigated diatom *Thalassiosira pseudonana* Hasle & Heimdal (Brunner et al. 2009; Ehrlich 2010a), the first diatom where the genome was successfully sequenced (Armbrust et al. 2004). From our point of view (Ehrlich 2010b), there are two possibilities for organic templates to be involved in the regulation of biomineralization. The first one is a direct regulation, and the second acts via the various functionally active and structurally diverse biomolecules which may become attached to the template. Therefore, chitin as biological material with crystalline highly ordered structure together with low-molecular weight biomolecules listed above may be responsible for biosilicification in diatoms.

3.1.1 Organic Templates Within Cell Walls of Diatoms

Thorough analysis of literature on organic templates which have been linked to biosilicification in diatoms leads to the following metabolic routes: Serine and Threonine, Hydroxiproline, Frustulins and Pleuralins, Silaffins, Long Chain Polyamine and Silicidins, Cingulins, and the Chitin routes.

3.1.2 The Serine and Threonine Route

The biochemical advances that led to our modern understanding of organic templates in diatoms' frustules began in the 1960s. The cell wall of diatoms was found to be composed of siliceous frustules with elegant architecture, which are encased in an organic coating (Reimann et al. 1965, 1966, for summary cf. Round et al. 1990). Even fossilized frustules can possess well preserved organic coating (Lewin 1961; Kamatani 1971). In a classic paper by Hecky et al. (1973), the sugar and amino acid composition of frustules from six diatom species (*Cyclotella cryptica*, *C. stelligera*, *Melosira nummuloides*, *M. granulate*, *Navicula pelliculosa*, *Nitzschia brevirostris*) have been described. According to this work, cell-wall protein is, in contrast to cellular protein, enriched in glycine, threonine and serine. At the same time it is characterized by the lower content of sulfur-containing, acidic, and aromatic amino acids. These authors reported both sufficient variability in frustular carbohydrates and amino acids. In some estuarine species, glucose is replaced by fructose.

Since the isolation procedure which aims to isolate organic matrix from biosilica structures plays a crucial role in experiments, we take the liberty to present a detailed description of the process. Hecky et al. (1973) proposed the following method. Harvested diatoms were re-suspended in 40 ml of triple distilled water, and then sonicated under selected conditions (settings and time). The effectiveness of sonica-

tion was monitored using light microscopy until the cell walls appeared free of cell contents. Selected sonicated subsamples were stained with phosphotungstic acid to check possible contamination by cellular debris using transmission electron microscopy. With exception of *Navicula pelliculosa*, the treatment effectively cleared the cell walls of cell contents in all diatoms studied. Differential centrifugation (1800 x g, 2 min) was used to collect frustules after sonication. The cell contents, which were localized in the supernatant after the first centrifugation, were collected and dried in vacuo over KOH pellets. This fraction was consequently analyzed to check the purity of the cell-wall preparation additionally. The frustules were re-suspended in triple distilled water, centrifuged again four times, and, finally, dried in vacuo over KOH. The hydrolysis procedure has been used for both the cell-wall and cell-contents fractions of selected diatoms. For example, 1.0–6.2 mg of frustules were hydrolyzed in 1.8 N HCl, at 100 °C for 4 h, under a nitrogen atmosphere, for determination of sugars. Also, under nitrogen, 1.7–7.7 mg of frustular material was hydrolyzed in 6 N HC1 for 22 h at 100 °C with the aim to determine amino acids. Obtained hydrolyzates were dried and re-dissolved in triple distilled water several times to eliminate the residual HC1. One ml of a pH 2.2 citrate buffer was added to the amino acid residue, and analyzed using amino acid analyzer (Hecky et al. 1973).

Using these techniques, the authors made the following conclusions: The hydroxyl-containing side-chains of serine and threonine are, probably, involved in

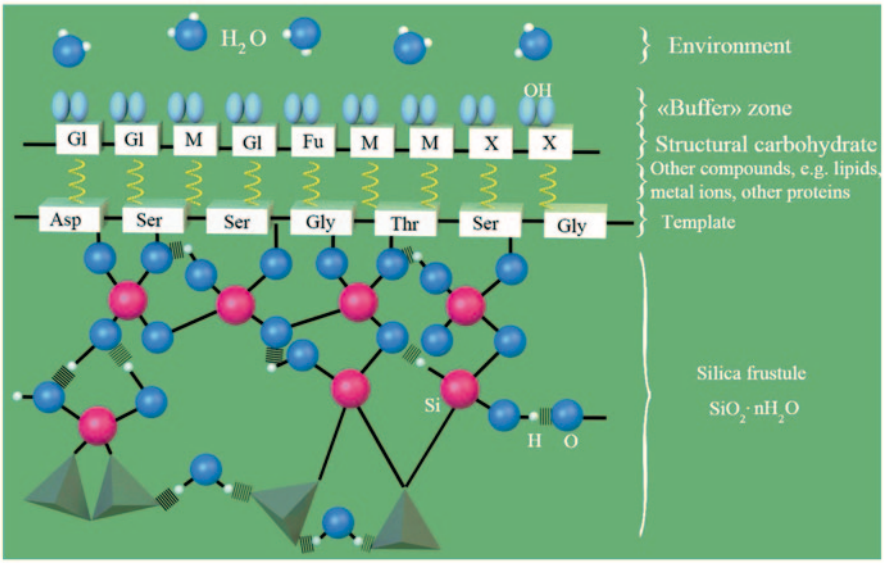

Fig. 3.1 Hypothetical distribution of organic layers in the diatoms frustule. The *outer layer* is of polysaccharide origin and consist of various sugars like glucose (*Gl*); mannose (*M*); fucose (*Fu*); xylose (*X*). Correspondingly, the *outward* directed hydroxyl groups of sugars are responsible for formation of the hydrophilic buffer zone. Amino acids like serine (*ser*), glycine (*Gly*), threonine (*Thr*), aspartic acid (*Asp*) are represented within the protein template. The hydrogen bonds are marked with *hatched lines*. The three dimensionality of the silicic acid (and resulting silica) with Si in fourfold coordination with oxygen atoms is represented in the form of *tetrahedral* geometry. (Image courtesy of Alexej Rusakov, inspired by Hecky et al. 1973)

Si-deposition. Such small amino acid as glycine may play a role of a spacer in the protein molecule. The function envisaged for the template protein is presented schematically in Fig. 3.1. It is proposed that the protein enriched in serine and threonine is localized on the the inner surface of membrane within which silica deposition occurs termed the silicalemma (Reimann et al. 1966). This protein is responsible for the formation of a layer of hydroxyl groups which are involved in silica condensation reactions with a consequent loss of water molecules. After that, the molecular layer of condensed silicic acid will be chemically attached to the protein template, in a geometric arrangement that will appropriate further polymerization of silicic acid. In contrast to simple interaction between the silicic acid molecules via random collisions, such a state is kinetically more favorable. Hypothetical support for the proposed interaction between serine and silicic acid comes from relatively high content of serine in relation to other amino acids with high resistance to thermal degradation found in geological record of ancient chert deposits (Hecky et al. 1973). Probably, the stabilization of serine due to its incorporation within the silica framework suggests the preferential serine-enrichment in the chert.

Thus, according to the model described by Hecky et al. (1973), the Si-depositing mechanism in diatoms may be based on condensation of silicic acid, using serine and threonine-rich protein template in epitaxial order. It was suggested that the solubility of diatom frustules under various environmental conditions is dependent on the nature of this template and the presence of polysaccharides in the frustule. The diversity of saccharides appears to be related to environmental factors, and can be useful in bio-systematic studies. Although from our point of view, the methods used in this study are very harsh and only provide supporting rather than convincing evidence for various speculations, the proposed model is very intriguing.

The Hydroxyproline Route

Contrary to Hecky et al. (1973), other researchers reported hydroxyproline related aminoacids within cell walls of diatoms. For example, Nakajima and Volcani (1969) reported 3,4-Dihydroxyproline, and Sadava and Volcani (1977) studied 4-hydroxyproline and 3,4-dihydroxy-L-proline in diatom frustules. These amino acids appear to originate from peptidyl proline. Cell-free extracts have been used to show the conversion of peptidyl proline to peptidyl hydroxyproline as well as the kinetic of this reaction using ^{14}C proline. Experimental data showed that dihydroxyproline does not arise from the further hydroxylation of peptidyl hydroxyproline. For example, a lag of several minutes between the incorporation of ^{14}C proline into protein and the appearance of ^{14}C hydroxyproline has been observed. However similar lag for the appearance of dihydroxyproline has not been registered. Additionally, it was shown that the formation of hydroxyproline was blocked by *a,a*-dipyridyl, but not the formation of the dihydroxypyroline from peptidyl proline. Being morphologically identical, frustules synthesized in the presence of dipyridyl showed minor difference in their chemical composition from frustules formed in its absence. The metabolism of ^{14}C dehydroproline occurs rapidly in the cells, with ^{14}C dihydroxyproline a main product. Increased synthesis of ^{14}C dihydroxyproline at the end of

cell separation have been reported in studies on conversion of ^{14}C proline to ^{14}C hydroxyproline at various stages of frustule formation (Sadava and Volcani 1977). Consequently, it was suggested that synthesis of dihydroxyproline plays a role in different developmental stages of the diatom cell wall formation.

Using slow-alkali etching of *Hyalonema sieboldi* glass sponge biosilica, we extracted the organic matrix, which was shown to be mostly represented by a hydroxylated fibrillar collagen with an unusual [Gly–3Hyp–4Hyp] motif (Ehrlich et al. 2010).This firstly discovered collagen motif determined in the studied deep-sea glass sponge is in a good agreement with the model of Schumacher et al. (2006), where 3(S)-hydroxyproline residues in the Xaa position of the collagen triple helix are described. This model offers a plausible molecular mechanism for the interaction between Gly–3Hyp–4Hyp polypeptides of isolated poriferan collagen template and polysilicic acid. The interaction between hydroxylgroups and orthosilicic acid is likely to be a hydrogen bond (Tilburey et al. (2007). The model proposed by us shows the possibility of existence of stable biocomposite based on hydrogen bonding between surfacely located hydroxyls of 3-Hyp and 4-Hyp and hydroxyl groups of polysilicic acid. Thus, the condensation reactions of silicic acid molecules with a consequent loss of water can be carry out on the surface layer with hydroxyl groups of the collagenous origin. Finally, similar to the model of Hecky et al. (1973), this initial layer of condensed silicic acid will be chemically bound into the hydroxylated collagenous template that will favor continuing polymerization of silicic acid according to specific geometric arrangement.

We hypothesized that this type of collagen that emerged at an early stage of metazoan evolution is a novel template for biosilicification in nature. The occurrence of additional trans-3-Hyp seems to play a key role in initiating of silica precipitation as well as in stabilizing of silicic acid molecules. The post-translational hydroxylation of proline and lysine residues in ancient collagens may have been linked to an increase of atmospheric oxygen during the Proterozoic (Exposito et al. 2002). The occurrence of skeletal silica- and hydroxylated collagen-containing biocomposites of the first multicellular organisms might be a co-evolutionary event.

The Frustulins and Pleuralins Route

In the 1990s, much attention was given to different kinds of calcium binding glycoproteins (Kröger et al. (1994), proteins with high weight molecular weight (Kröger et al. 1997), and proteins known as frustulins (Kröger et al. 1996) and pleuralin (Kröger and Sumper 1998). As reviewed by Kröger and Paulsen (2008), frustulins are proposed to be general diatom cell wall proteins that have been isolated and identified in both centric and pennate diatoms. The characteristic feature of frustulins is the presence of cysteine-rich domains (ACR) that contain ~50 amino acids including 10 highly conserved cysteine residues as well as multiple acidic domains. Short stretches of polyglycine side by side with proline rich regions (about 30% proline residues) are involved in spacing of the ACR domains, which can be also directly adjacent to each other. There are some specific differences in chemistry of the C-terminus of the ε-frustulin in different species. For example, that from *N.*

pelliculosa contains a tryptophan-rich domain (about 7 % W), however there is lack on this domain in frustulinsfrom *C. fusiformis* and *T. pseudonana* (Kröger et al. (1996). Ethylenediamine tetraacetate (EDTA) was effectively used for extraction of frustulins from the cell walls. This feature confirms a specific affinity of these proteins for Ca^{2+}ions. It is suggested that the Ca^{2+}-binding sites are localized within the ACR domains. Some kind of frustulins-based continuous protein coat that covers all parts of the frustule have been reported in *C. fusiformis* (de Poll et al. 1999. Both biochemical and immunocytochemical studies on the expression and localization of frustulins has been performed by de Poll et al. (1999) for *C. fusiformis*, *N. pelliculosa*, and *N. salinarum* in detail. The obtained results concluded that the frustulins were not apparently involved in the silicification process because they were not localized in the silicalemma of the newly formed SDVs. Consequently, the data reported by de Poll et al. (1999) imply a structural role of the frustulins in the casing of these algae rather than their regulatory function in biosilicification.

According to immunochemical investigations, the pleural (girdle) bands of the diatoms epitheca are the location places of pleuralins. For example, *C. fusiformis* contain 3–5 girdle bands in the overlap region. It is suggested that, in contrast to frustulins, pleuralins are more tightly bound to the frustules because they can be isolated only after treatment with anhydrous hydrofluoric acid. Interestingly, ammonium fluoride treatment at mildly acidic conditions, under which diatom silica dissolves completely, does not solubilize pleuralins. Probably, pleuralins are covalently cross-linked to an as yet unidentified frustular organic component, for example, a chitin that is resistant to HF-treatment. Four amino acids (proline, 22 %; serine, 11 %; cysteine, and 11 %; aspartate, 9 %) are the main structural compounds of the so called PSCD domain. This domain is characteristic for pleuralins, where the C-terminal parts are not related to the sequences which are typical for PSCD (Kröger et al. 1997).

The Silaffins, Long Chain Polyamine and Silicidins Route

The procedure that is based on treatment of diatoms frustules with acidified (pH 4–5) ammonium fluoride solution (10 M NH_4F,) lead to dissolution of siliceous layers and to extraction of are a family of phosphoproteins termed silaffins, or proteins with silica affinity (see for review Kröger et al. 1999, 2000, 2002; Kröger and Paulsen 2008). Because of this method, pleuralins, which can be extracted only using anhydrous HF, distinguishes from silaffins, which appear to be entrapped inside the silica. Even harsh solubilization methods based on mix of 2 % SDS at 95 °C, 8M urea, or 6M guanidinium·HCl at room temperature were no effective with respect to isolation of silaffins. Like the silaffins (Fig. 3.2a), long-chain polyamines usually abbreviated as LCPA, become isolated only upon dissolution of the silica that suggest their localization within the mineral phase. Identification of LCPA shows that all of known substances have either a putrescine, propylenediamine, or spermidine basis molecule with associated linear oligo-propyleneimine chains (Fig. 3.2b).

LCPA molecules are chemically very similar to the oligopropyleneimine modified lysine residues identified in silaffins. Sumper and Brunner (2006) reported that

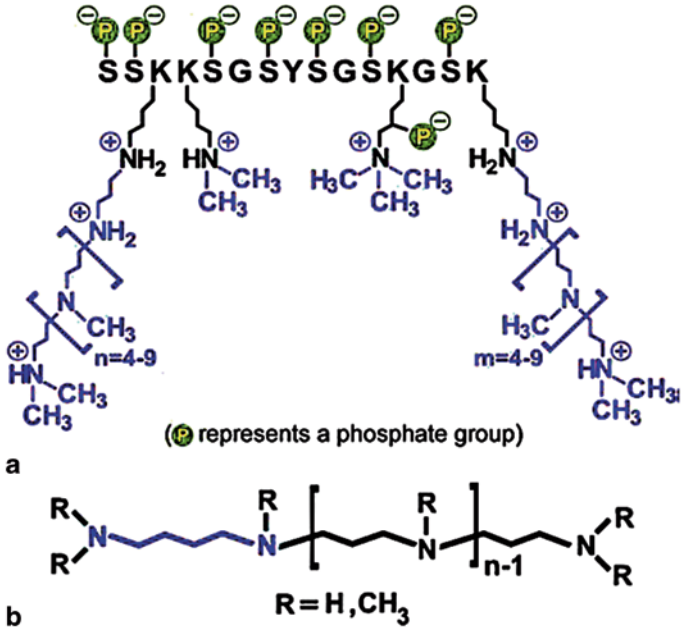

Fig. 3.2 Schematic representation of the common chemical formula of silaffins (**a**) and long-chain polyamines (**b**)

each diatom species may contain a characteristic mixture of LCPA molecules, which differ in the degree of N-methylation as well as in chain length. Usually, frustular silica from most diatom species studied to date contains practically equivalent content of silaffins and LCPA. However, such species as *Coscinodiscus asteromphalus*, *C. wailesii* and *C. granii*, appear to contain only LCPA (Sumper 2002). Because of evidently confirmed localization of both silaffins and LCPA within the silica, these biomolecules are suggested to be involved in diatom biosilicification. Moreover, detection of long-chain polyamines in siliceous skeletal structures of marine sponge *Axinyssa aculeata* (Matsunaga et al. 2007), suggest the possible role of them also in silica formation in multicellular organisms.

Wenzl et al. (2008) described the silicidins, a new class of aspartate/glutamate-rich and serine phosphate rich peptides within siliceous structures of *T. pseudonana*. Intriguingly, the discovery of silicidins was determined by a new demineralization procedure. These authors observed the following phenomenon. If silaffin-1/2 L is inserted after purification by size exclusion chromatography into 2M sodium chloride solution and again placed to size exclusion chromatography under high-salt conditions, a previously undetected component with low-molecular-weight can be separated readily from this silaffin. Three forms of silicidins have been isolated and separated from this material after treatment with anhydrous HF and purification by reversed-phase chromatography. The efficiency of these interesting peptides especially for phosphate anions to induce comparable amounts of silica precipitation is

remarkable. The concentration of silicidins must be at least two to three orders of magnitude higher, because the size of the silica nanospheres produced increase with the concentration of the silacidins when phosphate anions are present. According to modern hypothesis, silacidins can serve as the polyanion required in living diatoms for biosilicification regulated by polyamines (and/or silaffins) (Wenzl et al. 2008).

The Cingulins Route

According to recent work by Nils Kröger and co-workers, the silaffins are originally derived from some serine and lysine rich polypeptides, which are precursors with noncomplex amino acid compositions containing N-terminal signal chains for co-translational import into the endoplasmic reticulum. Their post-translational modifications consequently include the phosphorylation of numerous serine residues and alkylation of lysine residues. Nowadays, the amino acid composition-based bioinformatics approach enabled the identification of 86 silaffin-like proteins in the genome of the diatom *T. pseudonana* (Scheffel et al. 2010). However, the application of sequence homology-based tools for the identification of related proteins in diatom genome databases is not possible because silaffins from different diatom species do not show significant sequence homology.

Recently, the association of six silaffin-like proteins have been demonstrated in the girdle band region of the frustule which consists of multiple overlapping but independent siliceous microrings. These nanostructures constitute about half of the frustules in most diatom species. The term "cingulins" have been proposed for the six girdle band-associated silaffin-like proteins because of the name of the girdle band region known as "*cingulum*". Microrings with deeply integrated cingulins represent a nanostructured water insoluble organic matrix that is involved in biosilicification. The importance of the cingulins and the microrings in silica formation as common phenomenon in different species in diatoms is still under investigation.

Kröger and his team proposed the following demineralization approach to isolate the microrings and cingulins (Scheffel et al. 2010). Ammonium fluoride under acidic conditions was used for solubilization of the cingulins after dissolution of the mineral phase. This method was used previously for solubilization of LCPA, silaffins, and silacidins, but failed to solubilize the cingulins as was demonstrated below. Thus, strong GFP fluorescence was detected in the ammonium fluoride insoluble material (AFIM) from cingulin-GFP expressing transformants in contrast to the weak GPF fluorescence in the AFIM isolated from the tpSil3-GFP expressing transformants. In all cases the cingulin-GFP fusion proteins are visible as fluorescent rings. Between 64 and 100 % of the GFP fluorescence localized in the isolated biosilica from cingulin-GFP expressing diatoms strains was retained in the AFIM as have been quantified using fluorophotometry. It is not excluded that the insolubility of cingulins in *T. pseudonana* is a result of their association with or integration within the recently discovered chitin-based scaffold (Brunner et al. 2009).

The special test with chitin-indicating stain Calcofluor White showed that the AFIM from the cingulin-GFP expressing transformants contained chitin. The GFP

fluorescence was retained after specific treatment of the AFIM with chitinase. This enzymatic treatment, however, showed no effect on ring-shaped structures of the cingulin-containing insoluble material. Consequently, this data confirmed that cingulins of *T. pseudonana* are localized within an insoluble, but chitin-independent, ring-shaped matrix that is associated with the siliceous girdle band. The functional role of the insoluble cingulin-containing matrices in microrings probably consist in its tempating activity with respect to very special and oriented deposition of nonporous silica along "preferred sites" that possess silica-forming activity. The spaces in between these preferred sites may be responsible for the self-assembly of supramolecular aggregates of soluble biomolecules listed above that are suggested to template unique porous silica patterns.

3.1.3 Chitin in Diatoms

Depending on its source, chitin—the poly (β-(1–4)-N-acetyl-D-glucosamine- occurs in α, β and γ forms (Rudal and Kenchington 1973; Blackwell 1973), which can be accurate differentiated using X-ray diffraction, infrared and solid-state NMR spectroscopy (Rinaudo 2006). The most abundant form is the α-chitin that plays the crucial role as structural component in skeletal formations of numerous fungi, yeast, invertebrates like insects, crustaceans, aranoids, worms and sponges (see for review Ehrlich 2010a, b). Diverse protozoa (Herth et al. 1977; Herth 1980; Herth et al. 1986), polychaete (Lotmar and Picken 1950), pogonophoran and vestimetiferan worms (Blackwell et al. 1965; Gail et al. 1992), and squid pens (Rudall 1969; Rudall and Kenchington 1973) contain skeletal structures made of β-chitin that is the more rare form of this aminopolysaccharide.

Hierarchical organisation is one of the principal characteristic of broad variety of chitin-containing biological materials. Although the diversity of the occurrence of different chitin aggregation states within one organism, it include following hierarchical levels:

a. Molecular level with chitin chain oriented along the c-axis where hydrogen ions are laterally spaced by 0.475 nm with a monomer length of 1.032 nm.
b. Nanofibrillar level when nanofibrils of about 2–3 nm in diameter, each with19 chains of about 300 nm length. The lateral dimensions on this level are species dependent and can range from 2.5–25 nm (Goodrich and Winter 2007). The nanofibril must possess amounts of chains close to a minimum for stability but with an optimum surface area for interfacial interactions within chitinous structures (Vincent 2002).
c. Microfibrillar level when chitin microfibrils are formed and well visible under electron microscopes, for example in the form of shallow helices within the walls of stipe cells in some fungi (Kamada et al. 1991).
d. Fibre-level when microfibrills are bound in the structures with more than 1 μm in diameter (Al-Sawalmih 2007).

After pioneering work on chitin identification in diatom *T. fluviatilis* by McLachlan et al. (1965), a particularly pure form of β-chitin was identified in the spines produced by different diatom species (Herth and Barthlott 1979; Herth et al. 1986; Dweltz et al. 1968; Revol and Chanzy 1986). Also, the centric planktonic diatom *Cyclotella* synthesizes long fibrillar chitinous appendages (Blackwell et al. 1967), that slow down the sinking velocity of the cells (Walsby and Xypolyta 1977).

It was reported (Gooday et al. 1985) that the formation of β-chitin spines by the diatoms as well as their growth rates can be inhibited by the nucleoside antibiotic nikkomycin even at a minimum inhibitory concentration of 4 μM. In contrast to control cells, the chitin-free cells, which had been treated with nantibiotics, sedimented much more rapidly (Gooday et al. 1985).These chitinous spines are extremely stiff and crystalline and occur as up to 50 nm wide ribbons composed of parallel oriented nanofibrils which diameters between 5 and 30 nm. It was observed that diatom chitin forms broader ribbons and is more crystalline than those of fungal, or arthropodal origin (Herth and Zugenmaier 1977). The biological role of the chitinous spines in diatoms was also proposed. Thus, Gifford et al. (1981) suggested that the spines of marine diatom *T. weissflogii* can function as a protective mechanism that makes the diatom effectively larger and thus unavailable for consumption by small herbivores such as copepods.

The origin of chitin in diatoms has also been investigated. For example, the silica valve formations related to β-chitin fibril synthesis were studied in the centric diatoms *Cyclotella cryptica*, *C. nana*, *C. meneghiniana*, and *Thalassiosira fluviatilis*(=*T. weissflogii* (Grunow) G. Fryxell & Hasle) by use of transmission and scanning electron microscopy (Herth and Barthlott 1979a). For *T. fluviatilis,* the valves are described by a marginal ring of up to 86 processes and a central, less regular set of processes. Different supporting structures as well as a system of chambers surround the processes, which appear pore-like and may play an important role in fibril formation. It is thought that these processes give birth to the β-chitin fibrils. These fibrils, being attached in the pores, can be easily detached from the diatoms cells by aerating the cultures. Nascent β-chitin fibrils synthetized from diatom *Thalassiosira* sp. have been analysed by microdiffraction method. It was observed that that the c-axis of the crystal was oriented toward the diatoms (Sugiyama et al. 1999). Also the situation with respect to processes and chitin fibrils, the architecture of the pore apparatus and the valves in the investigated *Cyclotella* species, was similar. It is not excluded that the processes of the investigated centric diatoms are crucial structures which are responsible for the formation of β-chitin fibrils. According to Herth (1978), the unique membrane-associated chitin-fibril-synthesizing apparatus is the key player in formation of chitinous structures in the centric diatom *Cyclotella*. Electron microscopy methods have shown that in all species that synthesize chitin, the conical invaginations of the plasma membrane bear a special coat on their cytoplasmic face. This face shows also a specific hexagonal arrangement (Herth 1979).

Since 1997, the large scale production of β-chitin fibres (poly-GlcNAc) from diatoms for biomedical aims have been patented and established (see for details Vournakis et al. 1977a, b). However, up to publication by Brunner et al. (2009), the

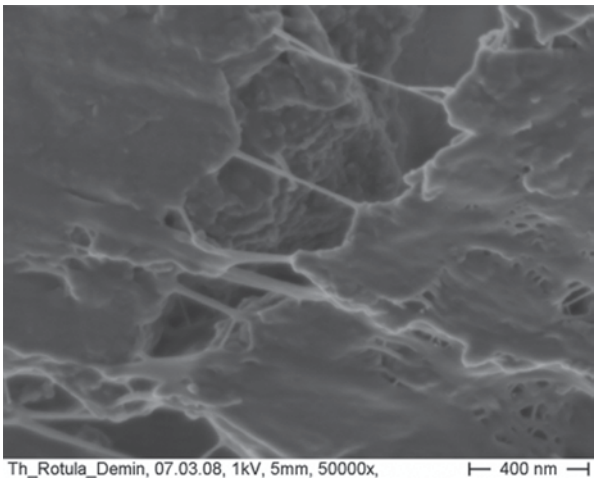

Fig. 3.3 Alkali treatment of *T. rotula* cells resulted in partial dissolution of the siliceous cell walls. The nano fibrillar network that is resistant to dissolution in 2.5 M NaOH at 37 °C became visible

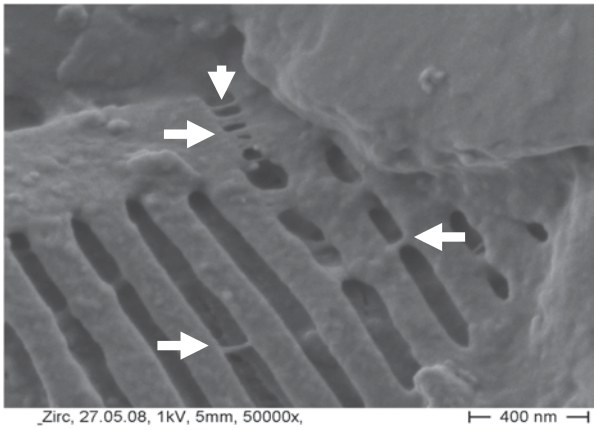

Fig. 3.4 SEM image of the *Pinnularia quadratarea*/ (A. Schmidt) Cleve var./minor/ (Østrup) Heiden from the Japan Sea bottom sediments. *Arrows* shows the nano fibrillar structures within disrupted cell wall

possible role of chitin as scaffolding as well as templating material in siliceous cell walls of diatoms was not investigated. The motivation to search for chitin within these structures in diatoms is based on observation made by Hermann Ehrlich and Vasiliy Bazhenov in March and May 2008 on partially demineralized *T. rotula* and dead marine diatom *Pinnularia quadratarea*, respectively. The original SEM images (never published previously) are presented here (Figs. 3.3, 3.4). The nano fibrils within partially disrupted cell wall of this species are well visible.

Chitin is very stable in alkali solutions even several months after insertion in contrast to amorphous silica and proteins with exception of collagen and elastin (see for details Hattori et al. 1999; Ehrlich 2010a, b; Ehrlich et al. 2010b). Therefore we have established an effective method for the desilicification of diatoms based on alkali treatment procedure. In experiments with glass sponges, alkali treatment at

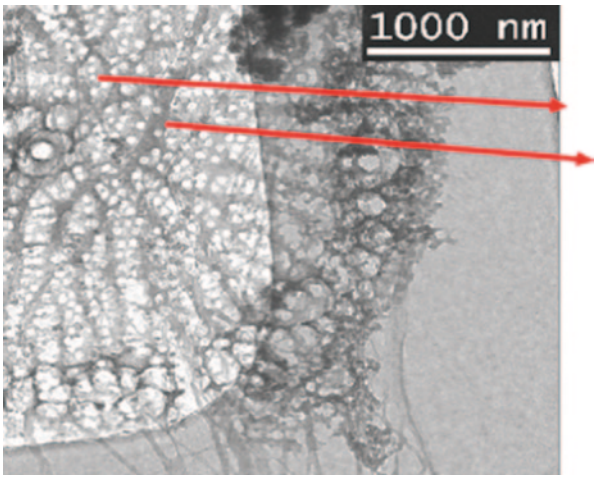

Fig. 3.5 TEM image of the completely demineralized *T. pseudonana* shows the presence of a nano fibrillar network. Both, internal nano fibrills originally localized within cell walls, as well external nano fibrils described in numerous papers previously, have been identified as β-chitin

37 °C is a more gentle demineralization procedure with respect to obtaining native organic matrices in contrast to rapid HF-based desilicification methods which can lead to artefacts (Ehrlich et al. 2010b). SEM studies (see images below) show strong evidence that alkali etching of cultivated and liophylized cells of *T. rotula* revealed organic templates of fibrillar nature.

We used *T. pseudonana* to carry out experiments on chitin identification within cell walls of diatoms. Intriguingly, Durkin et al. (2009) identified and described genes that encoded putative chitin synthases in a number of diatom genera, which indicates that the chitin-synthesizing ability is more distributed and probably plays a more significant role in algal biology than previously thought. Four phylogenetic clades have been reported for diatom chitin synthases. For example, three types of chitin synthases are encoding by six genes in *T. pseudonana*. Some environmental factors like short-term limitation by silicic acid or iron, or, even, short-term silicic acid starvation can increase the transcript abundance of the gene encoding one of these chitin synthase types. Furthermore, after long-term silicic acid starvation, transcript abundance of chitin synthase gene increased with a chitin-binding lectin localized to the girdle band region of the frustule. It can be assumed that chitin synthesis in diatoms is associated with their cell walls (Durkin et al. 2009).

Our results (Brunner et al. 2009) confirmed suggestions made by Virginia Armbrust and co-workers. This evidence showed that the siliceous frustules of the diatom *T. pseudonana* exhibit filigree nano structured internal chitin-containing networks (Fig. 3.5). The ^{13}C solid state NMR analysis suggested that this internal chitin contains a high amount of other bio-molecules, and seems to be amorphous. Moreover, SEM and TEM images showed that the nano- and microarchitecture of siliceous frustule of this diatom is strongly determined by structural features of chitin.

Further experiments on desilicification of *T. rotula* (Fig. 3.6) that use the alkali treatment revealed similar results to that of *T. pseudonana*. The SEM images

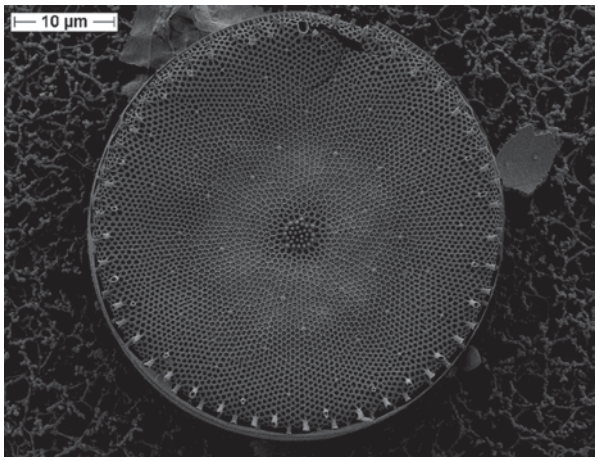

Fig. 3.6 The naturally occurring cell of *T. rotula*. (Image courtesy D. Krawczyk)

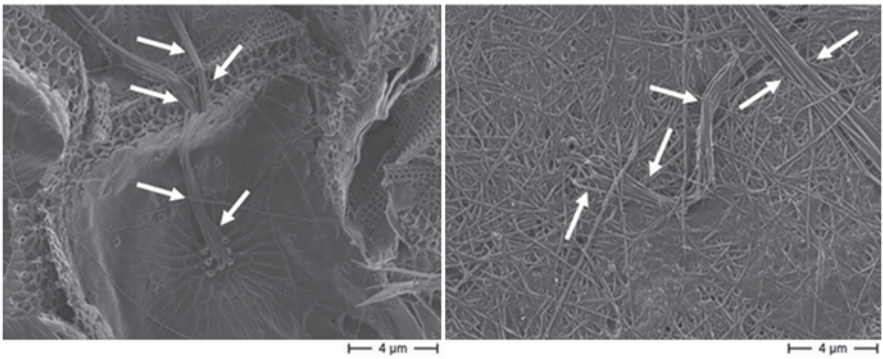

Fig. 3.7 SEM image: the cell of *T. rotula* prior (*left*) after 48 h of demineralization using 2.5 M NaOH at 37 °C. The presence of both, chitinous threads (*arrows*) and nano fibrils from dissolved cell wall are well visible

presented below (Figs. 3.7, 3.8 and 3.9) show that a nano structured chitinous network also is the base organic matrix for this diatom. The role of chitin in biosilicification in diatoms is still an open question. It was reported (Spinde et al. 2011) that poly-GlcNAc of diatomaceous origin can be biomimetically effectively silicified using such precursor as orthosilicic acid at pH 5.5. The silica-poly-GlcNAc nano composites obtained in this way show a homogeneous poly-GlcNAc dispersion. Evidence with regard to the preferential role of the OH group located at carbon position C-6 in the interaction between poly-GlcNAc and silica, that occur via hydrogen bonding, was obtained using solid-state ^{13}C NMR spectroscopy. In contrast to the situation observed for positively charged polymers, this weak interaction does not result in an acceleration of the silica poly-condensation process.

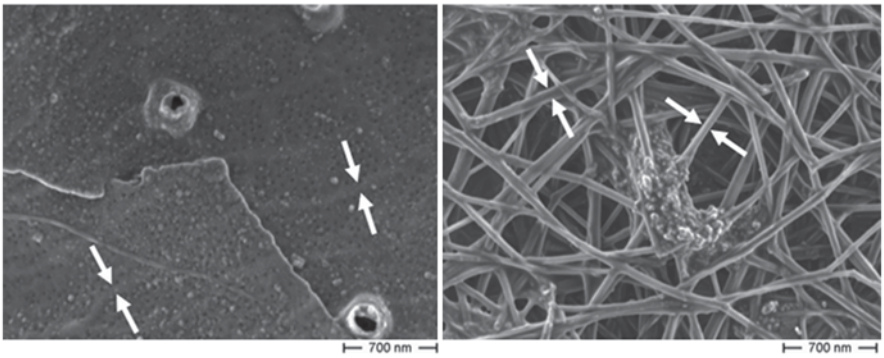

Fig. 3.8 SEM image: the nano fibrillar network of chitinous origin is well visible within cell walls of *T. rotula* prior (*left*) and after (*right*) alkali-based demineralization

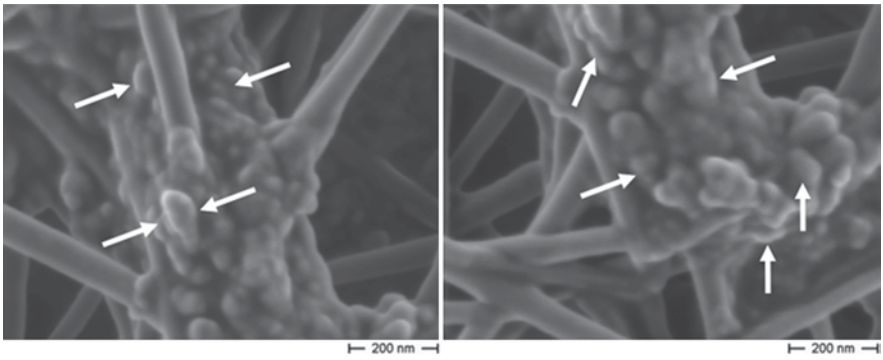

Fig. 3.9 SEM image: residual nanoparticles of silica (*arrows*) are tightly attached to the surface of chitinous nano fibers visible after gentle demineralization of *T. rotula* cells in alkaline solution at 37 °C

3.1.4 Discussion

Organic matter definitively plays a crucial role as principal structural material in diatoms' cell walls. The history of its investigation is long. Thus, as reported by Mangin (1908), the first mention of the structural association of organic membrane with the siliceous valves of diatoms was made by Bailey in 1851. The staining test prepared by Mangin showed absence of cellulose within frustules of diatoms. However, staining of selected diatoms specimens with methylene blue, naphthyl blue, ruthenium red, neutral red, safranin and alum haematoxylin showed positive results with respect to pectin. Also, after dissolution of siliceous cell walls with HF, some kind of "pectic" membranes and external envelopes, gelatinous pads and tubes remained.

Similar results were reported later also by Liebisch (1929). However, according to the modern points of view analyzed above, there is no "pectine route" confirmed

experimentally for diatom cell walls' silicification. Furthermore, Joyce Lewin reported in 1955 that cells of *Navicula pelliculosa* synthetized a gelatinous capsule after cell division. This phenomenon has been observed if phosphorus, nitrogen, or silica were eliminated from the culture medium. Capsular material was extracted using procedure, which is based on its solubility in 20 % sodium hydroxide. Finally, some kind of glucuronic acid—based biopolymer has been identified (Lewin 1955).

From the chronological point of view, the study of organic templates which are likely to be involved in biosilicification in diatoms, is a history of demineralization techniques. In contrast to naturally occurring dissolution of diatom cell walls in natural habitats (see for review Ehrlich et al. 2010b), all experiments in vitro were based on chemical reagents including HF- or alkali-based techniques. It can be suggested that the use of some novel reagents will result in the discovery of novel peptides or proteins. Probably, the best way to obtain true understanding about the biosilicification phenomenon in diatoms can be based on future joint projects, which will include experts in genomics, proteomics and molecular biology of these algae together with chemists and material scientists.

Another important aspect of the findings shown in this overview is that all the organic components presented here will certainly have an effect on the material properties of diatom silica. Since evolutionary processes, such as selection pressure caused by mechanical attacks of predators, are active on the finished frustule, it follows that nature, amount and orientation of the organic material within the frustule must be designed to optimize material properties. Therefore, it can be assumed that the formation process must be efficiently controlled by diverse organic components which are, at the same time, responsible for superior material properties.

Although the material properties of diatom silica are largely unknown, since only indirect data is available, first results suggest that the material properties (ultimate strength) are much better than those of hydrated silica (opal), which occupies more than 90 % of the volume (Round et al. 1990; Hamm et al. 2003). A similar effect has been described for nacre of abalone, where the strength is increased by a factor of 3000 compared to the most important component (aragonite). An understanding of the diatom frustule as a complete mechanical system would require detailed research on its nanostructure, chemical composition, and overall geometry. Compared to nacre, the spatial resolution of the analyses will have to be much higher, but recent developments of analytical methods, such as TOF-SIMS and Nano-SIMS, will enable us to analyze quality, quantity, and location of structural components of the diatom frustule in detail. Finally, the integration of an efficient formation process with superior material properties and geometry is an achievement which is highly attractive for a transfer into technological application. If successful, such a transfer could even improve the currently evolving techniques of rapid manufacturing.

Acknowledgements H.E. is very grateful to the German Research Foundation (DFG, Project EH 394/1) for financial support as well as to Vasily V. Bazhenov and Alexey Rusakov for their technical assistance. We cordially thank Alex Kraberg and Karen Wiltshire for specimens of *T. rotula* and Diana Krawczyk for images of *T. rotula*. Kevin McCartney is acknowledged for the revision of the English language of the manuscript.

References

Al-Sawalmih A (2007) Crystallographic texture of the arthropod cuticle using synchrotron wide angle X-ray diffraction. PhD Thesis, Rheinisch-westfälische Technische Hochschule Aachen

Armbrust EV et al (2004) The genome of the diatom *Thalassiosira pseudonana*: ecology, evolution, and metabolism. Science 306:79–86

Atkins EDT (1985) Conformation in polysaccharides and complex carbohydrates. J Biosci 8:375–387

Blackwell J (1973) Chitin. In: Walton AG, Blackwell J (eds) Biopolymers. Academic Press, New York, pp 474–489

Blackwell J, Parker KD, Rudall KM (1965) Chitin in pogonophore tubes. J Mar Biol Assoc UK 45:659–661

Blackwell J, Parker KD, Rudall KM (1967) Chitin fibres of the diatoms *Thalassiosira fluviatilis* and *Cyclotella cryptica*. J Mol Biol 28:383–385

Brunner E, Richthammer P, Ehrlich H et al (2009) Chitin-based organic networks: an integral part of cell wall biosilica in the diatom *Thalassiosira pseudonana*. Angew Chem Int Ed Engl 48(51):9724–9727

Cha JN, Shimizu K, Zhou Y, Christiansen S, Chmelka BF, Stucky GD, Morse DE (1999) Silicatein filaments and subunits from a marine sponge direct the polymerization of silica and silicones in vitro. Proc Natl Acad Sci U S A 96:361–365

De Yoreo JJ, Vekilov P (2003) Principles of crystal nucleation and growth. Rev Miner Geochem 54:57–93

Durkin CA, Mock T, Armbrust EV (2009) Chitin in diatoms and its association with the cell wall. Eukaryot Cell 8:1038–1050

Dweltz NE, Colvin JR, McInnes AG (1968) Studies on chitin (b-(1-4)-linked 2-acetamido-2-deoxy-D-glucan) fibers from the diatom *Thalassiosira fluviatilis*, Hustedt. III. The structure of chitin from X-ray diffraction and electron microscope observations. Can J Chem 46:1513–1521

Ehrlich H (2010a) Biological materials of marine origin. Invertebrates. Springer, New York, p 594

Ehrlich H (2010b) Chitin and collagen as universal and alternative templates in biomineralization. Int Geol Rev 52:661–699

Ehrlich H, Worch H (2007a) Collagen, a huge matrix in glass-sponge flexible spicules of meter-long *Hyalonema sieboldi*. In: Bäuerlein E (ed) Handbook of biomineralization vol. 1. The biology of biominerals structure formation, chapter 2. Wiley VCH, Weinheim, pp 23–41

Ehrlich H, Worch H (2007b) Sponges as natural composites: from biomimetic potential to development of new biomaterials. In: Custodio MR, Lobo-Hajdu G, Hajdu E, Muricy G (eds) Porifera research- biodiversity, innovation & sustainability. Museu Nacional, Rio de Janeiro, pp 303–312

Ehrlich H, Ereskovsky AV, Vyalikh DV, Molodtsov SL, Mertig M, Göbel C, Simon P, Hanke T, Heinemann S, Krylova DD, Pompe W, Worch H (2007a) Collagen in natural fibres of deep-sea glass sponge. In: Arias JL, Fernandez MS (eds) Biomineralization: from paleontology to materials science. Editorial Universitaria, Santiago de Chile, pp 439–448

Ehrlich H, Krautter M, Hanke T et al (2007b) First evidence of the presence of chitin in skeletons of marine sponges. Part II. Glass sponges (Hexactinellida: Porifera). J Exp Zool B Mol Dev Evol 308B:473–483

Ehrlich H, Heinemann S, Heinemann C, Bazhenov VV, Shapkin NP, Simon P, Tabachnick KD, Worch H, Hanke T (2008a) Nanostructural organisation of naturally occurring composites: Part I. Silica-collagen-based biocomposites. J Nanomat (available online doi:10.1155/2008/623838)

Ehrlich H, Janussen D, Simon P, Heinemann S, Bazhenov VV, Shapkin NP, Mertig M, Erler C, Born R, Worch H, Hanke T (2008b) Nanostructural organisation of naturally occuring composites: part II. Silica-chitin-based biocomposites. J Nanomat (available online doi:10.1155/2008/670235)

Ehrlich H, Koutsoukos PG, Demadis KD, Pokrovsky OS (2008c) Principles of demineralization: modern strategies for the isolation of organic frameworks. Part I. Common definitions and history. Micron 39:1062–1091

Ehrlich H, Deutzmann R, Capellini E, Koon H, Solazzo C, Yang Y, Ashford D, Thomas- Oates J, Lubeck M, Baessmann C, Langrock T, Hoffmann R, Wörheide G, Reitner J, Simon P, Ereskovsky AV, Mertig M, Vyalikh DV, Molodtsov SL, Worch H, Brunner E, Smetacek V, Collins M (2010a) Mineralization of the meter-long biosilica structures of glass sponges is template on hydroxylated collagen. Nat Chem 2:1084–1088

Ehrlich H, Demadis K, Pokrovsky O, Koutsoukos P (2010b) Modern views on desilicification: biosilica and abiotic silica dissolution in natural and artificial environments. Chem Rev 110:4656–4689

Exposito J-Y, Cluzel C, Garrone R, Lethias C (2002) Evolution of collagens. Anat Rec 268:302–316

Gaill F, Persson J, Sugiyama P, Vuong R, Chanzy H (1992) The chitin system in the tubes of deep sea hydrothermal vent worms. J Struct Biol 109:116–128

Gifford DJ, Bohrer RN, Boyd CM (1981) Spines on diatoms: do copepods care? Limnol Oceanogr 26(6):1057–1061

Gooday GW, Woodman J, Casson EA, Browne CA (1985) Effect of nikkomycin on chitin spine formation in the diatom *Thalassiosira fluviatilis*, and observations on its peptide uptake. FEMS Microbiol Lett 28:335–340

Goodrich JD, Winter WT (2007) Alpha-chitin nanocrystals prepared from shrimp shells and their specific surface area measurement. Biomacromolecules 8:252–257

Gordon R, Parkinson J (2005) Potential roles for diatomists in nanotechnology. J Nanosci Nanotechnol 5:35–40

Hamm CE, Smetacek V (2007) Armor: why, when and how? In: Falkowski P, Knoll A (eds) Evolution of primary producers in the sea. Elsevier, San Diego, pp 311–332

Hamm CE, Merkel R, Springer O, Jurkojc P, Maier C, Prechtel K, Smetacek V (2003) Architecture and material properties of diatom shells provide efficient mechanical protection. Nature 421:841–843

Hattori S, Adachi E, Ebihara T, Shirai T, Someki I, Irie S (1999) Alkali-treated collagen retained the triple helical conformation and ligand activity for the cell adhesion. J Biochem 125:676–684

Hecky RE, Mopper K, Kilham P, Degens ET (1973) The amino acid and sugar composition of diatom cell-walls. Mar Biol 19:323–331

Herth W (1978) A special chitin-fibril-synthesizing apparatus in the centric diatom *Cyclotella*. Naturwissenschaften 65:260–261

Herth W (1979) The site of β-chitin fibril formation in centric diatoms. II. The chitin-forming cytoplasmic structures. J Ultrastruct Res 68:16–27

Herth W (1980) Calcofluor white and congo red inhibit chitin microfibril assembly of *Poteriochromonas*: evidence for a gap between polymerization and microfibril formation. J Cell Biol 87:442–450

Herth W, Barthlott W (1979) The site of β-chitin fibril formation in centric diatoms. I. Pores and fibril formation. J Ultrastruct Res 68:6–15

Herth W, Zugenmaier P (1977) Ultrastructure of the chitin fibrils of the centric diatom *Cyclotella cryptica*. J Ultrastruct Res 61:230–239

Herth W, Kuppel A, Schnepf E (1977) Chitinous fibrils in the lorica of the flagellate chrysophyte *Poteriochromonas stipitata* (syn. *Ochromonas malhamensis*). J Cell Biol 72:311–321

Herth W, Mulisch M, Zugenmaier P (1986) Comparison of chitin fibril structure and assembly in three unicellular organisms. In: Muzzarelli R, Jeuniaux C, Gooday GW (eds) Chitin in nature and technology. Plenum Publishing Corporation, New York, pp 107–120

Kamada T, Takemaru T, Prosser JI, Gooday GW (1991) Right and left helicity of chitin microfibrils in stipe cells in *Coprinus cinereus*. Protoplasma 165:64–70

Kamatani A (1971) Physical and chemical characteristics of biogenous silica. Mar Biol 8:89–95

Kröger N, Paulsen N (2008) Diatoms—from cell wall biogenesis to nanotechnology. Annu Rev Genet 42:83–107

Kröger N, Sandhage KH (2010) From diatom biomolecules to bioinspired syntheses of silica- and titania-based materials. MRS Bull 35:122–126

Kröger N, Sumper M (1998) Diatom cell wall proteins and the cell biology of silica biomineralization. Protist 149:213–219

Kröger N, Sumper M (2004) The molecular basis of diatom biosilica formation. In: Baeueurlein E (ed) Biomineralization, 2nd edn. Wiley-VCH, Weinheim, pp 137–158
Kröger N, Bergsdorf C, Sumper M (1994) A new calcium binding glycoprotein family constitutes a major diatom cell wall component. EMBO J 13:4676–4683
Kröger N, Bergsdorf C, Sumper M (1996) Frustulins: domain conservation in a protein family associated with diatom cell walls. Eur J Biochem 239:259–264
Kröger N, Lehmann G, Rachel R, Sumper M (1997) Characterization of a 200-kDa diatom protein that is specifically associated with a silica-based substructure of the cell wall. Eur J Biochem. 250:99–105
Kröger N, Deutzmann R, Sumper M (1999) Polycationic peptides from diatombiosilica that direct silica nanosphere formation. Science 286:1129–1132
Kröger N, Deutzmann R, Bergsdorf C, Sumper M (2000) Species-specific polyamines from diatoms control silica morphology. Proc Natl Acad Sci U S A 97:14133–38
Kröger N, Lorenz S, Brunner E, Sumper M (2002) Self-assembly of highly phosphorylated silaffins and their function in biosilica morphogenesis. Science 298:584–586
Lewin JC (1955) The capsule of the diatom *Navicula pelliculosa*. J Gen Microbiol 13:162–169
Lewin JC (1961) The dissolution of silica from diatom cell walls. Geochim Cosmochim Acta 21:182–189
Liebisch W (1929) Experimentelle und kritische Untersuchungen uber die Pektinmembran der Diatomeen unter besonderer Berucksichtigung der Auxosporenbildung und der Kratikularzustande. Z Bot 22:1–97
Lotmar W, Picken LER (1950) A new crystallographic modification of chitin and its distribution. Experientia 6:58–59
Mangin LA (1908) Observations sur les diatomees. Ann Sci Nut Bot Biol Veg 8:177–219
Mann S (2001) Biomineralization principles and concepts in bioinorganic materials chemistry. University Press, Oxford, p 198
Marshall KE, Robinson EW, Hengel SM, Paša-Tolić L, Roesijadi G (2012) FRET imaging of diatoms expressing a biosilica-localized ribose sensor. PLoS One 7(3):e33771
Martin R, Hild S, Walther P et al (2007) Granular chitin in the epidermis of nudibranch molluscs. Biol Bull 213:307–315
Matsunaga S, Sakai R, Jimbo M, Kamiya H (2007) Long chain polyamines (LCPAs) from marine sponge: possible implication in spicule formation. Chem Biochem 8:1729–1735
McLachlan J, McInnes AG, Falk M (1965) Studies on the chitan (chitin: poly-N acetylglucosamine) fibers of the diatom *Thalassiosira fluviatilis* Hustedt. I. Production and isolation of chitan fibers. Can J Bot 43:707–713
Müller WEG, Rothenberger M, Boreiko A, Tremel W, Reiber A, Schröder HC (2005) Formation of siliceous spicules in the marine demosponge *Suberitues domuncula*. Cell Tissue Res 321(2):285–297
Nakajima T, Volcani BE (1969) 3,4-dihydroxyproline, a new amino acid from diatom cell walls. Science 164:1400–1401
Patwardhan SV (2011) Biomimetic and bioinspired silica: recent developments and applications. Chem Commun 47:7567–7582
Patwardhan S, Patwardhan G, Perry CC (2007) Interactions of biomolecules with inorganic materials: principles, applications and future prospects. J Mater Chem 17:2875–2884
Reimann BEF, Lewin JC, Volcani BE (1965) Studies on the biochemistry and fine structure of silica shell formation in diatoms. I. The structure of the cell wall of *Cylindrotheca fusiformis* Reimann and Lewin. J Cell Biol 24:39–55
Reimann BEF, Lewin JC, Volcani BE (1966) Studies on the biochemistry and fine structure of silica shell formation in diatoms. II. The structure of the cell wall of *Navicula pelliculosa* (Breb.) Hilse. J Phycol 2:74–84
Revol J-F, Chanzy H (1986) High-resolution electron microscopy of β-chitin microfibrils. Biopolymers 25:1599–1601
Rinaudo M (2006) Chitin and chitosan: properties and applications. Prog Polym Sci 31:603–632

Round FE, Crawford RM, Mann DG (1990) The diatoms: biology and morphology of the genera. Cambridge University Press, Cambridge, pp 747

Rudall KM (1955) The distribution of collagen and chitin. In: Brown R, Danielli JF (eds) Fibrous proteins and their biological significance. Symposia of society of experimental biology, No. IX, University Press, Cambridge, pp 49–71

Rudall KM (1969) Chitin and its association with other molecules. J Polym Sci 28:83–102

Rudall KM, Kenchington W (1973) The chitin system. Biol Rev 49:597–636

Sadava D, Volcani BE (1977) Studies on the biochemistry and fine structure of silica shell formation in diatoms formation of hydroxyproline and dihydroxyproline in *Nitzschia angularis*. Planta 135:7–11

Scheffel A, Poulsen N, Shian S, Kröger N (2011) Nanopatterned protein microrings from a diatom that direct silica morphogenesis. Proc Natl Acad Sci U S A 108:3175–3180

Schumacher MA, Mizuno K, Bachinger HP (2006) The crystal structure of a collagen-like polypeptide with 3(S)-hydroxyproline residues in the Xaa position forms a standard 7/2 collagen triple helix. J Biol Chem 281:27566–27574

Sheppard V, Scheffel A, Poulsen N, Kröger N (2012) Live diatom silica immobilization of multimeric and redox-active enzymes. Appl Environ Microbiol 78:211–218

Spinde K, Kammer M, Freyer K et al (2011) Biomimetic silicification of fibrous chitin from diatoms. Chem Mater 23:2973–2978

Subburaman K, Pernodet N, Kwak SY et al (2006) Templated biomineralization on self-assembled protein fibers. Proc Natl Acad Sci U S A 103:14672–14677

Sugiyama J, Boisset C, Hashimoto M, Watanabe T (1999) Molecular directionality of β-chitin biosynthesis. J Mol Biol 286:247–255

Sumper M (2002) A phase separation model for the nanopatterning of diatom biosilica. Science 295:2430–2433

Sumper M, Brunner E (2006) Learning from diatoms: nature's tools for the production of nanostructured silica. Adv Funct Mat 16:17–26

Tesson B, Hildebrand M (2010) Extensive and intimate association of the cytoskeleton with forming silica in diatoms: control over patterning on the meso- and micro-scale. PLoS One 5(12):e14300

Tilburey GE, Patwardhan SV, Huang J et al (2007) Are hydroxyl-containing biomolecules important in biosilicification? A model study. J Phys Chem B 111:4630–4638

van de Poll WH, Vrieling EG, Gieskes WWC (1999) Location and expression of frustulins in the pennate diatoms *Cylindrotheca fusiformis*, *Navicula pelliculosa*, and *Navicula salinarum* (Bacillariophyceae). J Phycol 35:1044–1053

Vincent JVC (2002) Arthropod cuticle: a natural composite shell system. Composites A 33(10):1311–1321

Vournakis J, Pariser ER, Finkielsztein S, Helton M (1997a) Poly-N-acetyl glucosamine. US patent # 5,623,064. Issued April 22, 1997

Vournakis J, Pariser ER, Finkielsztein S, Helton M (1997b) Method of isolating Poly-N-acetyl glucosamine from microalgal culture. US Patent # 5,622,834. Issued April 22, 1997

Walsby AE, Xypolyta A (1977) The form resistance of chitan fibers attached to the cells of *Thalassiosira fluviatilis* Hustedt. Br Phycol J 12:215–223

Weaver JC, Morse DE (2003) Molecular biology of demosponge axial filaments and their roles in biosilicification. Microsc Res Tech 62:356–367

Wenzl S, Hett R, Richthammer P, Sumper M (2008) Silacidins: highly acidic phosphopeptides from diatom shells assist in silica precipitation in vitro. Angew Chem 47:1729–1732

Wieneke R, Bernecker A, Riedel R, Sumper M, Steinem C et al (2011) Silica precipitation with synthetic silaffin peptides. Org Biomol Chem 9:5482–5486

Yang W, Lopez PJ, Rosengarten G (2011) Diatoms: self assembled silica nanostructures, and templates for bio/chemical sensors and biomimetic membranes. Analyst 136:42–53

Chapter 4
Mandibular Gnathobases of Marine Planktonic Copepods—Structural and Mechanical Challenges for Diatom Frustules

Jan Michels and Stanislav N. Gorb

4.1 Significance of Copepods in Marine Pelagic Food Webs

Crustaceans of the subclass Copepoda (Fig. 4.1) inhabit an impressively large variety of aquatic habitats (e.g. Huys and Boxshall 1991). In all regions of the earth they can be found in almost any body of water including habitats with extreme conditions such as the deep sea, active hot hydrothermal vents and very cold sea ice. Copepods are expected to contribute the largest amount of individuals to the metazoans, even larger than those contributed by insects and nematodes (Hardy 1970; Humes 1994). In the marine pelagial the abundance of copepods is particularly pronounced. As a result of this, in all ocean areas worldwide copepods represent the most numerous zooplankton group contributing 55–95 % of the total zooplankton individuals (Longhurst 1985). The diet of many copepod species contains large proportions of phytoplankton, and copepods are an important food source for various fish species and a large number of other organisms feeding on zooplankton. Accordingly, due to their dominance within the zooplankton, copepods are the main primary consumers and significant links between the primary producers and organisms of higher trophic levels. As such, they represent important food web components and very probably key organisms for processes such as carbon cycling and nutrient regeneration in the marine pelagial (e.g. Verity and Smetacek 1996; Turner 2004). In many ocean areas, diatoms account for a large proportion of the phytoplankton (e.g. Verity and Smetacek 1996; Smetacek 1999; Armbrust 2009 and citations therein). For this reason they often are an important food source for copepods, and the knowledge

J. Michels (✉) · S. N. Gorb
Department of Functional Morphology and Biomechanics, Institute of Zoology, Christian-Albrechts-Universität zu Kiel, Am Botanischen Garten 1–9, 24118 Kiel, Germany
e-mail: jmichels@zoologie.uni-kiel.de

J. Michels
Biological Oceanography, GEOMAR Helmholtz Centre for Ocean Research Kiel, Düsternbrooker Weg 20, 24105 Kiel, Germany
e-mail: jmichels@geomar.de

C. Hamm (ed.), *Evolution of Lightweight Structures,* Biologically-Inspired Systems 6,
DOI 10.1007/978-94-017-9398-8_4

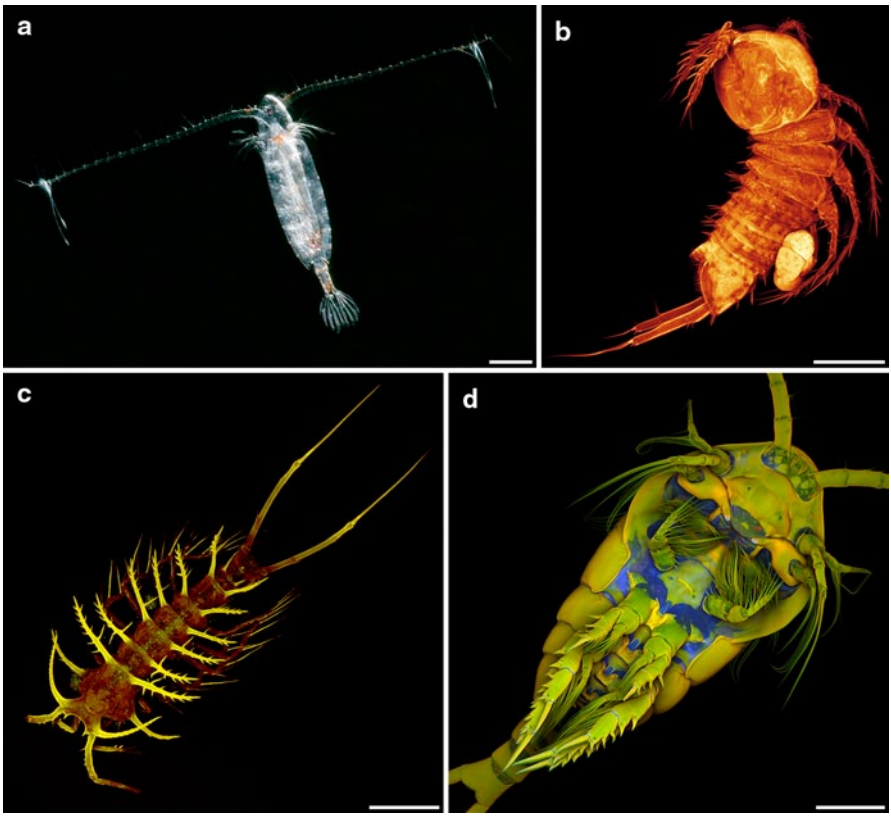

Fig. 4.1 Exemplary copepod species. **a** Female of *Calanoides acutus*, one of the dominant calanoid copepod species within the zooplankton of the Southern Ocean (dorsal view). **b** Female of the harpacticoid copepod genus *Mesocletodes*, collected from deep-sea sediment in the Southern Ocean (lateral view). **c** Female of *Ceratonotus steiningeri*, a harpacticoid deep-sea copepod species, collected from sediment in the Angola Basin at a water depth of 5389 m (dorsal view). **d** Female of the planktonic calanoid copepod species *Temora longicornis*, collected in the North Sea (ventral view). Scale bars = 1 mm (**a**), 100 µm (**b**, **c**), 200 µm (**d**). **a** Photograph (courtesy of Ingo Arndt). **b**–**d** Confocal laser scanning micrographs (maximum intensity projections). **b**–**d** Adapted from Michels and Büntzow (2010), Michels (2013) and Michels and Gorb (2012) with permission

of feeding interactions between these two groups of organisms is essential for the understanding of processes related to the food web and energy and particle fluxes in the marine pelagial.

4.2 Mandibular Gnathobases—Specific Feeding Tools with Morphologies Adapted to the Diets of the Copepods

Copepods usually possess five pairs of mouthparts (Fig. 4.2a), which are used to detect, collect and take up food organisms and particles (Koehl and Strickler 1981; Paffenhöfer et al. 1982; Strickler 1982; Price et al. 1983; Bundy and Vanderploeg

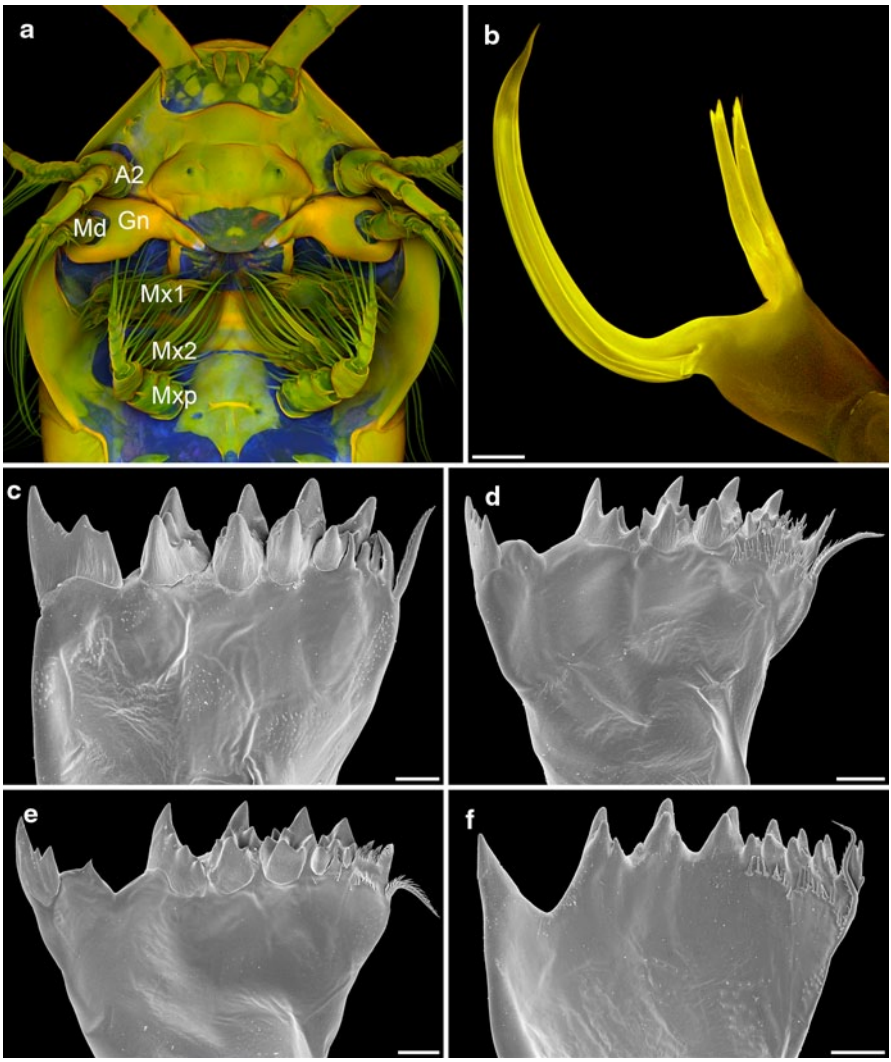

Fig. 4.2 Mouthparts and different types of mandibular gnathobases of calanoid copepods. **a** Section of the micrograph shown in Fig. 4.1d, indicating the location of the five pairs of mouthparts of *Temora longicornis*: **A2** second antenna, **Md** mandible, **Gn** mandibular gnathobase, **Mx1** first maxilla, **Mx2** second maxilla, **Mxp** maxilliped. (Only one mouthpart of each pair is marked.) **b** Confocal laser scanning micrograph (maximum intensity projection) showing the left gnathobase of a male *Heterorhabdus* sp. from the Southern Ocean (cranial view). **c**–**f** Scanning electron micrographs showing the left gnathobases from females of different Antarctic copepod species (all cranial view). **c** *Rhincalanus gigas*. **d** *Calanoides acutus*. **e** *Calanus propinquus*. **f** *Metridia gerlachei*. Scale bars = 50 µm (**b**), 25 µm (**c**–**e**), 20 µm (**f**). **b** Adapted from Michels (2007) with permission

2002; Malkiel et al. 2003; Koehl 2004). The mouthparts create water streams, so-called feeding currents, at the ventral side of the copepods' bodies and scan these currents for food organisms and particles by means of mechanoreceptors and chemoreceptors. After detection, the organisms and particles are evaluated with the aid

of these receptors, and the favoured ones are moved to the stoma of the copepods by additional movements of the mouthparts. Subsequently, the food items are grabbed and, if necessary, crushed and minced by the mandibular gnathobases, the basal parts of the mandibles, before being ingested. While, in general, the morphology of the mouthparts differs between species with different diets (e.g. Anraku and Omori 1963; Arashkevich 1969; Schnack 1989; Ohtsuka and Onbé 1991), the differences in the morphology of the mandibular gnathobases are particularly pronounced and clearly related to the diet of the respective copepod species (e.g. Anraku and Omori 1963; Arashkevich 1969; Itoh 1970; Schnack 1989; Michels and Schnack-Schiel 2005). The different gnathobase morphologies can be classified in three main groups: (1) gnathobases of copepods that are carnivorous and feed mainly on other zooplankton organisms have relatively long and sharp tooth-like structures (called 'teeth' in the following), and the number of teeth is smaller than those of the gnathobases of the other two groups (Fig. 4.2b); (2) copepod species that mainly feed on phytoplankton possess robust gnathobases with compact and relatively short teeth at their distal ends (Fig. 4.2c–e); (3) omnivorous copepods have gnathobases with a morphology representing an ecotonal form between the morphologies of the other two groups (Fig. 4.2f). The gnathobases of the first group are often rather specialised. Prominent examples for such a specialisation are the gnathobases of the calanoid copepod genus *Heterorhabdus*. They possess only a small number of teeth, and their ventral tooth exhibits a complex morphology that is comparable to the architecture of hypodermic needles and is strongly adapted to catching, anaesthetising and killing prey organisms (Nishida and Ohtsuka 1996). This tooth is hollow and features two openings, one at its base and another one at its tip. The lumen of such a tooth is filled with venom or anaesthetic secreted from glandular cells through specific labral pores, which are located close to the opening of the tooth base when the gnathobase is in its 'inoperative position' at the labrum. The ventral tooth of the left gnathobase is exceptionally long (Fig. 4.2b), and it is easily conceivable that this tooth can be efficiently used by the carnivorous copepods to spear prey and inject the venom or anaesthetic into its body. In general, the gnathobases of the first group are suitable to pierce and tear apart the prey with their long, pointed and sharp teeth and the reduced number of teeth. By contrast, due to their short, compact and relatively numerous teeth, the gnathobases of the second group seem to be very capable of crushing stable food items such as diatoms. The teeth of these gnathobases have usually been called 'grinding teeth' (e.g. Anraku and Omori 1963). However, a grinding function of these teeth to crush for example stable diatom frustules is not very conceivable. Many of the respective gnathobase teeth possess small cusps that would clearly decrease the efficiency of such a mechanism. It is much more likely that the copepods crush food items such as diatom frustules by exerting pressure with their gnathobase teeth and thereby concentrating the force on a clearly smaller area by means of the small teeth cusps. Especially in the case of the hollow diatom frustules the application of such a punctual pressure seems to be advantageous over a grinding mechanism and likely leads to a more effective disruption of the frustule structures.

4.3 Mandibular Gnathobases with Siliceous Teeth

In many calanoid copepod species, some of the gnathobase teeth obviously consist of another material than the rest of the gnathobases. This different appearance can easily be shown in an ordinary way by bright-field microscopy, and it becomes clearly evident when the gnathobases are visualized with scanning electron microscopy (e.g. Figs. 4.2c–e, 4.3a, 4.3c–e, 4.5a, 4.6a). Already several decades ago the application of simple preparation methods and microscopy techniques resulted in the assumption that such teeth are composed of silica (Beklemishev 1954). However, it was not until many years later that the presence of gnathobase tooth structures with similar material properties was mentioned and described for additional

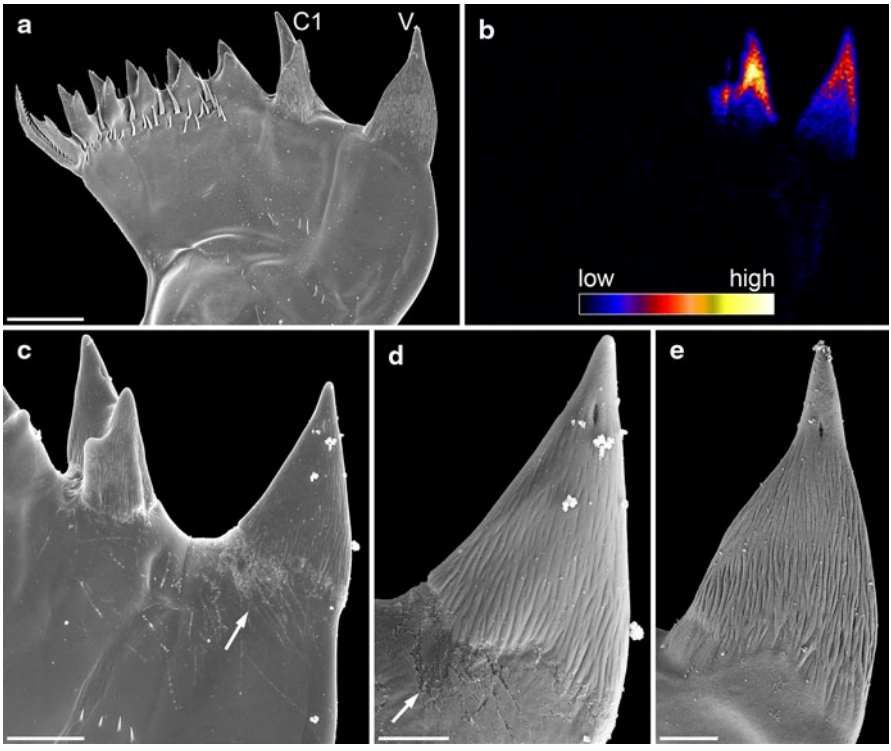

Fig. 4.3 Mandibular gnathobases of female *Centropages hamatus*. **a**, **c**–**e** Scanning electron micrographs (all cranial view). **a** Overview of the distal part of a gnathobase. **c** Overview of the ventral part of the distal gnathobase structures. **d** Detailed view of the ventral tooth shown in **c**. **e** Detailed view of the ventral tooth shown in **a**. **b** µ-PIXE mapping showing the distribution and concentration of silicon in the distal part of a gnathobase. The orientation of the gnathobase is similar to that of the gnathobase shown in **a**. The results of the elemental analysis indicate that the ventral tooth (**V**) and the first central tooth (**C1**) contain silica. Arrows indicate areas with a large number of scratches. Scale bars = 20 µm (**a**), 10 µm (**c**), 5 µm (**d**, **e**). Figure reproduced from Michels et al. (2012) with permission

copepod species (Sullivan et al. 1975; Vyshkvartseva 1975; Miller et al. 1980), and not earlier than several additional years later the application of microprobe and electron diffraction analyses confirmed the presence of silica in such teeth (Miller et al. 1990). The analyses indicated that the silica is present in the teeth in the form of opal, a hydrated amorphous type of silica. For this reason, the term 'opal teeth' was established. The application of both differential interference contrast microscopy and transmission electron microscopy revealed the morphogenesis of the siliceous teeth (Miller et al. 1990). They develop early in the pre-moult phase of the moult cycle. After the formation of fibrous tooth moulds, these moulds are connected via ducts to glandular tissue located in the proximal part of the gnathobase. It is assumed that unpolymerised silicic acid is released by this gland tissue and transported inside the ducts to the moulds where the silicification takes place. The final siliceous crown-like or cap-like structures are located on a socket consisting of chitinous exoskeleton material (Fig. 4.6b).

Recent studies revealed new insights into the architecture of the siliceous teeth. While the presence of silica in the gnathobase teeth was confirmed with modern high-resolution elemental analysis techniques and confocal laser scanning microscopy (Bechstein et al. 2011; Michels et al. 2012, 2015; Figs. 4.3b, 4.4c–e, 4.5b+d), the results of high-resolution transmission electron microscopy analyses clearly indicate that large proportions of the silica in the gnathobase teeth exhibit a nanocrystalline structure and consequently are not present in the form of amorphous opal (Michels et al. 2015). Evidence for a crystalline structure of the siliceous teeth had already been mentioned earlier but unfortunately without showing and describing any results (Miller et al. 1980). The recent analyses showed that the crystalline silica material present in the siliceous teeth is consistent with the mineral α-cristobalite (Michels et al. in 2015).

In nature, silica biomineralisation typically takes place on organic matrices composed of chitin or collagen that are preferential sites for nucleation and control the formation of the silica structures (see Ehrlich 2010). Siliceous diatom frustules, for example, contain an internal organic network of cross-linked chitin fibres that is assumed to be a scaffold for silica deposition (Brunner et al. 2009). After chemical removal of the silica from the gnathobases or fracturing the siliceous cap-like structures fibre networks become visible in the siliceous gnathobase teeth (Michels et al. 2015; Fig. 4.6b+c). The fibres are similar in appearance to those present in the diatom frustules, and they were shown to also be chitinous (Michels et al. 2015). It is very likely that the fibre networks serve as templates or scaffolds during the silicification process and are congruent with the fibrous tooth moulds mentioned above.

The silica-containing structures in the copepod gnathobases likely increase the mechanical strength and stability of the gnathobase teeth, and they are assumed to have coevolved with the siliceous diatom frustules (e.g. Hamm et al. 2003; Michels et al. 2012). For copepod species that mainly feed on phytoplankton this is certainly conceivable. However, the presence of silica in gnathobase teeth of carnivorous copepods (see Nishida and Ohtsuka 1996) suggests that siliceous teeth represent

an adaptation to frequent mechanical loads in general. In this context, the degree of silicification seems to be related to the mechanical stability of the main food items and thereby to the intensity of the prevalent loads. In siliceous teeth such as the cannula-like ones of *Heterorhabdus* spp. that are likely exposed to relatively moderate forces only the silica-containing structures are relatively small and not particularly pronounced (see Nishida and Ohtsuka 1996). By contrast, siliceous teeth regularly facing strong mechanical interactions with diatom frustules, which can be mechanically very stable (Hamm et al. 2003) and thus cause high forces affecting the teeth during feeding, typically exhibit very pronounced silica-containing structures, which seem to be rather compact and stable (e.g. Michels and Schnack-Schiel 2005; Figs. 4.2c–e, 4.5a, 4.6a). For this reason a coevolution between diatom frustules and gnathobases with very pronounced siliceous teeth is very likely.

Already relatively long ago the question regarding the origin of the silica in the gnathobase teeth arose (Sullivan et al. 1975). There are two potential sources. The copepods could either take up silicic acid from the seawater where it is present in all ocean areas (Tréguer et al. 1995; Pilson 2012), or they could utilise the silica that they ingest when they feed on diatoms or other copepods with siliceous teeth for the formation of their own siliceous teeth. Laboratory experiments showed that the copepods take up silicic acid from the seawater and are able to cover their silicon demand for the formation of siliceous teeth even at rather low silicic acid concentrations (Miller et al. 1980). The results indicate that the lowest natural marine silicic acid concentrations, found in oligotrophic ocean areas, are still high enough to sufficiently supply the copepods with silicon. Nevertheless, it is imaginable that the copepods use both potential sources and, besides taking up silicic acid from the seawater, also extract silicon from their diet where it is often present in high concentrations and therefore represents an efficient source. However, this hypothesis has never been investigated so far. In a respective experiment the frustules of living diatoms could be labeled with the radioisotope ^{32}Si, and the diatoms could be fed to copepodids (juvenile copepods) to test if ^{32}Si is included in the siliceous teeth of the copepods after moulting.

Up to now the mechanical stability of the silica-containing structures of gnathobase teeth has not been analysed. Such an analysis could potentially be performed using nanoindentation. However, because of the small dimensions of the structures it would be rather difficult to get reliable results. For insect mandibles, many of which are known to contain relatively high concentrations of zinc and manganese (e.g. Hillerton et al. 1984; Quicke et al. 1998), it has been shown that the metal incorporations increase the hardness of the mandible material (Schofield et al. 2002; Cribb et al. 2008). Copepod gnathobases often exhibit scratches caused by contact with stable food items. Interestingly, these scratches are typically only found on the surfaces of the chitinous material while the surfaces of the siliceous structures seem to be resistant to such abrasive damage (Fig. 4.3c+d). This indicates that the presence of silica very likely increases the hardness and stiffness of the gnathobase teeth and thus has a similar effect as zinc and manganese have in insect mandibles.

4.4 Mandibular Gnathobases, Diatom Frustules and the Evolutionary Arms Race

In addition to the presence of strong silica-containing structures, recent detailed analyses of the material composition of copepod gnathobases yielded further indication of a coevolution between diatom frustules and very pronounced siliceous teeth. The respective analyses had been inspired by the knowledge that structures consisting of hard and stable materials easily break because of local stress concentrations under strong mechanical loads when being in contact with other hard structures (Bhushan 2000). To test the idea that the non-siliceous gnathobase parts might have evolved specific properties that reduce the risk of wear and damage of the siliceous teeth, the materials embedding and bearing these teeth were recently investigated in the two calanoid copepod species *Centropages hamatus* and *Rhincalanus gigas* both of which have diets with significant proportions of diatoms (Michels et al. 2012, 2015). Interestingly, in the gnathobases of both species exoskeleton structures with high proportions of the elastic protein resilin were discovered. The results show that the architecture of the composite structures in the gnathobase teeth is much more complex than previously assumed. In *C. hamatus*, the siliceous teeth feature a cap-like structure that contains high resilin proportions. This structure is located on top of a chitinous socket and covered by another cap-like structure containing silica (Fig. 4.4). The siliceous teeth of *R. gigas* are characterised by a silica-containing cap-like structure that is situated on top of a chitinous socket (Fig. 4.5d). At the bases of the sockets of the siliceous teeth, the gnathobase exoskeleton features high proportions of resilin (Fig. 4.5c + d), while, by contrast, in the central and proximal parts of the gnathobase the exoskeleton is dominated by chitinous material (Fig. 4.5d).

Compared with chitinous exoskeleton material, resilin is very soft and elastic (e.g. Weis-Fogh 1961; Andersen and Weis-Fogh 1964). At first view it might be surprising that hard and stiff structures, which are supposed to be adapted to crushing stable diatom frustules, are combined with very soft structures. A possible explanation is that in some cases, while the copepods feed on diatoms, the pressure acting on the tips of the siliceous teeth might result in the local stress concentrations exceeding the breaking stress level and therefore in an increased risk of crack formation in and breakage of the teeth. A mechanical system that has to resist high amounts of stress under pressure will be more effective against damage and wear if it consists of a smart combination of materials with different mechanical properties (or a gradient in the material properties) since such an architecture leads to the minimisation of the probability of local stress concentrations (e.g. Gibson and Ashby 1988; Wang and Weiner 1998). It is conceivable that the soft and elastic resilin-containing structures of the siliceous teeth function as flexible supports of the hard and stiff tooth structures. In case the breaking stress level is reached, these structures might be deformed by compression and thereby reduce stress concentrations in the tooth material. Such a mechanism likely improves the resistance of the siliceous teeth to mechanical damages. In *C. hamatus*, additional structures with high resilin proportions, located at the dorsal edge of the central part and at the ventral edge of the proximal part of the gnathobases (Fig. 4.4a–c), might have a damping function

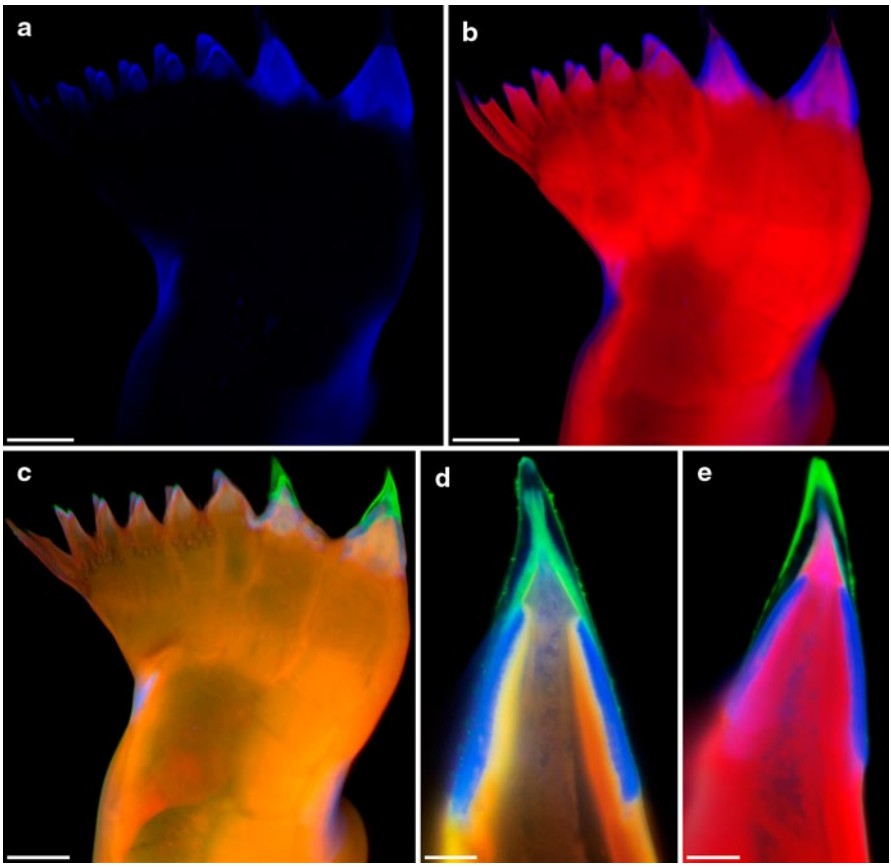

Fig. 4.4 Mandibular gnathobases of female *Centropages hamatus*. **a**–**e** Confocal laser scanning micrographs (all cranial view) (**a**–**c** maximum intensity projections showing the whole gnathobase; **d**, **e** 1-µm-thick optical sections through the ventral tooth). **a** Distribution of resilin. **b** Chitinous exoskeleton (red) and resilin-dominated structures (blue). **c**–**e** Chitinous exoskeleton (orange, red), resilin-dominated structures (blue, light blue) and silica-containing structures (green). Scale bars = 20 µm (**a**–**c**), 5 µm (**d**, **e**). Figure adapted from Michels et al. (2012) with permission

making the whole gnathobases resilient and therefore further reducing the risk of mechanical damage of the siliceous teeth.

Diatom frustules with their often complex architectures, which cause relatively high frustule stabilities and have very likely evolved to resist pressure exerted on the frustules from outside (Hamm et al. 2003), represent the most stable food items found in copepod diets. Intact diatoms can survive the passage through the guts of zooplankton organisms (Fowler and Fisher 1983). For this reason being able to crush and mince the diatom frustules is important for the copepods to better digest the diatom cells. However, successful crushing and mincing of such mechanically protected frustules demands the deployment of rather specific feeding tools. Accordingly, the presence of very complex composite tooth structures containing diverse materials such as resilin and silica supports the assumption that the respective siliceous copepod teeth have specifically coevolved with the stable diatom

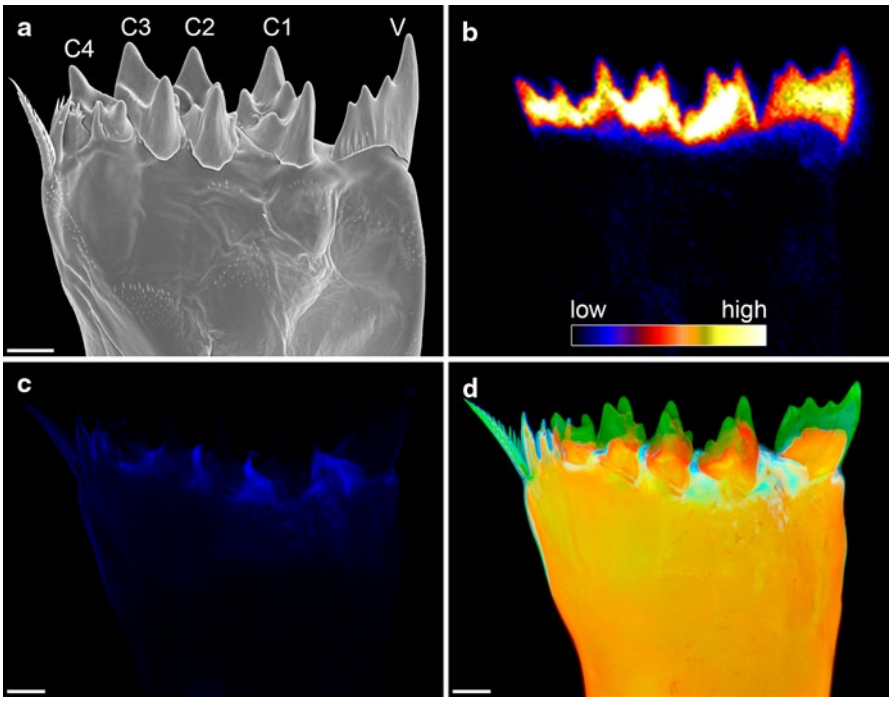

Fig. 4.5 Mandibular gnathobases of female *Rhincalanus gigas*. **a** Scanning electron micrograph showing the distal part of a gnathobase (cranial view). **b** μ-PIXE mapping showing the distribution and concentration of silicon in the distal part of a gnathobase. The orientation of the gnathobase is similar to that of the gnathobase shown in **a**. **c**, **d** Confocal laser scanning micrographs (maximum intensity projections) showing the material composition of the distal part of a gnathobase (caudal view). **c** Distribution of resilin. **d** Chitinous exoskeleton (orange), resilin-dominated structures (blue, light blue, turquoise) and silica-containing structures (green). The results indicate that the ventral tooth (**V**) and all central teeth (**C1**–**C4**) feature a silica-containing cap-like structure located on top of a chitinous socket. Scale bars = 25 μm. Figure adapted from Michels et al. (2015) with permission

frustules in an evolutionary arms race (for the explanation of the term 'arms race' see Dawkins and Krebs 1979) and enable the copepods to more efficiently feed on and utilise their main food organisms.

Plankton evolution is hypothesised to be mainly controlled by protection against specific 'attack systems' of grazers and predators, which has led to a large variety of morphologies and chemical and mechanical defence systems (Smetacek 2001). In this context, the copepod gnathobases featuring hard and stable biomineralised tooth structures with soft and elastic supports represent examples of highly-adapted 'attack systems'. A powerful operation of the gnathobases is ensured by pronounced mandibular muscles (Fig. 4.7). This combination enables the copepods to crush and mince the diatom frustules into small pieces (e.g. Turner 1978; Friedrichs et al. 2013). Large copepods such as the Antarctic species *Calanus propinquus* with pronounced siliceous teeth (Fig. 4.2e) are capable of destroying even the frustules of

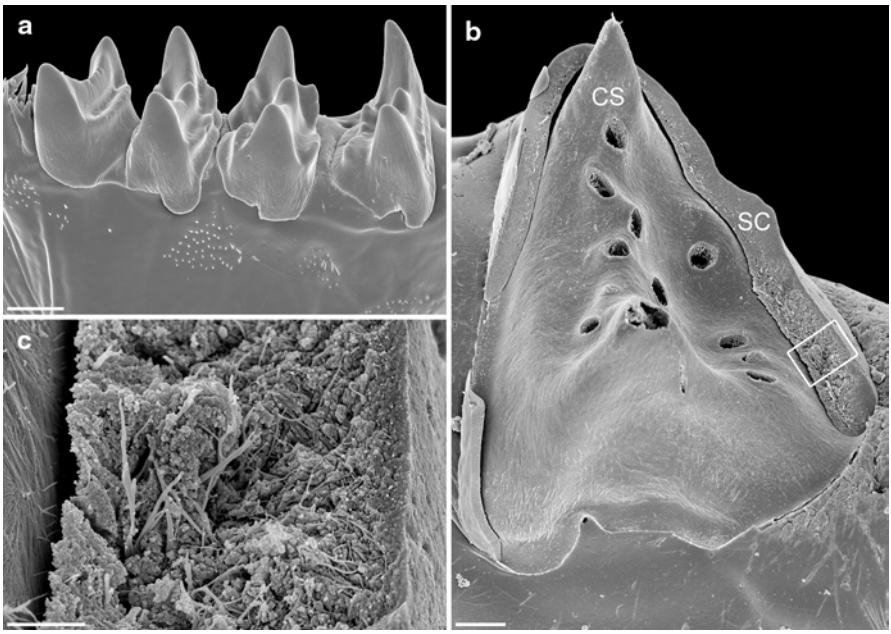

Fig. 4.6 Mandibular gnathobases of female *Rhincalanus gigas*. Scanning electron micrographs (all caudal view). **a** The four central teeth. **b** Central tooth after the removal of large parts of the silica-containing cap-like structure. **c** Detailed view of the structures marked by the rectangular frame in **b**. Scale bars = 20 µm (**a**), 5 µm (**b**), 1 µm (**c**). **CS** chitinous socket, **SC** silica-containing cap-like structure. Figure adapted from Michels et al. (2015) with permission

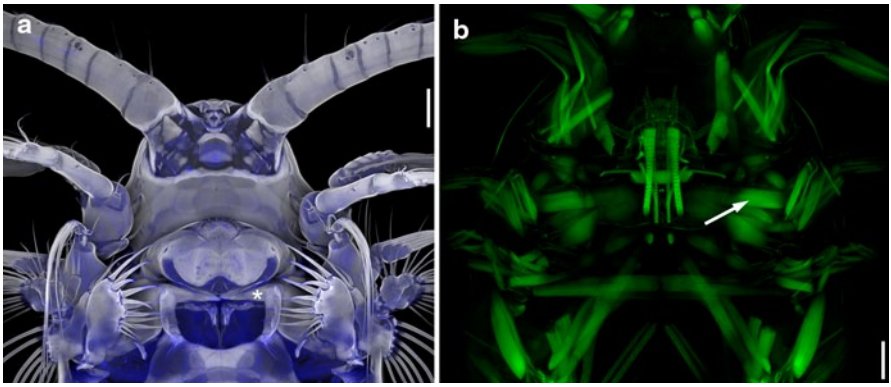

Fig. 4.7 Muscular system of the anterior part of *Centropages hamatus*. Confocal laser scanning micrographs (maximum intensity projections) showing ventral views of the exoskeleton (**a**) and the muscles (**b**) of female *C. hamatus*. Please note that the two micrographs show different sections of two different copepod specimens. The asterisk and the arrow indicate the positions of the left gnathobase and the strong muscles of the left mandible, respectively. Scale bars = 50 µm. Figure reproduced from Michels (2013) with permission

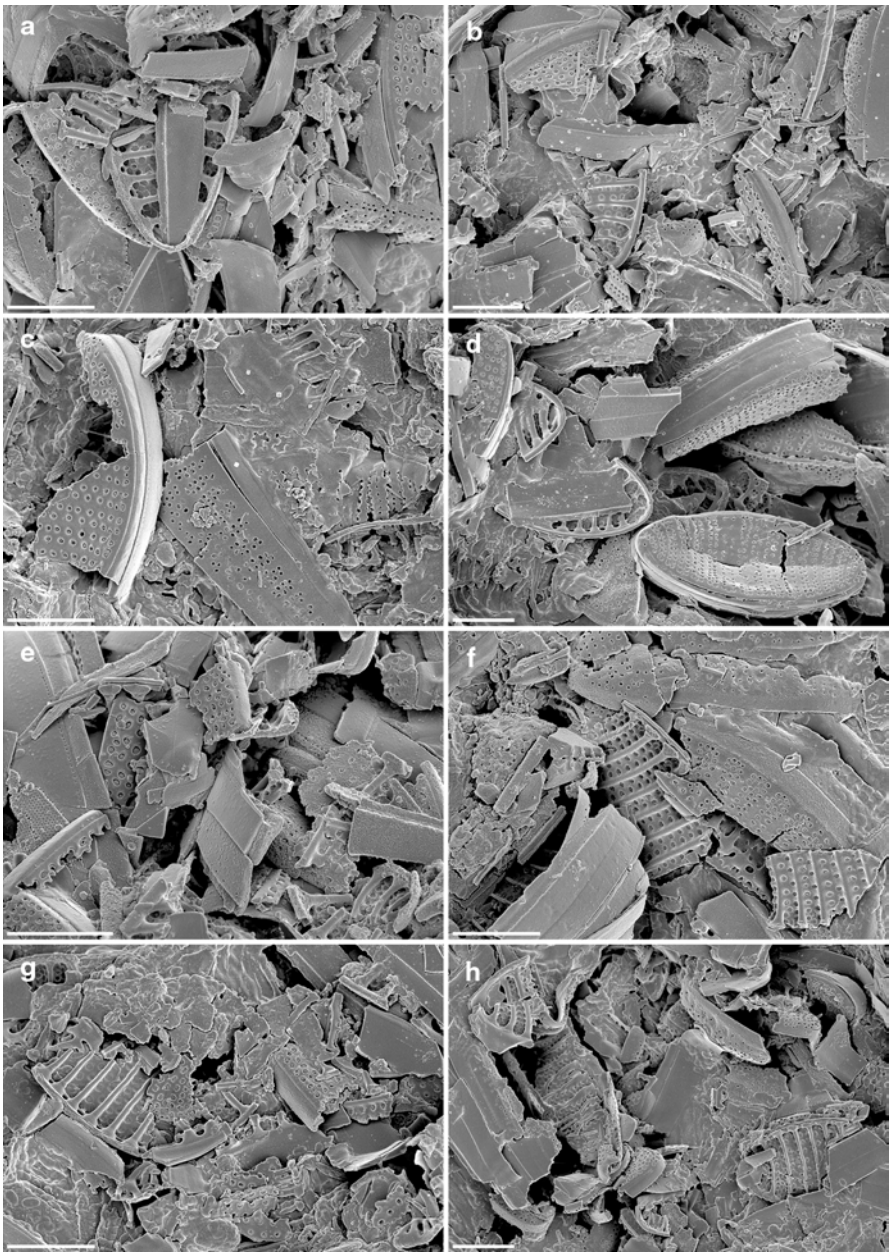

Fig. 4.8 Faecal pellets from feeding experiments with the diatom species *Fragilariopsis kerguelensis* and juveniles (copepodite stage V) of the Antarctic copepod species *Calanus propinquus*. **a**–**h** Scanning electron micrographs showing pieces of *F. kerguelensis* frustules present in the faecal pellets. Scale bars = 5 µm

the diatom *Fragilariopsis kerguelensis* (Fig. 4.8) that are particularly stable (Hamm et al. 2003). The copepods' ability to crush and mince diatom frustules certainly not only depends on the morphology and the material composition of the gnathobases but is also related to the dimensions of the copepods and their diatom food. In feeding experiments, for example, the relatively small copepod *Acartia clausi* was observed to damage only frustules of the small size fraction of the diatoms offered, while the larger species *Centropages hamatus* and *Temora longicornis* were able to also damage the frustules of the large size fractions (Friedrichs et al. 2013).

Besides their morphological adaptations, copepods exhibit specific feeding techniques and strategies enabling them to better utilise the available diatom food. Frustules of large diatoms such as *Coscinodiscus wailesii* are not always completely destroyed and ingested during feeding. *T. longicornis* was observed to break only small pieces out of the *C. wailesii* frustules, and subsequently it ingested the cell contents and dropped the frustules (Jansen 2008). In other experiments, *C. hamatus* exhibited a similar feeding strategy. While smaller *C. wailesii* frustules were broken in pieces, the large frustules were only 'opened' by breaking a hole in the girdle band, which was shown to be the frustules' weakest part (Friedrichs et al. 2013).

In general, the adapted gnathobase morphologies and material compositions combined with effective feeding techniques and strategies make copepods very powerful antagonists of diatoms in the evolutionary arms race. Copepod features such as the shape of the body, the antennae equipped with a high amount of sensors, powerful muscles enabling exceptional escape jumps, the capability to remotely detect and capture prey and efficient mate finding are assumed to be the basis for the success of the marine planktonic copepods (Kiørboe 2011). Nevertheless, it is conceivable that the development of the complex composite gnathobase structures that are adapted to efficiently capturing (or grabbing), crushing and mincing food items also accounts considerably for the dominance of the copepods observed today within the marine zooplankton.

Acknowledgements This project was financially supported by the virtual institute 'PlanktonTech' of the Helmholtz Association. Sigrid Schiel kindly provided copepod samples, and Ruth Alheit helped with the sorting of the samples. The provision of the photograph showing the live *Calanoides acutus* specimen by Ingo Arndt is gratefully acknowledged. This book chapter is adapted from the publication 'Michels J, Gorb SN (2015) Mandibular gnathobases of marine planktonic copepods—feeding tools with complex micro- and nanoscale composite architectures. Beilstein J Nanotechnol 6:674–685'.

References

Andersen SO, Weis-Fogh T (1964) Resilin. A rubberlike protein in arthropod cuticle. Adv Insect Physiol 2:1–65

Anraku M, Omori M (1963) Preliminary survey of the relationship between the feeding habit and the structure of the mouth-parts of marine copepods. Limnol Oceanogr 8:116–126

Arashkevich YeG (1969) The food and feeding of copepods in the northwestern Pacific. Oceanology 9:695–709

Armbrust EV (2009) The life of diatoms in the world's oceans. Nature 459:185–192

Bechstein K, Michels J, Vogt J, Schwartze GC, Vogt C (2011) Position-resolved determination of trace elements in mandibular gnathobases of the Antarctic copepod *Calanoides acutus* using a multimethod approach. Anal Bioanal Chem 399:501–508

Beklemishev KV (1954) The discovery of silicious formations in the epidermis of lower crustacea (in Russian). Dolk Akad Nauk SSSR 97:543–545 (english translation by McLean CA, Trans. 29, Ministry of Agriculture, Fisheries and Food)

Bhushan B (2000) Modern tribology handbook, 2. CRC Press, Boca Raton

Brunner E, Richthammer P, Ehrlich H, Paasch S, Simon P, Ueberlein S, van Pée K-H (2009) Chitin-based organic networks: an integral part of cell wall biosilica in the diatom *Thalassiosira pseudonana*. Angew Chem Int Ed Engl 48:9724–9727

Bundy MH, Vanderploeg HA (2002) Detection and capture of inert particles by calanoid copepods: the role of the feeding current. J Plankton Res 24:215–223

Cribb BW, Stewart A, Huang H, Truss R, Noller B, Rasch R, Zalucki MP (2008) Insect mandibles—comparative mechanical properties and links with metal incorporation. Naturwissenschaften 95:17–23

Dawkins R, Krebs JR (1979) Arms races between and within species. Proc R Soc Lond B 205:489–511

Ehrlich H (2010) Chitin and collagen as universal and alternative templates in biomineralization. Int Geol Rev 52:661–699

Fowler SW, Fisher NS (1983) Viability of marine phytoplankton in zooplankton fecal pellets. Deep-Sea Res 30:963–969

Friedrichs L, Hörnig M, Schulze L, Bertram A, Jansen S, Hamm C (2013) Size and biomechanic properties of diatom frustules influence food uptake by copepods. Mar Ecol Prog Ser 481:41–51

Gibson LJ, Ashby MF (1988) Cellular solids: structure and properties. Pergamon Press, New York

Hamm CE, Merkel R, Springer O, Jurkojc P, Maier C, Prechtel K, Smetacek V (2003) Architecture and material properties of diatom shells provide effective mechanical protection. Nature 421:841–843

Hardy A (1970) The open sea. The world of plankton. Collins, London

Hillerton JE, Robertson B, Vincent JFV (1984) The presence of zinc or manganese as the predominant metal in the mandibles of adult, stored-product beetles. J Stored Prod Res 20:133–137

Humes AG (1994) How many copepods? Hydrobiologia 292/293:1–7

Huys R, Boxshall GA (1991) Copepod evolution. The Ray Society, London

Itoh K (1970) A consideration on feeding habits of planktonic copepods in relation to the structure of their oral parts. Bull Plankton Soc Japan 17:1–10

Jansen S (2008) Copepods grazing on *Coscinodiscus wailesii*: a question of size? Helgol Mar Res 62:251–255

Kiørboe T (2011) What makes pelagic copepods so successful? J Plankt Res 33:677–685

Koehl MAR (2004) Biomechanics of microscopic appendages: functional shifts caused by changes in speed. J Biomech 37:789–795

Koehl MAR, Strickler JR (1981) Copepod feeding currents: food capture at low Reynolds number. Limnol Oceanogr 26:1062–1073

Longhurst AR (1985) The structure and evolution of plankton communities. Prog Oceanogr 15:1–35

Malkiel E, Sheng J, Katz J, Strickler JR (2003) The three-dimensional flow field generated by a feeding calanoid copepod measured using digital holography. J Exp Biol 206:3657–3666

Michels J (2007) Confocal laser scanning microscopy: using cuticular autofluorescence for high resolution morphological imaging in small crustaceans. J Microsc 227:1–7

Michels J (2013) Confocal laser scanning microscopy—detailed three-dimensional morphological imaging of marine organisms. In: Reynaud EG (ed) Imaging marine life: macrophotography and microscopy approaches for marine biology. Wiley-VCH, Weinheim, pp 69–91

Michels J, Büntzow M (2010) Assessment of Congo red as a fluorescence marker for the exoskeleton of small crustaceans and the cuticle of polychaetes. J Microsc 238:95–101

Michels J, Gorb SN (2012) Detailed three-dimensional visualization of resilin in the exoskeleton of arthropods using confocal laser scanning microscopy. J Microsc 245:1–16

Michels J, Schnack-Schiel SB (2005) Feeding in dominant Antarctic copepods—does the morphology of the mandibular gnathobases relate to diet? Mar Biol 146:483–495
Michels J, Vogt J, Gorb SN (2012) Tools for crushing diatoms—opal teeth in copepods feature a rubber-like bearing composed of resilin. Sci Rep 2:465
Michels J, Vogt J, Simon P, Gorb SN (2015) New insights into the complex architecture of siliceous copepod teeth. Zoology 118:141–146
Miller CB, Nelson DM, Guillard RRL, Woodward BL (1980) Effects of media with low silicic acid concentrations on tooth formation in *Acartia tonsa* Dana (Copepoda, Calanoida). Biol Bull 159:349–363
Miller CB, Nelson DM, Weiss C, Soeldner AH (1990) Morphogenesis of opal teeth in calanoid copepods. Mar Biol 106:91–101
Nishida S, Ohtsuka S (1996) Specialized feeding mechanism in the pelagic copepod genus *Heterorhabdus* (Calanoida: Heterorhabdidae), with special reference to the mandibular tooth and labral glands. Mar Biol 126:619–632
Ohtsuka S, Onbé T (1991) Relationship between mouthpart structures and in situ feeding habits of species of the family Pontellidae (Copepoda: Calanoida). Mar Biol 111:213–225
Paffenhöfer G-A, Strickler JR, Alcaraz M (1982) Suspension-feeding by herbivorous calanoid copepods: a cinematographic study. Mar Biol 67:193–199
Pilson, MEQ (2012) An introduction to the chemistry of the sea, 2nd edn. Cambridge University Press, New York
Price HJ, Paffenhöfer G-A, Strickler JR (1983) Modes of cell capture in calanoid copepods. Limnol Oceanogr 28:116–123
Quicke DLJ, Wyeth P, Fawke JD, Basibuyuk HH, Vincent JFV (1998) Manganese and zinc in the ovipositors and mandibles of hymenopterous insects. Zool J Linn Soc Lond 124:387–396
Schnack SB (1989) Functional morphology of feeding appendages in calanoid copepods. In: Felgenhauer BE, Watling L, Thistle AB (eds) Functional morphology of feeding and grooming in Crustacea. Balkema, Rotterdam, pp 137–151
Schofield RMS, Nesson MH, Richardson KA (2002) Tooth hardness increases with zinc-content in mandibles of young adult leaf-cutter ants. Naturwissenschaften 89:579–583
Smetacek V (1999) Diatoms and the ocean carbon cycle. Protist 150:25–32
Smetacek V (2001) A watery arms race. Nature 411:745
Strickler JR (1982) Calanoid copepods, feeding currents, and the role of gravity. Science 218:158–160
Sullivan BK, Miller CB, Peterson WT, Soeldner AH (1975) A scanning electron microscope study of the mandibular morphology of boreal copepods. Mar Biol 30:175–182
Tréguer P, Nelson DM, Van Bennekom AJ, DeMaster DJ, Leynaert A, Quéguiner B (1995) The silica balance in the world ocean: a reestimate. Science 268:375–379
Turner JT (1978) Scanning electron microscope investigations of feeding habits and mouthpart structures of three species of copepods of the family Pontellidae. Bull Mar Sci 28:487–500
Turner JT (2004) The importance of small planktonic copepods and their roles in pelagic marine food webs. Zool Stud 43:255–266
Verity PG, Smetacek V (1996) Organism life cycles, predation, and the structure of marine pelagic ecosystems. Mar Ecol Prog Ser 130:277–293
Vyshkvartseva NV (1975) Structure of the mandibles in the genus *Calanus* s.l. in relation to latitudinal zonality. In: Zvereva ZA (ed) Geographical and seasonal variability of marine plankton. Israel Program for Scientific Translations, Jerusalem, pp 186–199
Wang RZ, Weiner S (1998) Strain-structure relations in human teeth using Moiré fringes. J Biomech 31:135–141
Weis-Fogh T (1961) Molecular interpretation of the elasticity of resilin, a rubber-like protein. J Mol Biol 3:648–667

Chapter 5
Diatom Frustule Morphology and its Biomimetic Applications in Architecture and Industrial Design

Wiebe H. C. F. Kooistra and Göran Pohl

5.1 Introduction

Diatoms constitute a highly diverse group of unicellular, photosynthesizing eukaryotes that are common in marine and freshwater habitats. Many species abound in the passively drifting community, called plankton, whereas numerous others occur epiphytically, on rocks, in the sand and on mudflats. The defining feature of the diatoms is their multipart silica cell wall, called a frustule, whose architecture is highly diverse and often remarkably beautiful (for an overview of the morphological diversity, see Round et al. 1990). The enormous diversity in shape and ornamentation of the frustule elements can be appreciated using microscopy. Until the 1970's that meant, light microscopy. Intricate understanding of frustule architecture and fine structure arrived with the use of scanning and transmission electron microscopy (see Round et al. 1990), x-ray scattering (Vrieling et al. 2000) and atomic force microscopy (Crawford et al. 2001). From then on, biologists and biophysicists alike could observe frustule architecture in all its details and explore its functionality (Hamm et al. 2003). An overview of all this diversity is provided in part 5.2.

From a biomimetic perspective, diatom frustules form a source of inspiration for materials-science, architecture, nanotechnology, photonics and design of lightweight structures (Drum and Gordon 2003; Bradbury 2004; Townley 2011). Of course, frustule architectural details cannot be transferred directly into engineering, but many similarities and analogies render diatom frustules interesting study objects for research, technological development and innovation in professions such as architecture, engineering and industrial design (Townley 2011; Nachtigall and

W. H. C. F. Kooistra (✉)
Stazione Zoologica Anton Dohrn, Villa Comunale, 80121 Naples NA, Italy
e-mail: Kooistra@szn.it

G. Pohl
Faculteit Bouwkunde, Facade Research Group/office, TU Delft/Pohl Architekten,
Cyriakstr. 13, 99094 Erfurt, Germany
e-mail: g.pohl@pohlarchitekten.de

C. Hamm (ed.), *Evolution of Lightweight Structures,* Biologically-Inspired Systems 6,
DOI 10.1007/978-94-017-9398-8_5

Pohl 2013) for a number of reasons. Physical constraints on frustule architecture are often comparable to those familiar to architects and industrial engineers, despite the scales being vastly different. Analogies also abound between how diatoms construct frustule elements and constructors build large buildings in busy cities regarding how various elements are put together and how all the details of the construction process are managed. Yet, there are also clear differences, which prohibit a direct transfer of knowledge about form and function of frustule elements into architecture and technical design. These aspects are discussed in part in 5.3.

In the last part of this chapter (5.4) we present a series of features of frustules and their biomimetic applications in design, in particular in architecture, and we focus thereby on the utilisation of fibre reinforced composite materials. One of the overarching issues in diatom biology and design alike is the parsimonious use of materials. Diatom frustules and buildings alike can be viewed as a compromise among several requirements, specifications, and constraints dictated by a series of at times conflicting functions. In diatoms natural selection of the variation present in a population by a range of environmental pressures drives optimisation of frustule ultrastructural details, or more precisely, the processes that produce the optimised frustule; all this within the biophysical and biochemical limits of the construction process as well as of the finished product. Over time, changing selective pressures can change these details, often in radical ways. Some facets of these evolutionary principles now find applications in the search for optimal design of constructions and industrial products (see the example in 5.4.4).

5.2 The Diatom Frustule

The diatom frustule is an architectural marvel, consisting of a series of cell wall elements that envelop the living cell. It consists of two valves, each accompanied by a series of girdle bands. The valves resemble petri dishes; they are usually composed of a flat area, called valve face, and a rim, called mantle. The mantle overlaps the girdle bands. One valve together with its set of girdle bands is called the epitheca, and this set of elements overlaps a similar but slightly narrower set called the hypotheca (Round et al. 1990).

5.2.1 Construction of Silica Cell Wall Elements

During vegetative cell division, new thecae are constructed precisely inside the confines of the parental epitheca and hypotheca. In this way, the cell remains covered entirely by its silica wall throughout the cell division (Round et al. 1990). There is a drawback, however, namely miniaturization with on-going cell divisions. Newly formed thecae are always hypothecae. The one formed inside the parental epitheca

is of the same size as the parental hypotheca, but the one formed inside the parental hypotheca is minutely smaller. Consequently, average cell diameter diminishes and the variance in cell diameter increases in a clonal cell line until cells become so small and stunted that they are no longer viable.

The principal escape from this miniaturization-trap constitutes sexual reproduction. Cells can become sexualized when reaching a threshold window of cell sizes. Sexual reproduction includes meiosis and gamete formation, followed immediately by gamete fusion, and the swelling of the resulting zygote to form a so-called auxospore. Within this auxospore the initial vegetative cell is formed (see Round et al. 1990).

The reason why this is relevant for biomimetics is that processes during auxospore formation determine the overall shape of the initial diatom cell that "hatches" from the auxospore, and the shape of this cell delineates the shapes of its daughter cells upon division and so forth. In diatoms that are petri dish-shaped, swelling of the zygote proceeds isometrically, the resulting auxospore is globular and the valves of the initial cell are dome-shaped. This initial cell divides along its equatorial plane and, consequently, the valve faces of the daughter cells' newly formed valves are flat. Subsequent divisions generate cells that resemble cylinders. In diatom cells whose valves deviate from a petri dish-shape, swelling of the zygote is constrained anisometrically by the formation of silica bands, called properizonial or perizonial bands, formed in sequence to guide the swelling zygote into a range of species-specific shapes, from anything resembling a cigar, a perfume bottle, or a tri- or multipolar star. The initial valves are laid down against the inside of the auxospore wall and, consequently, follow the shape of the auxospore (see Round et al. 1990). For clarity, "polar" and "polarity" means valve faces deviating from a circular shape.

Construction of new silica cell wall elements proceeds in silica deposition vesicles (SDV; Schmid and Schulz 1979). Upon cell division, the daughter cells lay down SDV's in which new valves are constructed, and subsequently SDV's in which girdle bands are produced as the need for them arises in the growing cell. Dissolved silicic acid is actively taken up from the exterior and concentrated in the cytoplasm far above the level at which silica would polymerize. Precipitation in the cytoplasm is avoided because silicic acid transporter proteins bind the silica and transport it into the SDV. In the meantime, another class of peptides, silaffins, silacidins and long chain polyamines (LCPA's), are produced in the endoplasmatic reticulum and shuttled in vesicles to the Golgi Body. There, the peptides are modified and activated upon which they are shuttled in vesicles from the Golgi body to the SDV. Upon arrival in the SDV, the LCPA's and other peptides assemble into a matrix on which the supersaturated silica precipitates in an amorphous form (Hildebrand 2008; Kröger and Poulsen 2008). The density, nature and post-translational modifications of the peptides in particular regions within the SDV determine the structure and density of the precipitated silica. Invaginations in the SDV probably serve as casts guiding the formation of microscopic architectural details of the frustule elements. Once construction is completed, the frustule element is coated with an organic envelope and excreted through the cell membrane (see Round et al. 1990).

5.2.2 Frustule Shape and Ornamentation

Of the frustule elements, the valves are usually the architecturally most elaborate and provide the most inspiration for biomimetic purposes. The valve face generally shows a central area or a thickened midrib from which ribs extend towards the outer rim (Fig. 5.1). In the majority of species, the valves consist of a single layer, yet several species, especially larger ones, possess chambered valves consisting of an outer and an inner layer connected e.g., by a honeycomb matrix. The inner layer generally connects to the interior by means of a fine mesh of pores or a simple opening. Large species often have reinforced their valves on the interior side with thickened ribs, buttresses, flying buttresses, cross beams and other architectural aids. Figure 5.2 shows a valve of the centric diatom *Cyclotella atomus* exhibiting a primary layer of radiating ribs with small pores in between, which is reinforced by means of a large central area and a secondary layer of larger radial ribs.

Frustules need to be strong enough to resist, or at least hinder, the onslaught of herbivores (Hamm et al. 2003). But this is not the only function: transporting material through it is another. Rows of pores between the ribs permit exchange with the environment. Many species possess fields of tightly packed pores located at the valve apices. These pore fields exude sticky polysaccharides to form mucilage pads for attachment. Since these fields could impair structural integrity, they are often fairly thick and surrounded by support structures.

Most diatoms have tubular processes through their valve face. Labiate processes (= rimoportulae) constitute the most widespread ones and probably serve to excrete and/or ingest organic matter. Labiate refers to the lip-like internal end of the tube that is folded to the side. Another type of tube, the strutted process (= fultoportula; see Fig. 5.2), is found exclusively in the order Thalassiosirales (see Round et al. 1990) and is involved with the excretion of β-chitin fibres. These fibres extend into the environment or connect sister cells into a chain. The small struts surrounding these tubes anchor the tube into the surrounding cell wall, as structural reinforcements against the tensile stress of the chitin fibres. A third kind of process, called a raphe, consists of two slits that allow the cells to slide actively over the substratum by means of a cost-effective traction system (Edgar and Pickett-Heaps 1984). The slits usually flank the midrib and are “>” shaped in section through the cell wall. The raphe represents a structural weakness in the valve architecture. To avoid the valve from breaking along this weakness, many species possess series of bridge-like structures, called fibulae, over the raphe on the interior side of it, thus reinforcing the valve. Moreover, the ends of the slits are generally bent sideways or droplet-shaped to avoid cracking.

5.2.3 Diatom Taxonomy and Phylogeny

Diatoms have been ordered into groups of convenience based on characteristics of valve structures and processes (Kooistra et al. 2007). Radial centrics possess radially organized valves with ribs radiating from the centre, and labiate processes,

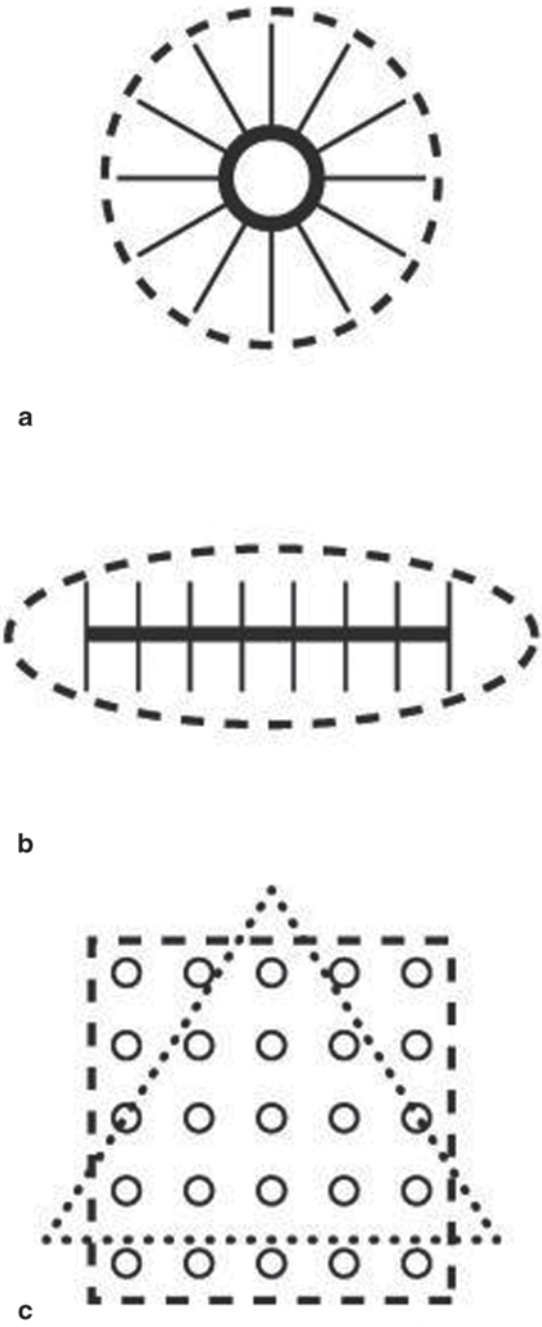

Fig. 5.1 Schematic organisation of: **a** a valve of a centric diatom in valve-view; **b** a valve of a pennate diatom; **c** organisation of a secondary layer in valves in certain centric diatoms, follow principles of repetition of structures. (© Nachtigall and Pohl 2013)

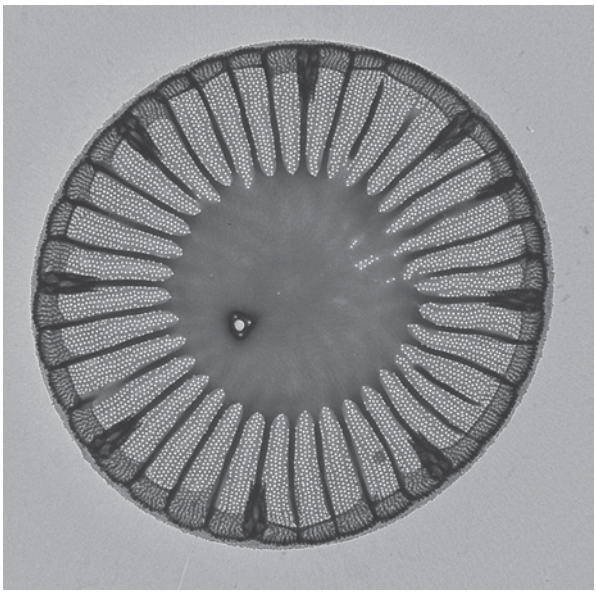

Fig. 5.2 Transmission electron micrograph showing a valve of the centric diatom *Cyclotella atomus* exhibiting a primary layer of radiating ribs with small pores in between, which is reinforced by means of a large central area and a secondary layer of taller radial ribs. Note the strutted process located off-centre permitting a view straight through its central tube. A further eight strutted processes are located along the valve perimeter (© Diana Sarno, SZN)

if present, usually located in a ring in the valve mantle or near the centre. Representatives of the radial centrics are, for example, *Actinoptychus, Asterolampra, Arachnoidiscus, Aulacoseira, Corethron, Coscinodiscus, Cymatosira, Ellerbeckia, Leptocylindrus, Melosira, Paralia, Rhizosolenia, and Stephanopyxis*.

Multipolar centrics also show a radial pore organization, but their cell outline is usually elongate, triangular or star-like, i.e., reveals polarity. This shape results from the aforementioned properizonial bands constraining the shape of the swelling auxospore from which the initial vegetative diatom cell emerges. Their valve poles possess pore fields, and their processes, if present, are situated usually within the central area or somewhat off-centre. Representatives are, for instance *Bacteriastrum, Biddulphia, Briggera* (fossil), *Chaetoceros, Ditylum, Eucampia, Helicotheca, Isthmia, Minutocellus, Odontella,* and *Triceratium*. The Thalassiosirales (e.g., *Lauderia, Porosira, Skeletonema, Thalassiosira*) exhibit a radial centric organization, but from an evolutionary perspective belong to multipolar centrics.

Pennate diatoms are elongated with a midrib, from which ribs extend out more or less perpendicularly. The pennates can be subdivided into raphid pennates, which possess raphe slits, and araphid pennates, which lack such slits, but instead have apical pore fields and apical labiate processes. Typical araphid pennate representatives are *Asterionella, Asterionellopsis, Fragilaria, Grammatophora, Licmophora, Lioloma, Staurosira, Synedra, Rhabdonema, Striatella, Thalassionema,* and *Thalassiothrix*. Typical raphid pennates include *Amphora, Bacillaria, Campylodiscus, Campyloneis, Cocconeis, Cylindrotheca, Fragilariopsis, Gomphonema, Navicula, Nitzschia, Phaeodactylum, Pseudo-nitzschia, Sellaphora,* and *Surirella*. Fine details of frustule ultrastructure of all these genera are documented lavishly in Round et al. (1990) with their book offering a great source of inspiration for biomimetic approaches.

Results of molecular phylogenetic studies (e.g., Medlin et al. 1993; Sinninghe-Damsté et al. 2004; Sorhannus 2004; Kooistra et al. 2007) show that diatoms are sister lineage to a group of extremely small, fast-swimming flagellated microalgae called Bolidomonadales (Guillou et al. 1999) and a small group of microalgae called Parmales (Ichinomiya et al. 2011). The latter form silica frustules as well, but these differ structurally from those of diatoms (Mann and Marchant 1989). Within the diatoms, radial centrics constitute the most ancient group, and multipolar centrics evolved from radial ancestry. Thalassiosirales appear like radial centrics but they form a lineage within the multipolar centrics indicating that their last common ancestor lost polarity secondarily. Multipolar centrics form a grade in most phylogenies because the pennates evolved from multipolar centric ancestry. Likewise, araphid pennates constitute a grade because the raphid pennates evolved from araphid ancestors.

5.2.4 Linking Structures

Many diatoms form chains composed of sister cells that hold on to one another—following cell division—by means of linking structures between adjacent valves in a number of ways (see Round et al. 1990 for examples). One mode of chain formation is by means of mucilage pads exuded through the apical pore fields, and is encountered in araphid pennates and in many centrics. Another form of connection is achieved by interlocking teeth or claws lined up along the rim of the valve face. These structures are laid down during valve formation. They are encountered all over the diversity of diatoms and probably have been acquired multiple times independently, originally often for entirely different purposes than chain formation. A third form of connecting valves is through the setae of diatoms in the family Chaetocerotaceae (*Chaetoceros* and *Bacteriastrum*). Setae are hollow tubes extended from the valve apices following valve formation (see Kooistra et al. 2010 for examples). They connect with the setae on the valve of the adjacent sister cell. A fourth type of connection constitutes the chitin fibres exuded through the strutted processes in the valve face of Thalassiosiralean diatoms (see e.g., Fig. 5.2). Within this group the diatoms of the genus *Skeletonema* possess strutted processes whose external tubes are elongated to such an extent that their ends interlock with those from the adjacent sister valve to form a stiff chain (Fig. 5.3; Sarno et al. 2005, 2007). To prohibit teeth or claws from becoming overly long in chains interlocked by strutted processes, a cell positioned in the middle of a chain produces daughters whose adjacent valves bear structures that do not interlock. This permits the daughter cells to become the terminal cells of two daughter chains, and drift apart without damage. The connecting structures between the cells are unlikely to have to endure strong tensile forces, but chains can be exposed to bending, which creates tension- and compression stresses over short distances in these elements.

Another form of linking structures, namely those that hold frustule elements within a cell in place, is found in the raphid pennate genus *Campyloneis* (De Ste-

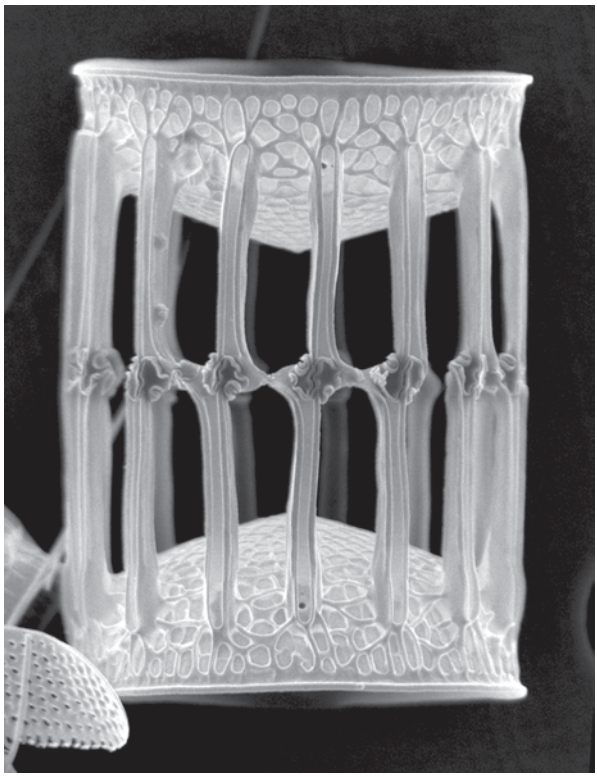

Fig. 5.3 Scanning electron micrograph of sibling valves belonging to adjacent sister cells of the centric diatom *Skeletonema japonicum*. Note the intricately interconnecting strutted processes. These are partially open towards the valve perimeter allowing a view inside the tube and showing the actual passage through the valve in two places (© Diana Sarno, SZN)

fano et al. 2003). Diatoms in this genus occur epiphytically on sea grass leaves and other flat surfaces where they have to resist, or at least counter, the scraping forces of radulas belonging to molluscan grazers. The hallmark of this genus is that its epitheca and hypotheca each include what effectively is a double valve. The inner valve is partly open to permit free passage to the cytoplasm (see e.g., Fig. 5.4 in De Stefano et al. 2003), and the outward facing side of the inner valve and the inward facing side of the outer valve are not physically connected. They are just piled on top of each other. Sliding sideways alongside each other is prevented in two ways. One constitutes a grid of bolt-like bosses on the surface of one valve that fit into openings in the other valve (see Figs. 5.4c and d in De Stefano et al. 2003). Another mode consists of clusters of raspberry-like bosses projecting from the outwards facing side on the ribs of the inner valve as well as from the ribs on the inward facing side of the outer valve (see Figs. 4f and g in De Stefano et al. 2003). Similar sets of bosses are found on the inward facing sides of the two inner valves. We believe that this system functions as follows: Lateral stresses in any direction due to pressure from the side or from above are countered by a slight deformation of the valves accompanied by a small movement. The raspberry bosses permit such movement by sliding in minute increments over one another's surfaces, depending on the intensity of the deformation. Following each increment of sliding, the bosses find themselves

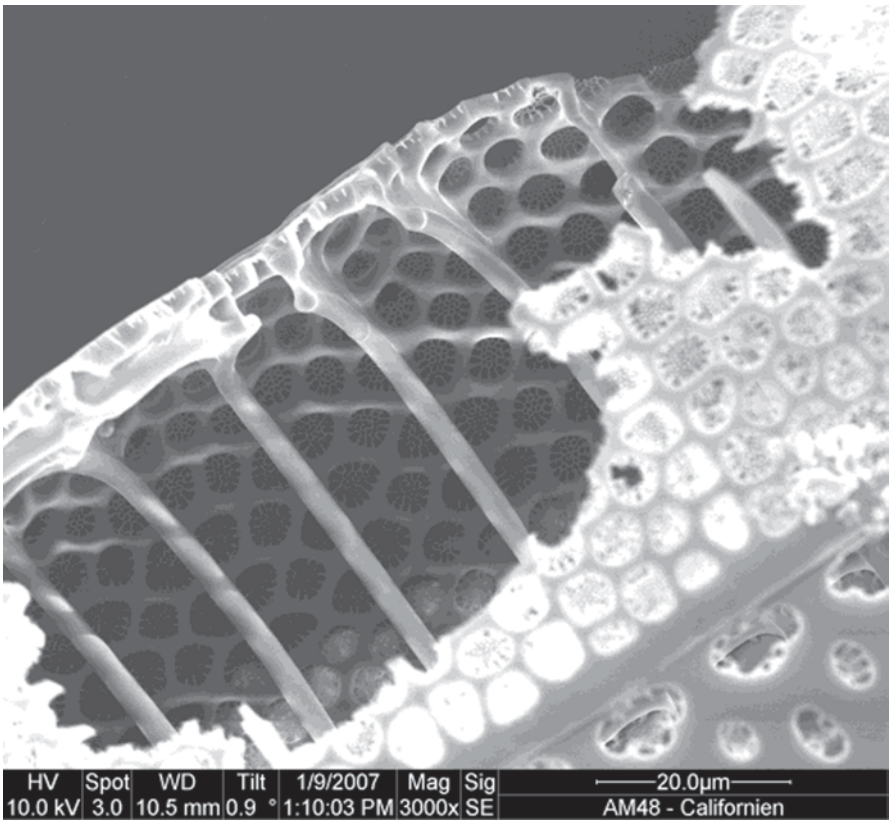

Fig. 5.4 Scanning electron micrograph showing concentric ribs in the valve of the bipolar centric diatom *Isthmia* (© AWI)

against one another in slightly different semi-stable positions. This way, modest deformations and movements are permitted whilst retaining structural integrity. As soon as the stress is gone, the bosses slide back into their relaxed positions.

5.2.5 The Fossil Record

Diatoms possess an extensive fossil record. Frustule elements are preserved, often in exquisite detail over millions of years (e.g., Gersonde and Harwood 1990; Harwood et al. 2004; Suto 2006; Ishii et al. 2011). Radial centrics first appear in the Jurassic, multipolar centrics are present in the Early Cretaceous, the pennates first appear in the Late Cretaceous, and the first raphid pennates are present unambiguously in the Paleogene (Rabosky and Sorhannus 2009). This sequence corroborates findings in phylogenetic studies of extant diversity. The fossil record is highly relevant from an architectural design viewpoint because several cell wall

designs, ornaments, and connection modes to form chains do not exist in the extant diversity. Examples of such fossil diatom architectures can be found among the genera illustrated in Gersonde and Harwood (1990) and Round et al. (1990). Often the valves and girdle bands are preserved in such exquisite ultrastructural detail that the ecological niches of these fossil diatoms, as well as the modes of chain formation can be reconstructed mathematically and inferred based on what is known from comparable, but unrelated, extant diatoms.

5.2.6 The Need for Shared Terminology

In order to enable diatomists, architects, designers, and civil engineers to communicate freely, their glossaries of architectural elements need to be compared. Their different ways of approaching design in diatom frustules and buildings need to be shared. Nachtigall and Pohl (2013) provide a series of schematic drawings (Fig. 5.1) of (a) a valve of a centric diatom in valve-view, showing a central ring and ribs radiating from it, (b) the valve of a pennate diatom showing a midrib or main supporting beam and perpendicular ribs, and (c) the organisation of a secondary layer in valves in certain centric diatoms, follow principles of repetition of structures, e.g. in the form of a honeycomb pattern (see Round et al. 1990).

Diatom frustules are built hierarchically and exhibit symmetries in different planes. In most of the centrics and virtually all of the pennates, the valves are structurally reinforced by means of ribs, as shown on the interior side of the valve of the bipolar centric diatom *Isthmia* (Fig. 5.4). The radially organized ribs in radial centric valves are in some species reinforced by concentric ribs perpendicular to the radial ones, as shown in *Arachnoidiscus* (Fig. 5.5). This pattern of ribs resembles the reinforcement structures of large domes. Examples are the glass domes over the Reichstag building in Berlin, Germany, and the Galleria Vittorio Emmanuele in Milan, Italy (Fig. 5.6). Many radial centrics possess valves in which ribs are organized in a honeycomb-pattern, as in e.g., the radial centric diatom *Actinoptychus* (Fig. 5.7), which provides strength against deformation whilst minimizing material

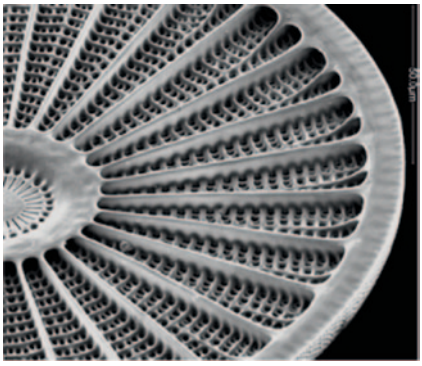

Fig. 5.5 Scanning electron micrograph of the inside of a valve of the radial centric diatom *Arachnoidiscus* (© AWI)

Fig. 5.6 The central dome of Galleria Vittorio Emmanuele at Milan, Italy; an example of a glass dome supported by a structure of radial and concentric ribs structurally and functionally similar to that in the valve of the radial centric diatom *Arachnoidiscus*. http://www.milanexpotours.com/milan-expo-project-2015/numbers/galleria-vittorio-emanuele.html

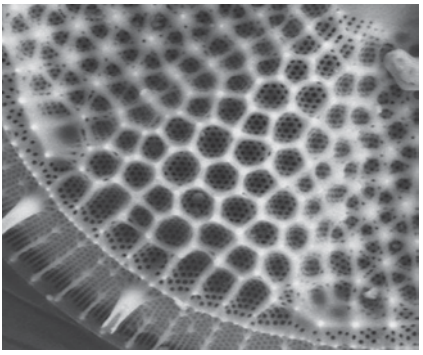

Fig. 5.7 Scanning electron micrograph showing a section in a valve of the radial centric diatom *Actinoptychus;* note the honeycomb-like secondary reinforcement on this valve (© AWI)

usage. Pennate valves possess a midrib which diatomists call "sternum", engineers "main supporting beam", and shipbuilders "keel." Perpendicular to this midrib is a row of ribs that diatomists call "interstriae" (the rows of pores in between them being the striae). Architects and shipbuilders call them crossbeams or ribs. Upon these ribs are often finer support structures. Given the symmetries, frustule elements can be perceived as a system of morphogenetic elements that can be translated into

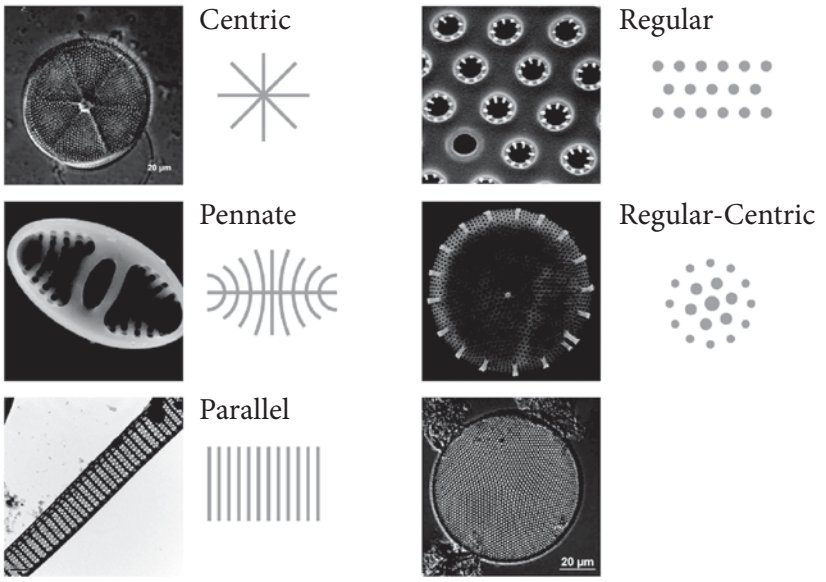

Fig. 5.8 Principal organization of valve architecture in centric,pennate,parallel rows, regular distribution with organization centre of secondary layers as defined in Nachtigall and Pohl (2013; © AWI, © Pohl Architekten)

"building blocks" in architectural applications. Symmetries and hierarchy are mostly self-similar copies in different scales.

To aid architects, engineers, and designers in defining these symmetries, Nachtigall and Pohl (2013) have added new specifications to the diatomists' terminologies that describe not only the primary organisation of the diatom valves with their ribs, but also the secondary layers with their honeycomb-like chambering in between the primary and secondary walls (Fig. 5.8).

5.3 Biomimetic Applications of Diatom Frustule Morphology

At the end of the nineteenth century Ernst Haeckel published his work "*Kunstformen der Natur* (Haeckel 1898), which found an eager readership not only among biologists, but also among designers and architects. "Art Nouveau—Jugendstil" architecture is replete with biomimetics examples, and these are not restricted to decorations. Another classic work that served as inspiration for architects is D'Arcy W. Thompson's "On Growth and Form" (D'Arcy Thompson 1917). During the 1970s and early 1980s, Otto, the architect of lightweight tent structures (Otto et al. 1985), botanist Johann-Gerhard Helmcke, and plant physiologists Schmid and Schulz (1979) analysed the fine structural details and genesis of diatom frustule

architecture in electron microscopy. Their work forms the foundation of on-going studies by architects, civil engineers, and industrial designers (Gruber 2010).

5.3.1 Analogies in Form and Function Between Diatom Frustules and Buildings

The similarities between form and function of parts in diatom frustules, and construction elements in works of architecture and engineering are obvious. And there are several reasons for that.

Biophysical constraints on frustule architectural design are often startlingly similar to the constraints architects and industrial engineers are confronted with. Of course, the building materials differ. Diatom frustules consist of nanometre-size spherules of amorphous silica precipitated onto an organic matrix of peptides (Hildebrand 2008; Kröger and Poulsen 2008), a material that has properties differing from materials such as steel, aluminium, glass, reinforced concrete, rock, wood, and a range of composite materials. Yet, the architectural solutions in diatom frustule elements to overcome those constraints are often remarkably similar to those deployed in architecture to enclose or bridge vast expanses. Truss, beam, frame, rib, outrigger, framework, and grid-shell can all be used to describe construction parts of frustule elements and technical structures (Otto et al. 1985). Yet, the analogies do not stop there.

Remarkable analogies exist between the way a diatom cell constructs frustule elements, and how constructors and engineers create complex structures. Casting of reinforced concrete and composites in construction exhibits analogies with how frustule elements are laid down in SDVs. In addition, the daunting logistics of building a skyscraper in a busy city closely resemble those of constructing diatom frustule elements: various materials are procured or pre-constructed elsewhere and then transported along different pathways to be delivered on time and in the right place and order, while surrounded by frantic, unrelated activities. In recent years, engineers increasingly focus on the possibilities of nanotechnology. Nano-engineering differs from how frustule elements are made, but aspects of what happens in SDVs may one day find application in nanotechnology.

Shape and structure of diatom frustules and buildings alike constitute a compromise among multiple functions and demands. For diatoms, dissolved silica is usually scarce and to be deployed parsimoniously to construct frustules that, nonetheless, need to resist deformation (Hamm et al. 2003). Frustules of planktonic species need to be lightweight not only to save material but also to avoid sinking. In a similar fashion, architects and industrial engineers have to be economical because materials are expensive, add weight and take up space. Apart from the defensive function, frustules must accommodate pores to allow exchange of nutrients and organic materials. In addition, the frustule is believed to have photonic properties, trapping, guiding, and focusing light waves to optimize photosynthesis (Parker et al. 2013). All these functions and demands impose constraints on the frustule architecture. Likewise, architects and material designers have to take into account

the technological and economic feasibility of their construction plans on top of limitations set by different functions, needs, and regulations of the finished product.

5.3.2 Challenges and Opportunities for Biomimetics in Knowledge Transfer

In spite of all the similarities discussed above, designers, architects, and engineers encounter challenges when transferring aspects of frustule morphology into their designs. To begin with, the scales are vastly different, and physical properties of the materials differ radically at these different scales, prohibiting isometric scaling-up. Also, diatoms construct frustule structures from locally fabricated organic compounds and imported silica (Hildebrand 2008; Kröger and Poulsen 2008), fine-tuned to requirements of on-site internal and external loads. Instead, engineers, architects, and industrial designers generally have to make do with standardized production processes offered by worldwide operating industries and have limited possibilities to adapt materials and production processes to the specific requirements of their constructions in different locations. Nature has developed gradient material, composites, and complex compounds while the abovementioned professionals are constrained by the economic reality of having to assemble pre-fabricated, relatively simple, semi-finished parts. New generic design methods, using parametric computer algorithms, are also restricted by the mechanical limitations of the machines building these parts.

The principal difference between natural systems and human-made structures seems to be the growth process of the former, which is far ahead of the additive process deployed in design, architecture or engineering. Nonetheless, diatom frustule elements constitute a great source of inspiration for biomimetics because once produced, they have become non-living structures, which cannot grow anymore, and in this aspect they are analogous to a building or a machine (Nachtigall and Pohl 2013).

5.3.3 Biomimetics to Enhance Material Development for Future Buildings

Technical limitations can be overcome if materials and construction processes are developed according to natural designer principles. Novel building materials provide examples of opening up new opportunities for biomimetics in knowledge transfer. Until recently, composites assembled from textiles and fibres have been applied mainly for high-tech purposes, but nowadays they are also increasingly applied in architecture and industrial engineering. Especially composites made of glass fibres or carbon fibres and a resin matrix seem to match demands on material efficiency, effectiveness, and lightweight, in combination with adaptability for changing needs. Additional aspects that are implicated in this composite material, concern free form-

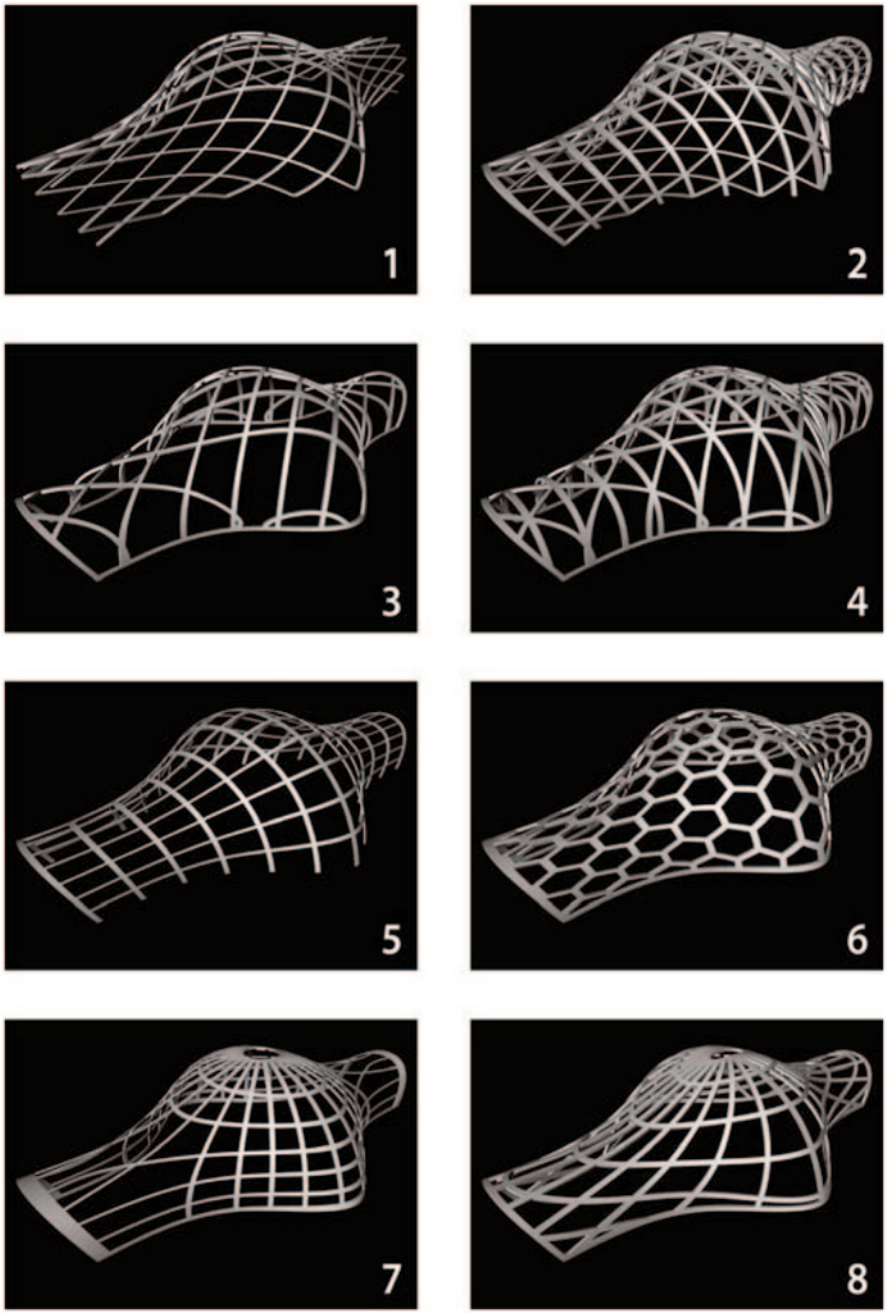

Fig. 5.9 Abstraction models, following organisation principles of diatoms and taking into account industrial production processes defined in Nachtigall and Pohl (© Pohl et al. 2012)

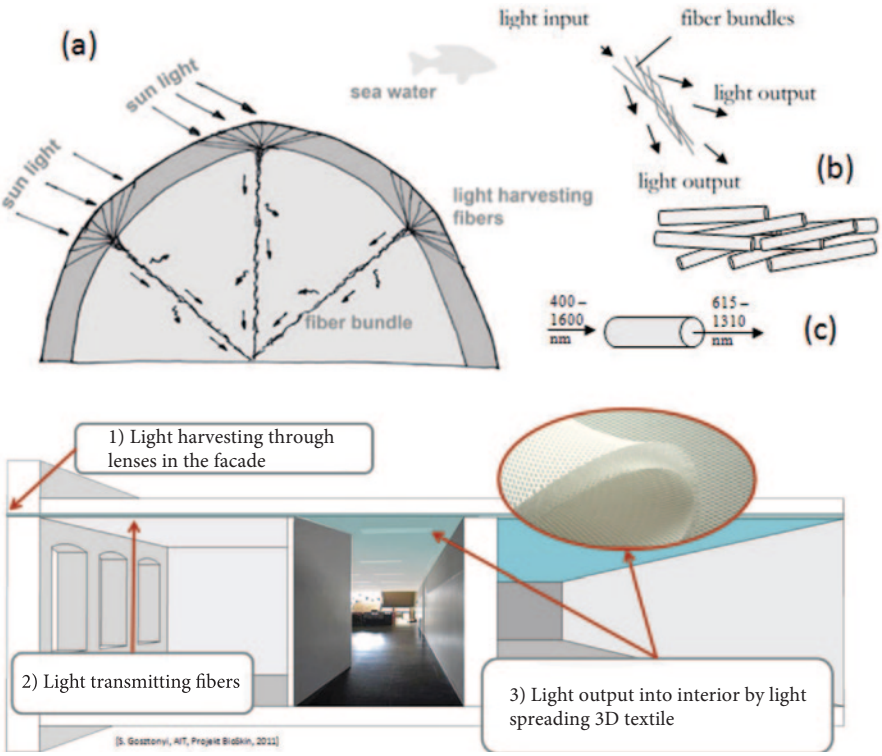

Fig. 5.10 Transmission of light, biomimetically transferred from the natural example of light bundles in deep-sea sponges of the genus *Thethya* into the application of daylight harvesting and transfer by buildings (© Gosztonyi et al. 2011a)

ability and anisotropy. In fibrous materials and building parts, fibres can be embedded into functional elements similar to how species deploy fibres in response to external and internal demands (see Fig. 5.9). These fibres can accomplish additional tasks as well, such as detection (Kroll et al. 2011) and conduction. Müller et al. (2006, 2007) described bionic applications of siliceous sponge spicules. Based on these scientific findings and on fundamental research by Zitzler (2008), Gosztonyi et al. (2011a), light transmission principles based on silica fibrous bundles where developed to illuminate buildings (Fig. 5.10).

Future buildings have to be constructed by following standards to minimize energy losses through their envelopes. In addition, these envelopes need to be flexible in response to changing conditions. Fibres can match these demands and will be able to help the production of multifunctional building envelopes (Gosztonyi et al. 2010; Gosztonyi et al. 2011b; Gruber and Gosztonyi 2010).

In view of this architectural potential, ultrastructural details of diatom frustules are often highly repetitious, and can therefore be regarded as a biomimetic base for structural implementations. Glass fibre reinforced composites are now used to

Fig. 5.11 The research structure COCOON_FS showing a modular structure composed of a restricted number of building block types reminiscent of the highly repeated patterns in diatom valves. Note that the assembly process of COCCON_FS differs radically from the way diatom frustules are formed. http:www.pohlarchitekten.de; http:www.planktontech.de (© G. Pohl)

develop architectural structures as well as to gather experiences with the opportunities the application of this material offers and problems it can solve (Ehrlich et al. 2011). The research structure COCOON_FS (Fig. 5.11), is a showcase of such a development, designing architecture with structural knowledge from biomimetics. Major progress can also be expected of novel ways to construct elements. Classical construction proceeds by means of assembling objects from different raw parts, or by etching or cutting away parts from a solid structure. Yet these methods have their limitations and disadvantages. The emerging field of using fibre reinforced composites for buildings may overcome some of these limitations, especially if used for building skins that embed extra functions.

5.3.4 Approaches to Knowledge Transfer in Biomimetics: Pool Research

How to transfer ample examples of design in diatom frustules via technological development and innovation into practical engineering applications? In a classical "biology-push" approach in biomimetics, a scientist observing a biological design might contemplate its possible applications. Unfortunately, biologists generally lack the technological background to fully appreciate the applicability of biological phenomena in engineering and architecture. In a "technology-pull" approach, an

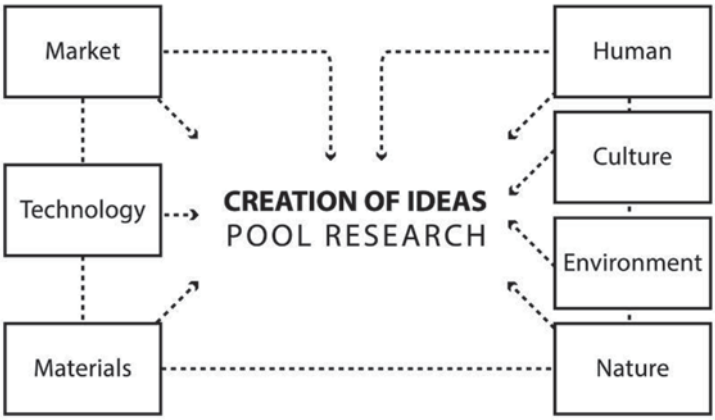

Fig. 5.12 Factors influencing creation of ideas in Pool research according to VDI Guideline 6226 in Nachtigall and Pohl (2013; © Pohl Architekten)

architect, engineer or designer confronted with a challenge may explore biodiversity to find a solution. The problem here however, is where to search. Architects and engineers usually do not have all the biological background knowledge to readily find the proper biological model.

In this context, a third method has been established which enriches all professions that deal with multiple-knowledge-based developments of technical products, as industrial designers or architects do. The whole complexity of natural solutions, technology, materials, inspirations by culture, environmental and market-driven needs, and finally the human scale can be seen as a data catalogue of knowledge. Based on network-methods that connect those multiple benefits and demands, ideal solutions can be developed and realized (Fig. 5.12). For this method, the term "pool research" has been established by Pohl et al. (2010), and has been implemented extensively in biomimetic research (Braun 2008; Gosztonyi et al. 2010; Gruber and Gosztonyi 2010).

Pool research is particularly well-suited for architects, structural engineers, and industrial designers who search for designs in nature and wish to transfer these into innovative solutions for technology, industry and architecture (Pohl et al. 2010; Anonymous 2013; Nachtigall and Pohl 2013). The methodology includes the collection of basic knowledge from biological systems to better understand biological form and function without any defined technical need in advance. Pool research is implemented throughout the whole working process of biomimetics. It starts with biological exploration, helps within the development phase, and focuses on practical application. It can be seen as the central tool for decisions of all collaborators involved. Its value is not merely a function of determinable combinations of rational aspects, but a synergistic combination of these aspects together with a sum of subjective and cultural influences (Anonymous 2013). In pool research, knowledge accumulation is at the core of the designer's methodology. In this way, the pool of accumulated biological knowledge and insights can be applied directly for design or technical development. Alternatively, ideas can be kept in store for

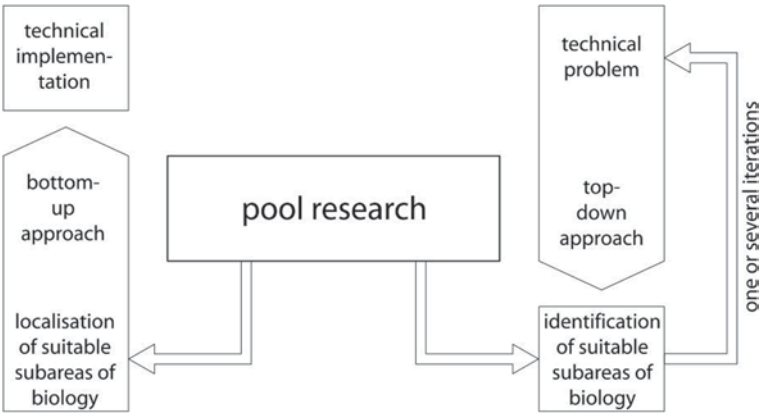

Fig. 5.13 Workflow in Pool research according to Pohl et al. (2012) and VDI Guideline 6226 (2013 © G. Pohl)

future applications when technological developments have overcome constraints of what can be realized, or when a demand for the product has developed, thus making realization economically feasible. The collected background knowledge of pool research can then readily translate biological designs into innovative technological and architectural designs.

Pool research also constitutes a practical strategy to shorten development times. Knowledge generated through pool research is important for all professions that can develop ideas inspired by the extensive diversity of nature-realized options (Fig. 5.13; Nachtigall and Pohl 2013).

5.4 Knowledge Transfer of Functional and Structural Elements from Diatom Frustules into Architecture

Many examples of knowledge transfer of functional and structural elements in diatoms into architecture exist (Otto 1975a, b; 1985, 1986; Teichmann and Wilke 1996). Nachtigall and Pohl (2013) review the state-of-the-art of current knowledge and give a preview of expected developments in architecture. In the following sections, examples are given of the range of actual and expected developments regarding knowledge transfer from diatom frustules into architecture.

5.4.1 Freeform Ribs

Valves of the radial centric diatom *Arachnoidiscus* (Fig. 5.5) offer a prime example of primary and secondary rib structures that can be translated into freeform architecture by using specialized computer algorithms. With the aid of these algorithms,

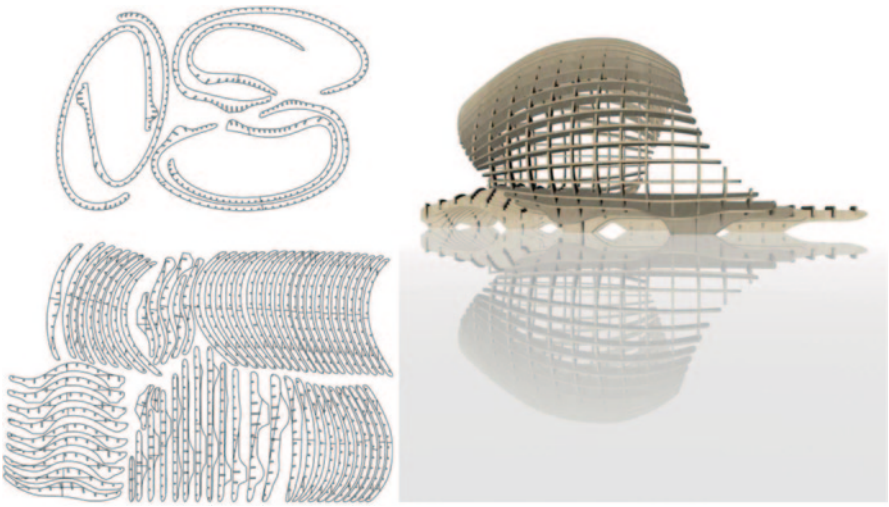

Fig. 5.14 Cutting design of building elements (ribs) and a 3D depiction of the assembled roof structure constructed with the building elements, student's design at the School of Architecture Saar, G. Pohl (© N. Feth)

the building substance is divided into structural ribs and filling elements that can be extracted and assorted to planar cutting elements (Fig. 5.14). This translation of geometrical complexity into flat surface structures helps fulfilling the technical demands of "easy-to-manufacture" and "easy-to-build" (Nachtigall and Pohl 2013).

5.4.2 Composite Materials for Grid Shell Structures

The valve exterior of the bipolar centric diatom *Isthmia* (Fig. 5.15; valve inside, see Fig. 5.4) provides an example of a structure in which stability is optimised while material usage in minimised. The fine structural solution deployed in this diatom lends itself ideally for transfer into the design of technical grid shell structures

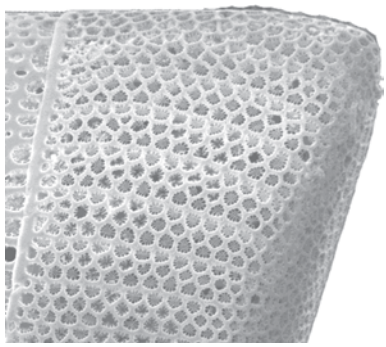

Fig. 5.15 Scanning electron micrograph of the exterior side of a valve belonging to the bipolar centric diatom *Isthmia* (See interior side, Fig. 5.4) (© AWI)

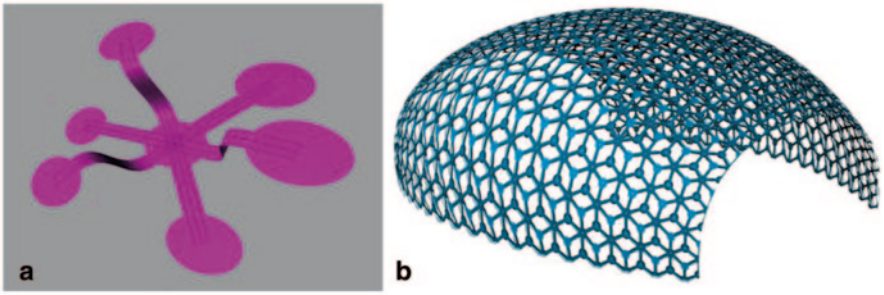

Fig. 5.16 Example of a loadbearing grid structure, with a flexible component on the left, and the technical structure showing the assembled components on the right, as in Nachtigall and Pohl (2013; © J. Otten and G. Pohl)

(Fig. 5.16). Lightweight structures consisting of a single or multiple building elements can be designed that still provide space cover, are stable and strong, and offer shading and protection. The technical task is to build these elements in a computer-aided cutting and bending process because of the great variety of elements used for multi-curved surfaces. For this purpose, parametric computer programming can solve design and manufacturing needs. The ideal material for such usages constitutes fibre reinforced plastic composites composed of knitted fibres embedded in a matrix (Nachtigall and Pohl 2013).

5.4.3 Hierarchical Structures

Hierarchical structures, as observed in *Actinoptychus* (Fig. 5.7) can be used as biomimetic examples to influence the layout of loadbearing structures developed by architects and civil engineers (Fig. 5.17). With the help of modern FEM-programs, it is possible to describe these forces in complex structures. Progress made in this field in recent decades helps with a more thorough understanding towards structural solutions found in natural systems and to implement the results into building structures (Nachtigall and Pohl 2013).

5.4.4 Combinations of Structural Elements

The BOWOOSS research pavilion, a timber construction by the B2E3 Institute for Efficient Architecture, Saarbrücken, Germany (Fig. 5.18) is a result of fundamental research on biomimetics in architecture (Pohl et al. 2012). Studies on diatom frustules have been compared using „Pool Research“. Natural and technical designs were structured, classified, and compared, and their possibilities for applications explored. As a result, the geometry of the building has been worked out in steps. Using evolutionary computer algorithms, a series of “individuals” was “mutated” in

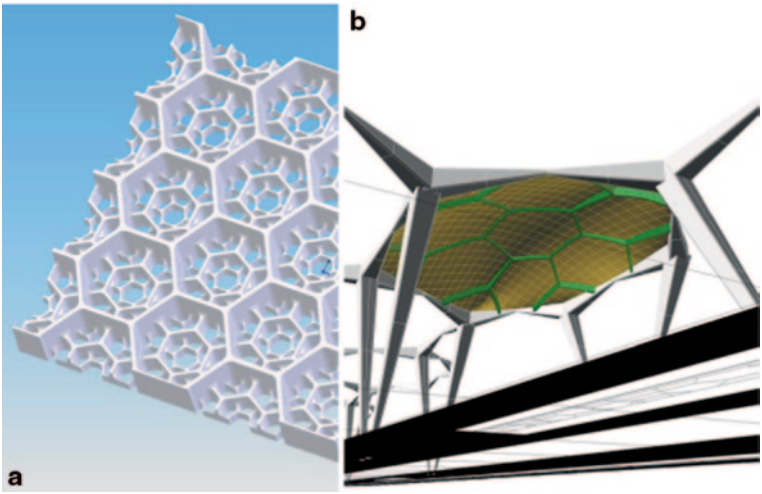

Fig. 5.17 Abstraction of hierarchical structures (© AWI) and hierarchical element of a roof structure for a design of the new railway station in Luxemburg-Cessange (© Knippers Helbig Advanced Engineering, Pohl Architects)

a sense that the "morphology" of each individual was changed subtly and randomly (see Fig. 5.18). The changed "individuals" were then exposed to "natural" selection by financial-economic, esthetical, and technical criteria. The ones exhibiting the best "morphology" were allowed to "survive" and give rise to a new cohort of "individuals," which in turn were "mutated" and so on until an optimal solution was encountered. The architecture translates natural design into technical foldings, uses rib structures and hierarchical structures and presents volumetry in a sensitive manner (Beautyman 2012). Diatoms of the species *Synedrosphenia, Actinoptychus* (Fig. 5.7) and *Arachnoidiscus* (Fig. 5.4) exhibit morphological specifications in their valve ultrastructure that have been of interest for this development. In computer calculations, their efficient load-bearing valves have been identified as a combination of three-dimensional ribs in combination with pore-like openings. The research pavilion BOWOOSS transfers these biological examples, integrating its load-bearing structure within the envelope (Fig. 5.17). The superstructure seems highly complex (Fig. 5.18) but is fabricated with the use of simple building elements (Fig. 5.19).

The structure is supported by laminated timber struts, which in a static sense form the primary and secondary structure, and are permanently fixed to the hull. The hierarchical system is multi-layered, as the biological examples of *Actinoptychus* and *Arachnoidiscus* reveal. Surfaces with pores are following the primary and secondary ribs, which in biological principles may follow multiple layers. The complex composite offers stability and envelops the hull in one. The organically formed ribs are made of 60-mm laminated European spruce, fixed permanently to 27-mm birch plywood foldings that give BOWOOSS a self-stabilizing effect. The hull filters natural light, offers ventilation and regulates transparency. The pore structures in the folding plates are designed using generative computer tools with holes placed

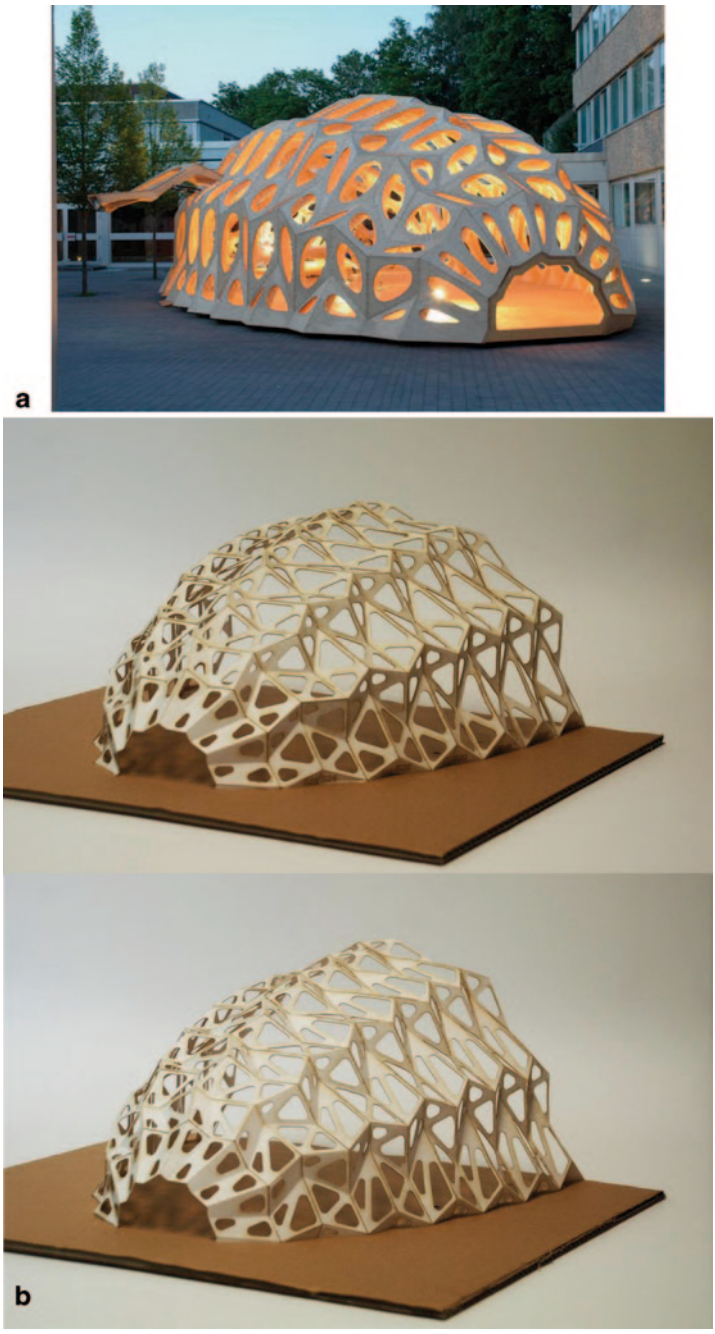

Fig. 5.18 **a** The BOWOOSS pavilion as installed in Saarbrücken, Germany in 2012, by the BOWOOSS research group, G. Pohl, B2E3 Institute for Efficient Architecture, HTW des Saarlandes. http:www.b2e3.de; http:www.pohlarchitekten.de (© G. Pohl) **b** models of two alternative variants of the BOWOOSS pavilion generated using evolutionary computer algorithms (© G. Pohl)

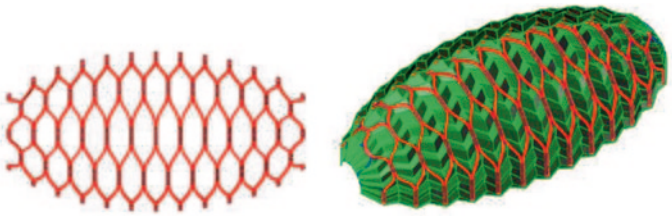

Fig. 5.19 The BOWOOSS pavilion, revealing a frame of ribs (in red) supporting the elaborately folded skin (in green). http://www.detail.de/architektur/themen/forschungspavillon-bowooss-019502.html (© N. Feth and G. Pohl)

in areas with minimal structural loads. Oval-shaped openings have been maximised taking into account static needs following tests of physical models. The pores save structural weight, which translates in low transportation costs and low installation weight. The individual pores are non-continuously curved as methods that can be recognized on structures of load-changes in plants (Pohl et al. 2012; Nachtigall and Pohl 2013).

5.4.5 Linking Structures Between Valves

Linking structures are difficult to incorporate in technical products. One possibility is to build structural knots with cast iron or aluminium to form the connecting parts into the material of beams. With 3D-printers, one could print plastic or metallic compound knots, but still the problem remains on how to integrate these into the building superstructure.

Strong internal forces caused by external loads on building elements are concentrated on structures connecting the building elements. Therefore, these linking structures need to be strong. Various connecting structures can be found between adjacent valves of sister cells in chain forming diatoms. A cell can build such structures permitting the adjacent structures to intertwine in such a way that it is impossible to take them apart without breaking the structure. An example of such intertwined linking structures between adjacent valves of sibling cells is shown at the tips of interconnecting strutted processes between adjacent valves of sibling cells in the centric diatom *Skeletonema* (Sarno et al. 2005, 2007; Fig. 5.3). This concept could be applied in massive loadbearing structures linking pillars to the frame of a roof (Fig. 5.20). This type of connectors may find applications in architecture and engineering, though it is no sinecure to prefabricate linking structures as shown in *Skeletonema*.

5.4.6 Load Bearing, Transmission and Detection: Natural and Technical Fibres

A promising development will be the production of fibre-reinforced knots with fibres layered to be optimally adapted to the load directions and load strength. Fibres

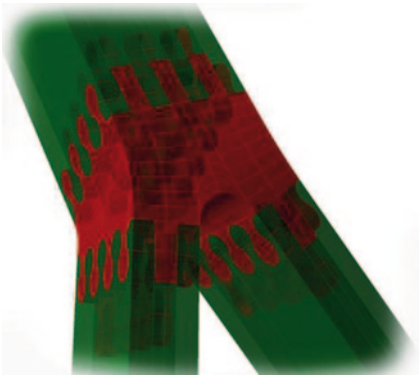

Fig. 5.20 Example of Y-shaped connection composed of interlinking structures reminiscent of those observed in *Skeletonema* (see Fig. 5.3, © BOWOOSS research group, Otten and Pohl)

for load bearing purposes exist in huge varieties in nature, in particular in higher plants and animals. Also the diatoms provide examples for natural solutions of structural enhancement. As explained before, the silica cell wall is not just glass, but instead a composite of peptides on which silica has precipitated (*see 5.2.1*). Another example constitutes the chitin fibres in Thalassiosirales connecting cells into chains. Natural and technical fibres have an enormous potential to carry tension forces (Ehrlich et al. 2011). For technical monitoring purposes, fibre reinforcements will embed embroidered sensors, for example for measuring compression and tension (Kroll et al. 2011). Such a sensory system is reminiscent of the nervous system with its bewildering assortment of sensory devices.

5.4.7 Anisotropic Skins: Fibre Reinforced Composites (FRC)

Skins of buildings are mostly made of added systems that exhibit the same specifications over the entire surface. Demanding requirements concerning energy and material efficiency will not match with this construction mode. Natural solutions in diatom frustules provide functional, structural, and design solutions that can be translated into architectural products, especially for complex, three-dimensional geometries. Fibre reinforced composites exist in natural systems that deploy material in quantity and quality precisely to what is required on the spot. Hence, thickness and fibre orientation may differ from spot to spot, depending on the strength required. Such principles are already deployed in the sails of racing vessels and will undoubtedly find application in technical composites of architectural hulls (Pohl and Pfalz 2010).

Facades are currently developed by combining raw materials by means of adding profiles. So far, technical research endeavours on fibre constructions for lightweight structural elements in architecture are mostly limited on load bearing or enveloping (Ehrlich et al. 2011). Solid parts made of biogenic fibres on one hand, and flexible hydro-pneumatically "blown" membranes on the other hand, for example in cell walls (Otto 1975a, b), are each specific and quantified to exterior and interior loads.

In the methodical approach of pool research in biomimetics, natural systems such as diatoms will need to be studied more thoroughly. Identifying the complex

functional systems in natural solutions will be necessary (e.g. load bearing, protection, semi-permeability, detection). Classification of the "ideal" natural models, especially using silica and silica reinforcement, tend to have an important potential for man-made productions. Structural elements, as they occur in broad varieties in diatoms, show an interesting transfer potential that has just started to be understood for architectural means. Within the facade research group at the Technical University Delft, the Netherlands, a major aim of the on-going research will be to implement the understanding of biological solutions to fibre reinforced systems for new facades in architecture. Anisotropic skins using fibres will, with the help of natural examples, be able to build smart facades that integrate load optimized construction systems and embed extra functions in skins for the overall need of next generation architecture (Gosztonyi et al. 2011b, Nachtigall and Pohl 2013).

Acknowledgments The authors acknowledge support from the COCOON_FS project Plankton-Tech www.planktontech.de. Ulrich Knaack and Tilmann Klein (Façade Research Group at TU Delft), Julia Pohl (Pohl Architekten) and Diana Sarno (SZN) provided constructive comments on the manuscript. Diana Sarno is thanked for providing electron micrographs and Susanne Gosztonyi for providing illustrations on light transferring structures based on glass fibres.

References

Anonymous (2013) VDI Richtlinie 6226, Bionik-Architektur, Ingenieurbau, Industriedesign. Beuth, Berlin

Beautyman M (2012) Jurassic Park-Pohl Architekten guided a school team's prehistoric-inspired campus pavilion at the Schule für Architektur Saar in Germany. In: Interior Design, New York, pp 135–137

Bradbury J (2004) Nature's nanotechnologists: unveiling the secrets of diatoms. PLOS Biol 2:1512–1515

Braun D (2008) Bionische Gebäudehüllen. Dissertation, University of Stuttgart

Crawford SA, Higgins MJ, Mulvaney P et al (2001) Nanostructure of the diatom frustule as revealed by atomic force and scanning electron microscopy. J Phycol 37:543–554

D'Arcy Thompson W (1917) On growth and form. Cambridge University Press, Cambridge

De Stefano M, Kooistra WHCF, Marino D (2003) Morphology of the diatom genus *Campyloneis* (Bacillariophyceae, Bacillariophyta), with a description of *Campyloneis juliae* sp. nov. and an evaluation of the function of the valvocopulae. J Phycol 39:735–753

Drum RW, Gordon R (2003) Star Trek replicators and diatom nanotechnology. Trends Biotechnol 21:325–328

Edgar LA, Pickett-Heaps JD (1984) Diatom locomotion. In: Round FE, Chapman DJ (eds) Progress in phycological research, vol 3. Biopress, Bristol, pp 47–88

Ehrlich A, Kroll L, Gelbrich S et al (2011) Einsatz von tragenden Faserverbundstrukturen in der Architektur. Paper presented at the 18th Symposium: Verbundwerkstoffe und Werkstoffverbunde, Chemnitz, 24 March-1 April 2011

Gersonde R, Harwood DM (1990) Lower Cretaceous diatoms from ODP Leg 113 site 693 (Weddell Sea) Part 1: Vegetative cells. Proc ODP Sci Results 113:365–402

Gosztonyi S, Brychta M, Gruber P (2010) Challenging the engineering view: comparative analysis of technological and biological functions targeting energy efficient facade systems. In: Brebbia CA, Carpi A (eds) Design & Nature 5, Comparing Design in Nature with Science and Engineering. WIT Press, Southampton, pp 491–502

Gosztonyi S, Judex F, Richter S et al (2011a) Bionischer Lösungsansatz für innovative Tageslichtnutzung im Sanierungsfall. Austrian Institute of Technology, Vienna

Gosztonyi S, Judex F, Brychta M et al (2011b) BioSkin-Bionische Fassaden, Potentialstudie über bionische Konzepte für adaptive energieeffiziente Fassaden. Austrian Institute of Technology, Vienna

Gruber P (2010) Biomimetics in Architecture: architecture of life and buildings. Springer, Vienna

Gruber P, Gosztonyi S (2010) Skin in architecture: towards bioinspired facades. In: Brebbia CA, Carpi A (eds) Design and Nature V, Comparing Design in Nature with Science and Engineering. WIT Press, Southampton, pp 503–513

Guillou L, Chrétiennot-Dinet M-J, Medlin LK et al (1999) *Bolidomonas*: a new genus with two species belonging to a new algal class, the Bolidophyceae (Heterokonta). J Phycol 35:368–381

Haeckel E (1898) Kunstformen der Natur. Bibliographisches Institut, Leipzig-Jena

Hamm CE, Merkel R, Springer O et al (2003) Architecture and material properties of diatom shells provide effective mechanical protection. Nature 421:841–843

Harwood DM, Chang KH, Nikolaev VA (2004) Late Jurassic to earliest Cretaceous diatoms from Jasong Synthem, Southern Korea: Evidence for a terrestrial origin. In: Abstracts of the 18th International Diatom Symposium, Międzyzdroje, 2–7 September 2004

Hildebrand M (2008) Diatoms, biomineralization processes, and genomics. Chem Rev 108:4855–4874

Ichinomiya M, Yoshikawa S, Kamiya M et al (2011) Isolation and characterization of Parmales (Heterokonta/Heterokontophyta/Stramenopiles) from the Oyashio region, western North Pacific. J Phycol 47:144–151

Ishii K-I, Iwataki M, Matsuoka K, Imai I (2011) Proposal of identification criteria for resting spores of *Chaetoceros* species (Bacillariophyceae) from a temperate coastal sea. Phycologia 50:351–362

Kooistra WHCF, Gersonde R, Medlin LK et al (2007) The origin and evolution of the diatoms: their adaptation to a planktonic existence. In: Falkowski PG, Knoll AH (eds) Evolution of planktonic photoautotrophs. Academic Press, Burlington, pp 207–249

Kooistra WHCF, Sarno D, Hernández-Becerril DU et al (2010) Comparative molecular and morphological phylogenetic analyses of taxa in the Chaetocerotaceae (Bacillariophyta). Phycologia 49:471–500

Kröger N, Poulsen N (2008) Diatoms-from cell wall biogenesis to nanotechnology. Ann Rev Genet 42:83–107

Kroll L, Wolf S, Müller S et al (2011) Characterisation of new embedded embroidered sensors for strain measurements in composite materials. In: Abstracts of the 10th Youth Symposium on Experimental Solid Mechanics, Chemnitz, 26-28 May 2011

Mann DG, Marchant HJ (1989) The origins of the diatom and its life cycle. In: Green JC, Leadbeater BSC, Diver WL (eds) The Chromophyte Algae: problems and perspectives. Clarendon Press, Oxford, pp 307–323

Medlin LK, Williams DM, Sims PA (1993) The evolution of the diatoms (Bacillariophyta). I. Origin of the group and assessment of the monophyly of its major divisions. Eur J Phycol 28:261–275

Müller WEG, Wendt K, Geppert C et al (2006) Novel photoreception system in sponges? Unique transmission properties of the stalk spicules from the hexactinellid *Hyalonema sieboldi*. J Biosens Bioelectron 21:1149–1155

Müller WEG, Wang X, Zeng L et al (2007) Phylogenetic position of sponges in early metazoan evolution and bionic applications of siliceous sponge spicules. Chinese Sci Bull 52:1372–1381

Nachtigall W, Pohl G (2013) Bau Bionik. Springer Verlag, Berlin

Otto F (1975a) Netze in Natur und Technik. IL Berichte 8. Institut für leichte Flächentragwerke, Stuttgart

Otto F (1975b) Wandelbare Pneus. IL Berichte 12. Institut für leichte Flächentragwerke, Stuttgart

Otto F (1985) Diatoms 1- Shells in nature and technics, morphogenetic analysis and character synthesis of diatom valves. IL Berichte 28. Institut für leichte Flächentragwerke, Stuttgart

Otto F (1986) Bambus. IL Berichte 31. Institut für leichte Flächentragwerke, Stuttgart

Parker AR, Lenau T, Saito A (2013) Biomimetics in optical nanostructures. In: Karthaus O (ed) Biomimetics in photonics. CRC Press, Taylor & Francis Group, Boca Raton, pp 55–116

Pohl G, Pfalz M (2010) Innovative composite-fibre components in architecture. In: Pohl G (ed) Textiles, composites and polymers for buildings. Woodhead Publishing, Cambridge, pp 420–470

Pohl G, Pohl J, Speck T et al (2010) The role of textiles in providing biomimetic solutions for construction. In: Pohl G (ed) Textiles, composites and polymers for buildings. Woodhead Publishing, Cambridge, pp 310–329

Pohl G, Feth N, Otten J (2012) BOWOOSS nachhaltige Bausysteme bionisch inspirierter Holzschalenkonstruktionen. Projektdokumentation Teilvorhaben 1, Biona- Forschungsbericht. B2E3, Institut für Effiziente Bauwerke. HTW des Saarlandes University Press, Saarbrücken

Rabosky DL, Sorhannus U (2009) Diversity dynamics of marine planktonic diatoms across the Cenozoic. Nature 457:183–186

Round FE, Crawford RM, Mann DG (1990) The diatoms. Biology and morphology of the genera. Cambridge University Press, Cambridge

Sarno D, Kooistra WHCF, Medlin LK et al (2005) Diversity in the genus *Skeletonema* (Bacillariophyceae): II. An assessment of the taxonomy of *S. costatum*-like species, with the description of four new species. J Phycol 41:151–176

Sarno D, Kooistra WHCF, Balzano S et al (2007) Diversity in the genus *Skeletonema* (Bacillariophyceae): III. Phylogenetic position and morphological variability of *Skeletonema costatum* and *Skeletonema grevillei*, with the description of *Skeletonema ardens* sp. nov. J Phycol 43:156–170

Schmid A-MM, Schulz D (1979) Wall morphogenesis in diatoms: deposition of silica by cytoplasmic vesicles. Protoplasma 100:267–288

Sinninghe-Damsté JS, Muyzer G, Abbas B et al (2004) The rise of the rhizosolenoid diatoms. Science 304:584–587

Sörhannus U (2004) Diatom phylogenetics inferred based on direct optimization of nuclear-encoded SSU rRNA sequences. Cladistics 20:487–497

Suto I (2006) The explosive diversification of the diatom genus *Chaetoceros* across the Eocene/Oligocene and Oligocene/Miocene boundaries in the Norwegian Sea. Mar Micropaleontol 58:259–269

Teichmann K, Wilke J (1996) Prozeß und Form "Natürliche Konstruktionen," Der Sonderforschungsbereich 230. Ernst & Sohn Verlag, Berlin

Townley HE (2011) Diatom frustules: physical, optical, and biotechnological applications. In: Seckbach J, Kociolek JP (eds) The diatom world; cellular origin, life in extreme habitats and astrobiology, vol 19. Springer Science and Business Media, Dordrecht, pp 273–289

Vrieling EG, Beelen TPM, van Santen RA et al (2000) Nano-scale uniformity of pore architecture in diatomaceous silica: a combined small and wide angle X-ray scattering study. J Phycol 36:146–159

Zitzler U (2008) Licht im Schwamm-Schwämme haben die ersten Glas-Lichtleiter erfunden. Pressemitteilung Universität Stuttgart

Chapter 6
Fibre Reinforced Building Envelopes Inspired by Nature: Pavilion COCOON_FS

Göran Pohl

6.1 Introduction

Analysing the biological load bearing systems of diatoms and planktonic organisms, as well as evaluating their technical potential as physical structure, led to an intense study of biological models of geometry, proportions, load bearing behaviour, functional complexity and the ability to adapt. Examining and systematising pore structures details, structural connections, node and fin structures and modular structure was part of the research project. Exploring the hierarchically organized structure of hull constructions led to the projects driving idea: the development of an optimised supporting structure.

Contrary to conventional structures, separating hull and supporting structure, both elements now merge into one. Considering the most efficient use of materials, the elements were simultaneously optimised and hierarchically structured, divided by self-optimising path-systems—emergent Voronoi-diagrams—for static stabilisation. The parametric definition and programming of the desired dependence simulated a self-controlling static system. Thus, a functional diversity, the integration of adaptive subsystems, is theoretically possible. Considering technical and availability reasons, the variety of material, that theoretically could be implemented in the structures, was limited.

In further research, one focus will lie on the benefits of new material compounds, allowing for the addition of functions to the elements (Figs. 6.1, 6.2, 6.3 and 6.4).

G. Pohl (✉)
Faculty of Architecture and The Built Environment, Architectural Engineering + Technology, TU Delft, Façade Research Group, Julianlaan 134, 2628BL Delft, The Netherlands
e-mail: g.pohl@pohlarchitekten.de; gpohl@htwsaar.de

C. Hamm (ed.), *Evolution of Lightweight Structures,* Biologically-Inspired Systems 6,
DOI 10.1007/978-94-017-9398-8_6

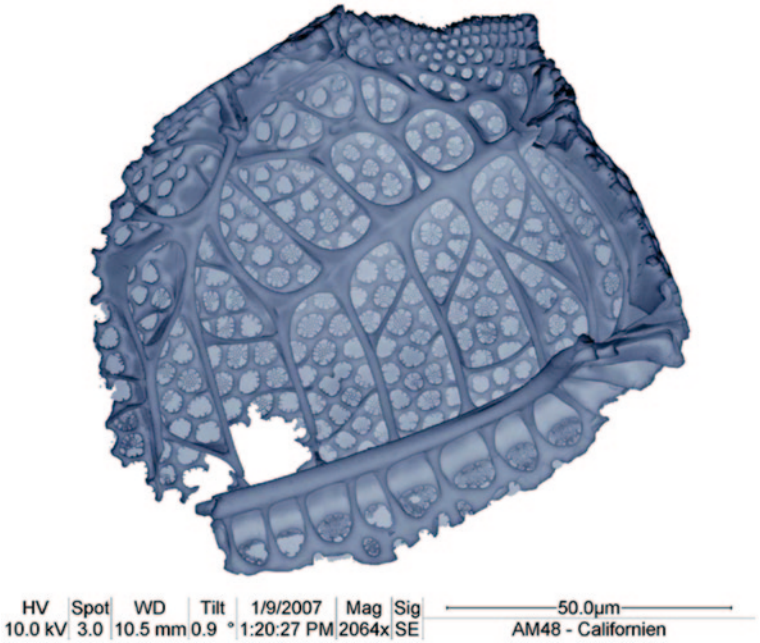

Fig. 6.1 Detail of diatom. (© Alfred Wegener Institute)

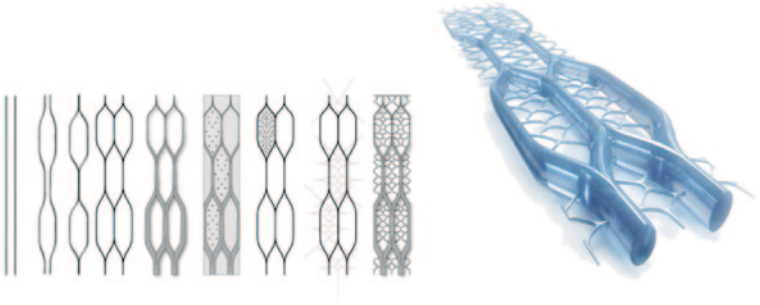

Fig. 6.2 Modular structure—Hierarchizations-Development steps to a constructive component. (© Göran Pohl/Leichtbauinstitut Jena)

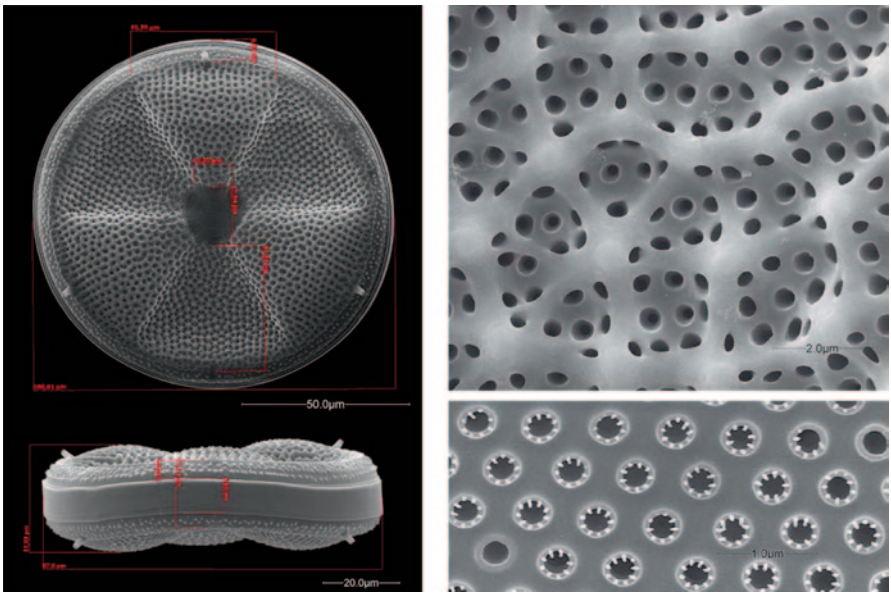

Fig. 6.3 Actinoptycus Senarius (*above*). (© Alfred Wegener Institute)

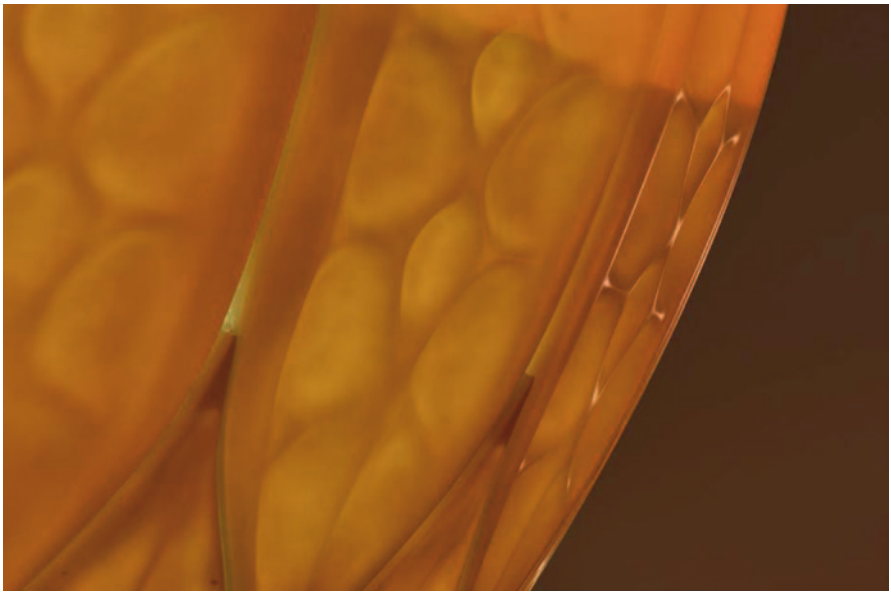

Fig. 6.4 Detailed view of COCOON_FS. Hierarchical structure with primary and secondary fins (*below*). (© Foto: Göran Pohl)

6.2 Morphogenetic Design

Derived from the Greek language, Morphé stands for “stature”, “shape”, while Genesis means “origin”, “emergence”.

Morphogenesis is understood in biology as the study of structure and shape.

Morphology describes macroscopically and microscopically visible features, starting with support structures and organs and organelles and further structural differentiations.

The classification of diatoms, i.e. plankton, is geared toward the characteristic fin structures (valves). Constructional characteristics differentiate between simpler circular structures (Centrales, mostly of fossil origin), and more complex symmetric multi-polar structures (Pennales). (Round et al. 1990)

Morphogenetic design can be described as the design of structure and form in regard to differentiations as shape, subdivision and detailization (Fig. 6.5). (Nachtigall and Pohl 2013)

Fig. 6.5 Night view. (© Foto: Roland Halbe)

6.3 Motivation

Erich Haeckel's findings in nature, as he called them "art forms in nature" (Haeckel 1898) have influenced a generation of architects, designing floral ornaments that have mostly been hand-made. In the later decades, planners followed archetypes of structuralism that have been supported by industrial mass production. Since the possibilities of computer generation grew, new constructive components in architecture are pushed by virtual three-dimensional geometry. For the generation of complex structures, computer programs allow the use of parametric tools, assembling building envelopes from multi-dimensionally twisted and refined elements. These forms of architecture are asking for technologically feasible solutions. Conventional building materials are hard to adapt to multipolar requirements. Construction technology is characterized by a fixation on conventional materials, which cannot put the computer-generated geometries and structural elements into effect. New materials promise a high potential for realizing complex shapes, but require appropriate data generation, iterative constructional development of computer data and manufacturing technologies, as well as verification of their specific applications. Research of sustainable materials inevitably goes hand in hand with finding new ways of generating solutions on all levels of the process chain. Constructional realization of parametrically generated architecture follows the tradition of lightweight constructions, starting after the end of WWII. Lightweight building technologies are firmly established in architecture since the 1950's and 1960's, the days of Buckminster Fuller, Kenzo Tange, Heinz Isler, Ulrich Müther and Frei Otto. Simple physical models were measured geodetically, and the resulting data was propagated onto concrete shells, (Jödicke 1962; Dechau 2000; Ramm and Schunck 2002) patterns for textile membranes (Otto and Rasch 1995) and sophisticated steel structures (Krausse and Lichtenstein 2000). Many biological paradigms were the findings of research and resulted in weight-optimized products (Teichmann and Wilke 1996; Hamm 2005) and led to nowadays established technical solutions. In contrast to these early methods, numerical tools allow the creation and evaluation of building geometry in a three-dimensional space, and the conversion into programmable manufacturing tools (Veltkamp 2007). In addition, modern construction materials can be further refined, and potentials for efficiency enhancement can be realized through load-appropriate anisotropies. This leads to a serious innovative push in construction technology. At the same time materials and manufacturing technologies are being introduced to facilitate the realisation of efficient architecture, allowing spatially complex structures. (Pohl and Pfalz 2010)

Nature has developed shapes which, in many species achieve their special characteristics through a hierarchical configuration. Biogenic structures only visible under an electron microscope reveal material configurations and connecting components

which are morphologically comparable to technical systems. Fibre bundles, made from biogenic silicate (Hildebrand 2008), create stable fin structures in diatoms, whose hierarchical valve structure creates a semipermeable shell, primary and secondary load-bearing elements and equalizing substructures from a single material component. (Hamm et al. 2003) Upon further examination of the diversity, assembly hubs were created from the same material and allow several other elements to be positively tied.

At the virtual research institute PLANKTONTECH, run by the Helmholtz Association, biologists from connected universities and institutes researched the characteristics of diatoms, which are a category of marine plankton. This can be seen as a new research, beginning from the point, Frei Otto and his collegues ended in the 1980's, already finding technical transfer potentials of diatom shells (Otto 1985). Generally all diatoms have hierarchically composed shell structures. The classification of diatoms is geared toward the characteristic fin structures (valves) and differentiates between simpler circular structures (Centrales), usually from extinct species, and more complex symmetric multi-polar structures (Pennales) (Round et al. 1990). Both designs form their silicate shells in stable, multi-finned husks. Biologists from Bremerhaven's Albert Wegener Institute, Freiburg's Albert Ludwig University, Berlin's Technical University, Harvard University and New Jersey's Rutgers University have been contributing to the findings of the research conglomerate. The Assembling and classifying of these findings under the topic of technical transferability was performed by the Institute of Lightweight Constructions Jena, led by Julia Pohl. Their implementation into technical fibre structures was part of the research done by Göran Pohl with support of Pohl Architekten and the Federal Institute for Textile and Process Technology, the ITV Denkendorf.

6.4 Methods of Transferring Natural Solutions into Architecture

The design methods of architects primarily base on knowledge about the human scale. This simple statement describes what architecture is for: buildings to be used in a social and cultural context. While looking for solutions only in the repertoire of technical developments, one will not match the standards of research. Werner Nachtigall, one of the best known experts in biomimetics, has been stating that if one doesn´t use the sources of natural developments, every research seems to be incomplete. Professional research does not allow disregarding even one source of knowledge-potential (Schultz 2011).

The knowledge transfer that this article is about uses the method Pool Research (corresponding to VDI guideline 6226 (2013), see also chapter "Diatom Frustule Morphology and its Biomimetic Applications in Architecture and Industrial Design"). The method was established by Pohl et al. (2010a) as design approach for architects and industrial designers using biomimetics. In the PLANKTONTECH research groups, broad research on diatom morphology provided the base of natural

solutions to be transferred into design systems. This pool of natural know-how has been examined and structurally classified. Finally, the morphogenetic structures of hierarchic systems in diatoms have been explored in depth. The outcome could be translated into structural demands of buildings like the pavilion COCOON_FS described here: self-supporting shell structures using lightweight material (silica) for integrated building envelopes. In diatoms structures are hierarchically organised for stability purposes. Ribs and beams as embedded supporting structures are naturally made from the same material as the cladding structure is: from biogenic silica. This morphological principle can be transferred directly in building-systems. First, silica as material does not seem to fulfil the demands, mostly being used for windows in technical systems and able to withstand pressure loads, as it is weak in terms of tension. From this point, technical developments help to match the needs evoked by the idea of natural hierarchic structures. Considering technical fibres such as glass fibres and the potential of fibre reinforced polymers (frp), emerging new typologies of facades will benefit from investigations on diatom structures. These facts show that a combination of various fields of research is needed, thus future architecture, meaning biomimetics, benefits.

6.5 Technique and Material

"Limits of technology are not limiting us, but inspiring us" (Frei Otto on November 18, 2011) at a conference on lightweight construction at Chemnitz Technical University (Otto 2011). With regards to frp materials, there is a huge potential which can be seen as ideal for anisotropic skins: super stable building skins have embedded extra functionality. Free mouldability of fibre-composite structures allows buildings to generate supporting-structures and envelopes in one single production process. Elements of construction can be configured load-appropriately and in seemingly any geometric shape. This construction material is usually composed of glass or carbon fibre and a matrix of polyester or epoxy resin to embed the fibres into a laminate. Other materials known for specific applications are aramid fibres or natural fibres (hemp, flax etc.) and matrices made from renewable resources. Natural fibres are already being used in the automotive industry, especially for lining components—their behaviour in crash situations is very favourable. Technology-transfer from the high technology industries benefits from natural structures which can be seen as the most influential factors for resource-efficient buildings in the future. A massive development stimulus in the building industry is recently ongoing in thin and free-form fibre-reinforced concrete elements which are mainly being used for veneer constructions. In the case of COCOON_FS, implementing pool research findings and technical inventions have provided new knowledge about fibrous materials and manufacturing methods for free-form lightweight building technologies. This lead to the experimental research prototype COCOON_FS. In further steps, the prototype will be refined for production readiness, and experiments have to be conducted regarding the properties and usability of other material combinations.

6.6 Milestones in PLANKTONTECH Research and Development of COCOON_FS

In a development step following Pool Research, the structural behaviour of diatoms can be characterized as follows:

Valves create hierarchical fin structures, which tie positively with the three-dimensionally arranged roof cover and result in a structured construction technique. Compared to the shells of the Clypeasteroida and similar sea urchins, which consist of separate, interlocked calcium carbonate plates, this technique appears to exhibit better rigidity and lower material usage, based on supporting fin and pore structures. This attribute can be reproduced in the technical implementation of self-supporting shell-fin-systems. The production of a prototype with the specific lightweight building characteristics of diatoms provides a deep insight on materiality as well as on production. The building shape is one factor and implementation of the entire process chain of the industrial manufacturing is another. When abstracted and projected onto the material-intrinsic requirements for numerical iterative tools, the design-to-production flow happens in several stages that can be seen as milestones:

a. Basic research of the PLANKTONTECH group members, assembling the member´s findings, evaluation and preparing for transfer as part of Pool Research
b. Design studies based on PLANKTONTECH Pool Research
c. Programming and preliminary design for COCOON_FS
d. Structural Morphogenetic Design for COCOON_FS: generic development steps of a hierarchical veneer and hull structure)
e. Static analysis
f. Constructional Morphogenetic Design for COCOON_FS: development of a cellular hull design in fibre-composite construction.
g. Testings and optimization steps due to material and manufacturing requirements
h. Production
i. Transport and Installation (Fig. 6.6)

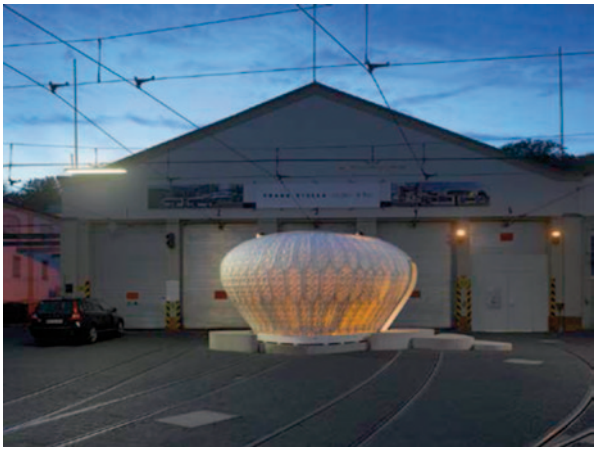

Fig. 6.6 Evening view with inside lighting. (© Foto: Roland Halbe)

6.7 Programming and Preliminary Design for COCOON_FS

The design-step programming reveals the functional needs of a building, while the preliminary design is based on these requirements. The results of programming can be characterized as requirements for the pavilion:

- Portable structure, easy to transport
- Installation has to be very quick, within 2–3 h
- Lightweight
- Translucent for illumination purposes, nightly attraction
- Optional elements for low volume-packaging
- Functional needs: space requirements for up to 2 persons (information desk) and for up to 5 persons (visitors).
- Display surfaces for small exhibitions on biomimetics (PLANKTONTECH results), design, and art.

The development of COCOON_FS has to match several criteria. Functional needs demanded a maximum of space. Given the transportation needs, a building was considered which would be able to either be cellular organised and built on site or to be transported as one piece. Demands on minimum weight with a maximum of stability forced a rethinking of the engineering process of construction buildings. The footprint of COCOON_FS was limited to a maximum of 10 m^2. The reasons for this limitation are the German regulations for official approval: more square footage would have required additional permissions which would have been subject to approval by the authorities and would have brought on additional costs rendering the research object ineffective and expensive. The space allocation plan was developed in line with the requirements of a minimal area and the maximization of usable space. On the base of this space allocation plan, the configuration was created (flexible layout, space for an information and cashier counter for two people, wall areas for research exhibits, catalogues and posters, space for up to 5 visitors at a time). As a result of these limiting factors, the hull is initially arched outwards and has a slightly curved roof, thus maximizing the available space.

6.8 Structural Morphogenetic Design

The pavilions geometric description is generated three-dimensionally by a universal CAD-System, Rhino.

The form-finding process is defined by several iterations until the volume contains all parameters.

Regarding use, maximum height and width, maximum basic area and geometric form, there are geometric requirements. Further steps refine the shell, considering

the production capability. The entire building structure is generated and gridded as a closed surface originating from the first form.

Single elements are extracted and constructively refined as cells. The parameterized image of the closed building structure in a 3D-CAD-System ensures accuracy and a precision fit of the final single forms.

4 mm were consistently defined as joint width between the cells.

COCOON_FS is a combination of individual cells. During further parametric development iterations the geometry of these cells was examined and confirmed. Their shape received a hierarchically layered structure consisting of primary and secondary fins, interconnected with the hull. Using the secondary fins as thickened hierarchical structures, it was possible to reduce the thickness of the outer walls to 3 mm, while the fins themselves were downsized to a 6 mm material gauge following load-bearing tests. Another side-effect using hierarchical structures is the equalization of thermal suspension and of production tolerances.

Further generative computer developments were necessary to convert the original geometry into a new shape, and to free-form a horizontal intersection which allowed a combination of equal or similar elements. These iterative optimization steps have been indispensable to reduce the cost of production.

Parametric studies of the transportability showed that the COCOON_FS structure can be built and transported very flexibly:

- Packaging of individual cells: A single panel van is sufficient to transport all components. Assembly happens on location, with permanent or detachable jointing. Components can be loaded and unloaded manually. A false work is required for assembly which can easily be created on location using a template.
- When the structure can be pre-assembled at the factory and shipped to its destination, the consistent assembly methods are advantageous. COCOON_FS can be transported on a flat-bed vehicle and loaded/unloaded with a crane.
- COCOON_FS can be broken apart into larger sub-assemblies and is therefore suitable for shipping in variably sized containers. Hull elements are assembled at the factory under controlled conditions. The element configuration is adjusted to container measurements.

6.9 Statical Analysis

Self-supporting elements-without substructure-adhesive bond (Fig. 6.7)

Weight of the whole pavilion: approx. 750 kg. The low weight requires the use of a heavy-weight base, or for the pavilion to be anchored to the floor.

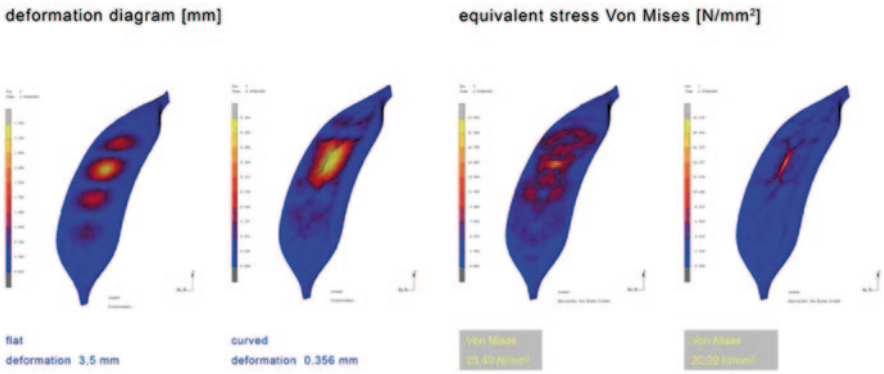

Fig. 6.7 The images above show the effects of increasing hierarchization (*left* to *right*): Adding a further substructure, the structured cell elements' deformation is reduced to 10% of its original dimensions. Given the same hierarchization step, stresses Von Mises are reduced by 15%. (© Alfred Wegener Institute)

6.10 Constructural Morphogenetic Design

The implementation of separate supporting structures would have been the traditional way of civil engineering. Like diatom frustule, integrated structures should match the demands of loadbearing and enwrapping in one. This leads to the development of self-supporting cell elements that could be assembled to a self-supporting building-structure. In the next step, individual cells have been verified to be produced. The following iterations have to construct every single element and to optimize this cellular system. Individual cells promised to be easy to produce and to improve transport flexibility. This view established the structural organisation of the pavilion. The constructural morphogenetic design considered all benefits and limits of the material as well as the specific needs for later installations (Figs. 6.8 and 6.9).

To create the elements of the construction, each element has to be exactly defined by 3D-data. This data shows the positive element, needing to produce a mould, a negative for each part. In this mould, the cells are laminated almost like a cake in a cake tin (Figs. 6.10 and 6.11).

The data of the positive elements has to be translated into data of negative moulds. The process is as follows:

Three-dimensionally created CAD-data was carried over into self-contained surfaces and exported into milling data for the CNC-controlled form cutters to produce the moulds. The data transfer runs via.iges or.step, which can be created from the

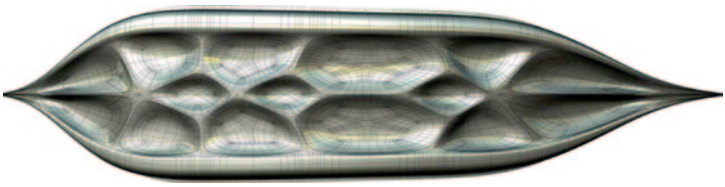

Fig. 6.8 One cell, showing ribs in the *centre* and leading to the fins that are necessary to connect each cell to the other (see pict. xx). (© Göran Pohl/Leichtbauinstitut Jena)

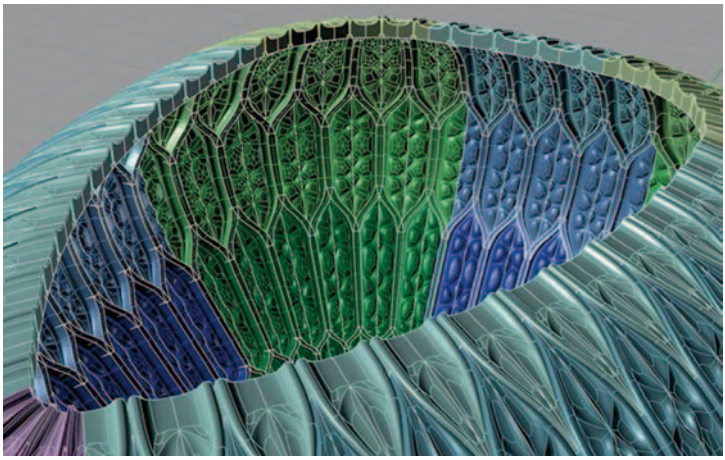

Fig. 6.9 Cells have to be constructed with high accuracy. Inside the construction, the fins of each cell are visible. Their function is the attachment of each cell to the other via gluing. (© Göran Pohl/Leichtbauinstitut Jena)

program *Rhinoceros*. The manufacturer needs data readable in *Catia*. Afterwards, shapes were milled from laminated MDF blocks and—ready to be laminated-coated in varnish. Parametric shape optimizations yielded 15 primary shapes and 8 non-standard parts, while the latter resulted from the basic shapes. Between 3 and 28 exemplars of the primary shapes, and 1–2 exemplars of each non-standard shape were cast (Fig. 6.12).

During the first tests, a 2-part mould was considered advantageous. However, first production results indicated that a change to a 3-part mould would be more beneficial due to the midrib that occurred from the 2-part mould. Despite a slightly higher production effort, less reworking and finishing was required (Fig. 6.13).

In addition, the first production results yielded important conclusions about the maximum bend and insertion radii of mattings and lattices, and about the flow behaviour of the embedding matrix. A parametrically programmed monitor visualized

Fig. 6.10 Overview of all 23 individual parts/forms. (© Göran Pohl/Leichtbauinstitut Jena)

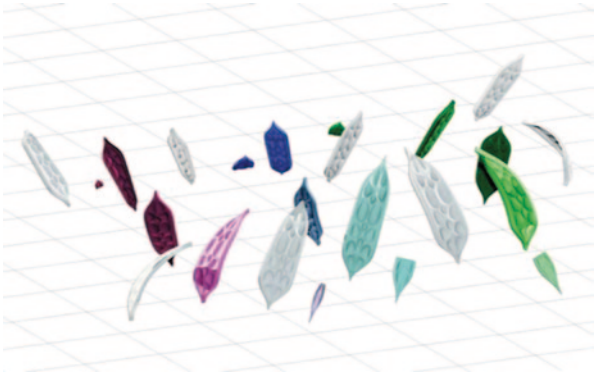

Fig. 6.11 Elementing as a result of manufacturing optimization requirements—Structural Morphogenetic Design (*right*). (© Göran Pohl/Leichtbauinstitut Jena)

the range of high-angle bend radii and large matrix accumulation. Subsequently, the fin radii were adjusted using the parametric system. The results are being compiled in a research report, which will be available for future free-form structures (Figs. 6.14 and 6.15).

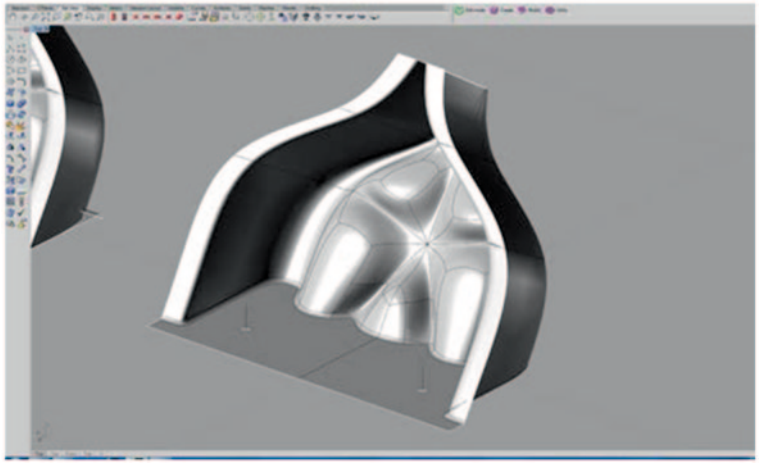

Fig. 6.12 Showing one of the non-standard elements which results from the basic element. This element is the base element that is connected to the floor. It differs by embedding an incline. (© Göran Pohl/Leichtbauinstitut Jena)

Fig. 6.13 2-part mould ready to laminate the first cells (*left*), 3-part-mould (*right*). (© Fotos: Göran Pohl)

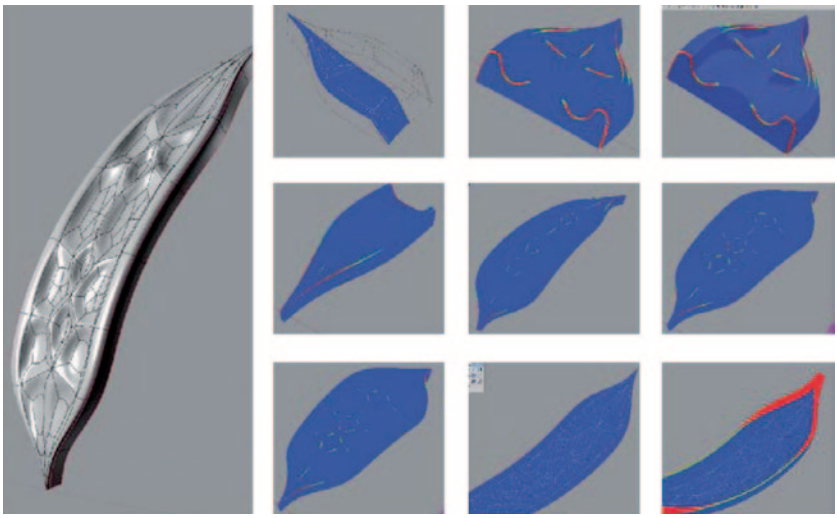

Fig. 6.14 Constructional Morphogenetic Design: Example of fibre structure optimization. The images above (*right and middle*) show areas in *red*. The fibres will not be embedded exactly in the mould (*right image*) and no fabrication problems will occur (*image in the middle*). The *red element* in the *bottom right corner* illustrates the areas of heavy forces due to connection when glued just in these areas. Finally, connections have been changed by identically spaced screwing during primary installation and gluing cell to cell at the end. (© Göran Pohl/Leichtbauinstitut Jena)

Fig. 6.15 Constructional elaboration (*above*). (© Göran Pohl/Leichtbauinstitut Jena)

6.11 Production

Lamination and Material Examinations

For the impressions of the cells, different glass fibre mats and fabrics were chosen and placed into polyester and epoxy resin. The first elements were manufactured as wet laminate in a handcraft lamination process. Easy moulding is the advantage of this process. However, personnel expenses are relatively high and the final composites' load bearing capacity is low. During the examinations, special fabrics and translucent resins were used to achieve high translucent cells. Given the material combination, resin flows too fast and the composites' homogeneity can't be ensured. Due to the production process and easily flowing resin, air inclusions became visible. In the beading, accumulations of resin didn't lead to an optically pleasing result. Therefore, a less translucent resin with white staining was chosen and the fabric was varied during the examinations. Thanks to these modifications, it was finally possible to generate a near perfect appearance. The best result was achieved by a combination of different mats with fleece placed inside.

Polyester resin served as a matrix. Apart from handcraft lamination, vacuum production was examined, using a unilateral form and a vacuum film with vacuum injections of resin. A counter mould was also considered. For the final production, the handcraft lamination process was chosen as it appeared to be the easiest way. Laminating the first samples of elements in a 2-part form, the fins thickness could be reduced to 60 mm. Evaluating first impressions, the originally estimated 100 mm seemed to deep, an assumption which was later confirmed by static calculations. Fins are significantly responsible for the stiffness of each cell and serve as adhesive flange, connecting the cells (Figs. 6.16, 6.17 and 6.18).

Coating coating of the elements was done using a polyurethane-based varnish, which is adjusted to result in a perfect exterior surface when used on both sides. The varnish has a high light transfer capacity, leading to great translucence.

Lighting Specifically for the pavilion, a lighting system was developed and optimized in cooperation with the manufacturer. The interior is illuminated using LED technology, turning COCOON_FS into a luminescent object at night (Fig. 6.19).

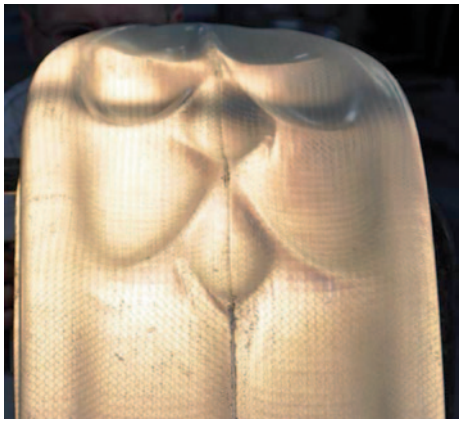

Fig. 6.16 High translucent cell. The 2-part form causes a seam in the centre. (© Foto: Göran Pohl)

Fig. 6.17 First samples of adhesive bonding, combining test cells (*left*). Different staining of test cells is clearly visible, based on different material compositions. (© Foto: Göran Pohl)

Fig. 6.18 Samples of elements after lacquer testing: the front element is fabricated by a 3-part form (*right*), the rear one by a 2-part form, visible by the middle bar. (© Foto: Göran Pohl)

Fig. 6.19 Interior view of the translucent hull. (© Foto: Roland Halbe)

6.12 Conclusion

The project's result is a free-form supporting structure in modular composites design, based on a new combination of materials.. Regarding fibre composites design, there have recently been further examinations of the choice and combination of materials. Acquired knowledge is thereby pursued, relating to the development of facade elements in fibre composites design. For economical implementations of these constructive innovations, the connection between manufactured and technological processes during production will be significant.

Future research focus could be on the following projects:

- Modification of textile, prefabricated structures, considering the ability to drape, fire and high-temperature behaviour
- Development of components' composition for inorganic, non-metallic sandwich-top layer-matrix and core layer.
- Implication of modified, prefabricated structures according to moulds' specific requirements
- Production of sandwich structures, based on textile reinforced sandwich top layers and non-flammable core layer.
- Development of a technology, supporting mass-production to fabricate non-flammable free-form supporting structures
- Application of function specific elements and monitoring fibres
- Implementing a flexible, modular mould system

Subsection

Acknowledgement Special thanks to Dr. Christian Hamm, AWI Bremerhaven, for the support, compiling biological foundations, and consulting.. Special thanks to Julia Pohl for doing the extensive work of Pool Research and providing systems that could be transferred to a technical context. Thanks to POHL Architects, supporting the project through the professional background, led by Julia Pohl. In the team, Jan-Ruben Fischer provided parametric programming and 3D-elaboration, and Jürgen Wilhelm graphic post-production.

Matthias Pfalz, Fibertech, and Andreas Ehrlich, TU Chemnitz have been partners in the discussion to find out the production material and technique to be used for COCOON_FS.

Prof. Dr. Martin Fischer, Friedrich Schiller University Jena, has been given the opportunity to install the prototype of COCOON_FS as an integrated part of the Frank Stella Art Exhibition 2011 in Jena. Thanks to Frank Stella, the outstanding artist, for his agreement to have the pavilion in the context of his exhibition in Jena and for his friendly comments.

Special thanks to Ulrich Knaack and Tilmann Klein, Façade Research Group at TU Delft, for the constructive comments to implement this chapter as part of my further research on fibre reinforced constructions used for building envelopes.

Realisation in the context of PLANKTONTECH Virtual Institute of the Helmholtz Association, in cooperation with Institute of LIGHTWEIGHT CONSTRUCTIONS INSTITUTE, POHL ARCHITECTS and with the support of Alfred Wegner Institute in Bremerhaven

Fibre Composite Realisation Fiber-Tech Group

Lighting Jenoptik AG and Dilitronics GmbH

References

Anonymous (2013) VDI Richtlinie 6226, Bionik—Architektur, Ingenieurbau, Industriedesign. Beuth, Berlin

Dechau W (2000) Kühne Solitäre, Ulrich Müther, Schalenbaumeister der DDR, DVA

Haeckel E (1898) Kunstformen der Natur. Bibliographisches Institut, Leipzig-Jena

Hamm, C (2005) Kieselalgen als Muster für technische Konstruktionen. Biospektrum 1(05):41–43

Hamm CE, Merkel R, Springer O et al (2003) Architecture and material properties of diatom shells provide effective mechanical protection. Nature 421:841–843

Hildebrand M (2008) Diatoms, biomineralization processes, and genomics. Chem Rev 108:4855–4874

Jödicke J (1962) Schalenbau. Dokumente der Modernen Architektur, Karl Krämer, Stuttgart

Krausse J, Lichtenstein C (2000) Your Private Sky, Richard Buckminster Fuller, Design als Kunst einer Wissenschaft, Lars Müller Verlag

Nachtigall W, Pohl G (2013) Bau Bionik. Springer, Berlin

Otto F (1985) Diatoms 1—Shells in nature and technics, morphogenetic analysis and character synthesis of diatom valves. IL Berichte 28, Institut für leichte Flächentragwerke, Stuttgart

Otto F (2011) Conference on lightweight construction, Chemnitz Technical University, 18 Nov 2011

Otto F, Rasch, B (1995) Gestalt Finden. Menges (ed), Stuttgart

Pohl G, Pfalz M (2010) Innovative composite-fibre components in architecture. In: Pohl G (ed) Textiles, composites and polymers for buildings. Woodhead Publishing, Cambridge, pp 420–470

Pohl G, Pohl J, Speck T et al (2010a) The role of textiles in providing biomimetic solutions for construction. In: Pohl G (ed) Textiles, composites and polymers for buildings. Woodhead Publishing, Cambridge, pp 310–329

Ramm E, Schunck E (2002) Heinz Isler, Schalen. VdF, Zurich

Round FE, Crawford RM, Mann DG (1990) The diatoms. Biology and morphology of the genera. Cambridge University Press, Cambridge

Schultz B (2011) Die Natur kopieren ist völlig sinnlos. In: Inspriation Bionik, Bauwelt 31.11, pp 14–17

Teichmann K, Wilke J (1996) Prozeß und Form "Natürliche Konstruktionen," Der Sonderforschungsbereich 230. Ernst & Sohn, Berlin

Veltkamp M (2007) Free form structural design. IOS Press, Amsterdam

Chapter 7
Biomimetic Engineering of Tailored, Ultra-Lightweight Fibrous Composites

Markus Milwich

7.1 Lightweight Constructions Using Fiber Reinforced Polymers

Fiber reinforced polymers (FRP's) are now in use for several decades. In using high strength fibers such as glass, carbon or aramid embedded in polymer, metal or ceramic matrices, very strong and lightweight composite materials and structures can be manufactured. Because of the strong interest of the automotive industry, research regarding FRP's is at full speed, mainly to reduce production cost with new materials and processes. The growing knowledge about the special handling and behavior of the materials in comparison to metals allows designing more complex and structural, i.e. highly strained, parts. Besides high strength and stiffness adherent with low weight, FRP's have many more advantages compared to un-reinforced plastic or metals, e.g. an excellent durability in different environments, very good fatigue behavior and low thermal conductivity (Henning and Moeller 2011). Fiber reinforced composites show an anisotropic behavior: fibers can carry loads very well in the direction of the fiber axis, whereas perpendicular to the fiber axis only the much weaker matrix carries the loads. This results in very different properties along or perpendicular to the fiber axis. Bearing this fact in mind, a big advantage of FRP's is, that the fibers can be laid in the direction of the stress lines. In future, mechanical properties will increasingly be tailored according to the stresses in the parts. On the other hand, in areas of the part where stresses are low, material is reduced thus reducing weight (Schürmann 2005).

Due to those manifold advantages, fibrous composites can be found increasingly in modern airplanes, sports goods, and in the industrial sector (primarily for wind turbines). The long term use and the wide experience made in racing cars are now successfully transformed into the automotive sector, especially in the field of

M. Milwich (✉)
Institut für Textil-und Verfahrenstechnik Denkendorf, Hochschule Reutlingen, Körschtalstraße 26, 73770 Denkendorf, Germany
e-mail: markus.milwich@itv-denkendorf.de

Hochschule Reutlingen, Alteburgstraße 150, D-72762, Reutlingen, Germany

C. Hamm (ed.), *Evolution of Lightweight Structures,* Biologically-Inspired Systems 6,
DOI 10.1007/978-94-017-9398-8_7

mobility. The FRP's help to save material and energy during manufacturing, during lifetime and also during recycling (Neitzel and Mitschang 2004).

7.2 Learning from Natural Role Models like Plankton, Plants and Animals

Plankton organisms, such as diatoms, have highly structured shells made of composite material. Although the shells are mechanically very strong, they have to be also light weight because they must float in near-surface water for the photosynthesis. In millions of years plankton developed a special ribbed shell structure to stay lightweight but also to protect itself against predator crustacean with a growing strength of the shell (Fig. 7.1).

Another natural basic principle is the composition of the tissue as a fibrous composite. That means that load carrying fibers are arranged into a form-giving load application matrix system. The high performance of natural composites results not only from the high mechanical properties of fibers and matrices, but result mostly from a smart anisotropic arrangement of bundled fibers on different hierarchical levels. This anisotropic structure of the tissue results in anisotropic material properties, where strength and Young's modulus of the tissues are adapted to size and direction of the external loads. Living tissue, e.g. bones and wood have an additional energy, material and weight saving property: overloaded zones react to the external forces in building up new material thus reducing the load per square inch, in underloaded zones material is removed and recycled.

Nature makes light and stiff structures by applying anisotropy: the fiber lay-up is according to the flux of the forces creating lowest weight and thus lowest consumption of resources.

The properties of natural systems are more defined by composite structure and less by the very few used materials: proteins, polysaccharides, Hydroxyapatite-ceramics

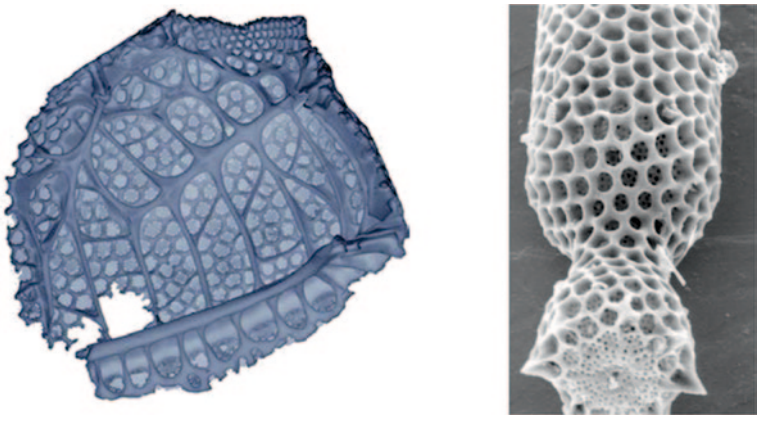

Fig. 7.1 Plankton Structures. (courtesy C. Hamm)

(Bones), $CaCO_3$-ceramics and silica-ceramics (Plants). Those basic materials form only four different natural fibers: cellulose in Plants, collagen in animals, chitin in insects/crustacean and spider silk. Natural fibers have a very high ability to carry loads, having a lower density as glass-, carbon-, or aramid fibers.

Very small changes in the chemical texture of natural fibers or tissue can result in very different mechanical properties. Thus, nearly identical collagen fibers (+ small amounts of hydroxyapatite) form highly loaded and very stiff bone structures, less stiff cruciate ligaments and highly dilative blood vessels. Most notably, nature combines two properties which are rather antithetic in technique: stiffness and ductility. Plankton shells and nacre are remarkable role models for bionic fiber reinforced composites which have high stiffness/strength and high ductility. Nacre is build up by a so called brick and mortar structure, where hard aragonite layers alternate with thin organic layers. The organic interface layers are up to 40 nm thick and consist of a mix of proteins and polysaccharides. They stand only for 5 % of the whole mass of the nacre and act as a template for the buildup of the hard aragonite layers. They act as crack arresters and distribute the external forces over a wider area. Stress peaks are avoided by deflection of the cracks along the organic layers resulting in high cracking resistance. This makes nacre double as hard and thousand fold more ductile than pure aragonite. Research work on nacre aims on biomimetically transferring that principle into technique to create new ductile and vibration damping materials.

The weight optimized properties are accompanied by environmental friendly production processes using low temperatures and solvent based processes.

Technical fibrous composites are constructed similar to nature: main aim is to reduce weight of a part in arranging fibers as good as possible (and with as low cost as possible) along the tension lines in the composite part, combining high young's modulus and high tenacity with low weight.

In the beginning of the use of FRPs, fibers in form of cut woven fabrics were draped and stacked into a mold. Due to the fixed 0°/90° fiber directions in the woven fabric, trade-offs had to be made regarding an optimal aligning of the fibers. Yet, nowadays different textile techniques like stitch weaving or robot-tape-laying are available, which effectively allow to lay the fibers in the path of the external forces, creating ultra-light-weight composite parts.

Composites are nowadays widely accepted as a good means to reduce weight, but more research work has to be done to develop faster production methods and better ways to transfer the very high Young's-Modulus and tenacity of the fibers into finished parts. Fibrous composites allow to integrating additional functions into the structures. Research work is done e.g. to actively damping of disturbing or harmful vibration with piezo-ceramic fibers (Monner 2005), to design passive, form-optimizing adaptive wings for maximum energy yield of airplane wings or wind turbine blades (Breitbach and Sinapius 2004) or to integrate (fibrous) glass sensors for damage control in bridges and airplanes.

Further weight savings in composites are anticipated by decoding multifunctionality of natural tissues and implementing the principles in composite structures. Biological multifunctionality is realized by the clever combination of fiber/matrix materials and gradient structures on different hierarchical levels. As an example,

mechanical properties like strength, stiffness and vibration damping are combined with water and mass transport. Multifunctional Composites combine different functions by either using new materials or by a clever combination of already existing materials. Desirable Additional Functions for composites are:

- Energy harvesting: solar heat, photovoltaic, piezo-fibers, thermal electric generators
- Comfort: Noise reduction and passive/active vibration damping
- Illumination, communication
- System Health Monitoring

7.3 Increasing use of Textiles for Fiber Reinforced Polymers

Not long ago, FRP'S were mostly laminated using short fibers or pre-impregnated unidirectional fibers. Because textiles are easier to handle, faster to process and have a better crash performance, textiles are increasingly used for composite parts (Cherif 2011). The use of textile composites is prominently shown in the automotive sector, mainly by the BMW's new i3 e-car, which has many textile parts in the car body (Fig. 7.2).

When composite structures are made with textiles, mainly non crimp fabrics (based on the warp knitting technology) and woven fabrics are used.

Fig. 7.2 BMW i3 e-car body made from carbon-fiber textiles

Like the construction of metallic car parts, the basic textiles are strengthened by framework substructures which are fixed onto them by stitching or sewing. Afterwards the whole assembly is infused with resin and heated to harden the resin.

Because the batteries of the e-cars are heavy, the car body itself should be as light as possible to save energy and to enhance the operating range of the e-car. Therefore, research work focuses on decreasing the weight of composite parts even further by inventing new technologies for an optimal fiber lay-up. In case of textile technology, textile techniques are developed where fibers can be lain in the calculated directions, the fiber lay-up copying as far as possible the given path of the forces in the part. Two newly developed textile technologies, the stitch weaving and a new developed non-crimp multiaxial multiply technique make it possible to produce a basic fabric and strengthen it with additional fibers which can be orientated according to the flux of the forces.

Figures 7.3 and 7.4 show the open-reed weaving machine principle and open-reed woven fabric with inwrought rovings.

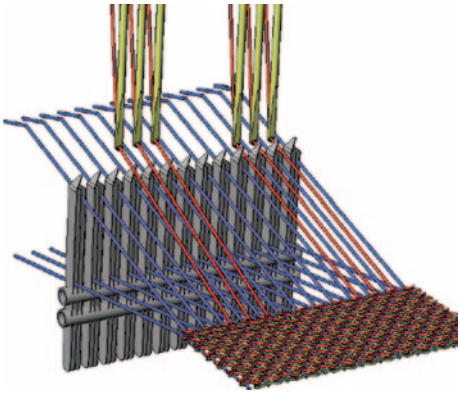

Fig. 7.3 Open reed weaving machine principle. (courtesy Dornier)

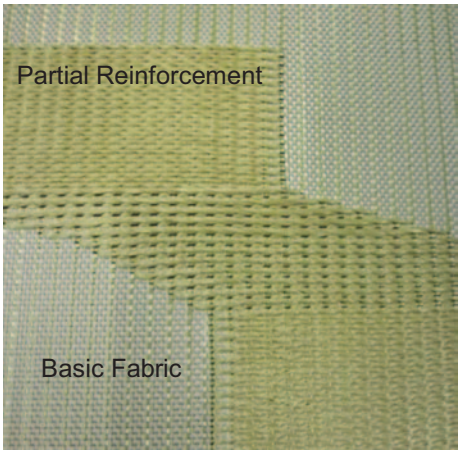

Fig. 7.4 Woven fabric with inwrought rovings. (courtesy Dornier)

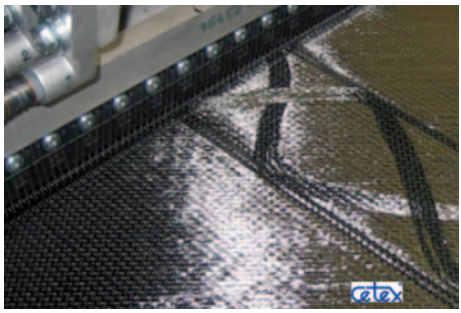

Fig. 7.5 Multiaxial non crimp carbon fabric with incorporated carbon strands. (courtesy Cetex)

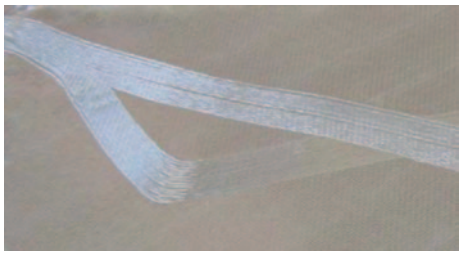

Fig. 7.6 Multiaxial non crimp glass fiber fabric with incorporated glass fiber strands. (courtesy Cetex)

Figures 7.5 and 7.6 show multiaxial non-crimp multiply fabrics with additionally incorporated fiber strands.

To reduce costly prepreg technology, research work is carried out to develop cost effective textile techniques or developing robot lay-up techniques for handling and draping the textiles into complex forms.

7.4 Biomimetic Transfer of Optimized Natural Fiber Reinforced Composites into Technical Structures

In principle, fiber composites are not a human invention. Bones, plant stems, and wood are fiber reinforced composites representing a highly optimized fiber lay up where the fibers run in the exact directions of effective loads (Mattheck 1998).

The Dragonfly-Thorax is a very good example of a multi optimized composite structure with a synergistic interaction of ribs from composite material. The ribs themselves are weight-optimized structures and are macroscopically arranged as weight-saving spacer structures connected by a thin layer of a belting outer skin (Fig. 7.7).

If one looks deeper into the ribs itself—and likewise into all other animal bones—an optimized fiber lay-up is to be seen, where the fibers are strictly aligned to the flux of forces in the bone (Fig. 7.8).

A sophisticated transfer from biological composites into technical applications dates back to the early 1980s and was accomplished by the group of R. Gordon, C.

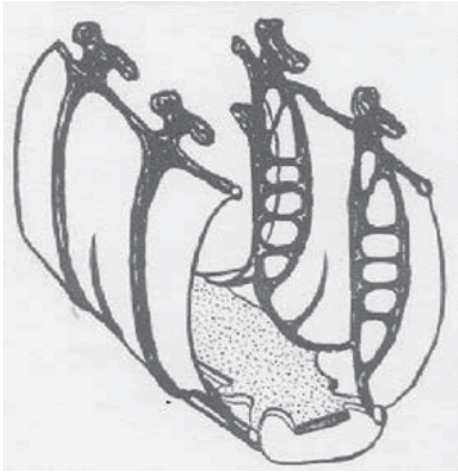

Fig. 7.7 Dragonfly thorax. (courtesy Nachtigall)

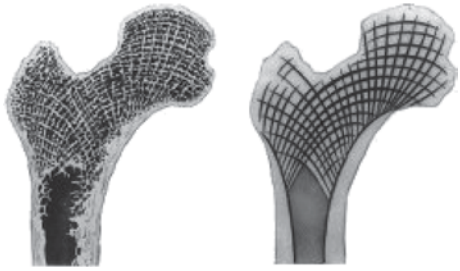

Fig. 7.8 Femur-Bone and extracted fiber-paths (courtesy: wissenschaft-online.de)

R. Chaplin, and G. Jeronimidis at Reading University. They patented a bio-inspired composite structural panel with high strength and toughness based on (ultra-)structural features in wood (Chaplin et al. 1983) (Gordon and Jeronimidis 1980). The orientation of the fibers in this biomimetic composite is based on angles found in micro fibrils of wood tracheids.

Design and production of these ultra-light-weight composites was supported by the development of adequate "finite element" computing methods, which facilitate the calculation of curved and irregular shapes. Claus Mattheck from KIT Karlsruhe investigates biological design rules, triggering the development of an optimized shape of naturally growing constructions. He developed computing methods to simulate force-controlled biological growth, which help to optimize technical constructions by a similar "organic" growth (as in trees) or even help to remove unnecessary volume and weight (as in bones or wood) and put the material into highly loaded zones of a part. His propagation of using tension force loaded machine elements instead of using pressure loaded elements propagates an even more extended use of fibrous materials and will further advance the use of custom-made composites (Mattheck et al. 2004). The results of those different optimizing programs are technical parts with high mechanical properties and low weight. A famous example for

such a bionic optimized structure is the SKO computed Mercedes Benz Bionic Car, where the weight optimized ribbed structure was topology optimized by Prof Mattheck (Fig. 7.9). The fibers are closely aligned along the flux of forces.

The Bionic car body work is 30 % lighter than conventional bodywork, but displays a comparatively complicated structure with many bifurcations. Whereas the assembly of such a car body with welded metallic profiles would be very costly, an assembly with the new fiber lay-up techniques in the composite sector would be simpler and lighter, because the fibers could be easily laid into the flux of the forces. Those fiber lay-up techniques are also so-called "gradient textile techniques." Similar to natural fibrous composites, these techniques allow to lay every single fiber strand exactly within the structure in the direction necessary to neutralize outer forces so that no unnecessary fibers or weight are incorporated.

As an example for a gradient textile process, Fig. 7.10 shows an extreme lightweight carbon fiber reinforced plastic Robot-arm of the German company Kuka Roboter GmbH, produced by a process called tailored fiber placement. This is a stitching process, where, on a slightly altered textile stitching machine, up to 10

Fig. 7.9 Bionic car. (courtesy Mercedes/Nachtigall)

Fig. 7.10 Ultra-Lightweight bicycle chain ring of Co. F + S

stitching heads place every single carbon fiber strand next to the preceding fiber strand (Fig. 7.11).

Another example for a biomimtic transfer of several role models into technique is the development of the “technical plant stem”. In close cooperation of Freiburg biologists and ITV engineers several functional natural principles were abstracted and incorporated into the fabrication of a “technical plant stem”. Role models are giant reed (Arundo donax) (Spatz et al. 1997) and horsetail (Equisetum hyemale). The stem of the horsetail consists of two cylinders connected by pillars (Fig. 7.12), creating remarkably large vallecular canals, which significantly reduces further the weight of the hollow stem. This sandwich structure represents an ultra-lightweight construction with high bending stiffness and high buckling resistance combined

Fig. 7.11 Tailored fiber Placement Technology (courtesy ACC)

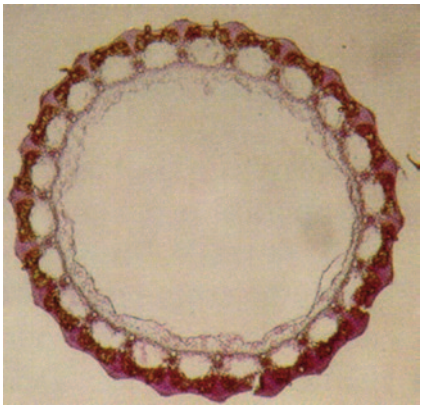

Fig. 7.12 Equisetum hyemale. (courtesy Plant Biomechanics Group Freiburg)

with a low material input, withstanding high wind loads and corresponding high vibrations.

This new product combines the ultra-lightweight sandwich construction of the horsetail with the superior vibration damping properties of the giant reed, disposing of a gradient of stiffness between fibers and matrix created by nano-particles.

Nevertheless, the production costs for this new product must also be taken into consideration. In case of composite beams like the technical plant stem, the pultrusion process is a cost-efficient production method for endless-fiber-reinforced plastics. Compared to metals, the pultruded composite profiles are corrosion resistant and maintenance free. The lower weight reduces installation costs, also lighter foundations can be realized.

In thermo-set pultrusion, matrix impregnated high-performance fibers are pulled through a form-shaping die and are consolidated by heat and pressure during the transit through the die (Fig. 7.13).

To incorporate diagonal fiber bundles into the technical plant stem, a braiding machine was installed into the pultrusion process. The braiding technique helically winds two different counter-rotating sets of intertwining fiber strands around a core system and an inner layer of unidirectional fibers. By varying the density, arrangement, and angles of the fibers in the different layers of the technical plant stem, technical structures can be produced which are optimally designed for a given load situation. With braid pultrusion technology, different hollow profiles with glass fiber

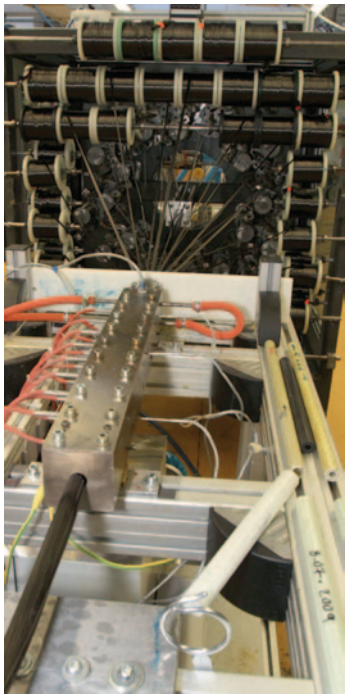

Fig. 7.13 Pultrusion line at ITV Denkendorf

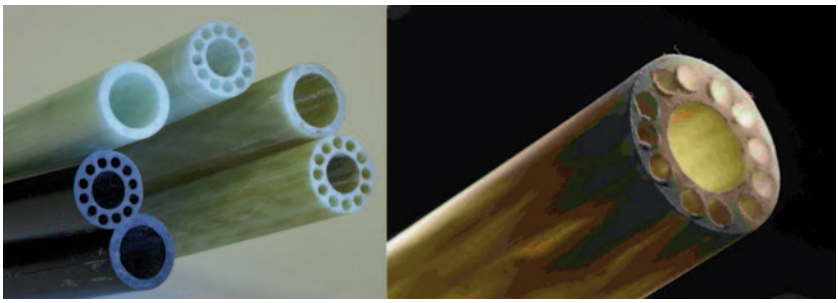

Fig. 7.14 Tubular profiles and "Technical plant stems" manufactured with pultrusion technique at ITV Denkendorf

and carbon fiber reinforcement were produced. To mimic the porous, optimized weight potential of the plant-matrix system, a polyurethane foam matrix was applied between the fiber bundles, resulting in a very lightweight specimen (Fig. 7.14). By combining this cost-efficient production method with the several advantages of the technical plant stem, this unique material will rapidly spread into manifold applications in the composite world like aerospace, transportation, industrial and sports (Milwich et al. 2006).

7.5 Nature's Ultra-Lightweight Structures are the Result of the Optimized Interaction of Different Hierarchical Levels

Within the PlanktonTech project, ITV and its research partners are learning from the role model Plankton to develop ultra-lightweight technical structures with optimized material, topology and fiber lay-up. The bio-mineralized shells of diatoms and Radiolarian are ultra-lightweight structures. Over 100.000 different plankton species with different geometries create a pool of role models for technical structures in different industries like transportation, machines or buildings. The most interesting question is how nature creates an abundance of hierarchical ordered lightweight structures by using only very few materials. ITV research work in PlanktonTech addresses this by developing materials and production methods to transfer those principles of structural/topological optimization and hierarchical ordering to build ultra-light-weight composite demonstrators. The pentagonal and hexagonal structures and substructures shown by Plankton are already generally known to result in stiff and strong structures in technique. Well known is the aramid honeycomb spacer in sandwich constructions, which is inserted between two strong outer layers resulting in a very bending resistant composite part (Fig. 7.15).

The research work in the PlanktonTech project goes along with other research projects at ITV and its research partners. One of the main topics is to understand

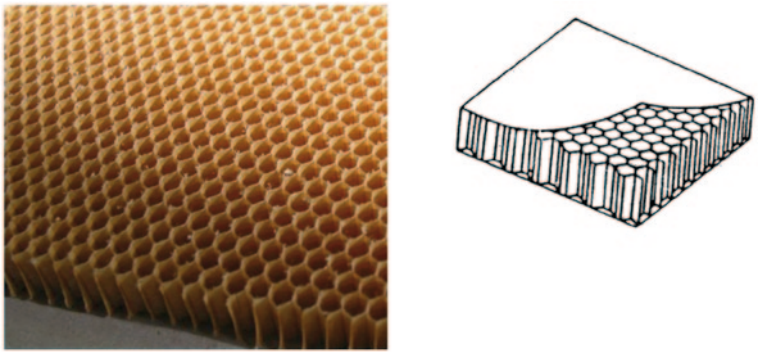

Fig. 7.15 Aramid fiber Honeycomb-Spacer

how the properties of the substructures on the different hierarchical levels create eventually the properties of the whole structure (Figs. 7.16, 7.17).

Well-investigated natural role models in the area of natural composites are plant stems like wood, horsetail and giant reed. Common attributes of those plant composite tissues are the combination of high mechanical or physical properties with lowest material and energy consumption. Main features of trees and giant reed are e.g. the outstanding damping of vibrations induced by wind and the tough, good natured breaking behavior with several smaller cracks before the final rupture takes place. In comparison to this, technical composite structures mostly show a

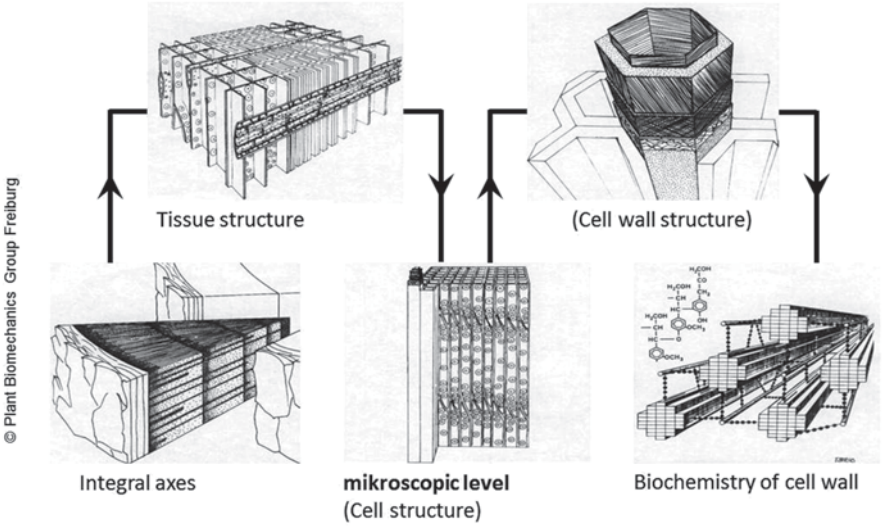

Fig. 7.16 Optimization of overall mechanical properties through optimization of several hierarchical levels by material selection and special fiber lay-up. (courtesy Plant Biomechanics Group Freiburg)

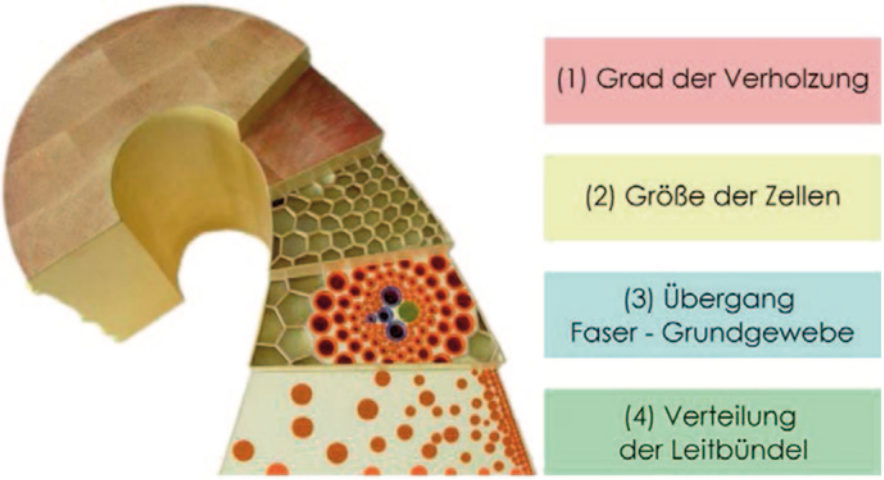

Fig. 7.17 Giant reed: Demonstrative example for a optimization of mechanical properties on several hierarchical levels. (courtesy Plant Biomechanics Group Freiburg)

catastrophic brittle breaking behavior without any pre-warning. The natural composites generate those special properties mainly by an elaborated, gradual stiffness transition between fibers and matrix tissue.

Research work on plants at MPI Potsdam and Freiburg University aim to get an even deeper insight onto the micro or nano-scale composition of the tissues and to extract the different mechanical properties e.g. by different Fiber lay-up i.e. microfibril-angle in the plant cell walls. With this insight, even better technical composite structures will be designed and manufactured.

7.6 Using Plankton-"Technology" to Develop Ultra-Lightweight Structures

The pentagonal and hexagonal structures and substructures are already known to result in stiff and strong structures (see Fig. 7.15). Yet to produce those special structures and their substructures with a well defined fiber lay-up, tape laying technologies have to be adapted and farther developed. Tailored fiber placement and tape laying processes are suited for flat structures. For three dimensional "Plankton-Tech" structures, ITV Denkendorf developed the "freeze-tape-laying" process for aligning the fibers to the 3D-load path in the composite part.

With the "freeze-tape-laying" process it is possible to place the fibers on 2D-and 3D-curved forms without breaking any of the brittle filaments of the high modulus carbon yarns (Fig. 7.18). With this technique, PlanktonTech framework parts were manufactured, among others a fiber lay-up which was inserted into a foam and connected to a carbon outer skin (Fig. 7.19).

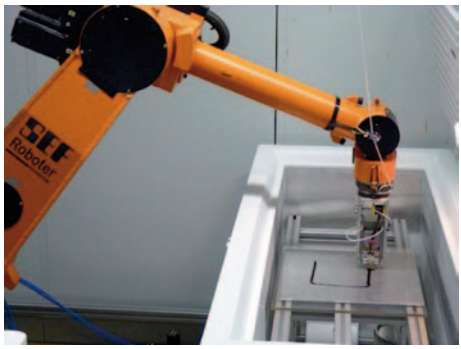

Fig. 7.18 Freeze tape laying

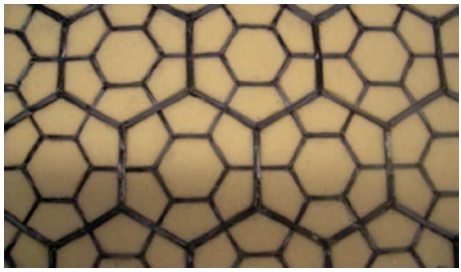

Fig. 7.19 PlanktonTech framework integrated in foam

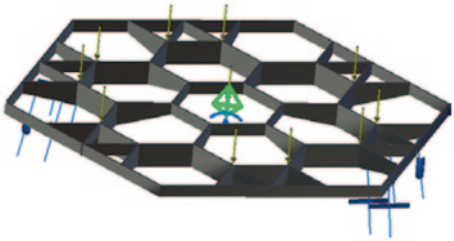

Fig. 7.20 Flat 3D-FEM model of PlanktonTech structure

The development of PlanktonTech manufacturing technologies were accompanied by a topology optimizing using Finite Element Analysis. The FEM calculation of a first flat PlanktonTech structure (Fig. 7.20) was optimized by several optimization steps regarding framework, wall thickness and strut height. This flat design was transferred into a CAD model of a more "natural" lentil like 3D-form (Fig. 7.21). With this form composite framework structures will be produced.

To manufacture the smaller substructures, another technology was developed, the so called "ITV-Fiber placement robot technology". In this case a carbon roving is impregnated directly in the process and deposited with a robot onto an grooved PlanktonTech form (Fig. 7.22).

With this technique several small and big PlanktonTech structures were produced and assembled (Fig. 7.23).

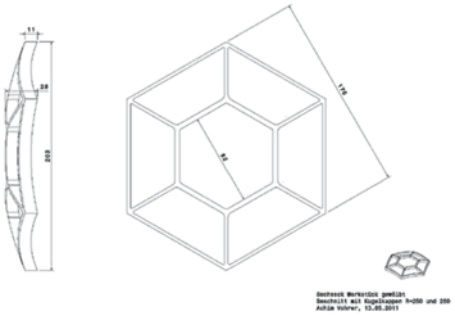

Fig. 7.21 Lentil-like, 3D-domed PlanktonTech composite framework

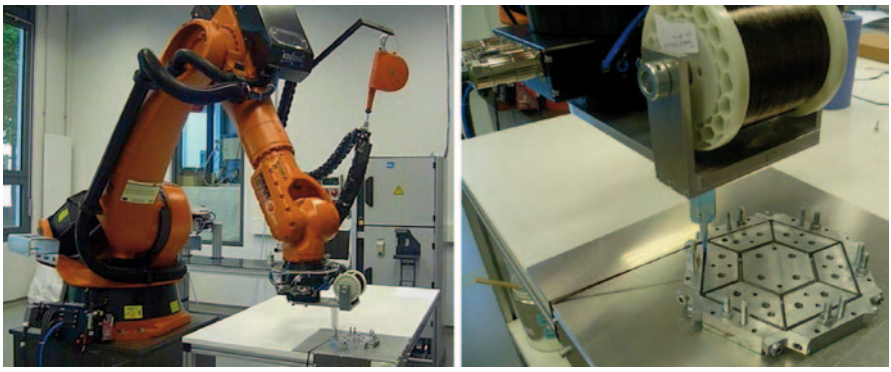

Fig. 7.22 Tape laying robot technology

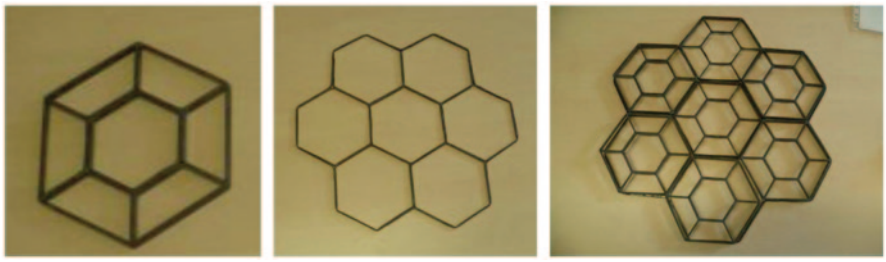

Fig. 7.23 Manufacturing of hierarchical PlanktonTech structure: First Level (*left*), Second Level (*middle*), assembled (*right*)

7.7 Using PlanktonTech "Technology" to Develop an Ultra-Lightweight Robotic Arm

The optimized fiber arrangement in biological materials finds is utilized in technique for an optimal macroscopic arrangement of struts for load-carrying structures e.g. robot arms. Figure 7.24 shows the cactus inspired DLR Rotex robotic arm, with

Fig. 7.24 Robot arm of DLR Stuttgart

0°, 90°-fiber bundles (tensile/compression/bending forces) and 45°-fiber bundles (torsional loads).

At ITV Denkendorf research work is done to find out, whether Plankton offers an even higher potential for lightweight framework structures. A PlanktonTech robot arm was designed, calculated and optimized with the Straus7 FEM-program and compared to the simulated DLR robot arm (Fig. 7.25).

After FEM optimization several PlanktonTech robot arms were fabricated at ITV (Fig. 7.26) and tested with the Universal testing machine on static mode (Figs. 7.27, 7.28).

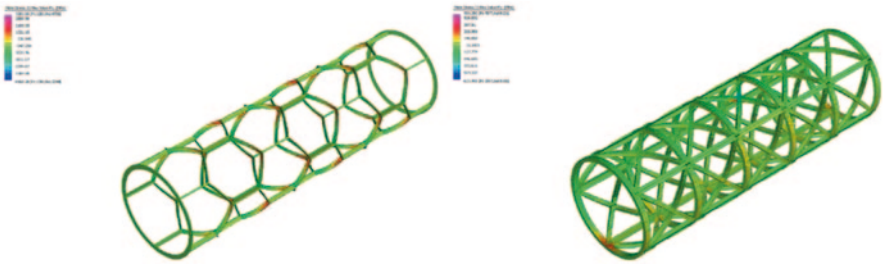

Fig. 7.25 FEM optimized PlanktonTech robot arm (*left*), compared to simulated DLR robot arm (*right*)

Fig. 7.26 PlanktonTech robot arms manufactured at ITV

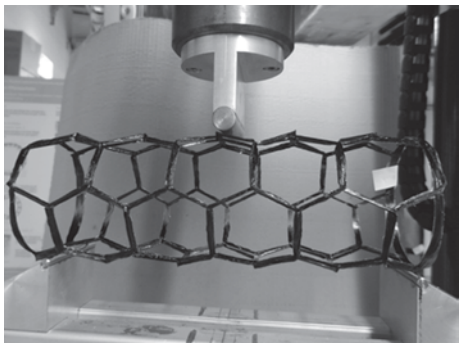

Fig. 7.27 3-Point-Bending test of PlanktonTech-Robot arm

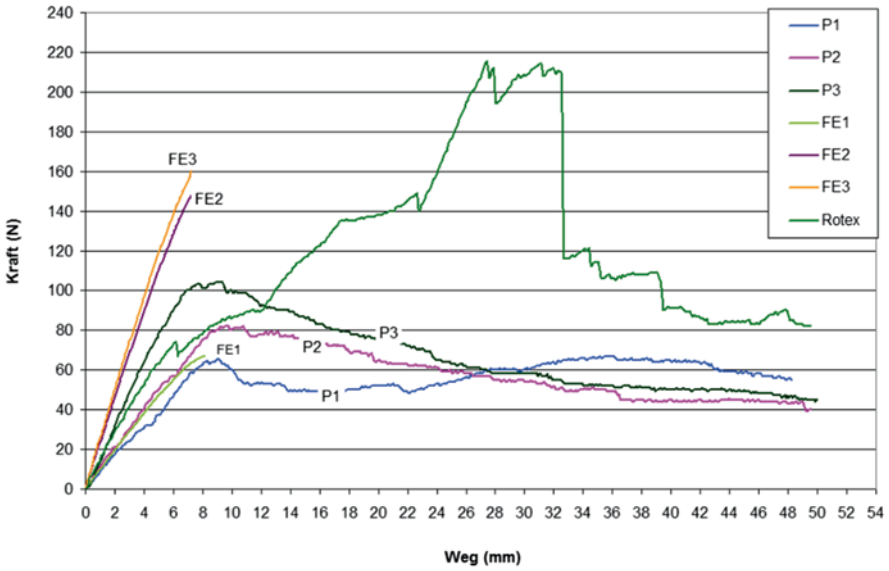

Fig. 7.28 3-Point static bending test of PlanktonTech robot arm and comparison to FE-Simulation. *P1–P3* Test results Hexagon; *FE1, FE2 FE*-Simulation Hexagon; *FE3 FE*-Simulation Double Hexagon

The test results showed a fairly good correspondence to the FEM calculation. Also the FEM comparison between PlanktonTech robot arm and DLR robot arm showed a significant better weight related stiffness of the PlanktonTech robot arm. Although the structure has been developed based on plankton structures, it resembles actually carbon nanotubes, which have been shown to have very advanced material properties.

7.8 Closing Remarks and Future Developments

The promising results of PlanktonTech structures regarding strength and stiffness will be pursued by further research work at ITV Denkendorf and PlanktonTech partners. Materials, fiber lay-up and Manufacturing methods will be further developed to obtain even more lightweight structures with less material cost. In case of natural materials, new, strong, lightweight and waterproof fibers based on silk proteins have been recently successfully produced.

Future will show whether fiber reinforced composites are made from silk fibers or silica-glass fibers (like from sea cucumber), the fibers being embedded into a biopolymer matrix similar to the high-strength and durable glue of rock barnacles.

References

Breitbach E, Sinapius M (2004) Stand und Perspektiven des Leichtbaus und der Adaptronik. Jahresbericht des DLR Instituts für Strukturmechanik, Braunschweig

Chaplin CR, Gordon JE, Jeronimidis G (1983) United States Patent. Composite Material. Assignee: Westvaco Corporation, New York (Application 351,777)

Cherif C (Hrsg) (2011) Textile Werkstoffe für den Leichtbau: Techniken—Verfahren—Materialien—Eigenschaften. Springer, Berlin. ISBN: 3642179916

Gordon JE, Jeronimidis G (1980) Composites with high work of fracture. Philos Trans R Soc Lond A 294:545–550

Henning F, Moeller E (Hrsg) (2011) Handbuch Leichtbau: Methoden, Werkstoffe, Fertigung. Hanser, ISBN 978-3-446-42891-1

Mattheck C (1998) Design in nature—learning from trees. Springer, Heidelberg

Mattheck C, Kappel R, Tesari I, Kraft O (2004) In Seilen denken–Einfache Anleitung fuer naturnahes Konstruieren. Konstruktionspraxis 9:26–29

Milwich M, Speck T, Speck O, Stegmaier T, Planck H (2006) Biomimetics and technical textiles: solving engineering problems with the help of nature's wisdom. Am J Bot 93:1455–1465

Monner HP (2005) Smart materials for active noise and vibration reduction. Proceedings of the Novem–Noise and Vibration: Emerging Methods, Saint-Raphael, France

Neitzel M, Mitschang P (2004) Handbuch Verbundwerkstoffe. Werkstoffe, Verarbeitung, Anwendung. Hanser, ISBN: 3446220410

Schürmann H (2005) Konstruieren mit Faser-Kunststoff-Verbunden. Springer, ISBN: 3540402837

Spatz H-Ch., Beismann H, Bruechert F, Emanns A, Speck T (1997) Biomechanics of the giant reed Arundo donax. Philos Trans of R Soc Lond B Biol Sci 352:1–10

Chapter 8
Echinoderms: Hierarchically Organized Light Weight Skeletons

James H. Nebelsick, Janina F. Dynowski, Jan Nils Grossmann and Christian Tötzke

8.1 Introduction

This overview of echinoderm skeletal structures is presented from a hierarchical point of view ranging from: (1) the complete organisms including all skeletal elements and soft part morphologies, to (2) coherent plate combinations including echinoid coronas and crinoid stems and arms, (3) single skeletal elements, (4) the micro-architecture of stereom types, and (5) ultrastructural aspects of biomineralization. This review mostly pertains to the echinoids and in part to the crinoids to which most attention has been directed in the literature. The consideration of skeletal hierarchies is accompanied by examining a suite of symmetries represented by the echinoderms as a whole or within the isolated elements. Usually beginning as free-swimming bilateral larvae, they undergo metamorphism to an organism based on a pentamerous arrangement, which as in the irregular echinoids and holothurians, can be overprinted by a return to

J. H. Nebelsick (✉)
Department of Geosciences, University of Tübingen, Sigwartstrasse 10, 72076 Tübingen, Germany
e-mail: nebelsick@uni-tuebingen.de

J. F. Dynowski
Stuttgart State Museum of Natural History, Stuttgart Rosenstein 1, 70191 Stuttgart, Germany

J. F. Dynowski
Department of Geosciences, University of Tübingen, Hölderlinstrasse 12, 72074 Tübingen, Germany

J. N. Grossmann
Institute of Zoology, Graduate Program: Bionics-Interactions across Boundaries to the Environment, University of Bonn, Meckenheimer Allee 169, 53115 Bonn, Germany

Zentrum für Wissenschafts- und Technologietransfer, Hochschule Bonn-Rhein-Sieg, University of Applied Sciences, Grantham Allee, 20, 53757 Sankt Augustin, Germany

C. Tötzke
Helmholtz-Zentrum Berlin for Materials and Energy, Hahn-Meitner-Platz 1, 14109 Berlin, Germany

C. Hamm (ed.), *Evolution of Lightweight Structures,* Biologically-Inspired Systems 6,
DOI 10.1007/978-94-017-9398-8_8

bilateral symmetry. Isolated elements can show radial symmetry in echinoids spines, pentamerous symmetry in the case of crinoid stalk elements, bilateral symmetry in the case of ophiuroid arm elements or can lack symmetry completely.

Echinoderms are marine organisms which belong as adults to the benthic realm on or within the substrate. They are important, and in some cases dominant, members of diverse benthic habitats in all depths of the seas. All echinoderms are light weight in that their skeletal elements are constructed of stereom, a variously arranged meshwork-like lattice made up of struts termed trabeculae. This stereom is highly variable as far as density and structure is concentrated ranging from chaotic to strictly directionally oriented to highly dense. The possession of stereom in the skeleton is one of the main diagnostic characters of echinoderms and allows even highly fragmented, single ossicles to be identified in the sedimentary rock record. The skeleton has long been an object of interest from a constructional design perspective and has been approached from various angles including the manner in which single elements are added to the skeleton and to how these elements, together with the whole skeleton, increase in size while retaining their general shape and structural integrity.

Echinoderm skeletons are mesodermal, similar to that of the bones of vertebrates. This means that the skeleton, with very few exceptions, is enveloped by soft tissue at all size scales: (1) the corona of echinoids and the calyx of crinoids surround and protect the major organs of the body, (2) muscle fibers and ligaments connect single plates to one another, (3) organic material (stroma) is present between the struts of the stereom and, at the lowest hierarchical level, (4) organic material is present within the skeletal struts themselves. The skeleton itself is constructed of high magnesium calcium carbonate which contains variable amounts of magnesium within the crystal lattice. Finally, the possession of a more or less durable skeleton has led to an impressive fossil record allowing the evolution of the echinoderms to be followed. There are a number of extinct taxa with, in part, even more bewildering and complex skeletal arrangements than among the five classes still present today.

8.2 Complete Skeletons and Basic Symmetry

The skeletons of echinoderms are highly variable and range from (1) loose ossicles in the body wall as found in the holothurians, to (2) serial rows of highly articulated skeletal elements connected by ligaments and muscle tissues as found in ophiuroids and many asteroids, to (3) rigid rows of plates locked together as in the corona of some, but not all, echinoids and the calyx of crinoids. There are many variations of these skeleton types and in most cases a combination can be present. In echinoids, the test consists of numerous plates that serve as an outer case of plates protecting the internal organs while serving as a platform for various appendages such as spines (Fig. 8.1) and pincher-like pedicellariae. Even the most compact and stable tests are penetrated by various holes including, among others, the mouth, anus and pore pairs of the ambulacral system. In crinoids, a clear tripartite organization can be present with the stems (if present) and arms of crinoids consisting of articulated elements attached to a rigid calyx.

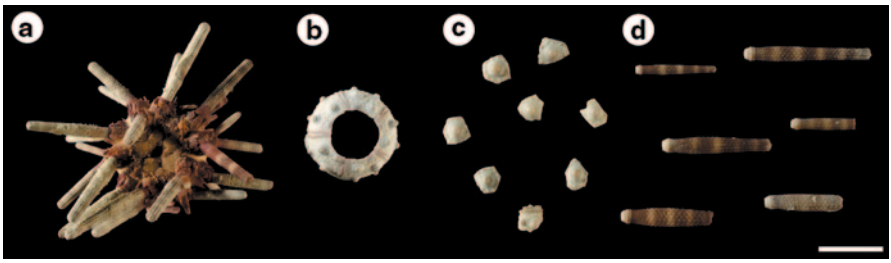

Fig. 8.1 *Eucidaris metularia* from the northern Bay of Safaga, Red Sea (see Nebelsick 1992). **a** Complete individual with spines and apical disc. **b** Denuded test lacking spines, note large primary tubercles which support the spines and sinuous ambulacral plate rows which harbor the tube feet. **c** Disarticulated plates, mostly single large interambulacral plates with primary tubercles. Lowermost element is fragmented and includes attached minute ambulacral plates. **d** Single primary spines showing banding patterning and surface protuberances. Scale bar = 1 cm.

Echinoderms are well known in showing a general five-fold pattern of body parts or plating pattern (Hotchkiss 1998; Smith et al. 2004; Morris 2007). Although most recent echinoderms generally follow this, there are notable exceptions. Recent sea stars often deviate from a fivefold pattern of arms and irregular echinoids show a clear bilateral symmetrical overprint. All echinoderm larvae show bilateral symmetry and undergo a complex metamorphism into adults (e.g. Smith 1997). Even those animals such as regular sea urchins in which clear pentamery can be readily recognized in adults, distinct asymmetry occurs in the position of specific single plates, such as the madreporite. Pentamery is not an apomorphic character for the echinoderms as basal echinoderms such as carpoids found only in the fossil record lack symmetry. The bilateral symmetry of crown group echinoderms was followed by asymmetrical skeletons and then by the familiar pentamerous extant echinoderms (see discussion in Smith 2005a; Zamora et al. 2012). The exact symmetry of irregular echinoids has also been subject to analysis with deviations being attributed to internal morphology or as a possible indicator of stress (Lawrence et al. 1988). Symmetry relationships can also be found between rows of plates as in echinoids or in the arms of ophiuroids and asteroids as well as in individual plates (see below). There have also been attempts to correlate phenotypic size variations of echinoderms to environmental parameters (Laurin et al. 1979; Laurin and David 1990; Dynowski and Nebelsick 2011).

8.3 Structural Analysis and Modeling of Echinoids and Crinoids

Echinoderm body shape can be highly mutable as in the holothurians with their leathery body walls containing minute calcite inclusions or more or less rigid skeletons as found in the corona of many echinoids and the calyx of crinoids. The echinoids have attracted the most attention as far as skeletal architectures and functional morphology is concerned. During their evolution, echinoids show a general

trend from having a uniform test shape, but variable test structure within Paleozoic stem groups to having a variable test shape and uniform test structure in the still extent crown group echinoids (Smith 2005b; Kroh and Smith 2010).

The echinoids shown in Fig. 8.2 thus show a variety of shapes and sizes among the regular and irregular echinoids. The regular echinoids differ in the size of plates,

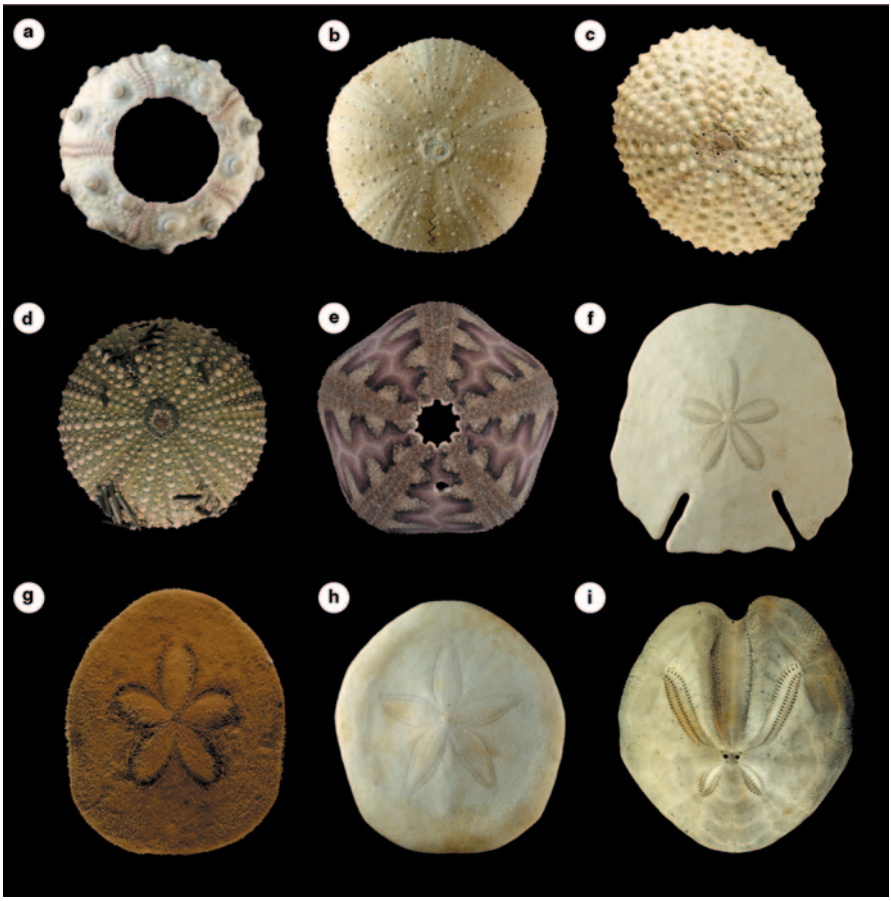

Fig. 8.2 Morphological comparison of tests of regular (*a–e*) and irregular (*f–i*) echinoids. *a–c*, *e–h*: Northern Bay of Safaga red sea, Egypt (see Nebelsick 1992), d and i: Northern Adriatic Sea. **a** The cidaroid *Eucidaris metularia* with large interambulacral tubercles and sinuous ambulacra. Test width = 1.4 cm. **b** *Tripneustes gratilla* with intact apical system and compound ambulacral plates. Test width = 4.5 cm. c) Oblong *Echinometra mathaei* with dense tubercles. Test length = 4.3 cm. **d** *Paracentrotus lividus* with a few attached primary spines. Test width = 4.7 cm. **e** *Microcyphus roussoui* with distinct naked area in the interambulacra. Apical disc is missing, predatory borehole also present. Test width = 5.3 cm. **f** Sand dollar *Echinodiscus auritus* showing petalodium and open posterior lunules. Test length = 9.2 cm. **g** *Clypeaster humilis* still covered by minute spines. Test length = 7.6 cm. **h** *Jacksonaster depressum* with distinct petalodium. Test length = 2.6 cm. **i** Spatangoid *Schizaster canaliferous* with deeply sunken anterior ambulacra and differentially curved paired ambulacra. Test length = 4.7 cm.

ambulacral plate compounding, the number of ambulacral pore pairs per ambulacral plate, the size and number of primary tubercle per plate and so on. The bilateral irregular echinoids show highly divergent morphologies among the flattened clypeasteroid and the more globose spatangoids with respect to, among others, their basic outline, the morphology of the ambulacralia and the size variations of plates. Clypeasteroids show a special constructional principle (see Seilacher 1979) showing not only interlocking plates but also internal supports connecting the upper and lower surface of the test (Fig. 8.3). Despite all these variations, the body form of echinoids is clearly recognizable and almost all extant taxa show double rows of ambulacralia (bearing the tube feet) and interambulacralia.

Echinoids have been the subject of a number of studies analyzing growth and test architectures (e.g. Moss and Mehan 1968; Raup 1968; Seilacher 1979; Johnson

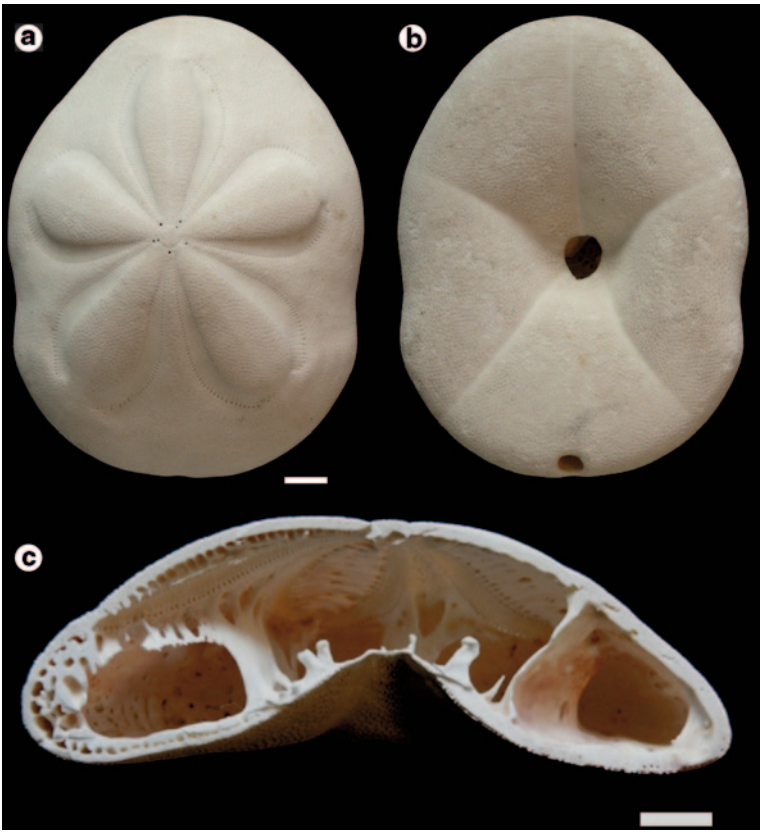

Fig. 8.3 Different views of the irregular clypeasteroid echinoid *Clypeaster rosaceus*. **a** Apical view showing petalodium with ambulacral pores. Apical disc at centre of test with 5 genital pores. **b** Oral view showing central peristome (*mouth*) and periproct near the posterior edge. Test covered by minute tubercles. **c** Cross section showing internal supports connecting the oral and apical side of the test. Double wall structure visible at the test anterior (*left*). Scale bars = 1 cm.

et al. 2002; Telford 1985; Phillipi and Nachtigall 1996; Zachos 2009; Chakra and Stone 2011; Mihaljević et al. 2011). A combination of simple membrane theory and static analysis was used by Telford (1985) to determine how stresses are carried in the skeleton. Ellers et al. (1998) demonstrated the importance of structural strengthening of these urchin skeletons by collagenous sutural ligaments which connect the plates. The interpretation of the echinoid skeleton as representing pressurized pneus (Moss and Mehan 1968; Seilacher 1979; Dafni 1986; 1988) at least during growth was convincingly challenged by Ellers and Telford (1992) who, upon measuring actual coelomic pressures within sea urchins, did not find increased pressure patterns or differences between growing (fed) and non-growing (starved) individuals. Measured pressure differences are caused by extruding and retracting the lantern during feeding which affected the displacement of internal fluids and the peristomal membrane, an area of soft tissue which surrounds the mouth.

The functional morphology of the regular echinoid *Echinus esculentus* performed by Philippi and Nachtigall (1996) using Finite Element Analysis (FEA) analyzed the reaction of the test to different types of loading and argue that test growth and shape cannot be due to internal pressure. Furthermore, the general test shape of regular echinoids is shown to be well adapted to the activity of tube feet. A three-dimensional model of growth is presented by Zachos (2009) which includes both plate addition and plate growth. Individual plate growth is considered along with the insertion of new plates which is continuous until a distance threshold is reached upon which a new plate is added.

Biomechanical considerations concerning crinoids have concentrated on the stalks and the arms using both recent as well as fossil examples. The arm arrangement of fossil crinoids is compared by Cowen (1981) to the distribution patterns found in banana plantations. The dependency of both systems on optimal transport efficiencies are shown in a cost-benefit analysis. A review of the morphology of crinoids and how this pertains to ecology is given by Baumiller (2008). Functional analyses of stalk morphologies comparing skeletal characteristics and the role of mutable collagenous tissue have been used to reconstruct postures of fossil crinoids by Baumiller and Ausich (1996). Baumiller and LaBarbera (1993) studied the structural characteristics of the stalk and the cirri of the crinoid *Cenocrinus asterius*. The mechanics associated with the surprising discovery that stalked crinoids can actually move over the substrate surface are presented in Baumiller and Messing (2007). Further studies on the skeleton and collagenous arm ligaments on crinoids have been made on the arms and their movement (Birenheide and Motokowa 1994, 1996, 1997; Motokawa et al. 2004).

8.4 Single Skeletal Elements

Single plates range in size from minute sclerites (such as in the body wall of holothurians; pedicellariae and tube feet supports in echinoids) to the massive spines of regular echinoids which can reach lengths of 10 cm or more. Individual plates are

present distributed loosely within the body wall, connected to one another by muscles and ligaments, or structurally locked by interconnecting trabecular extensions (see Seilacher 1979; Hidaka and Takahashi 1983; Smith et al. 1990). The single skeletal elements are highly variable in morphology and their detailed form can be closely related to functional aspects (Smith 1978; 1980a, b). Growth of echinoderm plates can occur in discrete increments leading to clear concentric banding which may or may not represent annual events (Raup 1968; Ebert 1975, 1985; Pearse and Pearse 1975). Resorption of skeletal material, though rare, has also been observed (Märkel and Röser 1983) becoming necessary in order to preserve the geometric integrity of the growing animals.

Echinoderm elements themselves also show a wide range of symmetries (Figs. 8.4, 8.5, 8.6, 8.7). Radial symmetry is present in the spines of echinoids. Pentamerous symmetry can be found in the stalk elements of crinoids, but is generally rare. Bilateral symmetric elements are present in ophiuroids and crinoid arms. Coronal plates of echinoids are flattened and show parallel surfaces while other elements show no symmetry at all. Two single echinoderm elements which have attracted special attention with respect to morphology and biomimetic potential are echinoid spines and teeth. Echinoid spines as single elements have been studied due to their relatively large size, growth characteristics and mechanical properties (e.g.

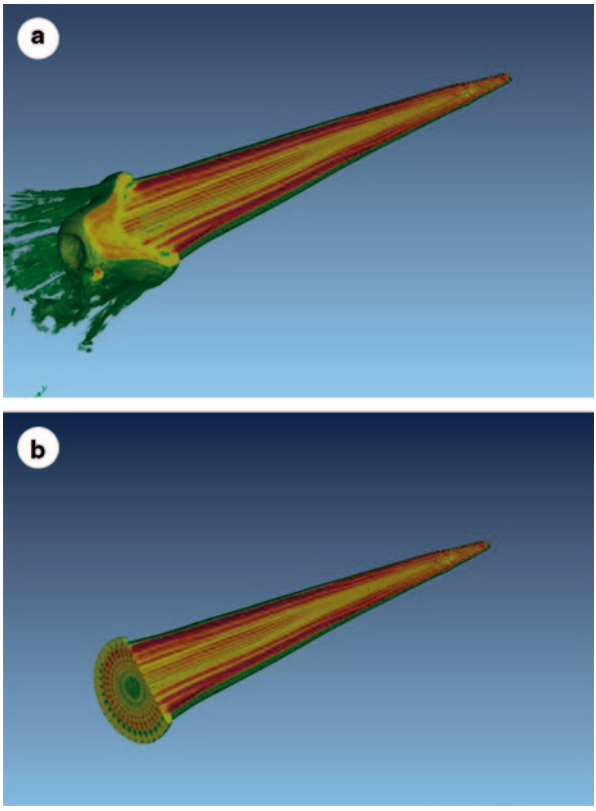

Fig. 8.4 CT-Scans of primary spine of *Echinometra mathaei* showing radial symmetry. **a** Longitudinal section showing consecutive growth stages of the spine. The base of the spine shows attached muscle fibers which attach the spines to the tubercles of the test plates. **b** As *above* with additional cross section at the level of the milled ring showing concentric layers. Length of spine = 2.5 cm.

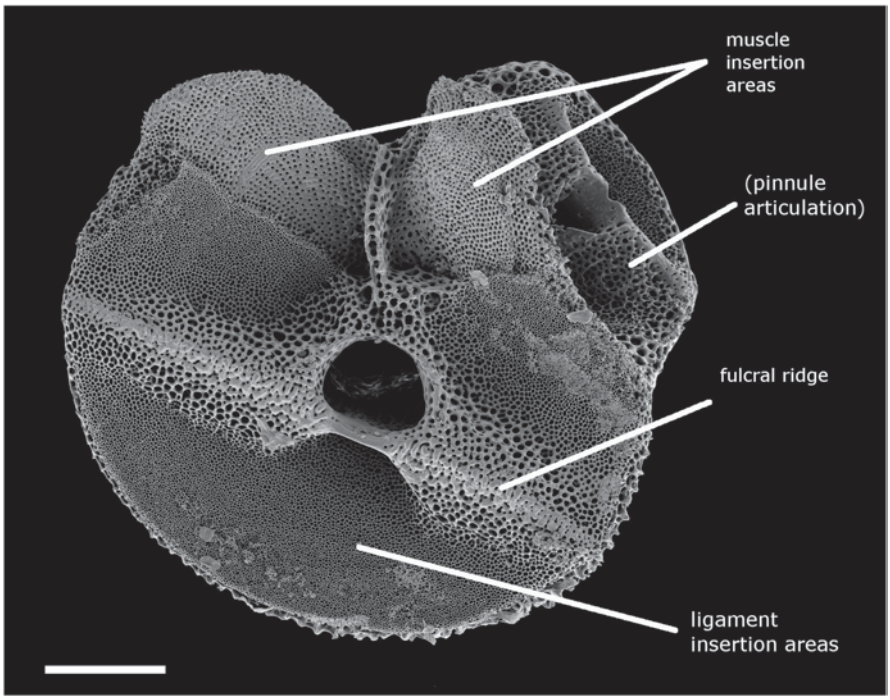

Fig. 8.5 Single arm plate of the stalkless crinoid *Antedon mediterranea* from the Tyrrhenian Sea, Giglio, Italy. Oblique muscular articulation is present with a central canal. Stereom differentiation is clearly developed (see text). Pinnular articulation to the *upper right*. Scale bar = 200 µm.

Strathmann 1981; Currey 1975; Burkhardt et al. 1983; Ebert 1986; Coppard and Campbell 2004; Davide et al. 2009; Presser et al. 2009; Moureaux 2010; Tsafnat et al. 2012; Grossmann and Nebelsick 2013a, b), Echinoid teeth are characterized by their complex morphology, continuous growth and hardness (e.g. Märkel and Gorny 1973; Stock et al. 2003; Wang et al. 1997; Gilbert and Weiner 2009; Robach et al. 2009; Killian et al. 2011; Veis et al. 2011; Ziegler et al. 2012).

8.5 Stereom Architecture

The presence of stereom within the skeletons is one of the features which characterize the echinoderms as a whole (Smith 2005a) and can be readily differentiated if under the scanning electron microscope (Figs. 8.5, 8.6, 8.7). Defined types of stereom include, for example, solid imperforate stereom, microperforate stereom containing few small pores, galleried stereom consisting of galleries of parallel arrangement of connected trabecular struts and chaotically arranged loose labyrinthic stereom (Smith 1980c, 1990). Stereom differentiation has been shown to be specifically

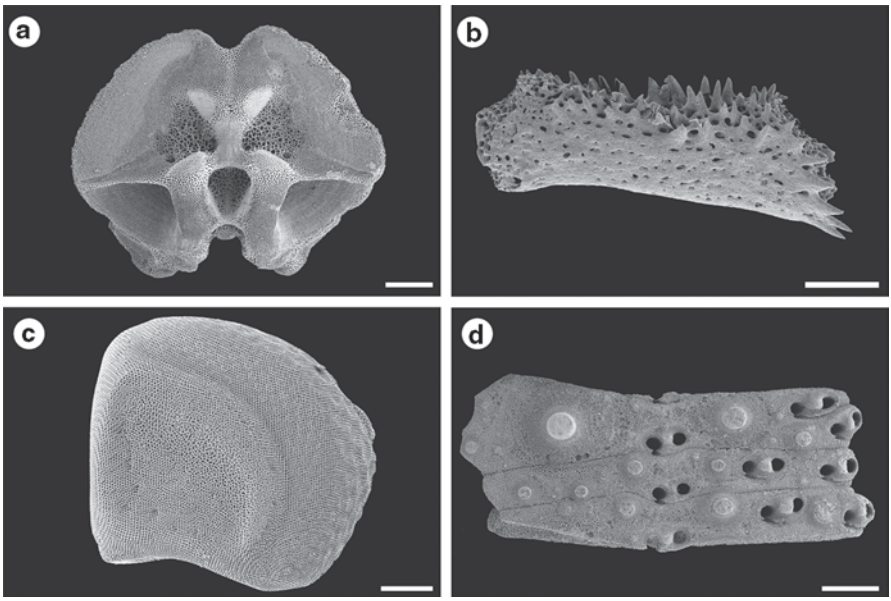

Fig. 8.6 Morphological and stereom variations among single ossicles (*a–e*) and conjoined plates of various echinoderms (*f*); *a, c* and *d* from sediment samples from San Salvador, Bahamas (see Dynowski 2012); *b* from the Tyrrhenian Sea, Giglio, Italy. **a** Bilateral symmetrical proximal face of an arm vertebra of the ophiuroid *Ophiocoma echinata*. Scale bar = 100 µm. **b** Single asymmetrical pinnular plate of *Antedon mediterranea* showing dense stereom and delicate spikes. Scale bar = 200 µm. **c** Marginal plate of the sea star *Astropecten duplicatus*. Scale bar = 400 µm. **d** Three conjoined compound ambulacral plates of the regular sea urchin *Tripneustes ventricosus*. Each compound plate is made of three elements resulting in *9* elements in all. Each compound plate bears three pore pairs and several tubercles. Tubercles show very dense stereom which serve as articulation surfaces. Scale bar = 400 µm.

correlated to the function of the skeletal elements or areas of the elements involved. Stereom can thus differ highly within single plates. In general, denser stereom is present where mechanical demands are high such as in the tubercles of echinoid plates on which the spine articulate. Highly structured stereom is needed where muscle fibers attach to the plates; loose stereom is found as a volume filler preserving the integrity plate shapes intact during growth (Smith 1980c, 1990).

A specific example for stereom differentiation and functionality is shown in Fig. 8.5 which shows a crinoid brachial with muscular articulation surfaces. Ligament insertion areas show stereom with an open mesh for the ligaments to attach deeply into the ossicles or even penetrate it. Muscle insertion areas have fine pores where the muscles attach but do not need to penetrate deep into the ossicles. The fulcral ridge consists of a robust dense calcite where adjoining ossicles form a kind of hinge for movement and have to withstand friction pressure. Further examples of stereom differentiation can be seen in Figs. 8.6 and 8.7.

The detailed structure of spines and their potential biomimetic applications has recently gathered more attention (Presser et al. 2009; Moureaux et al. 2010; Tsafnat

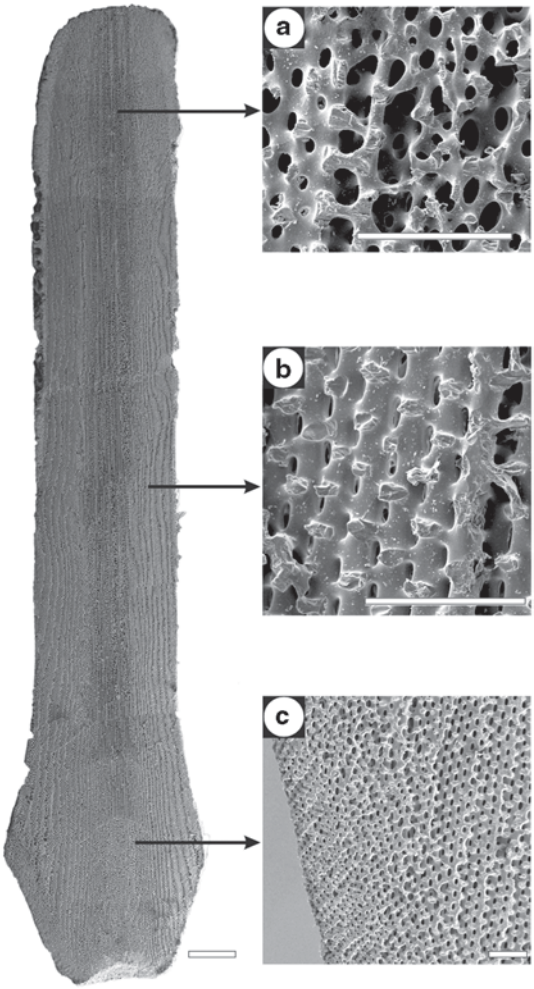

Fig. 8.7 Compiled SEM image of sectioned longitudinal oral primary spine of *Phyllacanthus imperialis* (to the *left*) and details of the stereom structure (to the *right*). **a** Medulla near the spine tip. **b** Radiating layer. **c** Spine base. Spine scale bar = 1 mm, detailed scale bars = 100 μm.

et al. 2012). Studies applied to the stereom of spines of cidaroid and camaradont echinoids by Grossmann and Nebelsick (2013a, b) have shown that a number of stereom types are present in the spines depending not only on the species involved, but also on the location of stereom with respect to position along the spines. Stereom types thus differ not only from the base to the tip (Figs. 8.4 and 8.7) but also radially from the centre of the spine to the outside. These stereom differentiations have structural implications as measured by three point bending tests (Grossmann and Nebelsick 2013b).

8.6 Calcification and Biomineralization

The mineralogy of the echinoderm skeleton as a high magnesium calcium carbonate material has attracted much attention (e.g. Raup 1966; Towe 1967; Weber 1969; Märkel et al. 1971; Blake et al. 1984; Emlet 1982; Tsipursky and Buseck 1993; Gilbert and Weiner 2009; see compilation in Kroh and Nebelsick 2010). Calcite forms in echinoderms after the transformation from amorphous calcite (Politi et al. 2004, 2008; Killian et al. 2011). Although echinoderm skeletal elements behave as single crystals of calcite in polarized light especially after diagenesis in the rock record, they are constructed of a mosaic structure with slight alterations in the orientation of sub-µm sized crystallite. This polycrystalline aggregate along with differential inclusion of magnesium even within single elements may be a factor in hindering crack propagation in the struts of the stereom, while also imparting the typical conchoidal fracturing found at the trabecular scale (Berman et al. 1988).

Ultrastructural research has been conducted on early calcification sites and on the mineralizing organic matrix (e.g. Märkel et al. 1986; Ameye et al. 1998, 2000 see reviews in Killian and Wilt 2008; Gilbert and Wilt 2011). Biomineralization in echinoderms has been studied in larval skeletons (Wilt 1999, 2002; Wilt et al. 2008), teeth (Kniprath 1974; Mann et al. 2010a, b; Veis 2011) and in spine regeneration. Although present in low levels, numerous proteins of the intracrystalline organic matrix of the echinoderm skeleton and have been identified at the molecular level (e.g. Albeck et al. 1996; MacKenzie et al. 2001; Peled-Kamar et al. 2002; Gilbert and Wilt 2011; Matraga et al. 2011). The skeletons of echinoderms thus represent composites of mineralized and organic materials.

8.7 Conclusions

The echinoderm skeleton has long attracted attention due to its highly unique morphological, structural and chemical characteristics. The skeleton and its many discrete elements can be observed at a number of hierarchical levels including: (1) complete organisms, (2) plate aggregates, (3) isolated single plate elements, (4) stereom architectures, and (5) the molecular level of biomineralization. These hierarchical levels can be seen in all five extant classes and in extinct taxa. Various types of symmetry are present within the different hierarchical levels ranging from bilateral to pentamerous to asymmetrical. Constructional principles have been studied in detail in echinoid coronas and in the stalk and arms or crinoids. Light weight architectures also become obvious at the level of single elements and in the different types of stereom present in all echinoderms.

Acknowledgments Funding provided by the Stiftung Baden-Württemberg, the DAAD and the German Science Foundation (DFG Project NE 537/24-1). Macroscopic photographs by Wolfgang Gerber, Tübingen. REM images of Figs. 8.5 and 8.6 by Susanne Leidenroth, SMNS.

References

Albeck S, Addadi I, Weiner S (1996) Regulation of calcite crystal morphology by intracrystalline acidic proteins and glycoproteins. Connect Tissue Res 35:365–370

Ameye L, Compere Ph, Dille J, Dubois Ph (1998) Ultrastructure of the early calcification site and of its mineralizing organic matrix in *Paracentrotus lividus* (Echinodermata: Echinoidea). Histochem Cell Biol 110:285–294

Ameye L, Hermann R, Dubois P (2000) Ultrastructure of sea urchin calcified tissues after high-pressure freezing and freeze substitution. J Struct Biol 131:116–125

Baumiller TK (2008) Crinoid ecological morphology. Annu Rev Earth Planet Sci 36:221–249

Baumiller TK, Ausich WI (1996) Crinoid stalk flexibility: theoretical predictions and fossil stalk postures. Lethaia 29:47–59

Baumiller TK, LaBarbera M (1993) Mechanical properties of the stalk and cirri of the sea lily *Cenocrinus asterius*. Comp Biochem Physiol 106A:91–95

Baumiller TK, Messing CG (2007) Stalked crinoid locomotion, and its ecological and evolutionary implications. Palaeont Electr 10(2A):10p

Berman A, Addadi L, Weiner S (1988) Interactions of sea-urchin skeleton macromolecules with growing calcite crystals—a study of intracrystalline proteins. Nature 331:546–548

Birenheide R, Motokawa T (1994) Morphological basis and mechanics of arm movement in the stalked crinoid *Metacrinus rotundus* (Echinodermata, Crinoidea). Mar Biol 121:273–283

Birenheide R, Motokawa T (1996) Contractile connective tissue in crinoids. Biol Bull 191:1–4

Birenheide R, Motokawa T (1997) Morphology of Skeletal Cortex in the Arms of Crinoids (Echinodermata: Crinoidea). Zool Sci 14:753–761

Blake DF, Peacor DR, Allard LF (1984) Ultrastructural and microanalytical results from echinoderm calcite: implications for biomineralization and diagenesis of skeletal material. Micron Microscopica Acta 15:85–90

Burkhardt A, Hansmann W, Märkel K, Niemann HJ (1983) Mechanical design in spines of diadematoid echinoids (Echinodermata, Echinoidea). Zoomorphology 102:189–203

Chakra MA, Stone JR (2011) Classifying echinoid skeleton models: testing ideas about growth and form. Paleobiology 37:686–695

Coppard SE, Campbell AC (2004) Taxonomic significance of spine morphology in the echinoid genera *Diadema* and *Echinothrix*. Invertebr Biol 123:357–371

Cowen R (1981) Crinoids arms and banana plantations: an economic harvesting analogy. Paleobiology 7:332–343

Currey JD (1975) A comparson of the strength of echinoderm spines and mollusc shells. J Mar Biol Ass UK 55:419–424

Dafni J (1986) Echinoid Skeletons as Pneu Structures. Konzepte SFB 230, Universität Tübingen und Stuttgart. Stuttgart 13:9–96

Dafni J (1988) A biomechanical approach to the ontogeny and phylogeny of echinoids. In: Paul CRC, Smith AB (eds) Echinoderm phylogeny and evolutionary biology. Oxford University Press, Oxford, pp 175–188

David B, Stock SR, De Carlo F, Hétérier V, De Ridder C (2009) Microstructures of Antarctic cidaroid spines: diversity of shapes and ectosymbiont attachments. Mar Biol 156:1559–1572

Dynowski JF (2012) Echinoderm remains in shallow-water carbonates at Fernandez Bay, San Salvador Island, Bahamas. Palaios 27:183–191

Dynowski JF, Nebelsick JH (2011) Ecophenotypic variations of *Encrinus liliiformis* (Echinodermata: Crinoidea) from the middle Triassic Muschelkalk of Southwest Germany. Swiss J Palaeont 130:53–67

Ebert TA (1975) Growth and morallity of post-larval echinoids. Am Zool 15:755–775

Ebert TA (1985) The non-periodic nature of growth rings in echinoid spines. In: Keegan BF, O'Connor BDS (eds) Echinodermata: proceedings of the International Echinoderm Conference, Galway, A.A. Balkema, Rotterdam, pp 261–267, 24–29 Sept 1984

Ebert TA (1986) A new theory to explain the origin of growth lines in sea urchin spines. Mar Ecol Prog Ser 34:197–199

Ellers O, Telford M (1992) Causes and consequences of fluctuating coelomic pressure in sea urchins. Biol Bull 182:424–434
Ellers O, Johnson AS, Moberg PF (1998) Structural strengthening of urchin skeletons by collagenous sutural ligaments. Biol Bull 195:136–144
Emlet R (1982) Echinoderm calcite: a mechanical analysis from larval spicules. Biol Bull 163:264–275
Gilbert PUPA, Weiner S (2009) The grinding tip of the sea urchin tooth exhibits exquisite control over calcite crystal orientation and Mg distribution. Proc Natl Acad Sci USA 106:6048–6053
Gilbert PUPA, Wilt FH (2011) Molecular aspects of biomineralization of the echinoderm endoskeleton. Prog Mol Subcell Biol 52:199–223
Grossmann JN, Nebelsick JH (2013a) Stereom Differentiation in spines of *Plococidaris verticillata*, *Heterocentrotus mammillatus* and other regular sea urchins. In: Johnson C (ed) Echinoderms in a changing World. Proceedings of the 13th International Echinoderm Conference, Tasmania, CRC Press, London, pp 97–104
Grossmann JN, Nebelsick JH (2013b) Comparative morphological and structural analysis of selected cidaroid and camarodont sea urchin spines. Zoomorph 132:301–315
Hidaka M, Takahashi K (1983) Fine structure and mechanical properties of the catch apparatus of the sea-urchin spine, a collagenous connective tissue with muscle-like holding capacity. J Exp Biol 103:1–14
Hotchkiss, FHC (1998) A “rays-as-appendages” model of the origin of pentamerism in echinoderms. Paleobiology 24(2):200–214.
Johnson AS, Ellers O, Lemire J, Minor M, Leddy HA (2002) Sutural loosening and skeletal flexibility during growth: determination of drop-like shapes in sea urchins. Proc R Soc Lond B 269:215–220
Killian CE, Wilt FH (2008) Molecular aspects of biomineralization of the echinoderm endoskeleton: Chem Rev 108:4463–4474
Killian CE, Metzler RA, Gong YT, Churchill TH, Olson IC, Trubetskoy V, Christensen MB, Fournelle JH, De Carlo F, Cohen S, Mahamid J, Scholl A, Young A, Doran A, Wilt FH, Coppersmith SN, Gilbert PUPA (2011) Self-Sharpening Mechanism of the Sea Urchin Tooth. Adv Funct Mater 21:682–690
Kniprath E (1974) Ultrastructure and growth of the sea urchin tooth. Calc Tiss Res 14:211–228
Kroh A, Nebelsick JH (2010) Echinoderms and Oligo-Miocene carbonate systems: potential applications in sedimentology and environmental reconstruction. Int Assoc Sedimentol Spec Publ 42:201–228
Kroh A, Smith AB (2010) The phylogeny and classification of post-Palaeozoic echinoids. J Syst Palaeont 8(2):147–212
Laurin B, David B (1990) Mapping morphological changes in the spatagoid *Echinocardium*: applications to ontogeny and interspcific comparisons. In: De Ridder C, Dubois P, Lahaye MC, Jangoux M (eds) Echinoderm research. Rotterdam, Balkema, pp 739–745
Laurin B, Marchand D, Thierry J (1979) Variations morphologiques du test chez *Echinocardium cordatum* (Pennant): étude qualitative et quantitative de cinq échantillons de Bretagne et de Normandie. Bull Soc Geol Normandie 65:895–906
Lawrence JM, Pomory CM, Sonnenholzner J, Chao C-M (1998) Bilateral symmetry of the petals in *Melitta tenuis, Encope micropora,* and *Arachnoides placenta* (Echinodermata: Clypeasteroida). Invertebr Biol 17:94–100
MacKenzie CR, Wilbanks SM, Barker MF, McGrath KM (2001) Biomineralisation in echinoderms: identification of occluded proteins. In: Barker M (ed) Echinoderms 2000. Swets & Zeitlinger, Lisse, pp 499–504
Mann K, Poustka AJ, Mann M (2010a) Phosphoproteomes of *Strongylocentrotus purpuratus* shell and tooth matrix: identification of a major acidic sea urchin tooth phosphoprotein, phosphodontin. Proteome Sci 8:6
Mann K, Wilt FH, Proustka A (2010b) Proteomic analysis of sea urchin (*Strongylocentrotus purpuratus*) spicule matrix. Proteome Sci 8:33
Märkel K, Gorny P (1973) Zur funktionellen Anatomie der Seeigelzähne (Echinodermata, Echinoidea). Zoomorph 75:223–242

Märkel K, Röser U (1983) Calcite-resorption in the spine of the echinoid *Eucidaris tribuloides*. Zoomorph 103:43–58
Märkel K, Kubanek F, Willgallis A (1971) Polykristalliner Calcit bei Seeigeln (Echinodermata, Echinoidea). Cell Tissue Res 119:355–377
Märkel K, Röser U, Mackenstedt U, Klostermann M (1986) Ultrastructure investigation of matrix-mediated biomineralization in echinoids (Echinodermata, Echinoidea). Zoomorph 106:232–243
Matranga V, Bonaventura R, Costa C, Karakostis K, Pinsino A, Russo R, Zito F (2011) Echinoderms as blueprints for biocalcification: Regulation of skeletogenic genes and matrices. Mol Biomin 52:225–248
Mihaljević M, Jerjen I, Smith AB (2011) The test architecture of *Clypeaster* (Echinoidea, Clypeasteroida) and its phylogenetic significance. ZooTaxa 2983:21–38
Morris, VB (2007) Origins of radial symmetry identified in an echinoderm during adult development and the inferred axes of ancestral bilateral symmetry. Proc R Soc B 294:1511–1516
Moss ML, Meehan MM (1968) Growth of the echinoid test. Acta Anat 69:409–444
Motokawa T, Osamu S, Birenheide R (2004) Contraction and stiffness changes in collagenous arm ligaments of the stalked crinoid *Metacrinus rotundus* (Echinodermata). Biol Bull 206:4–12
Moureaux C, Pérez-Huerta A, Compère P, Zhu W, Leloup T, Cusack M, Dubois P (2010) Structure, composition and mechanical relations to function in sea urchin spine. J Struct Biol 170:41–49
Nebelsick JH (1992) Echinoid distribution by fragment identification in the Northern Bay of Safaga, Red Sea. Palaios 7:316–328
Pearse JS, Pearse VB (1975) Growth zones in echinoids skeleton. Am Zool 15:731–753
Peled-Kamar M, Hamilton P, Wilt FH (2002) Spicule matrix protein LSM34 is essential for biomineralization of the sea urchin spicule. Exp Cell Res 272:56–61
Phillipi U, Nachtigall W (1996) Functional morphology of regular echinoid tests (Echinodermata, Echinoida): a finite element study. Zoomorph 116:35–50
Politi Y, Arad T, Klein E, Weiner S, Addadi L (2004) Sea Urchin Spine Calcite Forms via a Transient Amorphous Calcium Carbonate Phase. Science 306:1161–1164
Politi Y, Metzler RA, Abrecht M, Gilbert B, Wilt FH, Sagi I, Addadi L, Weiner S, Gilbert PU (2008) Transformation mechanism of amorphous calcium carbonate into calcite in the sea urchin larval spicule. Proc Natl Acad Sci USA 105:17362–17366
Presser V, Kohler C, Zivcová Z, Berthold C, Nickel KG, Schultheiß S, Gregorová E, Pabst W (2009) Sea urchin spines as a model-system for permeable, light-weight ceramics with graceful failure behavior. Part II. Mechanical behavior of sea urchin spine inspired porous aluminum oxide ceramics under compression. J Bionic Engin 6:357–364
Raup DM (1966) The endoskeleton. In: Boolotian RA (ed) Physiology of Echinodermata. Wiley, New York, pp 379–395
Raup DM (1968) Theoretical morphology of echinoid growth. J. Paleont 42:50–63
Robach JS, Stock SR, Veis A (2009) Structure of first- and second-stage mineralized elements in teeth of the sea urchin *Lytechinus variegatus*. J Struct Biol 168:452–466
Seilacher A (1979) Constructional morphology of sand dollars. Paleobiology 5:191–221
Smith AB (1978) A functional classification of the coronal pores of regular echinoids. Palaeontology 21:759–789
Smith AB (1980a) The structure, function and evolution of tube feet and ambulacral pores in irregular echinoids. Palaeontology 23:39–84
Smith AB (1980b) The structure and arrangement of echinoid tubercles. Phil Trans Roy Soc Lond B 289:1–54
Smith AB (1980c) Stereom microstructure of the echinoid test. Spec Pap Palaeont 25:1–83
Smith AB (1990) Biomineralization in Echinoderms. In: Carter JG (ed) Skeletal biomineralization: Patterns, process and evolutionary trends vol I. Van Nostrand Rheinhold, New York, pp 413–443
Smith AB (1997) Echinoderm larvae and phylogeny. Annual Rev Ecol Syst 28:219–241
Smith AB (2005a) The pre-radial history of echinoderms. Geol J 40:255–280

Smith AB (2005b) Growth and form in echinoids: The evolutionary interplay of plate accretion and plate addition. In: Briggs DEG (ed) Evolving form and function: fossils and development: proceedings of a symposium honoring Adolf Seilacher for his contributions to paleontology in celebration of his 80th Birthday. New Haven. Peabody museum of Natural History, Yale University, pp 181–193

Smith DS, del Castillo J, Morales M, Luke B (1990) The attachment of collagenous ligament to stereom in primary spines of the sea-urchin *Eucidaris tribuloides*. Tissue Cell 22:157–176

Smith AB, Peterson KJ, Wray G, Littlewood DTJ (2004) From bilateral symmetry to pentaradiality. The phylogeny of hemichordates and echinoderms. In: Cracraft J, Donoghue MJ (eds) Addembling the Tree of Life. Oxford University Press, New York, pp 365–383

Stock SR, Nagaraja S, Barss J, Dahl T, Veis A (2003) X-ray microCT study of pyramids of the sea urchin *Lytechinus variegatus*. J Struct Biol 141:9–21

Strathmann RR (1981) The role of spines in preventing structural damage to echinoid tests. Paleobiology 7:400–406

Telford M (1985) Domes, arches und urchins: the skeletal architecture of echinoids (Echinodermata). Zoomorph 105:114–124

Towe, KM (1967) Echinoderm calcite: Single crystal or polycrystalline aggregate. Science 157:1048–1050

Tsafnat N, Fitz Gerald JD, Le HN, Stachurski ZH (2012) Micromechanics of sea urchin spines. PLoS One 7(9):e44140. doi:10.1371/journal.pone.0044140

Tsipursky SJ, Buseck PR (1993) Structure of magnesian calcite from sea urchins. Am Min 78:775–781

Veis A (2011) Organic matrix-related mineralization of sea urchin spicules, spines, test and teeth. Front Biosci 17:2540–2560

Veis A, Stock SR, Alvares K, Lux E (2011) On the formation and functions of high and very high magnesium calcites in the continuously growing teeth of the echinoderm *Lytechinus variegatus*: Development of crystallinity and protein involvement. Cells Tissues Organs 194:131–137

Wang RZ, Addadi L, Weiner S (1997) Design strategies of sea urchin teeth: structure, composition and micromechanical relations to function. Phil Trans R Soc Lond B Biol Sci 352(1352):469–480

Weber JN (1969) The incorporation of magnesium onto the skeletal calcite of echinoderms. Am J Sci 267:537–566

Wilt FH (1999) Matrix and mineral in the sea urchin larval skeleton. J Struct Biol 126:216–226

Wilt FH (2002) Biomineralization of the spicules of sea urchin embryos. Zool Sci 19:253–261

Wilt FH, Killian CE, Hamilton P, Croker L (2008) The dynamics of secretion during sea urchin embryonic skeleton formation. Exp Cell Res 314:1744–1752

Zachos LG (2009) A new computational growth model of sea urchin skeletons. J Theor Biol 259:646–657

Zamora S, Rahman I, Smith AB (2012) Plated Cambrian bilaterians reveal the earliest stages of echinoderm evolution. PLoS One 7(6):e38296

Ziegler A, Stock SR, Menze BH, Smith AB (2012) Macro- and microstructural diversity of sea urchin teeth revealed by large-scale micro-computed tomography survey. In Stock SR (ed) Developments in X-Ray tomography VIII. Proceedings of SPIE 8506, 85061G

Chapter 9
Review: The Functions of Phytoliths in Land Plants

Inga C. Keutmann, Björn Melzer, Robin Seidel, Ralf Thomann and Thomas Speck

9.1 Introduction

Phytoliths have interested scientists for more than one hundred years (Fig. 9.1; Struve 1835; Ehrenberg 1846, 1854; Gregory 1855; Sachs 1862; Kohl 1889). Not only botanists were drawn to these fascinating, multifunctional structures, but also chemists, agronomists, geologists, palaeontologists and archaeologists (Cooke et al. 2011). Though the expression phytolith is most commonly associated with silica inclusions in plants, there are many different definitions of the term. Calcite inclusions, whether calcium carbonate or calcium oxalate, also known as cystholiths, and inclusions with combined silicate and calcite are described as phytoliths as well. In 2006 Sommer et al. proposed a definition for phytoliths *sensu stricto* as defined silicon precipitates of plant origin with a diameter >5 µm to separate them from 'undefined phytogenic silicon <5 µm'. This criterion is used in several recent publications as well as in this review.

Phytoliths are widely found in plants (Hodson et al. 2005), so it is not surprising that they have been the subject of much research. Especially in agronomy the influence of higher silicon uptake and therefore increased inclusion of silica as phytoliths and its importance as a nutrient in economic plants, like rice, sugar cane or wheat were studied (Takahashi 1968; Savant et al. 1999). In palaeontology, phytoliths were used for the determination of floral composition in fossil ecosystems and in

I. C. Keutmann (✉) · T. Speck · B. Melzer · R. Seidel
Plant Biomechanics Group, Botanic Garden of the Albert-Ludwig University, Faculty of Biology, Schänzlestraße 1, 79104 Freiburg im Breisgau, Germany
e-mail: thomas.speck@biologie.uni-freiburg.de

R. Thomann
Freiburg Materials Research Center (FMF) and Institute of Macromolecular Chemistry of the Albert-Ludwig University, Stefan-Meier-Str. 21–31, 79104 Freiburg im Breisgau, Germany

T. Speck
Freiburg Materials Research Center (FMF), Stefan-Meier-Str. 21–31, 79104 Freiburg im Breisgau, Germany

C. Hamm (ed.), *Evolution of Lightweight Structures,* Biologically-Inspired Systems 6,
DOI 10.1007/978-94-017-9398-8_9

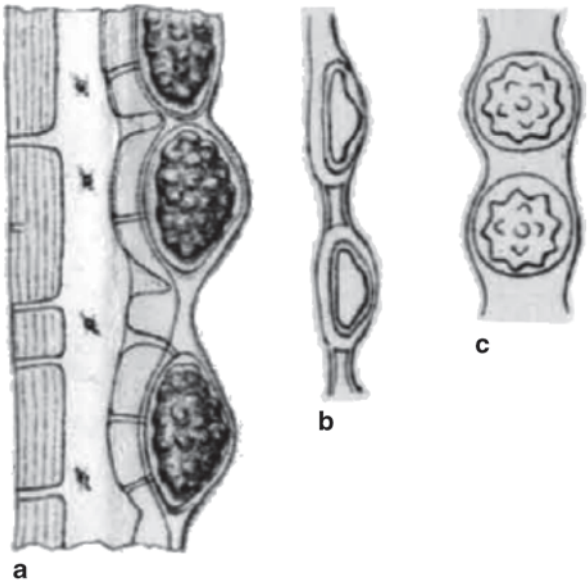

Fig. 9.1 Historical images of phytoliths from Kohl 1889. **a** *Masdevallia* spec., phytoliths with elliptic base and 'von Brod'—shape. **b** *Epidendrum nocturneum*, phytoliths as smooth caps. **c** *Phalaenopsis grandiflora*, phytoliths as warty balls

ethno-botany the composition of agricultural systems was analysed with the help of phytoliths (Tubb et al. 1993; Sangster et al. 2001). Interestingly, there is a striking chronological relationship between the evolution of angiosperms, especially grasses, and the radiation of diatoms found in the fossil record. This synchroneity seems to be linked to continental orogeny and hence enhanced erosion occurring at this time, which increased the supply of nutrients, and especially silica fluxes to the oceans. Probably, the silica fluxes intensified the production and diversification of diatoms. Later on, the expansion of grasslands pushed the diversification and massive increase of large herbivore abundances, especially ungulates (see Chap. 1c) with their teeth designed to process silica rich plant material. The concomitant marked rise of grasslands and large herbivore numbers biologically catalysed the availability of silica fluxes to the oceans, resulting in a concordant evolution of diatoms (Falkowski et al. 2004).

9.2 Amount and Appearance of Phytoliths in Land Plants and Soil

Silicon, after oxygen, is the second most abundant element in the Earth's crust. The amount of silicon in soil varies between <1% and 45% (Epstein 1999, 2001; da Cunha et al. 2008; da Cunha and do Nascimento 2009). Plants are an essential part of the silicon cycle (Fig. 9.2). They accumulate silicon as silicic acid [$Si(OH)_4$], with concentrations in soil ranging commonly between 0.1 and 0.6 mmol L^{-1} (Epstein

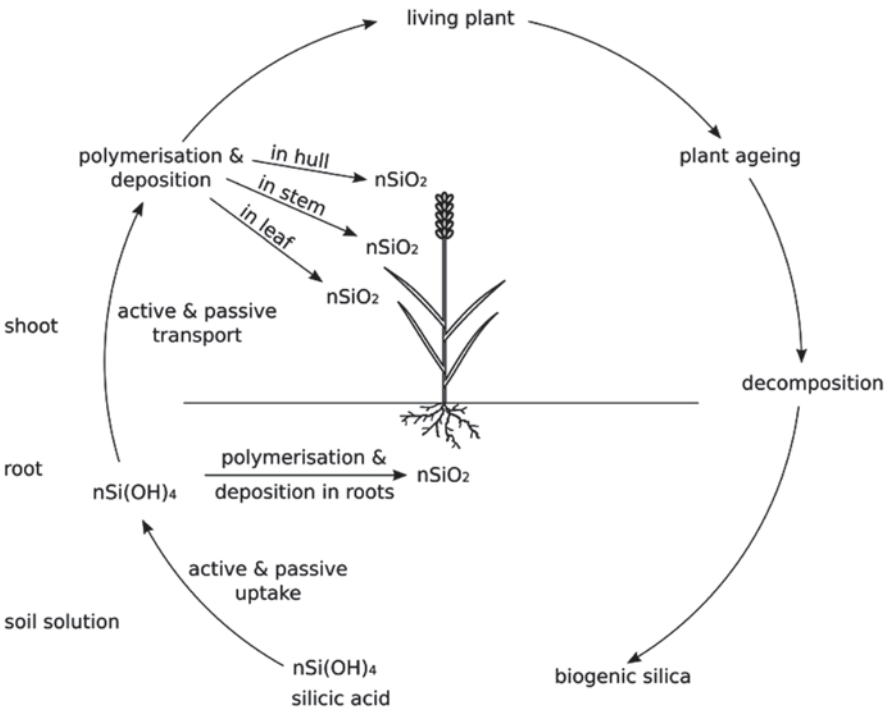

Fig. 9.2 Schematic illustration of the silicon cycle. Plants absorb silicic acid through the roots and transport it. Besides silica deposition in roots, it is also found in the shoot, where it is deposited in different plant organs. Due to plant ageing and following decomposition, biogenic silica becomes part of the soil again

1994, 1999), varying with soil types (Jones and Handreck 1965). Silicic acid occurs in soil due to rock weathering and the slow dissolution of biologically deposited SiO_2. The transport takes place in both a passive way through the transpiration stream and actively due to energy-dependent transporters (Ma et al. 2006; Ma and Yamaji 2006; Mitani and Ma 2005; Currie and Perry 2007). Furthermore, transpiration has been proven to be significantly correlated with silica content in plants (Euliss et al. 2005). The silicic acid is absorbed by roots, transported to the shoots and finally stored in different parts of the plant: in cell lumen, cell wall or outside of plant cells (Sangster et al. 2001; da Cunha et al. 2008; da Cunha and do Nascimento 2009). The accumulated silicon is stored as solid, amorphous, hydrated silica (SiO_2*nH_2O) forming phytoliths (Currie and Perry 2007) which is much more reactive than crystalline silica (Epstein 1999, 2001). The amount of silica in land plants varies from 0.1 to 10% of dry plant weight strongly depending on plant species and silicon content in the soil (Epstein 1999, 2001; Hodson et al. 2005; Ma et al. 2006; Currie and Perry 2007). This amount is comparable to or even exceeds the amount of various macronutrients in plants (Epstein 1999). The plant groups best known for their silica inclusions are Poales, Equisetales and Arecales, due to the fact that these orders have the highest

and most frequent silica concentrations and accumulation (>4% Si dry matter; Hodson et al. 2005; da Cunha et al. 2008; da Cunha and do Nascimento 2009).

Detailed analysis showed that not only the amount but also the form of phytoliths in plants is species dependent (Piperno 1988; Epstein 1994; 1999; Hodson et al. 2005). Variations in form are very pronounced, including e.g. conical, spherical, druse-like and dumbbell-shaped bodies to name just a few (Prychid et al. 2004). The uniqueness of phytoliths in a taxon is used especially in archaeology and palaeontology, e.g. for the determination of farming behaviour of earlier cultures or feeding behaviour of extinct animals.

Besides the variation in form, there is also great variation in size from 100 nm (Watteau and Villemin 2001) to over 1000 μm in diameter (Piperno 1988; Sommer et al. 2006) which partly defines the name of the specific phytolith structures, e.g. silica sand for many tiny particles in a cell (Prychid et al. 2004). Phytoliths are deposited in many different places and at all hierarchical levels in plants. However, their most common location is in the epidermis.

9.3 Functions of Silicon in Plants

Silicon is said to have many different functions in plants, including mechanical stability, growth promotion or defence against various biotic and abiotic stresses (Epstein 1994, 1999; Ma et al. 2001; Ma 2004). Up until now, some functions are proven and some are mere assumptions. Mostly, studies on the influence of silica were carried out with agronomically relevant plants like rice, soybean, maize, grains or sugar cane. Studies on plants without agronomic interest are scarce.

9.3.1 Mechanic Stability/Lodging

The term mechanical stability is used in many different contexts for plants. Some aspects of silica-influence on mechanical plant stability have not yet been analysed, such as the influence of silica inclusions on bending or torsion stiffness and on the respective moduli. Influence of silica on mechanical properties was mostly studied in relation to stem lodging of crop plants in agronomy. Different studies showed the reduction of lodging through fertilizing with silicon (Welton 1928; Tisdale et al. 1985; Hong et al. 2009), due to increased culm wall thickness and increased size of vascular bundles (Shimoyama 1958; da Cunha et al. 2008).

Leaf erectness which has pronounced influence on light interception is also increased by elevating the amount of silica in the plant (Yoshida et al. 1969, Ma 2004) and decreases the sensitivity to stem lodging amongst other causes due to an improved assimilation system (Takahashi 1968; Savant et al. 1999). Additionally, a high amount of silica in the cuticula, which can be increased by silicon fertilizing, gives enhanced mechanical stability against penetrators, such as stalk borers (Keeping et al. 2009) or pathogenic fungi (Haysaka et al. 2008).

9.3.2 Reduction of Climatic Stress

Climatic stresses are common for plants. They include water deficiency, cold temperatures and freezing (Savant et al. 1999; Liang et al. 2008) as well as mechanical (wind) loads and radiation.

Silicon in plants is able to reduce the extent of stress due to water deficiency. This is caused by the reduction of transpiration which is accomplished by the formation of a silica double layer in the cuticle leading to a reduced cuticular transpiration (Savant et al. 1999; Ma et al. 2001; Ma 2004). Additionally, silicon is proved to enhance water uptake in some plants due to an improvement in hydraulic conductance (Sonobe et al. 2009). However, there are many different factors involved and the different effects are still not completely analysed and understood (Sonobe et al. 2009). Another mechanism which needs additional investigation is the reduction of freezing stress in plant tissues due to increased silica content. Although it has been proven that additional silicon enhances water content of leaf tissues and reduces the amount of freezing injuries, the mechanism can only be guessed. Liang et al. (2008) assume that reductions of freezing injuries probably depend on higher antioxidant defence activity, lower lipid peroxidation, and membrane permeability.

9.3.3 Defence Against Chemical Stress

Lack or excess of nutrients and other elements might cause profound problems in plants. Silicon may mitigate effects of nutrition problems or chemical stress, as shown in many different studies. For example, silicon reduces excess toxicity of different elements, including manganese, iron, aluminium, cadmium, zinc (da Cunha et al. 2008; da Cunha and do Nascimento 2009) and phosphate (Ma and Takahashi 1990a, b; Ma et al. 2001).

In case of manganese the mechanism of preventing toxicity seems to be different depending on the plant species and has not been completely solved. Assumptions for this mechanism are a decreased uptake of manganese, but also binding of manganese by silicon, as well as increased enzyme activities (Shi et al. 2005; Shi et al. 2010) and two opposing assumptions: (a) a more distinct concentration of manganese (Iwasaki and Matsamura 1999), or (b) a more homogenous distribution of manganese in the leaves (Williams and Vlamis 1957; Horst and Marschner 1978; Savant et al. 1999). Even though the exact mechanism of how silicon interacts with manganese remains unclear, there is no doubt about the influence silicon has in alleviating excess toxicity of manganese.

Toxic Al^{3+} is probably bound by silicon in the plant (Cocker et al. 1998) as well as in the soil solution (Ma et al. 1997). The limiting effects of aluminium excess like reduced root growth and nutrition uptake are neutralized.

Cadmium and zinc are both found to build metal-silicate complexes in soil and in the plant, which decreases the availability of these two elements for the plant and supports detoxification of cells (da Cunha et al. 2008; da Cunha and do Nascimento 2009).

In case of phosphate, silicon has a great influence on both, phosphate deficiency and excess. With a sufficient phosphate supply there is no effect of silicon on the phosphate balance. However, with a lack of phosphate in soil, silicon has indirect beneficial effects on plant growth, due to a silicon-induced decreased manganese and iron uptake of the plants. Since phosphate binds manganese and iron, a decreased Mn and Fe uptake results in a higher availability of essential phosphate in the plant (Ma and Takahashi 1990; Ma et al. 2001). If the content of phosphate in soil is exceedingly high, silicon reduces the uptake of inorganic phosphate, which otherwise would affect growth negatively due to an inhibition of enzyme activity or inactivation of necessary metals like zinc (Ma and Takahashi 1990; Miyake and Takahashi 1978, 1982, 1985, 1986).

9.3.4 Defence Against Herbivores

Increased resistance against herbivores due to a higher amount of phytoliths in plants is the best known benefit of their occurrence in plants. Plants with high silica content have a rough surface, causing an increased abrasion of the teeth of herbivores and hence a reduced feeding on plants with higher silica content (Massey et al. 2007; Hunt et al. 2008). Comparing studies of pastures with different grazing intensity show that plants on heavily grazed land store much more silica than plants on lesser grazed land (McNaughton et al. 1985). The result can also be generated artificially by defoliation of the plants (McNaughton and Tarrants 1983), indicating higher silicon accumulation and therefore higher silica content in plants, as a defence against herbivores. However, not only plants adapted their silica content to grazing but also herbivores such as horses seem to have adapted their teeth to higher silica content in grass. It is thought that co-evolution took place in which, for example, North American Equidae evolved high-crowned molars due to the spread of grasslands (Falkowski et al. 2004; Mihlbachler et al. 2011).

9.3.5 Resistance Against Pathogenic Fungi and Germ Infections

Plants are highly endangered by pathogenic fungi, bacteria, and insects. It is proven that silica inclusions enhance the defence against the above mentioned organisms. Especially in the field of agriculture, the influence of fertilizing with silicon and hence the influence of a higher amount of silicates in plants is studied since the exact mechanisms of the protective effects are not yet understood (Cai et al. 2009). There are three different possible types of defence. Firstly, through a physical barrier due to the higher amount of silica in outer plant tissues and the resulting stronger defence against pathogenic penetration (Zhang et al. 2006; Hayasaka et al. 2008). Secondly, bio-chemically by inducing higher production rates of protective enzymes under stress (Yang et al. 2003; Fauteaux et al. 2006; Cai et al. 2009; Reynolds et al. 2009). Thirdly on the molecular level by up-regulation of genes known for their defence and pathogenic function under stress conditions (Watanabe et al. 2004; Fauteaux et al. 2006). Nevertheless, the exact defence mechanisms remain an interesting field of research.

9.3.6 Growth Promotion

Silica inclusions have great influence on plant growth. In addition to the reduction of negative stress effects, which would lead to growth reduction, silicon promotes several physiological processes in plants (Korndörfer et al. 2001). One example is an up to 50% higher activity of Rubisco in silica-rich plant leaves (Epstein 1999). Additionally, silicon acts as a growth stimulant, e.g. for larger leaves (McNaughton 1985) with a bigger biomass (Epstein 1999), and increases the yield of crop plants like sugar cane or rice (Savant et al. 1999; Korndörfer et al. 2001).

Because of multifunctional benefits in plants, the role of silicon in plant physiology is much discussed. In classic understanding, silicon does not belong to the necessary elements for most plants and as such is not considered to be one of the essential nutrients (Epstein 1999, 2009; Cooke and Leishman 2011). However, several researchers disagree with this position since the benefits of silicon for plants can easily be seen in phenotype and have definitely been proven by comparing the results of experiments on plants grown in soil with high and low silicon amounts (Epstein 1999, 2009; Korndörfer et al. 2001; Euliss et al. 2005; Currie and Perry 2007; Cooke and Leishman 2011). Despite this conflict, silicon is dealt with like every other nutrient element in plants with regards to the uptake mechanism (Epstein 2009).

9.3.7 Window Hypothesis

For a long time it had been speculated that silica bodies located in the leaf epidermis work as 'windows' to increase the transmission of light in the photosynthetic tissue. Agarie et al. (1996) however, could not support this hypothesis in their study. Even though only plants supplied with extra silicon built 'windows' in their leaves, the optical properties of leaf transmittance, reflectance, and absorbance spectrum were nearly the same which led Agarie et al. (1996) to reject the 'window hypothesis'.

9.4 Qualitative and Quantitative Detection of Phytoliths in Land Plants

9.4.1 Qualitative Analysis

There are different methods to detect phytoliths in plants and a comparison of the most commonly used methods is given in Blecher et al. (2012). The detection with the secondary electron microscope (SEM) by electron-dispersive X-ray detection (EDX; Fu et al. 2002; Sapei et al. 2007; Keeping et al. 2009) is most common, sometimes in combination with backscattered electron imaging (BSE; Dietrich et al. 2003; Laue et al. 2006). EDX is the classical method which is also element specific. BSE provides a higher special resolution than EDX, but is not specific to

silicon. Other possibilities are stains in light microscopy like methyl red and counterstaining with fast green (FG-MR) or crystal violet lactone and counterstaining with safranin (S-CVL) as proposed by Dayanandan (1983). These stains are not yet silica specific, and in case of some other colorants difficult in terms of security regulations. Raman analysis (Sapei et al. 2007; Gierlinger et al. 2008) is another silica specific method which not only determines the positions of phytoliths in the plant, but can also analyse the exact chemical composition of the phytoliths. Despite these advantages Raman is very complex in handling and interpretation and several possibilities of interference exist (Blecher et al. 2012). A short comparison of the listed methods is shown in Figs. 9.3 and 9.4.

In the end, the choice of method is tied to available equipment, even though only EDX and Raman provide reliable results.

9.4.2 Quantitative Analysis

The methodologies for quantitative analysis of silica in plants are manifold. The most frequent first step of quantitative silica analysis is isolation of the phytoliths, if the plant material is not measured directly by EDX (Keeping et al. 2009) or chromatographic methods (Fu et al. 2002). The isolation of phytoliths can generally be achieved in two different ways, wet ashing and dry ashing. Wet ashing means

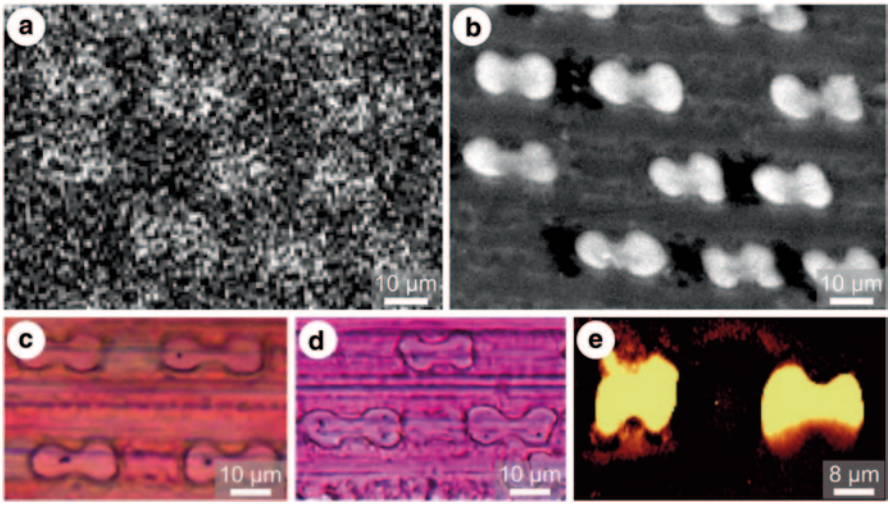

Fig. 9.3 Comparison of different silica-detecting methods using the dumbbell-shaped silica inclusions of *Miscanthus sinensis* (Poaceae) as an example. **a** EDX, dumbbells visible in average resolution. **b** BSE, dumbbells clearly visible. **c** light microscopic staining FG-MR, dumbbells visible, but surrounding tissue also stained (both *red*). **d** light microscopic staining S-CVL, dumbbells visible, but surrounding tissue also stained (both *violet*). **e** Raman imaging at wavelength 254–570 cm^{-1}, dumbbells clearly visible (*orange*)

characteristic / method	Si-specificity	study area	spatial resolution	comments
EDX	specific	small to large possible	acceptable, dependant on measurement time	time consuming for better resolution
BSE	not specific	small to large possible	good	confirmation of detection necessary
FG-MR	not specific	small to large possible	good	lignin also stained, staining inconsistent
S-CVL	not specific	small to large possible	good	lignin also stained, staining inconsistent
Raman	specific	small to large possible	good, dependant on measurement time	fluorescence & other interferences possible, time consuming, complex handling

Fig. 9.4 Comparison of different silica detecting methods with essential characteristics

isolation by chemical treatment, dissolving organic material, using chemicals like hydrogen peroxide, hydrochloric acid or nitric acid (Blackman and Parry 1968; Saccone et al. 2006; Saccone et al. 2007; Sapei et al. 2007; Mali and Aery 2008). Dry ashing means burning the plant material at high temperatures from 400 up to 600 °C (Jones and Milne 1963; Sapei et al. 2007; Keeping et al. 2009). A combination of both ashing procedures can also be done by applying the chemical treatment to the sample either before or after the heat treatment. A common procedure during the combination of both types of ashing is cooking the sample or the ash in hydrochloric acid (Euliss et al. 2005; Sapei et al. 2007). The ash, whether it is obtained by wet or dry ashing, can be analysed in different ways. Often the ash is weighed and compared to the dry weight of the used plant material or the ash content before the combined chemical treatment methods. Other possibilities include different spectroscopic methods (Fu et al. 2002) and colorimetric estimation where the ash is diluted, e.g. in sodium hydroxide solution. Then a reducing mix including a colorant is added and finally the colouration of the solution is measured at a specific wavelength (Blecker et al. 2007; Nwugo and Huerta 2008). A sole standard method cannot be found.

9.5 Conclusion

Although research on phytoliths has considerably increased over the last ten to fifteen years, several functions, especially their influence on the mechanical properties of plants, are still poorly understood. Conversely, it is expected that the role of silicon as an essential nutrient for plants will be revealed soon due to its manifold functions.

References

Agarie S, Agata W, Uchida H, Kubota F, Kaufman PB (1996) Function of silica bodies in the epidermal system of rice (Oryza sativa L.): testing the window hypothesis. J Exp Bot 47:655–660

Blackman E (1968) The pattern and sequence of opaline silica deposition in rye (Secale cereale L.). Ann Bot 32:207–218

Blackman E, Parry DW (1968) Opaline silica deposition in rye (Secale cereale L.). Ann Bot 32:199–206

Blecher IC, Seidel R, Thomann R, Speck T (2012) Comparison of different methods for the detection of silica inclusions in plant tissues. Int J Plant Sci 173:1–11

Blecker SW, King SL, Derry LA, Chadwick OA, Ippolito JA, Kelly EF (2007) The ratio of germanium to silicon in plant phytoliths: quantification of biological discrimination under controlled experimental conditions. Biogeochemistry 86:189–199

Cai K, Gao D, Chen J, Luo S (2009) Probing the mechanisms of silicon-madiated pathogen resistance. Plant Signal Behav 4:1–3

Cocker KM, Evans DE, Hodson MJ (1998) The amelioration of aluminium toxicity by silicon in higher plants: solution chemistry or an *in planta* mechanism? Physiol Plant 104:608–614

Cooke J, Leishman MR (2011) Is plant ecology more siliceous than we realize? Trends Plant Sci 16:61–68

Currie HA, Perry CC (2007) Silica in plants: biological, biochemical and chemical studies. Ann Bot 100:1383–1389

Da Cunha KPV, do Nascimento CWA (2009) Silicon effects on metal tolerance and structural changes in maize (Zea mays L.) grown on a cadmium and zinc enriched soil. Water Air Soil Pollut 197:323–330

Da Cunha KPV, do Nascimento CWA, da Silva AJ (2008) Silicon alleviates the toxicity of cadmium and zinc for maize (Zea mays L.) grown on a contaminated soil. J Plant Nutr Soil Sci 171:849–853

Dayanandan P (1983) Localization of silica and calcium-carbonate in plants. Scanning electron microscopy. Scanning Microsc Int 3:1519–1524

Dietrich D, Hinke S, Baumann W, Fehlhaber R, Baeucker E, Ruehle G, Wienhaus O, Marx G (2003) Silica accumulation in Triticum aestivum L. and Dactylis glomerata L. Anal Bioanal Chem 376:399–404

Ehrenberg CG (1846) Einige fernere Mittheilungen über die geformten unkrystallinischen Kieseltheile von Pflanzen, besonders über Spongilla Erinaceus in Schlesien und ihre Beziehung zu den Infusorienerde-Ablagerungen des Berliner Grundes. Bericht über die zur Bekanntmachung geeigneten Verhandlungen der Königlich Preußischen Akademie der Wissenschaften zu Berlin 4:996–1001

Ehrenberg CG (1854) Mikrogeologie. Voss, Leipzig, Germany

Epstein E (1994) The anomaly of silicon in plant biology. PNAS 91:11–17

Epstein E (1999) Silicon. Ann Rev Plant Physiol Plant Mol Biol 50:641–664

Epstein E (2001) Silicon in plants: facts vs concepts. In: Datnoff LE, Snyder GH, Korndörfer GH (eds) Silicon in agriculture, studies in plant sciences, vol. 8, Elsevier, Amsterdam and New York, pp. 1–10

Epstein E (2009) Silicon: its manifold roles in plants. Ann Appl Biol 155:155–160

Euliss KW, Dorsey BL, Benke KC, Banks MK, Schwab AP (2005) The use of plant tissues silica content for estimating transpiration. Ecol Eng 25:343–348

Falkowski PG, Katz ME, Knoll AH, Quigg A, Raven JA, Schofield O, Taylor FJR (2004) The evolution of modern eukaryotic phytoplankton. Science 305:354–360

Fauteaux F, Remus-Borel W, Menzies JG, Belanger RR (2006) Silicon and plant disease resistance against pathogenic fungi. Fems Microbiol Lett 249:1–6

Fu FF, Akagi T, Yabuki S (2002) Origin of silica particles found in the cortex of matteuccia roots. Soil Sci Am J 66:1265–1271

Gierlinger N, Sapei L, Paris O (2008) Insights into the chemical composition of equisetum hyemale by high resolution Raman imaging. Planta 227:969–980

Gregory W (1855) On the presence of diotomaceae, phytolitharia, and sponge spicules in soils which support vegetation. In: Datnoff LE, Snyder GH, Korndörfer GH (eds) Proceedings of the botanical society of Edinburgh., Elsevier, Edinburgh, pp 69–72
Hayasaka T, Fujii H, Ishiguro K (2008) The role of silicon in preventing appressorial penetration by the rice blast fungus. Phytopathology 98:1038–1044
Hodson MJ, White PJ, Mead A, Broadley MR (2005) Phylogenetic variation in the silicon composition of plants. Ann of Bot 96:1027–1046
Hong K, Cho HJ, Yoon CS, Hwang I (2009) Effects of silicate liquid fertilizer on the decrease of lodging and yield of rice. In: Datnoff LE, Snyder GH, Korndörfer GH (eds) The 9th international conference of the east and southeast asia federation of soil science societies., Elsevier, Amsterdam and New York, pp 662–663
Horst WJ, Marschner H (1978) Effect of silicon on manganese tolerance of bean plants (*Phaseolus vulgaris* L.). Plant Soil 50:287–303
Hunt JW, Dean AP, Webster RE, Johnson GN, Ennos AR (2008) A novel mechanism by which silica defends grass against herbivory. Ann Bot 102:653–656
Iwasaki K, Matsumura A (1999) Effect of silicon on alleviation of manganese toxicity in pumpkin (Cucurbita moschata Duch cv. Shintosa). J Soil Sci Plant Nutr 45:909–920
Jones LHP, Handreck KA (1965) Studies of silica in the oat plant III. Plant Soil 23:79–96
Jones LHP, Milne AA (1963) Studies of silica in the oat plant I. Plant Soil 18:207–220
Keeping MG, Kvedaras OL, Bruton AG (2009) Epidermal silicon in sugarcane: cultivar differences and role in resistance to sugarcane borer Eldana saccharina. Environ Exper Bot 66:54–60
Kohl FG (1889) Anatomisch-physiologische Untersuchung der Kalksalze und Kieselsäure in der Pflanze. N.G. Elwert, Marburg, Germany
Korndörfer GH, Snyder GH, Ulloa M, Powell G, Datnoff LE (2001) Calibration of soil and plant silicon analysis for rice production. J Plant Nutrition 24:1071–1084
Laue M, Hause G, Dietrich D, Wielange B (2006) Ultrastructure and microanalysis of silica bodies in Dactylis Glomerata. Microchim Acta 156:103–107
Liang Y, Zhu J, Li Z, Chu G, Ding Y, Zhang J, Sun W (2008) Role of silicon in enhancing resistance to freezing stress in contrasting winter wheat cultivars. Environ Exper Bot 64:286–294
Ma JF (2004) Role of silicon in enhancing the resistance of plants to biotic and abiotic stresses. J Soil Sci Plant Nutr 50:11–18
Ma JF, Takahashi E (1990a) Effect of silicon on the growth and phosphorus uptake of rice. Plant Soil 126:115–119
Ma JF, Takahashi E (1990b) The effect of silicic acid on rice in a P-deficient soil. Plant Soil 126:121–125
Ma JF, Yamaji N (2006) Silicon uptake and accumulation in higher plants. Trends Plant Sci 11:392–397
Ma JF, Sasaki M, Matsumoto H (1997) Al-induced inhibition of root elongation in corn, Zea mays L. is overcome by Si addition. Plant Soil 188:171–176
Ma JF, Miyake Y, Takahashi E (2001) Silicon as a beneficial element for crop plants. In: Datnoff LE, Snyder GH, Korndörfer GH (eds) Silicon in agriculture, studies in plant sciences, vol. 8, Elsevier, Amsterdam and New York, pp 17–40
Ma JF, Tamai K, Yamaji N, Mitani N, Konishi S, Katsuhara M, Ishiguro M, Murata Y, Yano M (2006) A silicon transporter in rice. Nature 440:688–691
Mali M, Aery NC (2008) Silicon effect on nodule growth, dry-matter production, and mineral nutrition of cowpea (Vigna unguiculata). J Plant Nutr Soil Sci 171:835–840
Massey F, Ennos RA, Hartley S (2007) Herbivore specific induction of silica-based plant defences. Oecologia 152:677–683
McNaughton SJ, Tarrants JL (1983) Grass leaf silicification: natural selection for an inducible defense against herbivores. PNAS 80:790–791
McNaughton SJ, Tarrants JL, McNaughton MM, Davis RD (1985) Silica as a defense against herbivory and a growth promoter in African grasses. Ecology 66:528–53
Mihlbachler MC, Rivals F, Solounias N, Semprebon GM (2011) Dietary change and evolution of horses in North America. Science 331:1178–1181

Mitani N, Ma JF (2005) Uptake system of silicon in different plant species. J Exp Bot 56:1255–126
Miyake Y, Takahashi E (1978) Silicon deficiency of tomato plants. J Soil Sci Plant Nutr 24:175–189
Miyake Y, Takahashi E (1982) Effect of silicon on the growth of cucumber plants in a solution culture. J Soil Sci Plant Nutr 53:15–22
Miyake Y, Takahashi E (1985) Effect of silicon on the growth of soybean plants in a solution culture. J Soil Sci Plant Nutr 31:625–634
Miyake Y, Takahashi E (1986) Effect of silicon on the growth and fruit production of strawberry plants in a solution culture. J Soil Sci Plant Nutr 32:321–326
Nwugo CC, Huerta AJ (2008) Silicon-induced resistance in rice (Oryza sativa). J Plant Nutr Soil Sci 171:841–848
Piperno DR (1988) Phytolith analysis—an archaeological and geological perspective. Academic press, San Diego
Prychid CJ, Rudall PJ, Gregory M (2004) Systematics and biology of silica bodies in monocotyledons. Bot Rev 69:377–440
Reynolds O, Keeping M, Meyer J (2009) Silicon-augmented resistance of plants to herbivorous insect: a review. Ann Appl Biol 155:171–186
Saccone L, Conley DJ, Sauer D (2006) Methodologies for amorphous silica analysis. J Geochem Explor 88:235–238
Saccone L, Conley DJ, Koning E, Sauer D, Sommer M, Kaczorek D, Blecker SW, Kelly EF (2007) Assessing the extraction and quantification of amorphous silica in soils of forest and grassland ecosystems. Eur J Soil Sci 58:1446–1459
Sachs J (1862) Ergebnisse einiger Untersuchungen über die in Pflanzen enthaltene Kieselsäure. Flora 20:33–38, 49–55, 65–71
Sangster AG, Hodson MJ, Tubb HJ (2001) Silicon deposition in higher plants. In: Datnoff LE, Snyder GH, Korndörfer GH (eds) Silicon in agriculture, studies in plant sciences, vol. 8, Elsevier, pp. 85–114
Sapei L, Gierlinger N, Hartmann J, Noske R, Strauch P, Paris O (2007) Structural and analytical studies of silica accumulation in Equisetum hyemale. Anal Bioanal Chem 389:1249–1257
Savant NK, Korndörfer GH, Datnoff LE, Snyder GH (1999) Silicon nutrition and sugarcane production: a review. J Plant Nutr 22:1853–1903
Shi Q, Bao Z, Zhu Z, He Y, Quian Q, Yu J (2005) Silicon-mediated alleviation of Mn toxicity in Cucumis sativus in relation to activities of superoxide dismutase and ascorbate peroxidise. Phytochem 66:1551–1559
Shi G, Quingsheng C, Liu C, Wu L (2010) Silicon alleviates cadmium toxicity in peanut plants in relation to cadmium distribution and stimulation of antioxidative enzymes. J Plant Growth Regul 61:45–52
Shimoyama S (1958) Effect of silicon on lodging and wind damage in rice. Report for the research funds granted by ministry of agriculture. Elsevier, Japan, p. 82
Sommer M, Kaczorek D, Kuzyakov Y, Breuer J (2006) Silicon pools and fluxes in soils and landscapes—a review. J Plant Nutr Soil Sci 169:310–329
Sonobe K, Hattori T, An P, Tsuji W, Eneji E, Tanaka K, Inanaga S (2009) Diurnal variations in photosynthesis, stomatal conductance and leaf water relation in Sorghum grown with or without silicon under water stress. J Plant Nutr 32:433–442
Struve GA (1835) De silica in plantis nonnulli. Phil. Diss. Berlin
Takahashi E (1968) Silica as a nutrient to the rice plant. Jpn Agr Res Q:1–4
Tisdale SL, Nelson WL, Beaton JD (1985) Soil fertility and fertilizers. Macmillan, New York
Tubb HJ, Hodson MJ, Hodson GC (1993) The inflorescence papillae of the triticeae: a new tool for taxonomic and archaeological research. Ann Bot 72:537–545
Watanabe S, Shimoi E, Ohkama N, Hayashi H, Yoneyama T, Yazaki J, Fujii F, Shinbo K, Yamamoto K, Sakata K, Sasaki T, Kishimoto N, Kikuchi S, Fujiwara T (2004) Identification of several rice genes regulated by Si nutrition. J Soil Sci Plant Nutr 50:1273–1276
Watteau F, Villemin G (2001) Ultrastructural study of the biogeochemical cycle of silicon in the soil and litter of a temperate forest. Eur J Soil Sci 52:385–396
Welton FA (1928) Lodging in oats and wheat. Bot Gaz 85:121–151

Williams DE, Vlamis J (1957) The effect of silicon on yield and manganese-54 uptake and distribution in the leaves of barley grown in culture solutions. Plant Physiol 32:404–409

Yang YF, Liang YC, Lou YS, Sun WC (2003) Influences of silicon on peroxidise superoxide dismutase activity and lignin content in leaves of wheat *Tritium aestivum* L. and its relation to resistance to powdery mildew. Sci Agric Sinica 36:813–817

Yoshida S, Navasero SA, Ramirez EA (1969) Effects of silica and nitrogen supply on some leaf characters of the rice plant. Plant Soil 31:48–56

Zhang GL, Dai QG, Zhang HC (2006) Silicon application enhances rice resistance to sheath blight (*Rhizocronia solani*) in rice. J Plant physiol Mol Biol 32:600–606

Chapter 10
The Influence of Silica on Bending Elastic Modulus of the Stalks of Two large Grass Species (Poaceae)

Inga C. Keutmann, Björn Melzer, Robin Seidel, Ralf Thomann and Thomas Speck

10.1 Introduction

Mechanical properties are vital for plants and plant organs in many different ways. Stiffness and strength, for example, influence stem and leaf erectness in cereals and other Poaceae. They also enhance photosynthesis, and provide the stability of stems, leaves and fructification organs against external mechanical loads and mechanical failure (e.g. lodging). The most important structural materials contributing to a plant's stiffness are cellulose and lignin. However, these bio-macromolecules are energetically expensive to produce, requiring 6957 kcal kg^{-1} for lignin or 4000 kcal kg^{-1} for cellulose (Jung et al. 1999). In contrast, increased silica content is considered to improve the mechanical stability as well, but at 10 to 20 times lower energy costs (Raven 1983). Increased silicon uptake by plants with increasing silicon availability in the soil has been demonstrated for different plant species (van der Vorm 1980; Dietrich 2003; Nwugo and Huerta 2008; Keeping et al. 2009). Various analyses were carried out to test the influence of silica content on the intensity of positive traits, such as metal tolerance (da Cunha 2008; Nwugo and Huerta 2008; da Cunha and do Nascimento 2009), penetration resistance (Keeping et al. 2009) or nodule growths (Mali and Arey 2008). Evidence of a correlation between silica content and mechanical stiffness and stability (see part 1 above), however, remains scarce. Consequently, the influence of increased silica content on bending mechanical properties

I. C. Keutmann (✉) · T. Speck · B. Melzer · R. Seidel
Plant Biomechanics Group, Botanic Garden of the Albert-Ludwig University, Faculty of Biology, Schänzlestraße 1, 79104 Freiburg im Breisgau, Germany

R. Thomann
Freiburg Materials Research Center (FMF) and Institute of Macromolecular Chemistry of the Albert-Ludwig University, Stefan-Meier-Str. 21–31, 79104 Freiburg im Breisgau, Germany

T. Speck
Freiburg Materials Research Center (FMF), Stefan-Meier-Str. 21–31, 79104 Freiburg im Breisgau, Germany
e-mail: thomas.speck@biologie.uni-freiburg.de

C. Hamm (ed.), *Evolution of Lightweight Structures,* Biologically-Inspired Systems 6,
DOI 10.1007/978-94-017-9398-8_10

(bending stiffness and bending elastic modulus) was tested on stalks of *Saccharum officinarum* grown with different levels of silicon availability in the soil.

Based on the findings of Schoelynck et al. (2010), who showed a correlation between increasing silica concentration and decreasing lignin concentration, as well as increasing cellulose concentration in wetland plants, the following hypothesis was tested: Is additional silica deposited as an accessory supporting agent in stalk regions of *Miscanthus sinensis* in situations of static mechanical bending stress where the stresses are applied?

10.2 Materials and Methods

10.2.1 Plant Cultivation

Saccharum officinarium plants as well as *Miscanthus sinensis* plants (both Poaceae) were cultivated at the University of Freiburg's Botanical Garden. *Saccharum officinarium* plants were cultivated in pots. Four types of soil were prepared by adding 50, 100 and 200 mg*kg^{-1} sodium metasilicate (Na_2SiO_3 $9H_2O$) respectively, according to concentrations given by Mali and Aery (2008). Sodium metasilicate was chosen because sodium silicate is said to increase the silicon supply in soil for plants (Tisdale et al. 1985). As a control, young plants were transferred to pots filled with prepared soil and pots without additional silicate. After 3 months the plants were harvested and used for 3-point bending analysis.

For *Miscanthus sinensis*, stalks were fixated to the ground so that they remained in a bent position (Fig. 10.1e, 10.1.f). After 4 months, fixated (B) and erect (E) reference plants were harvested. The plants were sectioned from the stalk base towards the tip in segments of 20 cm length (A1-A4, Fig. 10.1a). The number of test specimens was $n = 9$ for erect plant stems and $n = 8$ for pre-bent plant stems.

10.2.2 Microscopy

For low voltage high Contrast Detection (vCD), a scanning electron microscopes' (SEM) detection mode that uses backscattered electrons, samples were cross sectioned with a razorblade to a thickness of about 1 mm. Samples were mounted on a specimen holder using a conductive plate and observed at low vacuum with a chamber pressure of 100 Pa. These testing conditions allowed for a sample investigation without prior sputtering of the sample. vCD allows detection of pure material contrast and displays different materials with different brightness, e.g. a higher brightness corresponding to a higher atomic number of the incorporated elements. The experiments were carried out with a QUANTA FEG 250 (FEI, Eindhoven, The Netherlands). Samples for light microscopy were embedded in Technovite 7100 (Heraeus Kulzer GmbH, Wehrheim/Ts., Germany). The embedding procedure was conducted as described in the supplier's instructions for use but with double the time per step. After polymerization,

the samples were cut with a microtome (custom made by the Technical Workshop of the Biological Institute II/III of the University of Freiburg, Germany) to sections of 10 µm thickness and transferred onto glass slides. They were stained with toluidine blue for 1 min and after washing with water and alcohol embedded in Entellan® (Merck, Darmstadt, Germany), then capped with a cover slip. The coloured samples were investigated with an Olympus BX61 microscope (Olympus Europe GmbH, Hamburg, Germany) and images were taken with an Olympus DP 71 (Olympus Europe GmbH, Hamburg, Germany) camera and processed with the software CellP 2.8.

10.2.3 Bending Tests

Saccharum plant stalks were tested by 3-point bending tests. Each sample was placed on the setup as shown in Fig. 10.1c. The two supports were spaced at approximately 15 times the average sample diameter to minimize shear influence. *Miscanthus* segments were bent using 4-point bending in two directions: first in

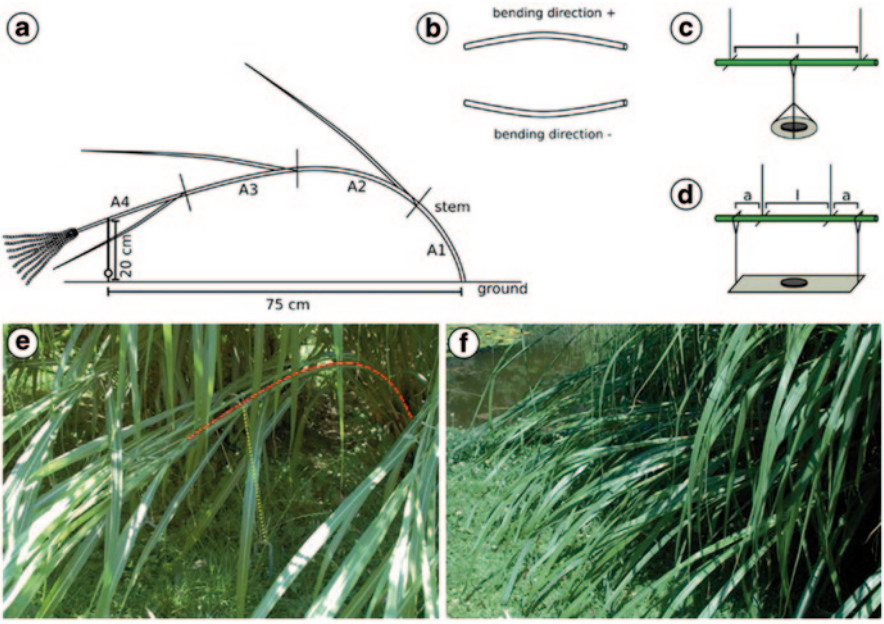

Fig. 10.1 **a** Schematic drawing of the experimental setup for pre-bent *Miscanthus* plants. The plants were fixated to the ground in a bent position with strings. A1 to A4 are the cut plant segments. **b** Bending directions. **c** Schematic drawing of the 3-point-bending apparatus with sample (*green*), support and pannier used for weight application. l is the distance needed for the determination of the bending elastic modulus. **d** Schematic drawing of the 4-point-bending apparatus with sample (*green*), support and two-armed pannier used for weight application. l and a are the distances needed for determination of the bending elastic modulus. **e** picture of the experimental setup of a stalk. The *red line* is positioned close above the pre-bent stalk. The *yellow line* indicates the string with which the stalk was fixated. **f** Experimental setup with several *Miscanthus* stalks bent to the ground

the direction in which the plants were pre-bent for 4 months (subsequently named +, Fig. 10.1b) and then opposite to the fixated pre-bending direction (subsequently named - Fig. 10.1b). For the erect plants, the + bending direction was chosen randomly and the - bending direction was 180° opposite to the + bending direction. For the bending procedure the sample was placed on the setup as shown in Fig. 10.1d.

For both plants, the weight was constantly increased in steps of 100 g and displacement was measured using a binocular with a dial gauge, 1 min after each weight increment. Bending elastic moduli were determined with the following standard equations for 3-point bending for *Saccharum* (10.1) and 4-point bending for *Miscanthus* (10.2):

$$E = \frac{l^3}{48b * I} \tag{10.1}$$

E = bending elastic modulus, I = moment of inertia, l = length between sample holders, b = slope of force-displacement graph.

$$E = \frac{l^2 * a}{16b * I} \tag{10.2}$$

E = bending elastic modulus, I = moment of inertia, l = length between supports, a = distance between support and respective arm of the two-armed pannier used for weight application and b = slope of force-displacement graph.

10.2.4 Determination of Silica Content for Saccharum Samples

Dried samples were weighed and afterwards ashed with a rapid incinerator (SVD 95, Harry Gestigkeit GmbH, Düsseldorf, Germany) at 400 °C for 48 h and weighed again. Then concentrated hydrochloric acid (HCl) was given to the ashes and boiled until all hydrochloric acid had evaporated. HCl was added again and heated to boiling point, then distilled water was added. The hot solution was filtered and washed with hot distilled water. The residue was heated again, this time at 600 °C for 3 h. After cooling, the residue was weighed again and the percent of silica per plant dry weight determined by the following formula:

$$silica[\%] = \frac{acid\ insoluble\ dried\ ash}{initial\ plant\ mass} * 100 \tag{10.3}$$

10.2.5 Statistics

Statistics were carried out using software R (version 2.13.2). Since the majority of data was not normally distributed, as tested using the Shapiro test in combination

with visualisations by histograms, the data was statistically analysed with a Wilcoxon U-test for *Saccharum* and for independent data of *Miscanthus* (testing of corresponding segments and bending directions of erect (E) against pre-bent plants (B), e.g. E-A1 + vs. B-A1 + and testing of different segments of pre-bent plants in the same direction, e.g. B-A1 + vs. B-A2 + vs. B-A3 + vs. B-A4 +). For dependent data of *Miscanthus* a paired Wilcoxon U-test for dependent data (same segment with different bending direction, e.g. B-A1 + vs. B-A1-) with Sidak correction of the significance level was carried out. The corresponding significance level is shown in the upper right edge of the figures showing the boxplot images (Figs. 10.3 and 10.4). For the tests with 4 groups (e.g. B-A1 + vs. B-A2 + vs. B-A3 + vs. B-A4 +) the significance level was 0.0085, whereas for the other tests with two groups it was 0.05.

10.3 Results and Discussion

Silicon uptake in *Saccharum* was successful and the percentage of silica in plant dry mass increased linearly (Fig. 10.2, R^2=0.9996) with increasing silicon content in the soil. Silica inclusions occur in sugar cane as dumbbells and in silica bands in the epidermis, but barely in cortex, vascular bundles or parenchyma (Keeping et al. 2009).

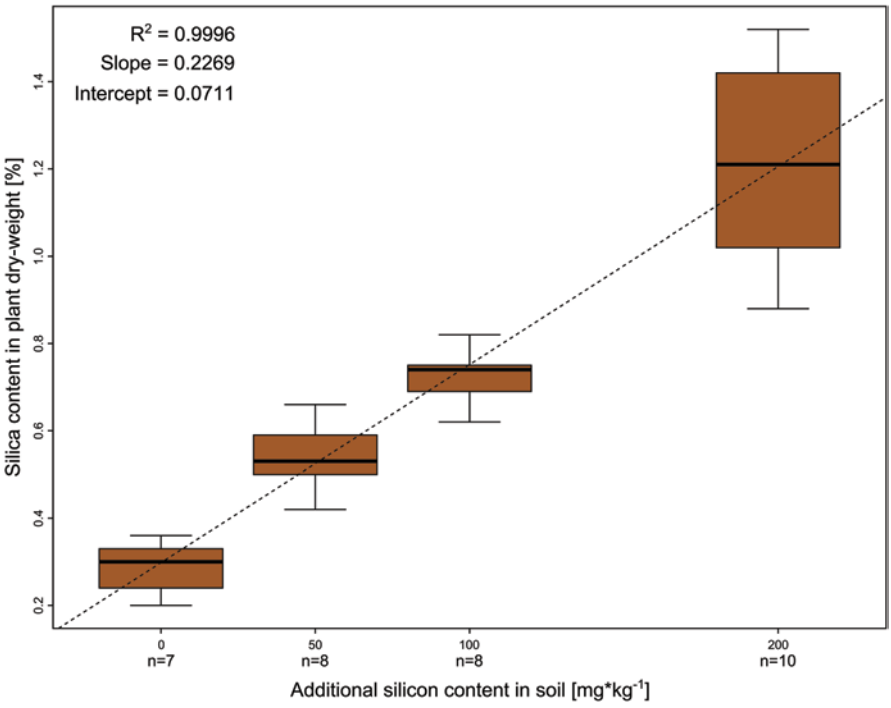

Fig. 10.2 Sugar cane: Silica content of plant dry-weight in percent plotted versus silicon addition to the soil. The increase with rising additional silicon content in the soil is linear

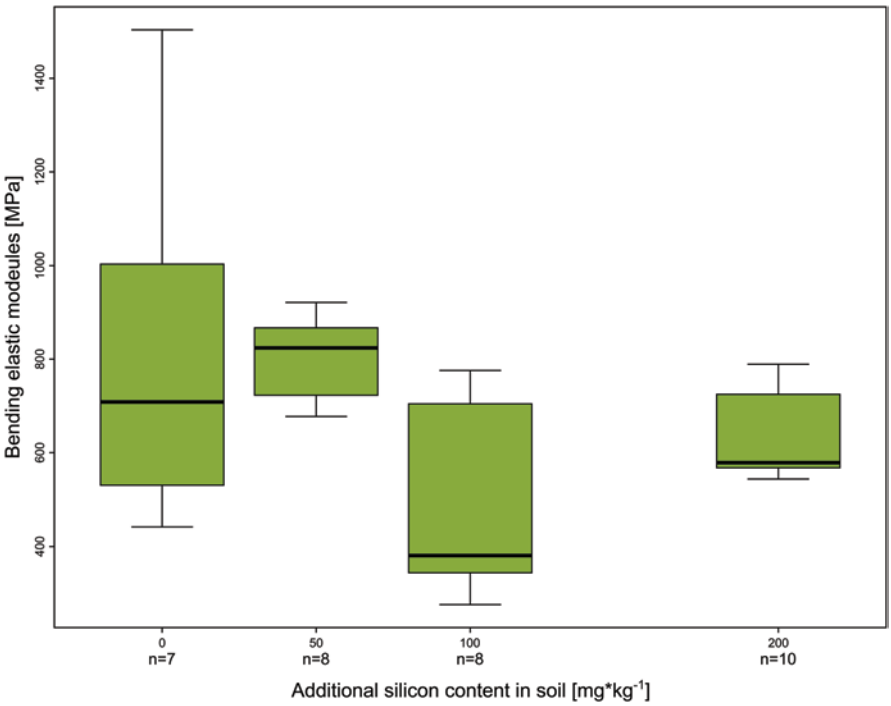

Fig. 10.3 Bending elastic moduli of stalks of sugar cane grown in substrates with different silicon addition. No significant difference can be found

The bending elastic moduli of the different test groups show no significant differences between reference plants grown in untreated soil and the plants grown with increased silicon content. The median values of the bending elastic moduli are very similar for reference plants and plants grown in soil with a silicon addition of 50 and 200 mg*kg^{-1} respectively, and varies between 824 and 580 MPa. Only the median for plants grown in soil with a silicon addition of 100 mg*kg^{-1} is with 381 MPa markedly lower but not significantly different due to the high variations (Fig. 10.3). Our data shows no consistent pattern, and the increase in silica content per plant dry-weight of 0.30% for the reference group to 1.21% for plants grown in soil with a silicon addition of 50 to 200 mg*kg^{-1} does not influence the bending elastic moduli significantly.

For *Miscanthus* stalks cross sections of pre-bent and erect stalks show that slightly more silica is deposited in the epidermis at the convex side of pre-bent stalks than in erect plants (Fig. 10.4a, 10.4e). Additionally, as a reaction to growth under static bending, the stem tissues at the convex side of the pre-bent plants show thickened cell walls as can be seen especially in the sclerenchymatous fibres arranged in the peripheral parenchymatous tissues (Fig. 10.4). The cell wall thickness is much more increased on the convex side of the pre-bent stalks, being under tension strain during growth compared to the concave side, which is under compressive strains.

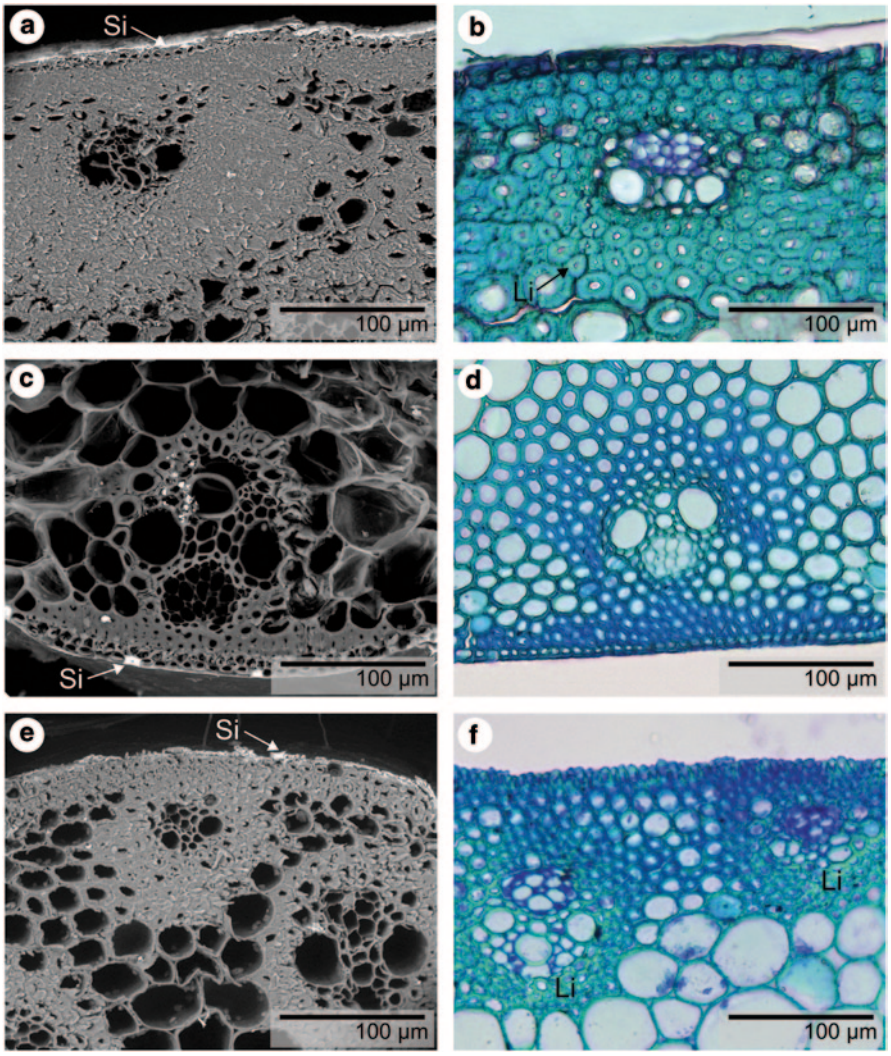

Fig. 10.4 *Miscanthus sinensis*: **a** vCD picture of the outer (convex) side of a pre-bent stalk. Silica deposit is seen as a *bright layer*. **b** Light microscopy picture of the outer (convex) side of a pre-bent stalk stained with *toluidine blue*. Lignin is stained *turquoise* (Li). The thickened cell walls are markedly lignified. **c** vCD picture of the inner (concave) side of a pre-bent plant stalk. Silica deposits are seen as a bright layer with several mass deposits. **d** Light microscopy picture of the inner (concave) side of a pre-bent plant stalk stained with *toluidine blue*. **e** vCD picture of an erect plant stalk. Silica deposits are shown as a bright layer with several mass deposits. **f** Light microscopy picture of an erect plant stalk stained with *toluidine blue*. Lignin is stained *turquoise*. The sample is partly lignified

Regarding cell wall thickness, the tissues of the concave side of pre-bent stems equals that of erect stems (Fig. 10.4). Moreover, in the cell walls of the convex side

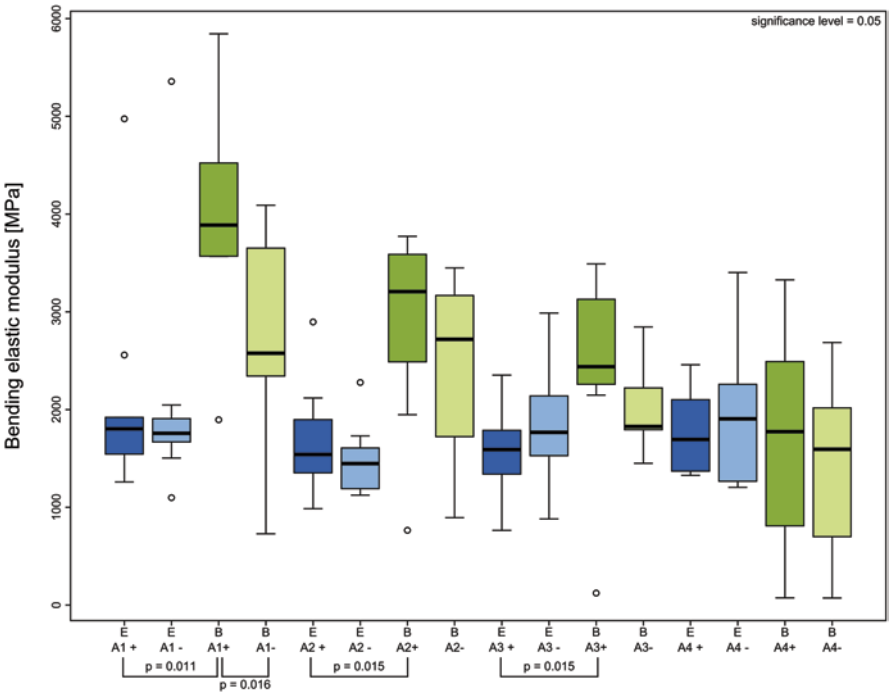

Fig. 10.5 Bending elastic moduli of *Miscanthus* stalks, arranged according to growth condition (erect (E) and pre-bent (B)) and tested stalk segment (A1-A4). The bending direction of pre-bent stalks is indicated by +/−. Significant differences are shown by brackets connecting the significantly different groups. The significance level which was tested for is shown in the upper right edge. As the respective segments of erect stalks show no significant difference as to the direction of 4-point bending (see Fig. 10.6), for statistical comparison with segments from pre-bent stalks, the erect segment with bending in the arbitrarily chosen +direction was always used.

of the pre-bent stems a higher lignification occurs compared to the wall tissues of the erect stems and the concave side of the pre-bent stems (Fig. 10.4b, 10.4d, 10.4f). The lignification of the concave side's stalk tissues of the pre-bent plants is comparable to or even lower than in the erect plant stalks (Fig. 10.4d, 10.4f).

The results of the bending tests fit in well with the observed structural and biochemical changes found in pre-bent and erect stalks. Due to the markedly increased cell wall thickening and the augmented lignifications of the peripheral stem tissues in the convex side of the pre-bent stalks, accompanied by a slightly higher silica deposition in the epidermis, pre-bent segments (B) in 4-point bending tests in direction of the pre-bent stalks (+ direction) show significantly higher bending elastic moduli than respective segments of erect stems (E) in the three basal segments A1 to A3 (Fig. 10.5): E A1 + (median: 1804 MPa) and B A1 + (median: 3887 MPa; $p = 0.0111$); E A2 + (median: 1541 MPa) and B A2 + (median: 3207 MPa; $p = 0.0152$); E A3 + (median: 1591 MPa) and B A3 + (median: 2439 MPa; $p = 0.0152$). Only for the uppermost segment A4, which is not strongly bent, no significant difference

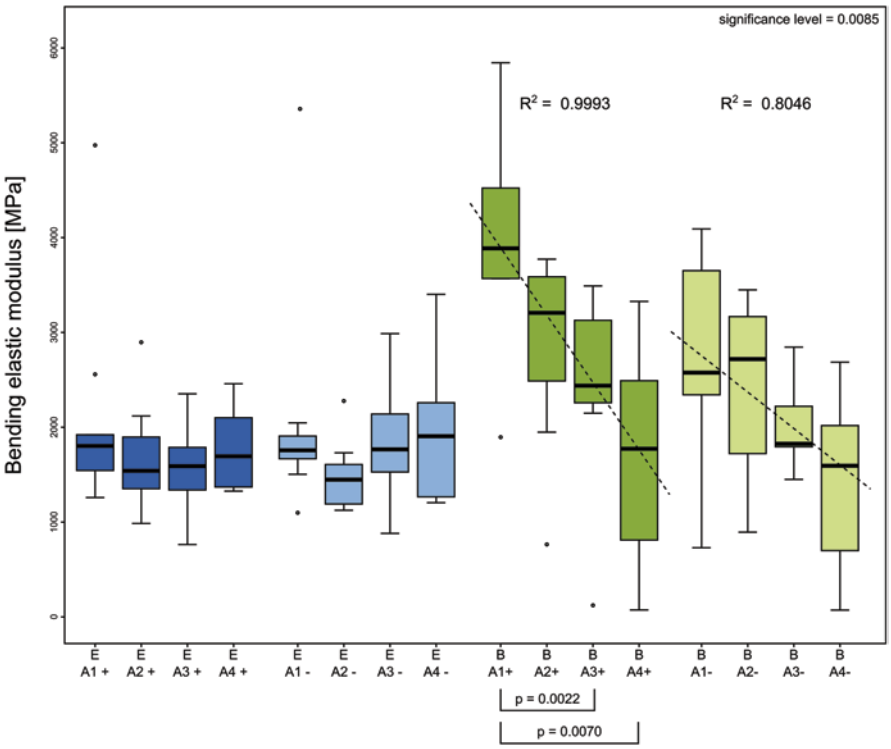

Fig. 10.6 Bending elastic moduli of erect (E) and pre-bent (B) *Miscanthus* stalks, sorted according to segment (A1-A4) and bending direction (+/−). Significant differences are shown by brackets connecting the significantly different groups. The significance level which was tested for is shown in the upper right edge. *Dashed lines* represent regression lines, displayed with corresponding R^2-factor

could be found. For bending tests against the direction of the pre-bent stalks (− direction) no significant differences to the respective segments of the erect stalks could be found, although the medians of segments A1 and A2 are markedly higher for pre-bent stalks (Fig. 10.5).

The bending elastic moduli for 4-point bending tests of the same segment with directions of bending differing by 180 ° are very similar for erect stalks, proving no anisotropy for this property in these stems. On the other hand, for pre-bent stalks the bending elastic moduli show pronounced differences for tests in the + and − direction for segments A1 to A3, indicating a pronounced mechanical anisotropy. For these segments the median of the moduli is always higher for bending in the direction of the pre-bent stalk (+direction). However, only segment B A1 showed statistically significant differences between the two bending directions (median+: 3887 MPa; median −: 2577 MPa; $p = 0.0156$; Fig. 10.5).

As shown in Fig. 10.6, where the bending elastic moduli are plotted against the tested segments for pre-bent and erect plants and both bending directions, a

marked difference between pre-bent and erect plants could be found. For erect plants the bending elastic modulus remains nearly constant along the stalks, and for none of the two bending directions a tendency to increase or decrease could be found (Fig. 10.6). For the pre-bent stalks on the other hand, pronounced variations along the stalks exist. For both bending tests, in + direction as well as against the direction of the pre-bent stalks (− direction), a marked decrease of the bending elastic modulus from stalk base to stalk apex could be found with R^2 values of $R^2 = 0.9993$ for + direction and $R^2 = 0.8046$ for − direction. Additionally, for bending in + direction, segment A1 (median: 3887 MPa) is significantly different to segments A3 (median: 2439 MPa; $p = 0.007$) and A4 (median: 1774 MPa; $p = 0.0022$).

Our results indicate that *Miscanthus sinensis* is able to adjust its stalk structure and cell wall biochemistry to the mechanical loads applied during the pre-bending experiments. This allows the plant to increase the bending elastic moduli in the pre-bent stems basipetally towards the most basal segments, i.e. the regions where the highest mechanical loads occurred due to pre-bending. This tendency could be found in bending tests in the + direction, as well as in bending tests going against the direction of the pre-bending (− direction). Besides, for the uppermost segment the bending elastic moduli are (markedly) lower for bending against the direction of the pre-bent stalks (− direction). This indicates that the predominant part of the reaction of the plant antagonizing the pre-bending takes place on the convex side. This reaction is vaguely reminiscent of the arrangement of tension wood formation in angiosperm trees where the 'mechanically reactive side' is also the convex side.

The observed results in *Miscanthus* lead to the conclusion that the assumed hypothesis of an increased deposition of silica at locations of high stress and strain, as replacement for the deposition of lignin, for energy-saving reasons could not be proved with our test procedure for *Miscanthus sinensis*. Even though silica content increases slightly in the epidermis of the convex side in pre-bent plants, lignin content increases as well (and probably more pronouncedly). Moreover, the main part of the increased bending stiffness and bending elastic modulus is brought about by a pronounced cell wall thickening in the stem tissues of the convex side. Assuming on the convex side of the stalks of *Miscanthus sinensis*, where the main part of the thickened cell wall consists of cellulose (despite the increased lignifications), a biochemically similar formation process and mode of function of the 'tension tissue' as described for tension wood in broad leaved trees (Scurfield 1973; Fournier et al. 1994; Bamber 2001; Pilate et al. 2004), an increased silica deposition (on the convex side) would not improve the mechanical performance of the pre-bent *Miscanthus* stalks.

Based on both the experiments presented, the general assumption of increased mechanical stability due to increased silica content could not be demonstrated in the case of bending elastic modulus (stiffness) for the two plant species tested with the experimental protocol used. Several studies report the reduction of lodging due to silicon fertilizing (Takahashi 1968; Savant et al. 1999), indicating an undefined higher mechanical stability. The improved lodging stability might be

based on additional deposition of silica in the root-stalk connection or just an adequate supply with silicon fertilizer for optimizing plant development. Mali and Aery (2008) observed in cow pea (*Vigna unguiculata*) shoots that additional silicon in lower concentrations seems to benefit plants more than higher silicon supply. Even though they analysed nodule growth and not stalk bending mechanics, their results indicate that additional silicon is only beneficial to a certain extent. Consequently, *Miscanthus* may in the pre-bending experiments 'rely' on lignin and cellulose as supporting agents, despite the costliness, and increases silica only slightly in the regions of mechanical stress. To summarize, very little research has been performed on exactly how additional silica may influence the mechanics of plants and plant organs. Therefore a wide field of research remains open in terms of improving our understanding of the influence of silica on plant mechanical properties. In particular, the direct mechanical influence of silica or its influence on mechanical properties via improved plant growth is of interest. In connection with this, it would be of economic significance whether an optimal amount of soil silicon for maximizing plant development and mechanical properties existed. Furthermore, the influence of distinct or bands of silica bodies versus the influence of continuous silica layers on mechanical properties may be a fruitful avenue to pursue.

References

Bamber RK (2001) A general theory for the origin of growth stresses in reaction wood: how trees stay upright. IAWA J 22:205–212

Da Cunha KPV, do Nascimento CWA (2009) Silicon effects on metal tolerance and structural changes in maize (*Zea mays* L.) grown on a cadmium and zinc enriched soil. Water Air Soil Pollut 197:323–330

Da Cunha KPV, do Nascimento CWA, da Silva AJ (2008) Silicon alleviates the toxicity of cadmium and zinc for maize (*Zea mays* L.) grown on a contaminated soil. J Plant Nutr Soil Sci 171:849–853

Dietrich D, Hinke S, Baumann W, Fehlhaber R, Baeucker E, Ruehle G, Wienhaus O, Marx G (2003) Silica accumulation in *Triticum aestivum* L. and *Dactylis glomerata* L. Anal Bioanal Chem 376:399–404

Fournier M, Bailleres H, Chanson B (1994) Tree biomechanics: growth, cumulative pre-stresses and reorientations. Biomimetics 2:229–252

Jung H-JG, Varel VH, Weimer PJ, Ralph J (1999) Accuracy of klason lignin and acid detergent lignin methods assessed by bomb calorimerty. J Agric Food Chem 47:2005–2008

Keeping MG, Kvedaras OL, Bruton AG (2009) Epidermal silicon in sugarcane: cultivar differences and role in resistance to sugarcane borer *Eldana saccharina*. Environ Exp Bot 66:54–60

Mali M, Aery NC (2008) Silicon effect of nodule growth, dry-matter production and mineral nutrition of cowpea (*Vigna unguiculata*). J Plant Nutr Soil Sci 171:835–840

Nwugo CC, Huerta AJ (2008) Silicon-induced cadmium resistance in rice (*Oryza sativa*). J Plant Nutr Soil Sci 171:841–848

Pilate G, Chabbert B, Cathala B, Yoshinaga A, Leplé J-C, Laurans F, Lapierre C, Ruel K (2004) Lignification and tension wood. CR Biol 327:889–901

Raven JA (1983) The transport and function of silicon in plants. Biol Rev 58:179–207

Savant NK, Korndörfer GH, Datnoff LE, Snyder GH (1999) Silicon nutrition and sugarcane production: a review. J Plant Nutr 22:1853–1903

Schoelynck J, Bal K, Backx H, Okruszko T, Meire P, Struyf E (2010) Silica uptake in aquatic and wetland macrophytes: a strategic choice between silica, lignin and cellulose? New Phytol 186:385–391
Scurfield G (1973) Reaction wood: its structure and function. Science 179:647–655
Takahashi E (1968) Silica as a nutrient to the rice plant. Jpn Agric Res Quart 3:1–4
Tisdale SL, Nelson WL, Beaton JD (1985) Soil fertility and fertilizers. Macmillan, New York
Van der Vorm P (1980) Uptake of Si by five plant species, as influenced by variations in Si-supply. Plant Soil 56:153–156

Chapter 11
ELiSE—An Integrated, Holistic Bionic Approach to Develop Optimized Lightweight Solutions for Engineering, Architecture and Design

Christian Hamm and Sebastian Möller

11.1 Introduction

Gravity is a dominating factor for life on earth. It influences all organisms, except for the very smallest (sizes of 1 μm and smaller, e.g. some bacteria and viruses) and those, which have virtually the same density as their surrounding medium, such as jellyfish. Reducing mass while maintaining mechanical strength provides many evolutionary advantages. For example, it saves resources, allows faster movement, and reduces sinking velocity which is crucial for the survival of planktonic organisms. Especially the first two aspects have become very important in the modern world, as efficient mobility is being regarded a basic necessity for mankind, but resources become more and more limited. Throughout history, civilizations have optimized factors that were decisive for their success, such as tools, weapons and buildings. These objects often had to be light and strong. Although all this led to many intriguing solutions, there is still plenty of room for improvement. Many books and articles describe methods to find and apply appropriate tools for optimization of lightweight structures. But at the same time, almost any problem to develop a technical lightweight component has so many potential solutions, that computing power and time to design, vary, calculate and optimize such products and sufficiently consider all valuable approaches using conventional methods would by far exceed reasonable and economic values.

Within the biosphere, optimization processes occur simultaneously in inconceivable numbers. Mutation, recombination, and natural selection cause adaptation to many different environmental factors such as physical and chemical challenges

C. Hamm (✉) · S. Möller
Bionic Lightweight Constructions and Functional Morphology, Alfred-Wegener-Institut Helmholtz-Zentrum für Polar- und Meeresforschung, Bremerhaven, Germany
e-mail: chamm@awi.de

S. Möller
e-mail: smoeller@awi.de

C. Hamm (ed.), *Evolution of Lightweight Structures,* Biologically-Inspired Systems 6,
DOI 10.1007/978-94-017-9398-8_11

originating from the inorganic world. These factors range from forces, temperatures, nutrients and, to a considerable extent, to those originating from other organisms Although there is no single goal (*sensu* Adams 1979) in these optimization efforts, the processes are very efficient and have created millions of species with amazing technical solutions, including some of the most amazing lightweight constructions.

Compared to products of the apparent "creativity" of nature, which result from these processes, even the amazing developments of scientists, designers and engineers can appear humble. The drive for improving these developments has led to the forming of a community of scientists and engineers has evolved who dedicate their efforts to the transfer of technical principles found in nature. They call it "Bionics", "Biomimetics" or "Biomimicry", the choice of words depending on their cultural background. Although the potential for technology transfer from nature is huge and the discipline has received much public attention, the invested resources and consequently the number of realized innovations are still moderate. The question remains how the processes and principles present in nature can be used most efficiently to create innovative solutions. Here we present several principles, which lead to the evolution of stable lightweight constructions in nature and present a systematic approach which combines all these principles found in ecosystems within a single product development process.

11.2 Lightweight Optimization in Nature and Corresponding Bionic Approaches

11.2.1 Lightweight Principles

How Nature Does It

One might expect that lightweight solutions are ubiquitous in nature, because building structures always requires energy and time, and sometimes limited raw materials. Moving organisms move faster if their stabilizing components are light, and especially flying is easier if an organism is built lightly. But there are also conflicting demands: organisms have to store water, nutrients, and energy, generate forces using need muscles, or have to insulate their metabolism against low temperatures with the help of fat storage and growing fur and feathers. Consequently, lightweight solutions occur in many organisms, but are often masked because extra functions are added to the properties of being mechanically strong and light. Typical examples are found among higher plants and animals. Large plants, especially trees, are restricted in their ability to grow a lightweight construction, because their growth process is purely additive. As a result, tree trunks may well reduce (notch) stress, but do not possess the complex framework of a true lightweight construction. Many vertebrates, especially birds (Dumont 2010) or fast runners such as cheetahs or antelopes, have bones, which are typical stable lightweight constructions. However,

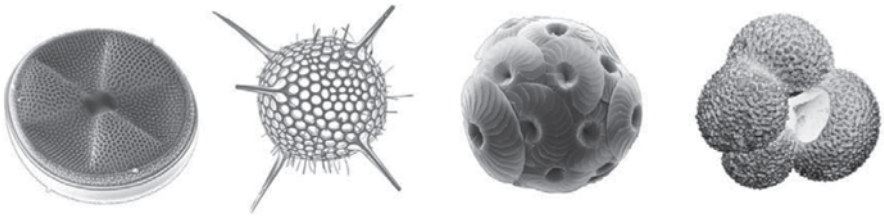

Fig. 11.1 Diatom, Radiolaria, Coccolithophorid (by courtesy of Gerald Langer, Cambridge University), Foraminifera (by courtesy of Jelle Bijma, Alfred Wegener Institute)

their overall structures are difficult to transfer to technical solutions, because these bones are part of an endoskeletons, meaning they only work well together with tendons, ligaments, and muscles (Fig. 11.1).

Transfer

A good approach is to identify lightweight principles with a high potential for transfer and use them for buildings, constructions or products. Especially the shell geometries of planktonic organisms mentioned above, such as diatoms, but also radiolaria, tintinnids, acantharia, and foraminifera have been described together with potential mechanical effects in many publications (Burkhard and Bach 1990; Hamm and Smetacek 2005, Kooistra and Pohl 2014, this issue). Since these principles follow the rules of physics, a transfer to technical solutions by people with a background in mechanics will often considerably improve the state of the art. A main problem, however, remains the fact that technical load cases and materials, but also the possibility to produce complex structures economically, differ considerably from those the organisms experience in nature. Therefore, a substantial adaptation to the technical load cases, technical materials and production techniques is usually necessary. From a technical viewpoint, the results remain mostly suboptimal, since subsequent optimization processes are very laborious and require very special expertise, which is often not available. However, they are excellent for rapid realization as prototypes or demonstrators and give crucial impulses as innovative approaches for radically new construction concepts (Fig. 11.2).

Fig. 11.2 Design object suspended lightweight railway (design Simon Szameitat 2013). Weight reduction and functional details based on constructional principles of diatom shells

11.2.2 Diversity

How Nature Does It

The presence of a high diversity of organisms within an ecosystem is typically a significant advantage if a new challenge arises (McCann 2000; Elmqvist et al. 2003). Usually, the presence of different solutions for all sorts of challenges bears a high potential to include an appropriate answer to a newly aroused challenge. There is no reason to believe that the optimization of stable lightweight constructions is an exception to this mechanism. As mentioned above, optimization is a complex, difficult task because the solutions for most problems cannot be described by one simple optimum but by a multi-peak optimization landscape. In nature, adaptations just occur as a function of selection pressure. Thus, if a new mechanical challenge arises, for instance, caused by a new type of grazer, the corresponding selection pressure will act on all organisms within the susceptible size range. Consequently, optimization processes leading to better adapted lightweight solutions will occur in several or even many organisms at the same time. Although this process has not been observed yet in the highly fluctuating planktonic ecosystems, it is well known from the beaks of different species of Darwin finches, which are directly influenced by the mechanical properties of their food, i.e. an increase of the percentage of hard seeds will lead to the simultaneous adaptation of the beaks of different species (Grant and Grant 2001) (Fig. 11.3).

Even if a certain design has an advantage over the others in the beginning, it is extremely difficult to predict which design will end up as the best answer to the mechanical challenge after the optimization process.

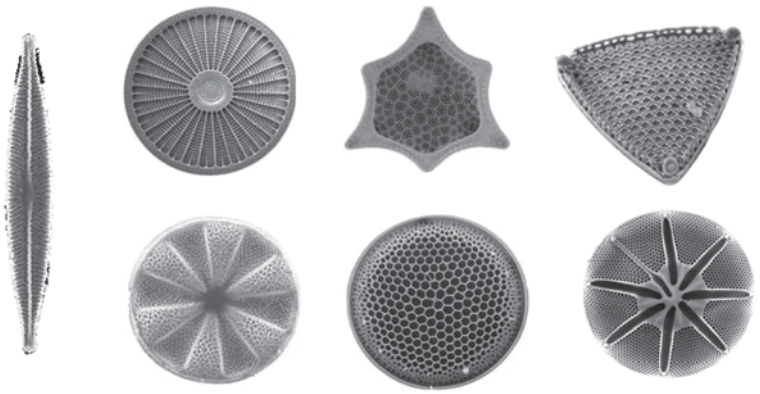

Fig. 11.3 Diversity among diatoms: Although all diatom frustules fulfill the criteria as stable lightweight constructions, they have very different overall geometries as well as substructures. Their respective potential to adapt to a new mechanical challenge, e.g. caused by a predator, is likely to differ considerably. Here we show 7 of an estimated 100,000 species

Fig. 11.4 Two Variants of new developments for automotive lightweight wheels. The most important loadcases were tested and revealed very good performances, but an adaptation using evolutionary algorithms has not been executed yet. The left concept has been designed for a realization in anisotropic materials, such as fiber reinforced plastics, the solution on the right is for isotropic materials (e.g. metals)

Transfer

It is obvious that an engineer is more likely to get an excellent result for his lightweight problem if he is able to start with different lightweight concepts for a technical solution. But unlike in nature, it matters whether few or hundreds of concepts are tested, because the effort to create 3D (CAD) models, analyze them, adapt them to restrictions of production processes, create an FE-Mesh and calculate is quite considerable. It is, therefore, essential to select high-potential candidates for specific lightweight solutions. The main challenge is therefore: how can the potential of a certain lightweight principle be rated? Usually, the criteria for a pre-selection depend on the matching of general forms and the potential to manufacture lightweight principles. Compared to the integration of just one principle, manufacturers appreciate the possibility to choose between several concepts of technical solutions for a specific component. However, the results are likely to remain far beneath their optimal performance as stable lightweight construction, if a professional optimization step is missing (Fig. 11.4).

11.2.3 Evolutionary Processes/Optimization

How Nature Does It

The elegance of evolutionary processes is based on simplicity and effectiveness. Several parameters or traits can be altered by mutation at the same time; recombination by sexual reproduction strongly augments the difference between individual offspring. The continuous creation of new, slightly altered generations and them being tested by environmental factors which decide, in turn, their reproductive success leads to an automatic adaptation of their properties to changing environmental factors. Although these principles are very powerful, adaptations in nature underlie certain restrictions, which are not attractive for an engineering process. One characteristic of natural evolution is that the alterations from one generation to the

next are, in general, minute. Therefore, it takes a very long time until a new species evolves. Even then, the differences between the old and the new species often remain small (Theriot et al. 2006). A complication for evolutionary processes in nature is that once a certain group of organisms has had time to adapt to and occupy a certain ecological niche, it is difficult for other taxa to start a similar adaptation based on other morphological/ physiological principles. In other words, had the dinosaurs not died out to a catastrophic event at the end of the Creatceous, mammals would never have had the chance to evolve in such an enormous diversity of forms and sizes.

Transfer

When transferring the evolutionary process to technology (i.e. using genetic algorithms, Rechenberg 2000) it is most remarkable that it can work even more efficiently than it does in nature. The main advantage of the technical approach is speed: several parameters of a lightweight structure can be varied, several variants can be tested and the best offspring can be selected in a very short time. If the structure is not too complex and the number of parameters is not too big, several hundreds of generations can be simulated in reasonable time. Another big advantage is that changes in geometry are not restricted to small steps which are allowed by the genetic setup as is the case in nature. Structural changes, which would, in nature, mark the evolution of a new species can be simulated in only one generation. A main technical challenge is the selection of adequate geometric models. The effectiveness of evolutionary strategies is restricted in such a way that they ideally need starting points which already possess certain properties that have a high potential for a superior solution after the adaptation process.

11.2.4 Growth Processes

How Nature Does It

A powerful tool to optimize lightweight structures is growth and/or reduction of structural components based on high low mechanical stress values within a living organism. It is known that trees react with selective growth to high stress and thus reduce notch stress and even create structures such as I-beams. However, since they only add structure and do not remove it, their freedom to create diverse efficient lightweight solutions is extremely restricted. Therefore, it is amazing that trees still grow a large variety of interesting forms, which are interpreted as a result from their “mechanical load history” (Mattheck 1991). In contrast, the processes which lead to the inner structures of bones and their resulting structures are more sophisticated: bone cells can add and remove material, depending on the level of stress found in an area of the whole structure. This leads to very complex

constructions, of which the most famous is probably the human femur, where the stress trajectories are manifested as an intricate framework of an apatite composite. As in trees, orientation and dimensions of bone structures reflect their mechanical load history, but in contrast to them, unnecessary or over-dimensioned structures can be reduced. This leads to considerable weakening of bones of astronauts or immobile persons, but allows both reduction and reinforcement as a function of mechanical loads.

A special case of growth processes are found among the cell covers of protists, especially the silica frustules of diatoms, whose geometries are extremely complex. Here, silica structures grow within hollow forms (silica deposition vesicles, SDVs), which are manipulated by the cytoskeleton into fantastic geometries, which in turn allow the production of very complex shells with a superior performance as stable lightweight constructions. In contrast to bone, there is, to our knowledge, no change of geometry possible once the structure is completed. This is consistent with current technical manufacturing methods and most likely leads to a certain robustness of the shell structures: although they are adapted to mechanical challenges posed by their most numerous and effective predators, they cannot afford to be completely unprepared (i.e. mechanically weak) with regards to diverging mechanical attacks and other load cases, which they encounter less frequently.

Transfer

There are already several algorithms, which are based on growth processes and are suited to generate 3D-Data for new stable lightweight constructions. Although different mathematical and programming solutions have been developed for this purpose, all of them use the available design space, apply the technical load cases relevant for construction, and reduce material where FE-calculations display small stress values, while conserving load-bearing, high stress structures. This approach to reduce weight is completed by the reverse method: growth is allowed wherever stress values become high. This method efficiently reduces notch stress. These approaches are widely used and have successfully helped to reduce material while maintaining mechanical strength, or improving strength while using as much material as before. However, in cases where the geometries, the load cases, the materials, or the production processes are complex, this approach tends to have limitations to the extent that a realisation is not feasible. In addition, the result of such an optimization is always a simple framework with no potential for fundamentally different solutions, and the results in most cases have a low robustness, because unexpected loads have few options to be compensated for by alternative stress paths.

The growth processes of diatoms and radiolarians have not yet been transferred to the technical loads, but two aspects appear to have a considerable potential for future applications: (1) a mathematical simulation of their morphogenesis for the generation of high-quality, robust structures, and (2) a physical system of membranes which can be manipulated to generate complex casts as do the SDV's of diatoms.

11.2.5 Beauty

How Nature Does It

Most natural structures, especially lightweight structures, are perceived as being beautiful. This is not only the case where organisms have to be eye-catching because they have to attract mating partners. Beautiful structures can also be found in higher and lower plants, for instance in their leaves, pollen grains, and, again and most strikingly, among protist cell covers, such as those of diatoms and radiolarians. According to Plato, beauty resides in proper measure and proper size, and of parts that fit harmoniously into a seamless whole. To St. Augustine, geometric form and balance create beauty, and Plotinus postulated that beauty must be present in details as well as the whole, and that it cannot be constructed out of ugliness, but its law must run throughout (Etcoff 2000). Although these authors could not know it, these descriptions are consistent with mechanically well-designed constructions.

Transfer

It is a common and long established practice to transfer beautiful natural forms to products and buildings. These forms are usually selected according to personal taste and combined with ideas and design preferences of individual designers, architects and engineers. There are many examples where this has been done quite successfully. Where necessary, the resulting products are often embellished according to their mechanical function. However, while well-designed stable lightweight constructions usually have a beauty in the sense mentioned above, beautiful structures are not automatically optimized for the mechanical loads they experience—neither in nature, if they meet a new challenge, nor in the technical world, where they always meet a new challenge. In both cases, it is necessary to test a number of different designs in order to find an ideal solution, and both require a serious adaptation process (that is, evolution in nature and genetic algorithms in the technical world).

11.2.6 Synthesis and the ELiSE Lightweight Process

Organisms, which develop lightweight solutions within ecosystems, for instance planktonic ecosystems, integrate all of the mentioned processes just by living, reproducing and growing. They inherit powerful lightweight principles from their predecessors, are usually present in a certain diversity, adapt without extra effort using evolutionary processes, form their shells in a sophisticated growth processes, and are beautiful just because their proportions are “right”. This means they are not angular but possess smooth transitions, are (basically) symmetrical, harmonic and often possess a self-similarity of forms at different size scales of their structures. In

order to transfer the potential of the natural processes mentioned above effectively, a corresponding combination of principles and mechanisms is necessary for the product development process.

To combine the biomimetic potential of lightweight structures evolved in nature, especially in diatoms and radiolarians, with the principles of evolution in a technical context, the holistic lightweight optimization process ELiSE (Evolutionary Light Structure Engineering) was developed. As mentioned before, this process is composed of five different steps, which base on each other in a systematic order. These steps shall be described in detail and are shown in the figure at the end of this chapter.

1. Technical specification
   The success of an optimization is highly dependent on the technical setup defined in this first step of the ELiSE lightweight process. The technical part which has to be optimized can be characterized by different parameters such as material, production process and load cases. All these parameters influence the performance of an optimized part and have to be considered during the optimization process. If a relevant load case is neglected an immense reduction of the quality of the final optimization will be the consequence. At this point the ELiSE lightweight process does not differ from other optimization methods or engineering approaches to new product developments in general. As the use of CAD and FEM is an integral part of ELiSE later on, the definition of a fully assessed CAE setup is a key point in this step. At the same time the main optimization goal is defined, as lightweight design can be introduced by reducing weight or stress within the material or by increasing the overall stability of a construction.
2. Screening and selection of powerful archetypes
   Based on the previously defined optimization goals the systematic search for valuable archetypes starts with this step. Approximately 100,000 different species of diatoms and radiolarians are available. The Friedrich Hustedt Diatom Study Centre located at the Alfred Wegener Institute, Helmholtz Centre for Polar and Marine Research (AWI) offers direct access to a database storing information on taxa, accessions and publications. In addition, a second database is available providing engineering information on diatoms and radiolarians and thus containing CAD models or FE results of calculations made so far. Within this database a selection of powerful, biological archetypes can be identified using similarity search algorithms. This procedure enables engineers to find suitable archetypes in a semi-automated way. To summarize, engineers have the possibility to find manifold data about the shells of diatoms and radiolarians.
3. Abstraction to concept models
   In most cases, the complexity of natural lightweight structures prevents a direct transfer of design principles to technical applications. Restrictions of the production process or costs in general make it necessary to reduce the high level of details. The lightweight principles have to be understood and evaluated

by competent engineers or experts with a similar background. Still, specific solutions found in the biological archetype and peculiar structures of the shells are difficult to understand even by experts. In this step these structures have to be investigated and it has to be decided how a natural structure can be simplified without losing its functionality.

In a next sub step the simplified and abstracted structure is designed using CAD: a parametric CAD model of a bio-inspired concept is the result. Now the basic principles of evolution play an important role. It is not possible to guarantee that a bio-inspired concept is better than the original reference model. Therefore, several concepts are created based on different design principles found during the screening of nature. All concepts are forced into competition and therefore, it is pretty likely that the dominant concept will be superior when compared to the performance of the reference model.

4. Finite element analyses and optimization
   FEM is used to benchmark the design concepts created in the last step and to compare the best concept with the reference model. With the numerical calculation of deformation and stress values within digital concept models under given load cases, the performance of every concept can be estimated. One advantage of natural shells is the fact that they are robust against several different load cases. Using the similarity search algorithms in step 3, only those biological archetypes were chosen that showed a high possibility of possessing structures suitable for the given load cases. Nevertheless, the final concept has to be optimized primarily for the load cases defined in step 1 and the bio-inspired concepts are not necessarily optimized for these load conditions. Therefore, an optimization of each concept changes the structure in order to increase the performance under given loads. This optimization has to be regarded as a meta-level of implementing the principles of evolution to the ELiSE lightweight process. In this specific sub step each concept is optimized without comparing it to other principles. This is an analogy to the change of species during the course of evolution. One main optimization tool is the Evolutionary Strategic Optimization which is based on the change of parameters within the parametric CAD model. In addition, further optimization tools are used to improve the concept models, e.g. CAO and SKO which were described previously.
5. Assessment of the final structure
   The final step of the ELiSE lightweight process is the assessment of all calculated results. Every concept was designed using bio-inspired design principles from shells of diatoms and radiolarians. All concepts were optimized to fit the load conditions defined at the beginning. In this final step all concepts are compared to each other and to the reference model. Due to the implementation of principles of evolution and the use of pre-optimized biological structures for all concepts the possibility is high that engineers were able to design at least one concept which shows a better performance than the reference model.

   Although several steps of the ELiSE process include semi-automated methods to reduce the amount of work for an engineer, e.g. the similarity search

algorithms or the Evolutionary Strategic Optimization, the holistic process remains an abstract strategy to transfer high potential lightweight structure from nature to technical applications. For this reason, the quality of the final lightweight design is strongly dependent on the expertise of the engineers. Consequently the best way to use the ELiSE lightweight process is to combine the knowledge of different experts (biologists, experts in Biomimetics and engineers) within an interdisciplinary project team (Figs. 11.5, 11.6).

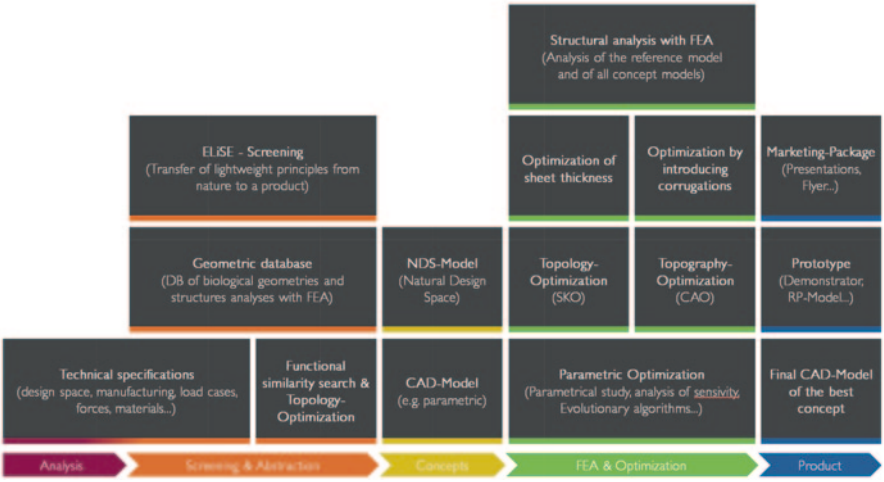

Fig. 11.5 The EliSE process, consisting of a set of conventional and biomimetic tools arranged in 5 general steps which describe the full product development

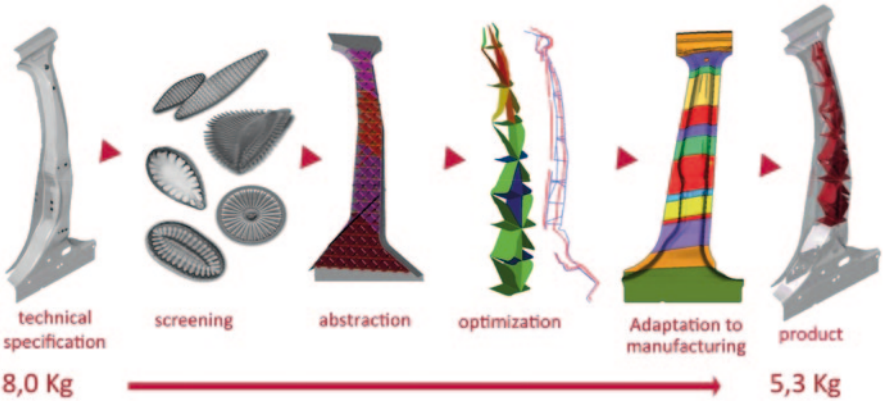

Fig. 11.6 The EliSE process, based on an example (b-pillar) from the automotive industries. It shows the potential for weight reduction, if a combination of steel and FRP materials is allowed and optimized according to the steps described above (Fig. 11.5)

11.3 Conclusion

The optimization of lightweight structures is an extremely challenging and complicated task. Currently we see that both mathematical and bionic methods to optimize lightweight constructions have improved considerably over the last decade, and it is very likely that they continue to do so. In nature, several principles which individually already help in the development of new lightweight solutions in technology work together. The ELiSE process combines these principles in a similar way and thereby leads to solutions which are very efficient but differ significantly from those created by standard methods such as topology optimization. In addition, it can usually provide several solutions to the same problem, a phenomenon which is also observed in the natural world.

References

Adams D (1979) The Hitchhiker's guide to the galaxy. Pan Books, UK, p 180

Bach K and Burkhardt B (eds., 1984) Diatoms I, Shells in Nature and Technics (Cramer, Braunschweig)

Dumont ER (2010) Bone density and the lightweight skeletons of birds. Proceedings of the Royal Society of London B, 2193–2198

Edward C, Theriot SC, Fritz CW, Daniel JC (2006) Late quaternary rapid morphological evolution of an endemic diatom in Yellowstone Lake, Wyoming. Paleobiology 32(1):38–54

Elmqvist T, Folke C, Nyström M, Peterson G, Bengtsson J, Walker B, Norberg J (2003) Response diversity, ecosystem change, and resilience. Front Ecol Environ 1:488–494

Etcoff N L (2000) Survival of the prettiest: the science of beauty. Doubleday, New York, 325 pp.

Grant, P.R. and Grant, B.R. (2002) Unpredictable Evolution in a 30-Year Study of Darwin's Finches, *Science* 296: 707–711.

Hamm, C.E. and Smetacek, V. (2007) Armor: Why, When and How? In: P. Falkowski and A. Knoll (eds.): Evolution of Primary Producers in the Sea. Elsevier, San Diego p. 311–332.

Kooistra and Pohl (2015), in Hamm (ed.) this issue.

Mattheck C (1991) Trees — the mechanical design. Springer, Berlin, Heidelberg, 121 pp.

McCann KS (2000) The diversity-stability debate. Nature 405:228–233

Rechenberg I (2000) Case studies in evolutionary experimentation and computation. Computer Meth. Appl. Mech. Eng. 186: 125–140.

Storn R, Price K (1997) Differential evolution—a simple and efficient heuristic for global optimization over continuous spaces. J Glob Optim 11:341–359

Szameitat S (2013) Bionic Lightweight Metro – Bachelor's Thesis (Design) University of Applied Science, Potsdam, 92 pp.

Chapter 12
Offshore Foundation Based on the ELiSE Method

Christian Hamm, Daniel Siegel, Nils Niebuhr, Piotr Jurkojc and Rene von der Hellen

12.1 Introduction

According to the energy policy objectives of the German government, Germany targets a phasing out of nuclear energy until 2022 (Knopf et al. 2011). Therefore the demand for power plants using renewable energy will increase. The prognosis of market research institutes show that between today and 2022, the power output of offshore wind energy could increase to a value of approx. 10 GW. To meet this target, up to 2000 offshore wind turbines will have to be installed in German offshore areas (Wab e. V. 2012). Due to political decisions and technical challenges, it is possible that the process of installing this capacity will be considerably prolonged. To install wind energy plants in the offshore field, a strong mechanical connection of the energy plant to the sea ground is required. This kind of connection is called offshore foundation. The design of these foundations depends on diverse environmental factors such as water depth, currents, wave regime and sedimentology

C. Hamm (✉) · D. Siegel · N. Niebuhr · P. Jurkojc
Bionic Lightweight Constructions and Functional Morphology, Alfred-Wegener-Institut Helmholtz-Zentrum für Polar- und Meeresforschung, Bremerhaven, Germany
e-mail: chamm@awi.de

D. Siegel
e-mail: dsiegel@awi.de

N. Niebuhr
e-mail: nniebuhr@awi.de

P. Jurkojc
e-mail: pjurkojc@awi.de

R. von der Hellen
Weserwind GmbH Offshore Construction Georgsmarienhütte GmbH, Riedemannstr. 1, 27572 Bremerhaven, Germany

WeserWind GmbH Offshore Construction Georgsmarienhütte, Riedemannstraße 1, 27572 Bremerhaven, Germany
e-mail: r.vonderhellen@weserwind.de

C. Hamm (ed.), *Evolution of Lightweight Structures,* Biologically-Inspired Systems 6,
DOI 10.1007/978-94-017-9398-8_12

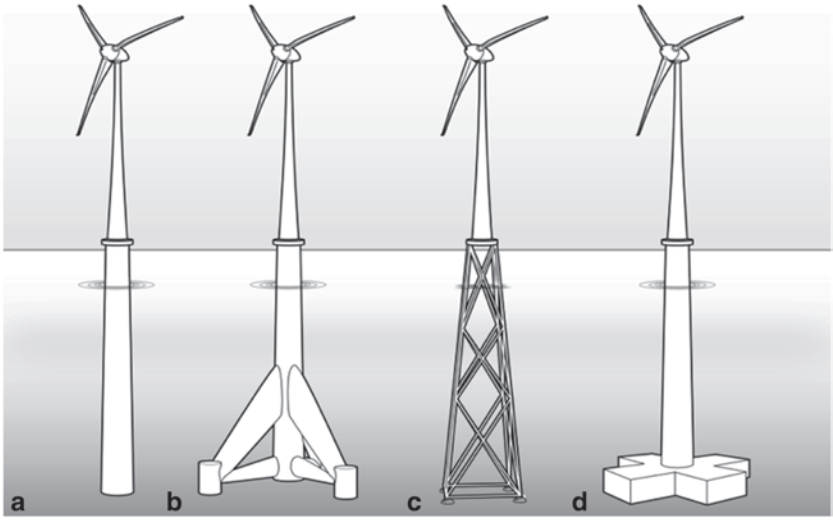

Fig. 12.1 Variation of different key foundation designs for offshore wind energy plants. **a** monopile **b** tripod **c** jacket d gravity base

(Byrne and Houlsby 2003). Therefore there are many different designs necessary alone on the basis of differing technical requirements. In addition, it is still under debate, which fundamental design is the most cost- effective and sustainable solution for any given offshore location. Today the most common foundation designs are monopile, tripod, jacket, tripile, gravity base, and suction bucket (Zaaijer, 2003) (see Fig. 12.1).

The different kinds of foundations also vary in the demand of material, in most cases steel. The weight of the primary structure of a tripod for 30 m water-depth is ca. 840 t. One of the lightest substructures available on the market today is the jacket foundation. For the same water-depth the jacket has a weight of around 425 t (Seidel 2007). Disadvantages are the fact that the four piles of the jacket require a costlier piling process, and the complexity of the structure makes it expensive to manufacture. Therefore the BIONA-research project "*Offshore foundations based on ELiSE procedure*" (OFE) focused on a structure with less than four piles. The following were requirements for a new, bionic structure for offshore wind energy plants for a water-depth of 30 m:

1. The structure must have, like the tripod, only three fastening structures for piles.
2. The geometry should be relatively simple to keep production costs low.
3. The new design should use standard steel pipes (such as those used for pipeline construction with diameters of up to 1500 mm, offshore steel (S355 or S420)).
4. The structure should be at least 25 % lighter than the currently produced tripods.
5. The structure should represent the best solution from a selection of at least three constructional principles.

The ELiSE method (see chap. 10) uses structural principles from nature for the development of technical products. One of the main challenges for bionic lightweight

developments is how to transform biological structures into useful technical structures. These are made of completely different materials, have a reduced complexity but are often several times larger, and experience different load cases. ELiSE systematically solves such technical problems with the help of a large variety of pre-optimized planktonic lightweight structures in combination with an optimization procedure.

Many planktonic organisms have elaborate, stable biomineralized exoskeletons with an extremely low weight. The reason for this development in nature is the protection against predators in combination with the fact that they can only survive in upper water levels, which provide sufficient nutrients (Hamm and Smetacek 2007). The necessity to be light and mechanically strong is also the main characteristic of modern lightweight developments.

Typical, planktonic shells are composed of many substructures, which are difficult to implement in the design of a technical product. Within the framework of this project it was necessary to use planktonic structures with a comparable design to an offshore tripod construction, and transform their structural principles into a weight-minimized steel foundation for offshore wind energy plants.

12.2 Material and Methods

Our research in this project showed that using radiolarians as structural archetypes have a high potential in optimizing the weight of foundations. Radiolarians are part of the marine plankton. They take their name from the radial symmetry, often marked by radial skeletal spines, characteristic of many forms (Boltovskoy 2002). The transformation of the radiolarian into an offshore foundation was done with the ELiSE method. The design of the new foundation is related to the Tripod Offshore foundation structure from WeserWind. This structure was therefore taken as reference for all FE-calculations in order to evaluate the potential of new constructional principles.

The structure of this section represents the use of the innovative lightweight construction method “Evolutionary Light Structure Engineering” (compare Chapter 10—ELiSE). This method consists of five steps. Every step of this method will be described in more detail in the following text, with the corresponding results to illustrate the development.

12.3 Results

12.3.1 Screening

The new foundation structure should maintain an innovative structure design which reflects a completely new approach to the construction of foundation structures. The idea of the innovative structure design was found in the nature. Diverse lightweight construction principles can be found in the protective skeletons of small plankton

structures like diatoms and radiolarians. These structures consist of effective lightweight designs with principles of nature that proved value during evolutionary processes (Hamm 2005). The objective of the work step screening was the selection of appropriate diatoms and radiolarians which have design principles that can be applied to buildings such as foundation structures.

12.3.2 Search for the Biological Archetype

Selection criteria such as geometrical similarities have been set up to reduce the huge amount of about 100,000 different species with diverse, high efficient light weight geometries (Hamm 2005). Matches for the tripod foundation were primarily found among radiolarians. The Alfred Wegener Institute owns samples of radiolarians coming from the west coast of Africa. These samples were examined with the light microscope. Radiolarians that match the geometrical criteria were prepared for scanning electron microscope (compare Fig. 12.2). For future implementation, recordings were made of appropriate structures using scanning electron microscopy, which served as a template for the subsequent design phase. Since the structures of radiolaria have been described in detail in diverse publications, and the Alfred Wegener Institute, we used literature data in addition to SEM-pictures (Fig. 12.3).

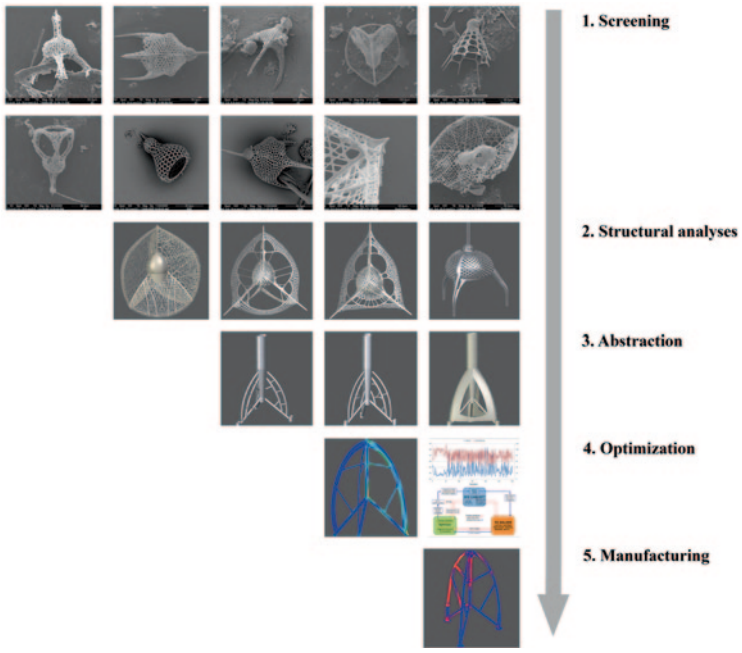

Fig. 12.2 Development of an offshore foundation based on the five-step approach of the Evolutionary Light Structure Engineering procedure

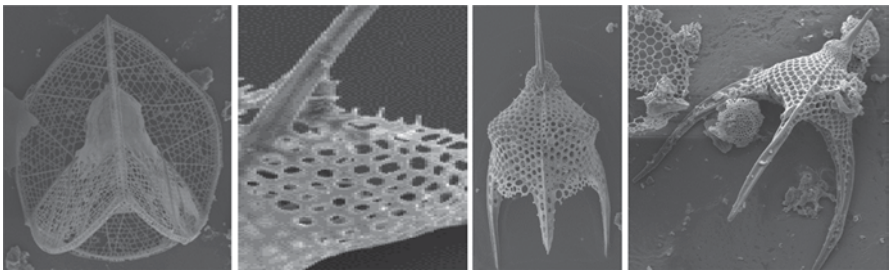

Fig. 12.3 Examples of scanning electron microscope images of suitable radiolarians for a further offshore development

12.3.3 Structural Analysis

The selected biological organisms had to be tested for their suitability for the foundation structure because the technical load cases naturally did not correspond with the loads they would experience in nature. For this reason the plankton structures were analyzed with the technical load cases (forces, moments and supports) to localize imported design components which are necessary for the stability of an offshore foundation. Detailed CAD models (constructed in the CAD program Solid Works) were built with the help of scanning electron microscope recordings and literature data from the screening phase. The geometries of the selected radiolarians tests were transferred exactly to the models in order to obtain an accurate understanding of the mechanical principles. After the construction process the models were analyzed with FE-Software tools (MSC Marc/Mentat). For that purpose the constructed organisms were scaled to the size of the foundation structure and loaded with the technical load cases provided by the manufacturer. Evaluation criteria for the selection of a suitable archetype were a homogeneous stress distribution, maximum comparative stresses according to v. Mises and low maximum deformation values. In addition, the potential for structural simplification in order to meet the manufacturing requirements were assessed. Important mechanisms of action were found after the analysis of the calculated models. The work package “Structural analysis” was completed with the comparison of all FE-results. Five biological organisms could be determined as potential archetypes for an innovative foundation.

12.3.4 Abstraction

The results of the structure analysis were the basis for the abstraction of the organisms. The process of abstraction is necessary because the skeletons of radiolarians have a complex design which cannot be realized with conventional production technologies. The biological organisms have to be reduced to the essential structural elements to ensure the successful transfer of the biological lightweight principles to a technical product. In the beginning of the abstraction process, the five best results were selected from the structural analysis. With the information of the stress

analysis, the structures were simplified with only essential components remaining. Elements with no supporting functions were removed.

The Radiolarians illustrated in Fig. 12.4 are shown with v. Mises stresses. The results of the FEM calculations on the best rated *C. teuscheri* show a homogeneous stress distribution as a sign that most areas lie within the flow of forces. Higher stresses are only concentrated on the outer arc of the structure. This arc is strongly bent and would therefore buckle easily as a function of typical load cases (moments originating from wind pressure on the rotor). However, since this buckling can only take one direction, the arc can be stabilized by thin struts, which are only charged with tensile stress and connected to the main inner beams of the structure. This principle was transferred to an abstracted and simplified first draft of a foundation structure. Analogous to the implementation described above, a further investigation of other organisms and their abstraction took place. After the abstraction of the biological archetypes, all constructions were analyzed with the load cases of the reference foundation structure. The benchmark of all abstracted constructions showed that the design of the Radiolarian *Clathrocorys teuscheri* offered the best potential for further development.

12.3.5 Optimization

In phase four optimization tools were applied. An optimization loop, which connected the necessary programs, has to be configured. In this case there were three programs involved: SFE concept, MSC.Nastran and the optimization tool. The abstracted *Clathrocorys* model was parameterized with five design parameters. These parameters were able to change the location of the central node, the strut connection and the radial food print. The wall thickness was also defined as a design parameter. SFE Concept was responsible for the shape variation and the generation of new models and input decks. These generated input decks were used from MSC.Nastran to calculate results like mass, displacement and stresses. The third part, the optimization loop, was the brain of the loop. It decided how the new design variables had to be changed for the next run (see Fig. 12.5) (Fig. 12.6).

The objective was to minimize mass by a maximal allowable displacement from 100 mm as a constraint. Two different algorithms were used for optimization, which will later be compared in the results and discussion. First of all, a simple gradient search based algorithm was applied. The optimization tool DAKOTA from Sandia National Laboratories was used to handle this purpose. The design n parameters were defined as $x_1,\ldots,x_n$ and concluded in the vector $\vec{x}$. The following objective function was applied:

$$f(x_1^0,\ldots,x_n^0) = F(\vec{x}^0) = optimum \tag{12.1}$$

The gradient is defined as an n-dimensional vector.

$$\vec{g} = \nabla f(\vec{x}) = \left(\frac{\partial f}{\partial x_1},\ldots,\frac{\partial f}{\partial x_n} \right)^T \tag{12.2}$$

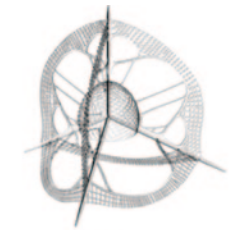

(1) *Clathrocorys teuscheri:*

- homogeneous stress distribution
- simple principle in spite of complex geometry
- buckling prevented by tensile structures
- high potential for realisation in steel
- first choice for the next steps within ELiSE

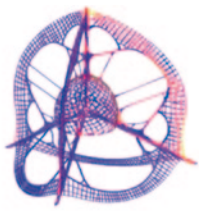

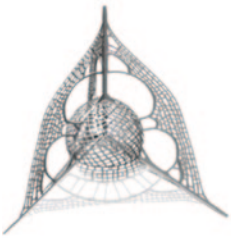

(2) *Chlathrocorys murrayi*

- homogeneous stress distribution
- principle similar as in (1)
- higher complexity than in (1)
- potential for realization in steel: medium

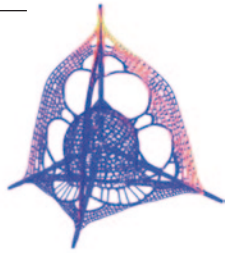

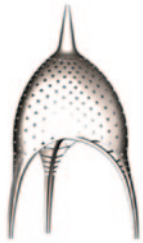

(3) *Pterocenium*

- Outer shell and internal structure
- average stress distribution
- shell structure difficult to manufacture
- effective, elegant abstraction required
- interesting for future foundation developments

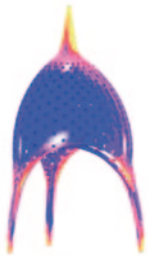

(4) Pterocanium trilobum

- poor stress distribution
- transition to piles have a high potential
- shell difficult to manufacture
- poor potential for abstraction
- potential use for other products possible

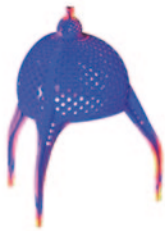

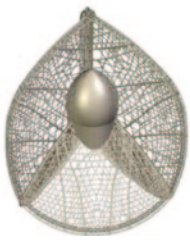

(5) Callimitra carolotae

- homogeneous stress distribution
- extreme complexity
- framework structure difficult to manufacture
- high potential for innovative production methods
- high potential for other products

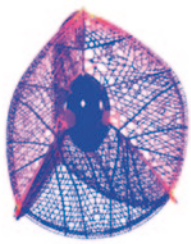

Fig. 12.4 *Radiolaria* as biological archetypes with screening criteria. *left***:** CAD construction *right***:** stress analysis with conventional FEM-Tools

Fig. 12.5 Foundation models on the basis of simplified radiolarian geometries. *Left*: abstraction of Pterocenium, *middle:* Callimitra and *right*: Clathrocorys. This step contains an arbitrary component

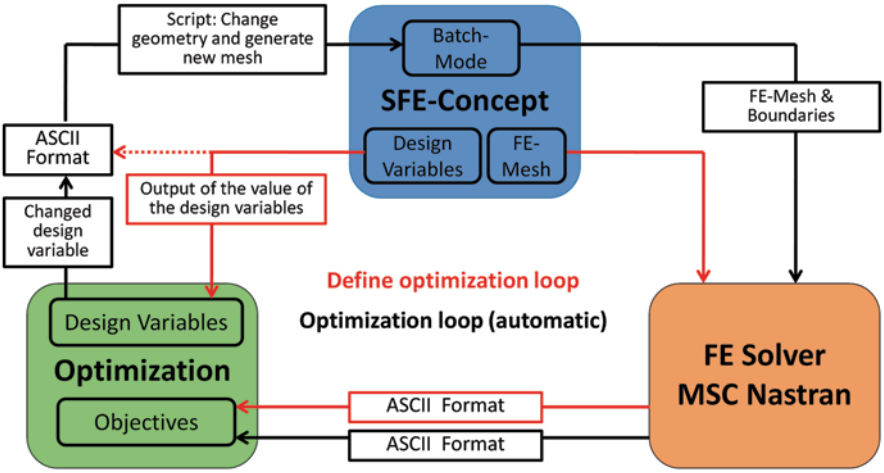

Fig. 12.6 Optimization loop (modified after a scheme drafted by SFE Concept GmbH, Berlin)

The vector shows in every point in the direction of the highest scope. The single mode was selected as an optimization strategy and the optimization model was single. The convergence criterion was 10^{-6} and the maximal number of interaction was restricted to 300.

The evolution strategy was used as a second optimization algorithm. This algorithm is part of the stochastic principle and was coded into VBA. It was applied through the help of Microsoft Excel 2007. The evolutionary strategic optimization (ES) consists of μ parents which created λ mutated offspring. The best offspring λ will survive and will be passed into the next generation. Within the optimization a (1,5)-ES strategy was applied (Rechenberg, 1994) (Fig. 12.7).

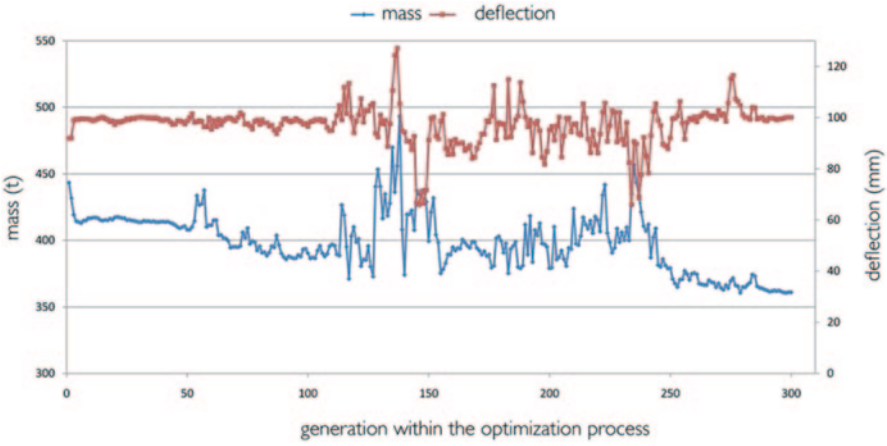

Fig. 12.7 Optimization progress of the used evolutionary strategy. The best parameter setting was achieved in generation 297 with 361 t and 997 mm displacement

12.3.6 Manufacturing

Aspects concerning manufacturing take place during the last step. Based on the optimized results of the bio-inspired structure, a similar pipe design was created. The offshore steel S355 and the product range of the company Europipe were considered to achieve the most cost effective production afterwards. The delivery program consisted of pipes with an outer diameter between 508 and 1524 mm and a wall thickness between 7 and 40 mm.

Another requirement was the connection to the sea belt (Fig. 12.8).

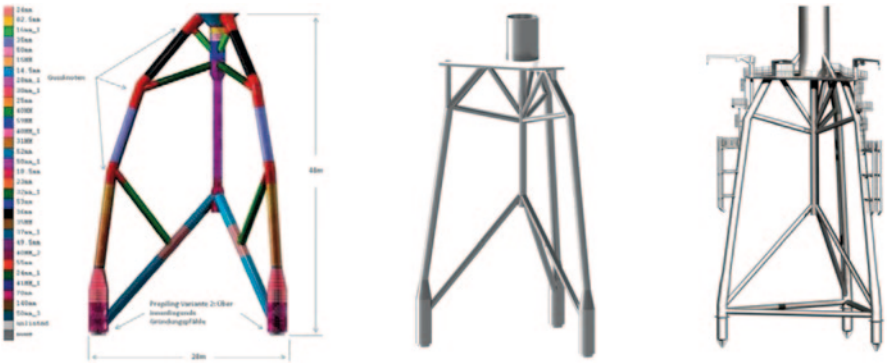

Fig. 12.8 Details showing the adaptation of the structure to the manufacturing process (composition of straight steel pipes, *left*, simplified angular bending instead of continuous curves, (*middle)* and necessary addition of secondary steel (boat landings, platform, cranes))

12.4 General Discussion

The development of lightweight structures, compared to that of new materials, seems like an uncomplicated, well-established procedure. All structural lightweight principles are based on classical mechanics and have been described in detail (Quote Leichtbau-Katalog). However, even seemingly simple tasks, such as the construction of a bridge, can be solved by many different designs (Gordon 1978). Natural structures, which are under selection pressure to be strong and light, must obviously follow the same principles as do technical structures with the same profile. Even more than technical lightweight solutions, they are realized in a wide variety of forms. There are three reasons that their geometries can differ significantly from those known in technical solutions or generated by topology optimization: (1) They fulfill additional functions (e.g. permeability, vibration damping, robustness against unexpected loadcases, (2) they present an alternative (potentially better) solution, e.g. by applying a higher structural complexity, differentiated material properties, or using purely tensile structural elements, and (3) the load cases of the natural structures differ fundamentally from those of the technical solutions.

In turn, natural lightweight solutions have a high potential for technical lightweight developments, if they have (1) a clearly defined profile as stable lightweight constructions, (2) a large spectrum of different geometries, and (3) not too many additional functions. In the case of biomineralized plankton shells which serve mainly as armor against predators, and which exist in many different forms, these conditions are fulfilled.

Although the ELiSE process has a high potential to improve many different lightweight structures, no guarantee can be given that it can improve a technical solution before the first steps have been passed. It is crucial to find natural models, whose construction principles are consistent with those of the technical specifications of the product which has to be optimized. The load cases lightweight structures experience in nature will never be exactly the same as those experienced in the technical world. In addition, a considerable upscaling of the size of the structures is necessary. The offshore foundation described here is a prime example for that. This deficiency can be partly compensated by the optimization step within the ELiSE procedure, which is based on the technical specifications. Still, the transfer is more likely to be successful if the technical load cases bear some resemblance to those which led to the evolution of natural solutions.

Plankton shells are subject to extremely diverse and complex load cases, which are generated by the feeding tools of many different predators. Thereby, the most abundant and active predators will have the strongest influence on the evolution of these shells. Still, less abundant predators must also have an effect, thus we expect that most plankton shells will be generalists, that is, they will have no explicit mechanical weakness. Based on such a principal geometry of a plankton shell, adaptations to an altered spectrum of predators are possible. Indeed, different geometric characteristics based on the same structural design can be seen within a plankton genus.

The fact that plankton shells are adapted to a mixture of different mechanical challenges also facilitates adaptations to technical load cases. In the case of the

offshore foundations, a prerequisite was that the structure should have three anchor points, which could be fixed with piles in the sediment. These had to somehow converge into a single tube, representing the transition to the tower section. Such a tetrahedral geometry is hard to find among diatoms, as they are basically boxes (Round et al. 1990). Fortunately, there are many other planktonic groups with biomineralized armor. Among them, the radiolarians are particularly interesting for the challenges described here, as some of their taxa possess complex open frameworks within a tetrahedral design space. In contrast to the photosynthetic diatoms, which need only pores with a diameter in the nm range, radiolarians feed on small organisms and particles and are therefore forced to use open skeletal structures.

Although all radiolarians selected for mechanical assessment complied with the requested design, they had fundamentally different geometries. *Chlathrocorys* was analyzed in two variants, and we chose the species which could be simplified more easily. *Callimitra* displayed a very complex network of structural reinforcements, which completely fills each sector. In addition, the rim is reinforced by a bent lattice truss consisting of triangles. Both *Callimitra* and *Chlathrocorys* have a relatively small central capsule. *Pterocanium* is much bigger and has a very large central capsule, which is internally reinforced by thin structures.

All these structures displayed good stress distribution as a function of the technical load cases. *Pterocenium*, the heaviest structure, had large areas without stress, thus much material was useless and we saw little potential to reduce it in the optimization step. We finally chose to use *Clathrocorys teuscheri* for further optimzation because it had the highest potential for a transfer of its structural principles even in a simplified format: Its outward bent structures trigger a controlled buckling as a function of the typical load cases of an offshore construction, which was prevented by thin purely tensile elements.

12.4.1 Outlook

The optimization of an offshore foundation with three piles using the EliSE method shows the high potential of the bionic approach even for very large, unusual structures. As a case study, using a simplified technical specification, the development was extremely successful and met all requirements. In the next stages, it will be necessary to include all crucial load cases and optimize for strength, low weight and low cost at the same time. In addition, an effective way to adapt the foundations to different offshore sites with specific ground mechanics, water depths, current and wave regimes, respectively and produce them efficiently will be necessary to compete on this dynamic but very cost-sensitive market.

This will require:

- Considerable input from different manufacturers
- Information on usefulness and prices of semi-finished products such as steel pipes of different dimensions and quality
- Technical specifications for foundation depending on individual construction sites with the highest potential

The potential for technical constructions which allow more structural detail is, obviously, even higher. Examples are components that can be produced by casting processes or by additive manufacturing. Such manufacturing methods are increasingly applied in the aerospace and automotive industries.

References

Boltovskoy SA (2002) radiolarian.org. http://www.radiolarian.org. Accessed: 20 Aug 2012

Byrne BW, Houlsby GT (2003) Foundations for offshore wind turbines. Philos Trans A Math Phys Eng Sci (compiled by Thompson JMT) 361:2909–2930

Gordon, J.E. (1978) Structures or Why Things Don't Fall Down. Penguin Books, London, 395 pp.

Hamm C (2005). Kieselalgen als Muster für technische Konstruktionen. BIOspektrum 1:41–45

Hamm C, Smetacek V (2007) Armor: why, when, and how. In: Falkowski PG, Knoll AH (eds) Evolution of primary producers, Elsevier, Boston, S. 311–332

Knopf B, Phale M, Edenhofer O, Kondzielle H, Götz M, Bruckner T et al. (2011) Der Einstieg in den Ausstieg: Energiepolitische Szenarien für einen Atomausstieg in Deutschland

Rechenberg I (1994) Evolutionsstrategie'94. Frommann-Holzboog, Stuttgart

Round F, Crawford R, Mann D (1990) The diatoms: biology & morphology of the genera. Cambridge University Press, Cambridge

Seidel M (2007) Jacket substructures for the REpower 5 M wind turbine. Conference Proceedings European Offshore Wind 2007. Berlin

Wab e. V (2012) Fragen und Antworten zur Offshore-Windenergie

Zaaijer MB (2003) Comparison of monopile, tripod, suction bucket and gravity base design for a 6 MW turbine. Offshore windenergy in Mediterranean and other European seas (OWEMES conference). Naples